CONFIGURATION OF CROSSLINKED MULTI-POLYMERIC MULTI-UNITS FOR SITE-SPECIFIC DELIVERY OF NICOTINE

NEHA SINGH

A Dissertation submitted to the Faculty of Health Sciences, University of the Witwatersrand, Johannesburg in the fulfilment of the requirements for the Degree of Master of Pharmacy

2007

Supervisor: Prof. Viness Pillay, Department of Pharmacy and Pharmacology, University of the Witwatersrand, Johannesburg, South Africa

Co-Supervisor: Prof. Michael P. Danckwerts, Department of Pharmacy and Pharmacology, University of the Witwatersrand, Johannesburg, South Africa

Declaration

I, Neha Singh declare that this dissertation is my own work. It is being submitted for the degree of Master of Pharmacy in the Faculty of Health Sciences at The University of the Witwatersrand, Johannesburg, South Africa. It has not been submitted before for any degree or examination at this or any other University.

This 28th day of February 2007.

ABSTRACT

Parkinson's Disease (PD) is a progressively debilitating neurodegenerative disease that affects the central nervous system and leads to severe difficulties with body movements. PD occurs due to the selective degeneration of neurons in the region of the brain known as the substantia nigra pars compacta. To date PD remains an incurable disease. Currently prescribed drugs provide only symptomatic relief to patients. Furthermore, they have considerable side effects and are often ineffective in the later stages of the disease or need to be used in combination in order to be effective. The role of neuroprotectants as a preventative measure in PD therapy is consequently receiving a great deal of attention and is being subjected to extensive research. This study sought to develop a novel prolonged-release drug delivery device for providing site-specific administration of newly researched neuroprotective agents. Nicotine was employed as the model neuroprotectant to incorporate in a novel reinforced crosslinked multiple-unit multi-polymeric drug delivery device. The study was the first of its kind to develop and employ the alkaloid for this purpose in a formulated delivery system. The device was intended to be one that provided zero-order prolonged release of the drug over a period of 1-2 months. The device was formulated such that its design was in keeping with the potential for implantation into the substantia nigra pars compacta to provide site-specific drug delivery. In order to do so, polymers, with biocompatible and bioerodable characteristics were selected to incorporate the drug within a reinforced crosslinked matrix. The study elucidated the mechanism of crosslinking of ionotropically crosslinked alginate spheres (gelispheres) with a variety of crosslinking agents through an evaluation of physicomechanical properties of the crosslinked system. The presence of barium in the crosslinked matrices generated densely networked gelispheres which retained their robustness following exposure to hydrating media and displayed promising potential for

entrapping drug molecules and retarding their release. The system was reinforced employing hydroxyethylcellulose (HEC) and polyacrylic acid (PAA). A Design of Experiments approach employing a Plackett-Burman screening design enabled optimisation of the proposed device in terms of reinforcing polymers (HEC and PAA) and crosslinking agents (barium and calcium). In order to further attenuate drug release rate the optimised crosslinked gelispheres were exposed to dilute hydrochloric acid (HCl) which significantly decreased gelisphere matrix swelling and erosion following exposure to simulated cerebrospinal fluid (CSF). These gelispheres were thereafter incorporated into a compressed release-rate modulating polymeric discs. Zero-order drug release was observed for a period of 50 days in simulated CSF when the optimised gelispheres were incorporated into compressed poly(lactic-co-glycolic) acid (PLGA) discs. Alternative approaches to modify drug release kinetics were also evaluated including the use of PLGA coatings on compressed hydroxypropylmethylcellulose-polyethylene oxide (HPMC-PEO) discs incorporating gelispheres and the use of crosslinked alginate-pectinate gelispheres as carrier systems to deliver PLGA-PLA (polylactic acid) microparticles incorporating drug. A Box-Behnken statistical design was employed to formulate and optimise the drug carrying PLGA-PLA microparticles. In both of the abovementioned cases we obtained sustained zero-order drug release.

SUMMARY

Configuration of Crosslinked Polyspheres for Site-Specific Delivery of Neuroprotectants

Parkinson's Disease (PD) is a progressively debilitating neurodegenerative disease that occurs due to the selective degeneration of neurons in the region of the brain known as the substantia nigra and leads to severe difficulties with body movements. To date PD remains an incurable disease. This study sought to develop a novel prolonged-release drug delivery device for providing site-specific administration of a newly researched neuroprotective agent, nicotine, incorporated in a novel reinforced crosslinked multiple-unit polyspheric drug delivery device. The device was intended to be one that provided zero-order prolonged release of the drug over a period of a few months. In order to do so, polymers, with biocompatible and bioerodable characteristics were selected to encapsulate the drug within a reinforced crosslinked matrix. The study elucidated the mechanism of gelation of ionotropically crosslinked alginate spheres (gelispheres) within a unique combination of reinforcing biopolymers, hydroxyethylcellulose (HEC) and polyacrylic acid (PAA) which was formulated employing a variety of crosslinking agents. A Plackett-Burman screening design enabled identification of independent factors which influenced the behaviour of the proposed device in terms of drug release (DR) and drug entrapment efficiency (DEE). In order to attenuate DR, matrix swelling and disintegration, the optimised crosslinked gelispheres were exposed to dilute HCl. The optimised gelispheres were incorporated into release-rate modulating compressed polymeric discs. Alternative approaches to modify drug release kinetics were also investigated including the use of PLGA coatings on compressed polymeric discs incorporating gelispheres and the use of crosslinked gelispheres as carrier systems to deliver PLGA-PLA microparticles incorporating nicotine.

PUBLICATIONS

Formulation and Statistical Optimisation of Novel Double-Incorporated PLA-PLGA Microparticles within an Alginate-Pectinate Platform for the Delivery of Nicotine. Journal of Microencapsulation. Volume 23(2):153 - 167. N. Singh, F. Seedat, J.L. Sweet, V. Pillay and M.P. Danckwerts. 2006.

Review Paper: Advances in the Treatment of Parkinson's Disease. Progress in Neurobiology. Volume 81(1):29 - 44. N. Singh, V. Pillay and Y.E. Choonara. 2007.

PRESENTATIONS

POSTERS

A Novel Double–Encapsulated Crosslinked PLA-PLGA Polyspheric Glycosidic Scaffold for Controlled Delivery of Nicotine to the Brain. N. Singh, V. Pillay, F. Seedat, J.L. Sweet and M.P. Danckwerts. Conference of the Controlled Release Society, Florida, United States of America, 18th - 22nd June 2005.

A Novel Multi-Unit System for the Delivery of Neuroprotectants in Parkinson's Disease. N. Singh, V. Pillay and M.P. Danckwerts. Conference of the Academy of Pharmaceutical Sciences, Port Elizabeth, South Africa, 29th September - 2nd October 2005.

The Influence of Barium and Calcium on the Hydrational and Physicomechanical Properties of Nicotine-Loaded Alginate-Hydroxyethylcellulose Gelispheres. N. Singh, V. Pillay, Y.E. Choonara and M.P. Danckwerts. International Conference on Pharmaceutical and Pharmacological Sciences, Johannesburg, South Africa, 20th - 23rd September 2006.

Influence of Crosslinking Reagents on the Hydration and Physicomechanical Properties of Nicotine-Loaded Alginate-Hydroxyethylcellulose Gelispheres. N. Singh, V. Pillay, Y.E. Choonara and M.P. Danckwerts. Conference of the American Association of Pharmaceutical Scientists (AAPS), Texas, United States of America, 29th October - 2nd November 2006.

A Novel Multi-Polymeric Crosslinked Glycosidic Platform for Site-Specific Delivery of Neuroprotectants. N. Singh, V. Pillay and Y.E. Choonara. Neurological Association of South Africa Conference, Johannesburg, South Africa, 28th March - 1st April 2007.

PODIUM PRESENTATIONS

Design and Development of a Multi-particulate System for Parkinson's Disease. Therapeutic Sciences Research Afternoon, University of the Witwatersrand, Johannesburg, South Africa, 11th August 2005.

Biodegradable Glycosidic Multi-Polymeric Devices for Drug Delivery. Biomaterials Symposium, University of the Witwatersrand, Johannesburg, South Africa, 4th September 2006.

A Novel Multi-Polymeric Crosslinked Glycosidic Platform for Site-Specific Delivery of Neuroprotectants. Young Scientists Competition, International Conference on Pharmaceutical and Pharmacological Sciences Johannesburg, South Africa, 20th - 23rd September 2006.

ACKNOWLEDGEMENTS

I would like to firstly thank my family, Ma, Pa and Priyanka for your unbounded love and support. You have given me the capacity to always believe in capabilities (even when I didn't believe in them myself) and teaching me that quitting is never an option.

I would like to thank my supervisor, Professor Viness Pillay for believing in me. Without you I would never have had the opportunities that I have had, not just to pursue this Masters. Thank you for pushing my boundaries and being a constant source of support and encouragement. I would also like to thank my co-supervisor Professor Michael P. Danckwerts for having faith in me. Thank you Yahya E. Choonara for your most valuable and constructive advice on this manuscript.

I would like to thank my friends, who have been my extended family these past few years.

Thank you, Gauri Jain, for inspiring me to read Paolo Cohelo's 'The Alchemist' and helping me to see the reason in life when it feels like there isn't any and believing that the mind is powerful enough to create miracles. Thank you for being the one I am allowed to lean on.

Thank you, Lisa Claire du Toit for being my confidant and for putting up with me for the past 2 years in 8M16. You have taught me patience and what it really takes to be better than what you think is your best.

Thank you, Maria P. Paraskeva for listening to everything and anything I have ever needed to say and also for putting up with my 37 (I'm sure there are more!) personalities. Your endurance puts the energiser bunny to shame.

Thank you, Sheri-Lee Harilall for your friendship, and most of all, for caring. I am grateful for the fact that you have treated me like family and made me realise the value of being able to embrace your past, present and future.

I would also like to thank some of the phenomenal women, without whom I would never have survived the past few years. Thank you (in alphabetical order) Jeanette Lotter, Kerushini Naidoo, Oluwatoyin Kolawole, Poonam Mistry and her family, Samantha Pillay, Sibongile Sibambo and Shirona Naidoo and for enriching my life through your friendship.

Thank you, Ashok E. Prasad, Naveen Kumar, Jayachandran T. Paul and his family for continuing to push me on when I needed the motivation and for being my guardians in everyway.

Thank you, Mr. David N. Bayever for making sure I never gave up hope even when success seemed impossible. You reminded me that 'perseverance *always* wins'.

Thank you, Nani ma and Daddyji and your beautiful family that I feel incredibly privileged to be a part of. You have ensured that I always keep my feet on the ground.

I also thank The University of the Witwatersrand for its support during my studies and for giving me the opportunity to purse my education at this institution in this wonderful country. Also, I would like to thank Sandy van Vuuren for her ready assistance and for very kindly giving me permission to use her lab. I would also like to thank Busi, Elizabeth, Florence, Sello and Tebogo at the Department of Pharmacy and Pharmacology for their patience and support.

I would also like to thank Investec for the Stella and Paul Lowenstein travel grant that gave me the opportunity to attend the Controlled Release Society (CRS) Conference in Miami, Florida, USA in 2005. It was an experience that has enriched my Masters degree immeasurably.

Finally, I would like to thank the Almighty, for helping me realise that I am loved and that He has a plan for me. Thank you for sending your Angels.

You will pass through storms and you may suffer defeat. The essence of creative life is to persevere in the face of defeat and to follow the rainbow within your heart.

- Diasaku Ikeda

DEDICATION

I dedicate this dissertation to my Mom.

You are my inspiration.

TABLE OF CONTENTS

Abstract....3

Summary....5

Publications....6

Presentations....7

Acknowledgements....9

List of Figures....18

List of Tables....24

Declaration....2

***Chapter 1*....26**
Parkinson's Disease – The Benefits of a Novel Drug Delivery System for Neuroprotective Agents

1.1 Introduction....26
1.2 Current Therapies and their Limitations....32
1.3 Neuroprotection as a Treatment Strategy for the Management of PD....35
1.4 Nicotine as a Neuroprotectant for PD....37
1.5 Challenges Associated with Drug Delivery to the Brain....41
1.6 Implantable Therapeutic Systems....44
1.7 Rationale and Motivation for Study....46
1.8 Aim and Objectives of This Study....48
1.9 Synopsis of Dissertation....49
1.10 Potential Benefits of This Study....52

***Chapter 2*....54**
Elucidation of the Properties of Crosslinked Alginate Gelispheres as a Platform for Drug Delivery through Physicomechanical Analysis

2.1 Introduction....54
2.2 Materials and Methods....61
2.2.1 Materials....61
2.2.2 Preparation of Alginate Gelispheres....62
2.2.3 Textural Analysis of Unhydrated Gelispheres....62
2.2.4 Textural Analysis of Hydrated Alginate Gelispheres....65

2.2.5 Analysis of Alginate Gelisphere Erosion....65
2.3 Results and Discussion....66
2.3.1 Textural Analysis of Unhydrated Alginate Gelispheres....66
2.3.1.1 Influence of G/M-Ratio on the Textural Properties of Unhydrated Alginate Gelispheres 68
2.3.1.2 Influence of Crosslinking Agent on the Textural Properties of Unhydrated Alginate Gelispheres....69
2.3.2 Textural Analysis of Hydrated Alginate Gelispheres....72
2.3.2.1 Influence of the Co-ordination Number of Crosslinking Agent on Matrix Hydration ...79
2.3.2.2 Influence of G/M-Ratio on Matrix Hydration....80
2.3.2.3 The Influence of G-Unit Selectivity for Crosslinking Agents on Matrix Hydration....81
2.3.2.4 Barium as a Matrix Re-inforcer for G-rich Alginates....82
2.3.3 Erodibility of the Crosslinked Alginate Gelispheres....83
2.3.3.1 Influence of G/M Ratio and Crosslinking Agent on Matrix Erosion....84
2.4 Concluding Remarks....88

***Chapter 3*....91**
Evaluating the Role of Hydroxyethylcellulose and Polyacrylic Acid on the Modifying Drug Release Rates of Crosslinked Alginate Gelispheres

3.1 Introduction....91
3.2 Materials and Methods....101
3.2.1 Physiochemical Properties of Nicotine....101
3.2.2 Standard Curve for Nicotine....106
Three Phase Approach Employed to Develop and Optimise the Crosslinked Multi-Polymeric Gelispheres....107
3.2.3 PHASE I: Elucidating the Effect of Crosslinking Agent and Post-Curing Exposure to Dilute HCl on Multi-Polymeric Reinforced Gelispheres....108
3.2.3.1 Formulation of Crosslinked Reinforced Alg-HEC Gelispheres....108
3.2.3 PHASE II: Formulation and Evaluation of Reinforced Multi-Polymeric Gelispheres Employing a Design of Experiments Approach....111
3.2.4.1 Formulation of Alg-HEC-PAA Gelispheres in Accordance with a Plackett-Burman Screening Design....111
3.2.4 Determination of Drug Entrapment Efficiency....112
3.2.5 Evaluating *In Vitro* Drug Release Characteristics of Alg-HEC and Alg-HEC-PAA Gelispheres....113
3.2.6 Textural Analysis of Hydrated of Alg-HEC and Alg-HEC-PAA Gelispheres....114
3.2.7 Analysis of Gelisphere Volume Changes following Hydration....114
3.2.8 Thermal Analysis of Alg-HEC and Alg-HEC-PAA Gelispheres....115
3.2.9 Analysis of Polymer-Polymer and Drug-Polymer Interactions Employing FTIR Spectroscopy....115
3.2.10 Analysis of Changes in Surface Morphology of Hydrated Alg-HEC-PAA Gelispheres....116
3.2.12 PHASE III: Formulation Optimisation Studies....116
3.2.12.1 Statistical Optimisation of Alg-HEC-PAA Gelispheres....116

3.2.12.2 Precipitating Alginic Acid in Optimised Formulations as a Means to Retard Gelisphere Swelling....117
3.3 Results and Discussion....117
3.3.1 PHASE I: Elucidating the Effect of Crosslinking Agent and Post-Curing Exposure to Dilute HCl on Multi-Polymeric Reinforced Gelispheres....117
3.3.1.1 Analysis of Physicomechanical Properties of Drug-free Alg-HEC Gelispheres....117
3.3.1.2 Analysis of Physicomechanical Properties of Drug-loaded Alg-HEC Gelispheres....121
3.3.1.3 Swelling Behaviour of Hydrated Alg-HEC Gelispheres....129
3.3.1.4 Evaluation of Drug-Polymer Interactions Employing FTIR Spectra....132
3.3.1.5 Evaluating Changes in Surface Morphology of Unexposed and HCl-Exposed Gelispheres following Hydration....135
3.3.1.6 Evaluation of the Drug Entrapment Efficiency of Alg-HEC Gelispheres....137
3.3.1.7 Elucidation of *In Vitro* Drug Release from Crosslinked Alg-HEC Gelispheres....139
3.3.1.8 Elucidation of Polymer-Polymer Interactions Employing FTIR Studies....142
3.3.1.9 Analysis of Native and Crosslinked Polymer Thermal Transitions Employing Differential Scanning Calorimetry....145
3.3.2 PHASE II: Formulation and Evaluation of Reinforced Multi-Polymeric Gelispheres Employing a Design of Experiments Approach....147
3.3.2.1 Alg-HEC-PAA Gelisphere Yield – Evaluation of Reaction Efficiency....147
3.3.2.2 Evaluation of the Drug Entrapment Efficiency (DEE) of Alg-HEC-PAA Gelispheres ……..…..149
3.3.2.3 Elucidation of *In Vitro* Drug Release from Alg-HEC-PAA Gelispheres....150
3.3.2.4 Thermal Analysis of Alg-HEC-PAA Gelispheres....152
3.3.2.4 Evaluation of Physicomechanical Properties of Alg-HEC-PAA Gelispheres....154
3.3.3 PHASE III: Formulation Optimisation Studies....159
3.3.3.1 Statistical Analysis of the Alg-HEC-PAA Gelispheres....159
3.3.3.2 Formulation and Evaluation of Optimised Gelispheres....166
3.3.3.3 Elucidating the Effect of Precipitating Alginic Acid on Optimised Gelispheres....167
3.4 Concluding Remarks....169

***Chapter 4*....172**
Modulation of Nicotine Release via Formulation of a Compressed External Polymeric Matrix Incorporating Crosslinked Gelispheres

4.1 Introduction....172
4.2 Materials and Methods....177
4.2.1 Evaluation of Powder Flow Properties and Compressibility of Polymers....178
4.2.1.1 Carr's Compressibility Index (CCI) of Polymers Employed to Formulate External Compressed Matrices....178
4.2.1.2 Evaluation of Angle of Repose (ϕ) of Polymers Employed to Formulate External Compressed Matrices....179
4.2.2 Formulation of Compressed Polymeric Discs Incorporating Gelispheres....180
4.2.3 Evaluation of *In Vitro* Drug Release Characteristics of the Compressed Polymeric Discs Incorporating Gelispheres....181
4.2.4 Evaluation of Friability of External Polymeric Matrices....181

4.2.5 Textural Analysis: Evaluation of Brinell Hardness Number (BHN) of Compressed Polymeric Discs 182
4.2.6 Evaluation of Conductivity Changes Following Disc Gelation 183
4.2.7 Evaluation of Matrix Erosion of Compressed Polymeric Discs Following Hydration..... 184
4.2.8 Evaluation of Changes in Disc Porosity Following Hydration 184
4.2.9 Kinetic Modelling of Release Kinetics from Compressed Polymeric Discs 184
4.3 Results and Discussion 189
4.3.1 Powder Flow and Compressibility of Polymers Employed to Formulate Compressed Discs..... 189
4.3.1.1 Carr's Compressibility Index (CCI) of Polymers Employed to Formulate Compressed Discs: Evaluating Powder Compressability 189
4.3.1.2 Angle of Repose (ϕ) of Polymers Employed to Formulate Compressed External Matrices: Evaluating Powder Flowability 191
4.3.2 Evaluation of *In Vitro* Drug Release from Optimised Alg-HEC-PAA Gelispheres Incorporated within Compressed Polymeric Discs 192
4.3.3 Friability of Compressed External Polymeric Matrices 194
4.3.4 Changes in Brinell Hardness Number (BHN) of Compressed External Polymeric Matrices Following Hydration 194
4.3.5 Evaluation of Erosion of Compressed External Polymeric Matrix 196
4.3.6 Changes in Conductivity of Compressed External Polymeric Matrices Following Hydration..... 200
4.3.7 Kinetic Modelling of Release Kinetics from Compressed Polymeric Discs..... 201
4.4 Concluding Remarks 202

Chapter 5 **..... 204**
Alternative Approach to Modify Nicotine Release: (I) PLGA-Coated Polymeric Discs Incorporating Crosslinked Calcium-Alg-HEC Gelispheres

5.1 Introduction 204
5.2 Materials and Methods 208
5.2.1 Formulation of PLGA-Coated (PC) Polymeric Matrices 209
5.2.2 Determination of *In Vitro* Drug Release Characteristics 209
5.2.3 Kinetic Modelling of Drug Release from Compressed Polymeric Discs 210
5.3 Results and Discussion 210
5.3.1 Evaluating *In Vitro* Drug Release from PLGA-Coated (PC) Polymeric Matrices 210
5.3.2 Kinetic Modelling of Drug Release from PLGA-Coated Compressed Polymeric Discs..... 213
5.4 Concluding Remarks 214

Chapter 6 **.....215**
Alternative Approach to Modify Nicotine Release: (II) Application of Novel Crosslinked Alginate-Pectinate Double-Encapsulated Approach for Delivering a PLA-PLGA Microparticulate System

6.1 Introduction.....215
6.2 Materials and Methods.....219
6.2.1 Preparation of PLA-PLGA Microparticles.....219
6.2.2 Determination of Drug Entrapment Efficiency.....221
6.2.3 Determination of *In Vitro* Drug Release Characteristics.....222
6.2.4 Optimisation of the PLA-PLGA Microparticles.....222
6.2.5 Double Entrapment of PLA-PLGA Microparticles into Crosslinked Alginate-Pectinate Polyspheres.....223
6.2.6 Elucidating Surface Morphology of the Developed Systems.....224
6.3 Results and Discussion.....224
6.3.1 Yield of Microparticles.....224
6.3.2 Evaluation of Drug Entrapment Efficiency.....226
6.3.3 Evaluation of *In Vitro* Release of Nicotine from the Microparticles.....226
6.3.4 Statistical Optimisation Studies.....228
6.3.5 Statistical Inferences between the Experimental and Predicted Values for Responses Measured.....229
6.3.6 Main Effects on the Responses.....233
6.3.7 Response Surface Behaviour of Microparticulate System.....235
6.3.8 Double-Entrapment of PLA-PLGA Microparticles within an Alginate-Pectinate Platform.....236
6.3.9 Yield of Crosslinked Polyspheres.....237
6.3.9.1 Zinc-Alginate Platform.....238
6.3.9.2 Zinc-Pectinate Platform.....238
6.3.9.3 Combined Zinc-Alginate-Pectinate Platform.....239
6.3.10 Evaluation of Drug Release from Polyspheres.....239
6.4 Concluding Remarks.....241

Chapter 7 **.....242**
Conclusions and Recommendations

7.1 Conclusions.....242
7.2 Recommendations.....245

References 249

LIST OF FIGURES

Figure 1.1: Summary of the pathological process involved in PD (Source: Adapted from Dipiro et al., 2001). Abbreviations: DOPAC: 3,4-dihydroxyphenylacetic acid; MAO-B: monoamine oxidase inhibitor B; GSH: glutathione; GSSH: glutathione disulfide; H_2O_2: hydrogen peroxide; $OH^{\cdot}$: hydroxyl free radical and OH^- hydroxyl ion…… 29

Figure 1.2: A schematic of free radical involvement as a common intermediary risk factor for many neurotoxic events in the pathogenesis of PD. Abbreviation: mtDNA: mitochondrial DNA (Source: Adapted from Prasad et al., 1999)…….……31

Figure 1.3: Sites of action of pharmacological therapies currently prescribed for PD (Source: Adapted from Katzung, 2001)…….....32

Figure 1.4: Proposed neuroprotective mechanisms of nicotine in the brain involved in preventing the onset and progression of PD…….. 40

Figure 2.1: Chemical structure of alginate and its monomers mannuronic acid (M) and guluronic acid (G). (Source: Draget et al., 2003)……...……...…55

Figure 2.2: Chemical structure of alginate and its monomers guluronic acid (G) and mannuronic acid (M) in an 'egg-box' arrangement when crosslinked with divalent cations (depicted by the red circles in the diagram) (Source: FMC BioPolymer Novamatrix, CRS Conference, 2005)……...…56

Figure 2.3: A calcium ion packed in a GG pocket between two alginate strands. Crosslinking between the carboxyl ends of the saccharide units alters the stereochemistry of the two approaching pockets considerably. (Source: Adapted from Al Musa et al., 1999)..……58

Figure 2.4: Typical textural profiles generated for crosslinked alginate gelisphere matrices (a) matrix resilience (%), (b) fracture energy (Nm) and (c) deformability modulus (N/mm)……...64

Figure 2.5: Profiles depicting the relationship between, (a) matrix resilience (%), (b) deformability modulus (N/mm) and (c) fracture energy (Nm) of unhydrated gelispheres crosslinked with zinc, calcium, barium and various binary combinations of the cations…… 67

Figure 2.6: Spatial arrangement of (a) zinc (b) calcium and (c) barium ions……..69

Figure 2.7: The interaction of divalent barium ions with carboxylic acid groups on alginate G-units and water molecules (octahedral arrangement) within the polymeric matrix (Source: Adapted from Berceńo et al., 2002)……70

Figure 2.8: Schematic illustration of the hydration mechanism and erosion of ionically crosslinked gelispheres……73

Figure 2.9: Matrix resilience (%) of hydrated alginate gelispheres crosslinked with (a) calcium, (b) zinc, (c) barium, (d) calcium and zinc, (e) calcium and barium, (f) barium and zinc, (g) calcium, barium and zinc over a period of 96 hours……..……...75

Figure 2.10: Deformability modulus (N/mm) of hydrated alginate gelispheres crosslinked with (a) calcium, (b) zinc, (c) barium, (d) calcium and zinc, (e) calcium and barium, (f) barium and zinc, (g) calcium, barium and zinc over a period of 96 hours……..……77

Figure 2.11: Fracture energy (Nm) on hydrated alginate gelispheres crosslinked with (a) calcium, (b) zinc, (c) barium, (d) calcium and zinc, (e) calcium and barium, (f) barium and zinc, (g) calcium, barium and zinc over a period of 96 hours……..……...79

Figure 2.12: Matrix erosion (%) of gelispheres following hydration crosslinked with (a) calcium, (b) zinc, (c) barium, (d) calcium and zinc, (e) calcium and barium, (f) barium and zinc, (g) calcium, barium and zinc over a period of 96 hours……88

Figure 3.1: The chemical structure of cellulose composed of linear 1,4-β-D'-glycosidically-linked β-D-glucospyranose units (Source: Ludwig, 2005)…….93

Figure 3.2: The chemical structure of the cellulosic ether hydroxyethylcellulose (HEC). (Source: Ludwig, 2005)..... ……...……95

Figure 3.3: Schematic illustrating the mechanism of crosslinking of alginate G-units with divalent calcium ions…….…....95

Figure 3.4: X-ray diffraction (XRD) profile observed for the G-rich sodium alginate (FMC BioPolymer) selected for further studies……. 97

Figure 3.5: The chemical representation of the monomer in Carbopol® 934; the covalently crosslinked branched chain polymer employed to coat the crosslinked reinforced alginate gelispheres……98

Figure 3.6: The 2-dimensional representation of the S-enantiomer of nicotine. The (*) indicates the location of the chiral carbon. (Source: Armstrong et al., 1998)…..……102

Figure 3.7: FTIR spectra of nicotine……103

Figure 3.8: Typical (a) DSC and (b) X-ray diffraction (XRD) profile observed for the model neuroprotectant nicotine…….105

Figure 3.9: UV spectrum for nicotine…….....106

Figure 3.10: Standard curve for nicotine at a wavelength of 245nm in 0.1M PBS at pH 7.4…...107

Figure 3.11: Schematic illustrating the methodology employed to formulate and analyse the Alg-HEC gelispheres…… 110

Figure 3.12: (a) Fracture energy (Nm), (b) Deformability modulus (N/mm) and (c) Matrix resilience (%) of drug-free unexposed Alg-HEC gelispheres and (d) Fracture energy (Nm), (e) Deformability modulus (N/mm) and (f) Matrix resilience (%) of drug-free HCl-exposed Alg-HEC gelispheres, over a period of 12 hours (N=3) following exposure to simulated CSF…….118

Figure 3.13: Stereomicrographs (Magnification x16) indicating changes in surface morphology of drug-free Alg-HEC gelispheres crosslinked with (a) $BaCl_2$, (b) $CaCl_2$, (c) $ZnSO_4$, (d) $BaCl_2$/dil. HCl, (e) $CaCl_2$/dil. HCl, and (f) $ZnSO_4$/dil. HCl, following exposure to PBS (0.1M; pH 7.4; 37°C; 50rpm) over a period of 12 hours……..….120

Figure 3.14: Textural analysis indicating the (a) Fracture energy (Nm), (b) Deformability modulus (N/mm) and (c) Matrix resilience (%) of unhydrated drug-loaded Alg-HEC gelispheres crosslinked with various crosslinking agents…….122

Figure 3.15: Changes in the physicomechanical properties observed in the (a) Fracture energy (Nm), (b) Deformability modulus (N/mm) and (c) Matrix resilience (%) of drug-loaded Alg-HEC gelispheres and (d) Fracture energy (Nm), (e) Deformability modulus (N/mm) and (f) Matrix resilience (%) of drug-free HCl-exposed Alg-HEC gelispheres, following exposure to simulated CSF, over a period of 12 hours……. 125

Figure 3.16: Stereomicrographs (Magnification x16) indicating changes in surface morphology of nicotine-loaded Alg-HEC gelispheres crosslinked with (a) $BaCl_2$, (b) $CaCl_2$, (c) $ZnSO_4$, (d) $BaCl_2$/dil. HCl, (e) $CaCl_2$/dil. HCl, and (f) $ZnSO_4$/dil. HCl, following exposure to simulated CSF, over a period of 12 hours……..128

Figure 3.17: Change in gelisphere volume (mm^3) of hydrated crosslinked Alg-HEC gelispheres drug-free (ND) (a) unexposed to dilute HCl and (b) exposed to dilute HCl and drug-loaded gelispheres (c) unexposed to dilute HCl and (d) exposed to dilute HCl following exposure to simulated CSF, over a period of 12 hours……..……129

Figure 3.18: Flowchart illustrating the process of hydration and subsequent chain disentanglement following hydration of the polymeric matrix……..131

Figure 3.19: FTIR spectra for (a) native alginate, (b) alginate and nicotine and (c) crosslinked alginate incorporating nicotine indicating the interactions between the alginate, calcium and nicotine……..... 134

Figure 3.20: Proposed mechanism of interaction of nicotine with alginate monomers at a molecular level…….. 134

Figure 3.21: Scanning electron micrographs of unhydrated drug-loaded (a) unexposed barium-crosslinked (magnification 1300x; 30 nanoamps) and (b) HCl-exposed barium-crosslinked gelispheres and hydrated (magnification 300x; 30 nanoamps) (c) unexposed barium-crosslinked and (magnification 1300x; 30 nanoamps) (d) HCl-exposed barium-crosslinked (magnification 6500x; 30 nanoamps) gelispheres following exposure to simulated CSF after 50 hours……..…….136

Figure 3.22: Drug entrapment efficiency (%) (Where, Formulation 1:$BaCl_2$, 2:$BaCl_2$/dil.HCl, 3:$CaCl_2$, 4:$CaCl_2$/dil. HCl, 5:$ZnSO_4$, 6:$ZnSO_4$/dil. HCl) of nicotine within crosslinked Alg-HEC gelispheres following exposure to simulated CSF, over a period of 50 hours.....137

Figure 3.23: % Drug release of nicotine from (a) unexposed Alg-HEC gelispheres crosslinked with zinc, calcium and barium and (b) Alg-HEC gelispheres exposed to dilute HCl following curing, over a period of 50 hours in simulated CSF. The four phases (Ia, IIa, Ib and IIb) of release are also depicted……..……..……. 139

Figure 3.24: Schematic illustrating the mechanism of sequestration…… 142

Figure 3.25: FTIR spectra of (a) HEC and (b) HEC and alginate……..143

Figure 3.26: Schematic illustrating the proposed mechanism of hydrogen bonding (H-bonds) forming between alginate M-units and HEC resulting in a reinforced gelisphere matrix…….. 144

Figure 3.27: Typical DSC profiles obtained for the G-rich Alginate (FMC BioPolymer) and (b) HEC (Hercules Inc., Natrosol® Pharm) selected for formulating the proposed drug delivery system and (c) the unexposed calcium-crosslinked Alg-HEC gelispheres…….....147

Figure 3.28: % Drug released over a period of 50 hours from the Alg-HEC-PAA gelispheres following exposure to simulated CSF…….……...…151

Figure 3.29: Typical differential scanning calorimetry (DSC) profiles of (a) Formulation 2, (b) Formulation 4 and (c) Formulation 7……..……...153

Figure 3.30: Changes observed in the (a) Matrix resilience (%) (b) Fracture energy (Nm) and (c) Deformability modulus (N/mm) of Alg-HEC-PAA gelispheres over 50 hours following exposure to simulated CSF……...……157

Figure 3.31a: Main effects plots indicating the influence of input parameters on (i) % drug release t=1 hour (i.e. the burst effect) and (ii) % DEE (where, Carb refers to PAA)……..…160

Figure 3.31b: Interaction plots correlating the pair-wise influence of input parameters (i) % drug release t=1 hour and (iv) % DEE. The red lines indicate the upper limits of the parameters, while the black lines indicate the lower limits……..161

Figure 3.32: Response surface plots correlating % drug entrapment efficiency (DEE) and the influence of (a) polymer concentration (alginate and HEC) and (b) the concentration of crosslinking ions, barium and calcium and (c) % drug release (DR) at t=1 hour (i.e. the burst effect) and the influence of alginate and HEC concentration…… 163

Figure 3.33: % Drug release from optimised formulations exposed to simulated CSF over 50 hours……..167

Figure 3.34: % Drug release from unexposed optimised formulation and HCl-exposed optimised formulation to over 120 hours to simulated CSF……...…. 169

Figure 4.1: The chemical structures of (a) hydroxypropylmethylcellulose (HPMC), (b) polyethylene oxide (PEO) and (c) poly(lactic-co-glycolic acid) (PLGA). (Source: Ludwig, 2005)……..175

Figure 4.2: Typical force-distance profile obtained for the calculation of BHN for the compressed polymeric discs exposed to simulated CSF……183

Figure 4.3: Carr's Compressibility Index (%) of polymers employed to formulate compressed discs……189

Figure 4.4: Angle of Repose (degrees) of polymers employed to formulate compressed discs……191

Figure 4.5: % Drug released from optimised gelispheres (Chapter 3) compressed into polymeric discs following exposure to simulated CSF over a period of 50 days……192

Figure 4.6: Changes in the Brinell Hardness Number (BHN) (N/mm^2) of compressed polymeric discs following exposure to simulated CSF over a period of 30 days……195

Figure 4.7: Matrix erosion (%) of compressed polymeric discs following exposure to simulated CSF over a period of 30 days……196

Figure 4.8: Scanning electron micrographs (Magnification 65x) of compressed (a) PLGA, (b) HPMC-PLGA and (c) PEO-PLGA discs following exposure to simulated CSF after 21 days……199

Figure 4.9: Changes in conductivity (μSiemens) of compressed polymeric discs following exposure to simulated CSF over a period of 30 days……..……200

Figure 5.1: X-ray diffraction (XRD) profile observed for the calcium-crosslinked Alg-HEC gelispheres selected for incorporation into external polymeric discs coated with PLGA…….208

Figure 5.2: % Drug released from Ca-Alg-HEC gelispheres over a period of 50 hours after exposure to simulated CSF……..…….…… 210

Figure 5.3: % Drug released over a period of 500 hours (or 21 days) from the gelispheres compressed into native PLGA and PLGA coated (PC) polymeric discs following exposure to simulated CSF…….…….. 213

Figure 6.1: Chemical structure of polylactic acid (PLA), polyglycolic acid (PGA) and poly(lactic-co-glycolic) acid (PLGA)…….. 215

Figure 6.2: Scanning electron micrographs of (a) fragmented microparticles and (b) optimal spherical microparticles……225

Figure 6.3: Typical scanning electron micrograph of a highly porous PLA-PLGA microparticle……..227

Figure 6.4: % Drug released from optimised PLA-PLGA microparticles as per Box-Behnken design and ANN algorithm…….……...229

Figure 6.5: Linear relationship between the experimentally-derived and Box-Behnken predicted values for (a) Drug release (fractional) after 0.5 hours, and (b) Drug entrapment efficiency……..230

Figure 6.6: Typical profiles for (a) the normal probability plot of the residuals, and (b) the residuals versus the fitted values……232

Figure 6.7: (a) Main effects plots (data means) for Drug Entrapment (%), and (b) % Drug release at 0.5 hours…… 233

Figure 6.8: Response Surface Plots for (a) Drug encapsulation vs. Polymer type and [Span 80]; and (b) Drug release in 0.5 hours vs. Stirring time (hours) and Polymer type (1 – PLA; 2 – PLA and PLGA and 3 – PLGA)…….235

Figure 6.9: High resolution scan of PLA-PLGA microparticles double-incorporated within a zinc-alginate polysphere……239

Figure 6.10: Drug release studies of double-encapsulated microparticles from multiparticulate polyspheres. (Insert clearly shows the second phase of drug release)……240

LIST OF TABLES

Table 1.1: Currently prescribed drugs for the management of PD symptoms and their limitations……34

Table 1.2: Agents selected by CINAPS as potential neuroprotective agents for assessment in clinical trials for the treatment/prevention of PD……..36

Table 1.3: Properties of the BBB which limits the delivery of neuroactive agents to the CNS (Source: Adapted from Abbot et al., 2006)……..... 42

Table 2.1: Commercial uses of alginates…… 59

Table 2.2: Alginates of varying G/M-ratios……61

Table 2.3: Parameter settings for measurement of the physicomechanical properties of gelispheres……63

Table 2.4: Range of matrix erosion for the various alginate gelispheres crosslinked with various combinations of divalent cations after 24 hours of exposure to hydration……85

Table 3.1: The chemical properties of nicotine. (CRC Handbook, 2004)…….....102

Table 3.2: Crosslinked Alg-HEC gelispheres prepared for Phase I.…..… 109

Table 3.3: The Plackett-Burman design template employed to optimise drug-loaded Alg-HEC-PAA gelispheres indicating the various combinations and permutations of polymers (alginate, HEC and PAA) and crosslinking agents (calcium and barium) that were employed. ……..……112

Table 3.4: Gelisphere yield efficiency ($\%^{w}/_{w}$) for the Alg-HEC-PAA formulations……..148

Table 3.5: Response outcomes for the Alg-HEC-PAA formulations…….…….. 150

Table 3.6: Response outcomes for textural analysis of unhydrated (t=0hr) and hydrated (after 9 hours of exposure to simulated CSF gelispheres of the Alg-HEC-PAA Formulations……..158

Table 3.7: Summary of results for % drug release (DR) t=1 hour (i.e. the observed burst effect) and drug entrapment efficiency (DEE) for Alg-HEC-PAA gelispheres…… 164

Table 3.8: Summary of results for % drug release (DR) t=1 hour (i.e. the observed burst effect) for Alg-HEC-PAA gelispheres…….....165

Table 3.9: Summary of results for % DEE for Alg-HEC-PAA gelispheres……..165

Table 3.10: Optimised formulations developed…….166

Table 3.11: Drug entrapment efficiency (%) for optimised formulations…….166

Table 3.12: Drug entrapment efficiency (%) for unexposed optimised formulation 1 and HCl-exposed optimised formulation…….....168

Table 4.1: Investigated polymer compositions for the external matrix……..181

Table 4.2: Typical test parameters employed for analysis of the Brinell Hardness Number (BHN) of compressed polymeric matrices exposed to simulated CSF…….. 182

Table 4.3: The relationship between the geometry of the polymeric matrix and mechanism of drug release. (Source: Siepmann and Peppas, 2001)…….187

Table 4.4: Friability results for polymeric matrices expressed as % weight loss (% WL) after 4 and 20 minutes in a friabilator at a rotation 25rpm……..194

Table 4.5: Release kinetics obtained from the various diffusion, relaxation and erosion models for compressed PLGA discs incorporating optimised gelispheres.……..……...201

Table 5.1: Various categories of coatings investigated and their properties..... 205

Table 5.2: Investigated polymer compositions for the external compressed polymeric matrix incorporating Ca-Alg-HEC gelispheres…….209

Table 5.3: Release kinetics obtained from the various diffusion, relaxation and erosion models for PLGA-coated compressed HPMC-PEO discs incorporating Ca-Alg-HEC gelispheres.....213

Table 6.1: General properties and typical applications of the biodegradable polyester polymers polyglycolic acid (PGA), polylactic acid (PLA), and their copolymer poly(lactic-co-glycolic) acid (PLGA)……..217

Table 6.2: Independent variables evaluated using the Box-Behnken Design…….220

Table 6.3: Values of responses obtained from the formulation of nicotine-loaded PLA-PLGA microparticles…… 227

Table 6.4: Optimised parameters used to generate experimental values……..... 228

Table 6.5: Comparison between desired and experimental output parameters with respect to selected data-modelling tools…….228

Table 6.6: Salient Parameters employed according to Andersoñ-Darling statistic……232

Table 6.7: Responses obtained for re-incorporated microparticles……238

Chapter 1

Parkinson's Disease – The Benefits of a Novel Drug Delivery System for Neuroprotective Agents

---

'Involuntary tremulous motion, with lessened muscular power, in parts not in action and even when supported; with a propensity to bend the trunk forwards, and to pass from a walking to a running pace: the senses and intellects uninjured.'

- An Essay on the Shaking Palsy, Dr. James Parkinson, 1817

1.1 Introduction

Parkinson's Disease (PD) or *Paralysis Agitans* was first documented in 1817 by Dr James Parkinson as the "shaking palsy" that afflicted his gardener who led a life of "sobriety" (Critchley, 1955). Since then the relationship between personality and the potential for developing PD has been extensively investigated. The inverse relationship between the "novelty-seeking" personality (verses the law-abiding, contentious and cautious "reduced-novelty seeking" personality displaying a 'certain intellectual and moral rigidity' (Critchley, 1955)) and subsequent development of PD is widely documented (Menza et al., 1990; Menza et al., 1992; Benedetti et al., 2000). Smoking, alcohol, coffee, cocaine, amphetamine and opiate abuse have all been shown to have somewhat of a preventative effect in the onset of PD (Paulson and Dadmer, 1991; Menza et al., 1993; Fujii at al., 2000). As a direct paradox, to this phenomenon, currently prescribed drugs for managing this condition have now been demonstrated to have a link between patients seeking a "reward-seeking" lifestyle subsequent to initiating therapy (Uitti et al., 1989; Dodd et al., 2005; Klos et al., 2005;

Stocchi, 2005). Such etiological data only confirms the pathological affliction associated with PD by depletion of the 'rewarding' dopaminergic neurons in the brain.

PD is a disease of the central nervous system (CNS) that leads to severe difficulties with body motions. Typical symptoms include tremor, rigidity, slowed body movements (bradykinesia), unstable posture and difficulty in walking (characterized by the patient's shuffling gait). To date PD remains an incurable disease. The currently available pharmacological and non-pharmacological treatments are able to offer only symptomatic relief for patients (Katzung, 2001). Available therapies aim to improve the functional capacity of the patient for as long as possible; however they do not modify the progression of the neurodegenerative process. The need for newer and more effective agents is consequently receiving a great deal of attention and consequently being subjected to extensive research.

In neuropathological terms, PD is characterized by the presence of intracytoplasmic inclusions from protein aggregates called Lewy bodies (LBs) (Burke, 1998) and the depletion of pigmented DA-containing neurons in the region known as the substantia nigra pars compacta (Forno, 1996). LBs consist of a heterogeneous mixture of proteins and lipids. The lipoidal core of these inclusions is surrounded by the peripheral filamentous elements which can comprise a variety of proteins, including ubiquitin, neurofilament, various proteasomal elements, and α-synuclein, which may be oxidatively modified (Fahn and Cohen, 1992; Zhang et al., 2000). Approximately 80% of

dopaminergic neurons in the susbtantia nigra are already irreversibly destroyed when the first symptoms of PD become significantly visible.

Affecting one in every 100 persons above the age of 65 years, it is the second most common neurodegenerative disease after Alzheimer's disease (de Rijik, et al., 2000). Apart from a documented relationship between personality-type, PD generally presents itself in the population as a sporadic condition. However an atypical presentation arising from gene defects inherited, by Mendelian trait have also been observed (Lev and Melamed, 2001; Vila and Przedborski, 2004). Among such inherited forms, abnormalities in the genes coding for the protein α-synuclein have been documented (Polymeropulous et al., 1997). Secondary causes of this condition include infection (post-encephalitic PD), drugs (e.g. antipsychotics such as haloperidol and thiordazine, antiemetics such as promethazine and metaclopramide (Standaert and Young, 2001)), chronic intoxication (among many substances, manganese and more rarely carbon bisulphide or carbon monoxide (Critchley, 1955)) and stroke.

Over the past few decades a large volume of data generated from clinical studies, autopsies and *in vitro* and *in vivo* experimental models have been accumulated, which has allowed us to gain some understanding of the pathogenesis of sporadic PD. Studies that have investigated this multifactorial cascade have thus far been primarily, if not exclusively, studied in toxic experimental animal models of PD, in particular from models that have been produced by the parkinsonian neurotoxin 1-methyl-4-phenyl-1,2,3,6-tetrahydropyridine (MPTP) (Emborg, 2004).

Studies demonstrated that soon after the systemic administration of MPTP, its active metabolite, MPP^+, (1-methyl-4-phenylpyridinium ion) (Srivastava et al., 1993), concentrates in the mitochondrial matrix, where it binds to complex I of the electron transport chain (ETC) (Gluck et al., 1994). This binding interrupts the movement of electrons along the ETC, leading to an increased production of reactive oxygen species (ROS), particularly superoxide radicals (Figure 1.1). This MPP^+-related disruption in electron flow is consequently associated with a drop in adenosine triphosphate (ATP) production. This phenomenon is found only in susceptible areas of the brain such as the ventral midbrain and striatum (Khan et al., 2005).

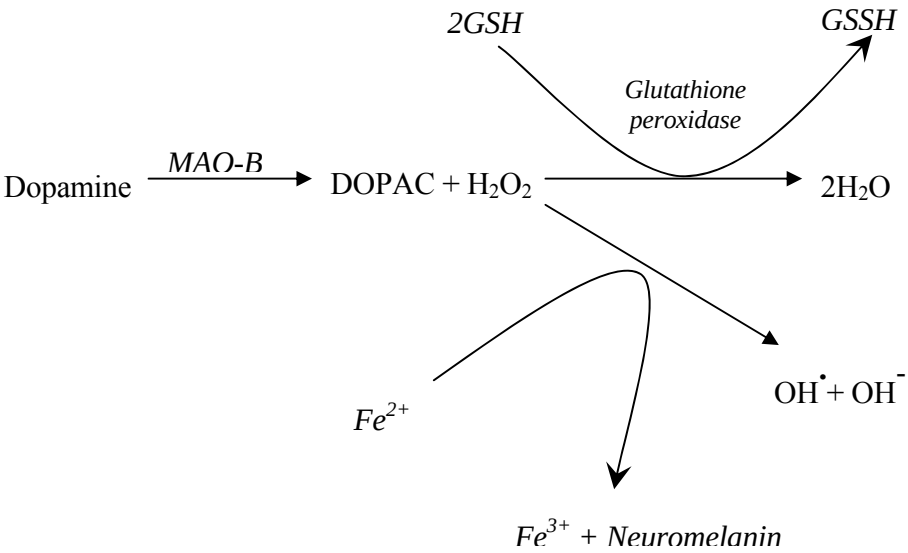

Figure 1.1: Summary of the pathological process involved in PD (Source: Adapted from Dipiro et al., 2001). Abbreviations DOPAC: 3,4-dihydroxyphenylacetic acid; MAO-B: monoamine oxidase inhibitor B; GSH: glutathione; GSSH: glutathione disulfide; H_2O_2: hydrogen peroxide; $OH^{\cdot}$: hydroxyl free radical and OH^- hydroxyl ion.

In addition to aggravating mitochondrial oxidative stress and energy depletion, MPP^+ also interacts with synaptic vesicles by binding to vesicular monoamine transporter-2 (Przedborski and Jackson-

Lewis, 1998; Przedborski, 2005). Thus, MPP^+ translocates into synaptic vesicles and stimulates the release of synaptic DA (Fabre et al., 1999). The resulting extruded cytosolic DA readily undergoes autoxidation, thus generating a burst of ROS, subjecting nigral neurons to oxidative stress (Fabre et al., 1999). Some theories suggest that the oxidation of cytosolic DA could also be catalyzed by enzymes such as cyclo-oxygenase-2 (Teismann and Ferger, 2001).

With reference to Figure 1.1, studies by Fahn and colleagues (Fahn, 1991; Fahn, 1992a; Fahn and Cohen, 1992b) have described the role of the oxidative pathway on dopaminergic neuronal degeneration and the role that antioxidants may play in the prevention of PD. Finally, the role of glutathione (GSH) in the degradation of DA neurons has been described by Bharath and colleagues (2002). They reported that age-related depletion in GSH levels may precipitate the accumulation of oxidizing free radicals such as hydrogen peroxide, hydroxyl ions and superoxide in the brain. This depletion in GSH has been attributed to the progressive mitochondrial dysfunction in the brain which has a drastic impact on ATP synthesis and usage. Furthermore, it enhances the formation of the LBs described earlier. Figure 1.2 summarizes the role that antioxidants may play in the treatment of PD.

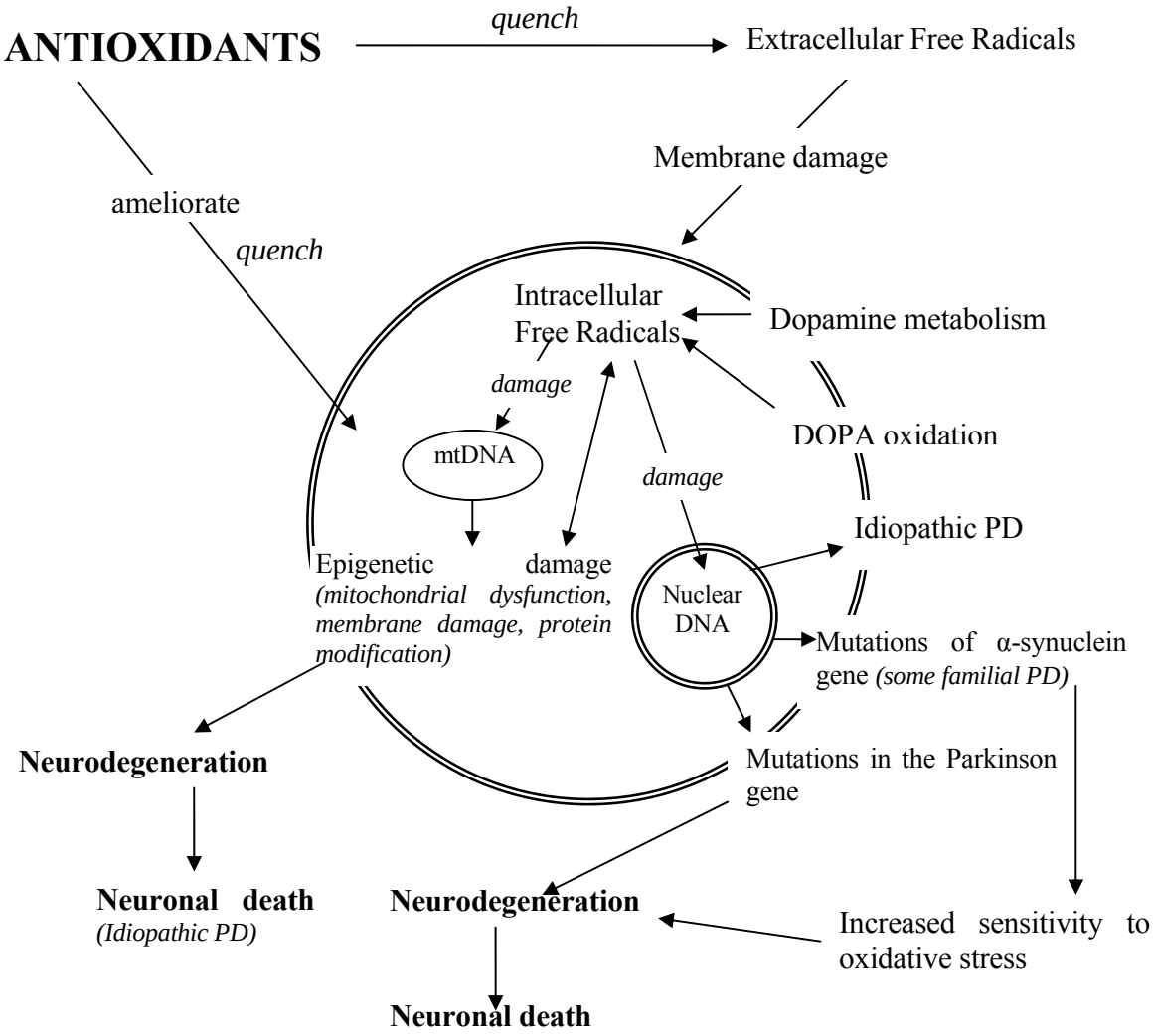

Figure 1.2: A schematic of free radical involvement as a common intermediary risk factor for many neurotoxic events in the pathogenesis of PD. Abbreviations: mtDNA: mitochondrial DNA (Source: Adapted from Prasad et al., 1999).

1.2 Current Therapies and their Limitations

There is no cure for PD, since currently available therapies can neither arrest nor reverse the progression of the disease. However, the symptoms can be managed with several different drugs. The drugs used to treat PD either boost the levels of DA in the brain or mimic the effects of DA.

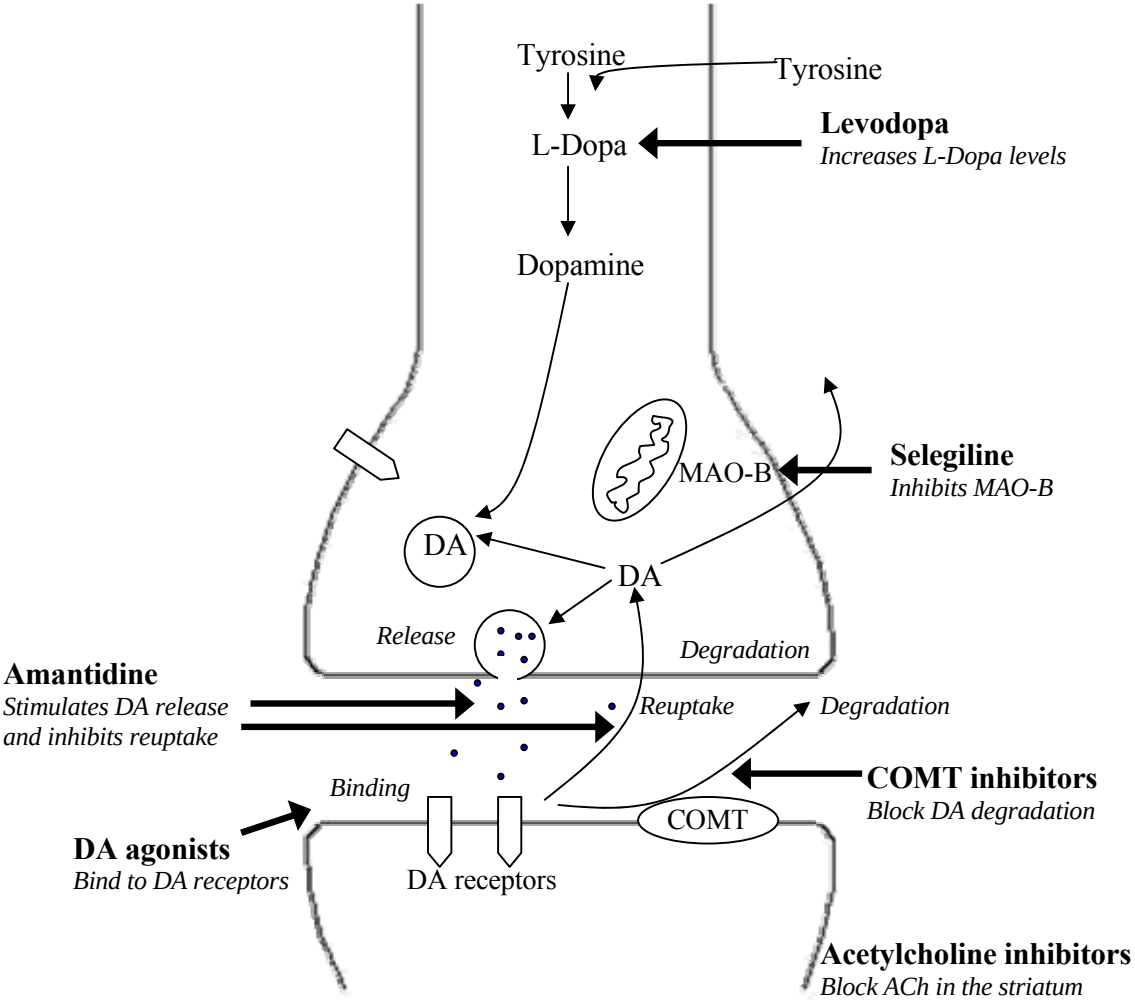

Figure 1.3: Sites of action of pharmacological therapies currently prescribed for PD (Source: Adapted from Katzung, 2001).

Most patients who begin treatment with only a DA receptor agonist eventually need to add levodopa within a few years (Silver and Ruggieri, 1998). To minimize side effects, very low doses are used initially and gradually titrated up. It is significant to mention here that exposure of patients to the 'gold standard' of PD therapy (Mercuri and Bernardi, 2005), levodopa results in fluctuations of motor responses in approximately 30-50% of patients exposed to therapy for as little as 5 or more years (Hutton and Morris, 1995). The most common fluctuation experienced is the so called 'on-off' phenomenon that results in an unpredictable transient loss of therapeutic effect (Riley and Lang, 1993). Furthermore, older patients can be particularly sensitive to the adverse effects of these drugs, which may cause symptoms of confusion, hallucinations, orthostatic hypotension and fatigue. Apart form levodopa, drugs that are currently prescribed for the management of PD include DA receptor agonists, selegiline, amantadine, catechol-O-methyl transferase (COMT) inhibitors and anticholinergics. Table 1.1 highlights the relative benefits of the currently prescribed therapies.

Table 1.1: Currently prescribed drugs for the management of PD symptoms and their limitations.

LEVODOPA	SELEGILINE	AMANTADINE	ANTICHOLINERGICS	DA RECEPTOR AGONISTS	COMT INHIBITORS
This is the key compound in the treatment of PD, acting as a precursor of DA. When levodopa is administered orally it is rapidly decarboxylated and only a small portion of the dose enters the CNS unchanged. Thus a high dose is required for the desired effect; this induces nausea and vomiting in the sufferer. Cardiac arrhythmias are also a concern for patients with a history of heart disease. It has also been linked to depression, insomnia, agitation and anxiety (Obeso et al., 2000; Olanow et al., 2004; Jankovic, 2005). In some cases dyskinesias can be so severe that they impede speech, swallowing, respiration, and balance (Koller and Hubbard, 1990). Although levodopa reduces many of the motor symptoms of PD, it does not affect non-motor symptoms (Cools, 2005) nor is it able to halt the progression of the degeneration of dopaminergic nigral neurons. Fluctuations in drug response are a common phenomenon. For many patients, however, after 4 to 6 years of therapy, there is an ever-shortening duration of response to levodopa. These so called 'off' periods are marked by severe akinesia that can extend over many hours (Brotchie et al., 2005). This commonly requires an adjustment of the dose of levodopa and "drug holidays" to allow for continuation of the therapy (Forzese, 1997; Jankovic, 2000). The optimal period for such an intervention is extremely patient specific. Even in those patients that do respond favourably, subsequent recurrences and fluctuations in the 'on-off' phenomenon are not uncommon and in many instances the beneficial effects are short lived (Olanow et al., 2004).	This monoamine oxidase B (MAO-B) inhibitor prevents the metabolism of DA in the body. As a result when used in combination with levodopa, it enhances and prolongs its antiparkinsonian effects. Thus allowing for the dose of levodopa to be reduced. Its main use is as adjunctive therapy with levodopa to allow a reduction in the fluctuating response that patients experience with its long term use. Some studies have shown that it may protect neuronal cells from the consequences of oxidative stress (Wadia et al., 1998, Am et al., 2004, Yamada and Yasuhara, 2004, Magyar and Szende, 2004; Mandel et al., 2005) and promoting the release of neural growth factors (Kontkanen and Castrén, 1999; Mizuta et al., 2000). The underlying mechanism is believed to be associated with decreased hydrogen peroxide (H_2O_2) (Magyar and Szende, 2004). Studies suggest that concurrent use with levodopa may lead to potentiated adverse effects. On its own it has been shown to cause insomnia in patients when taken later during the day. Studies do suggest that Selegiline may retard disease progression and significantly delays the need for levodopa (Cohen and Spina, 1989; Rinne et al., 1991; Macleod et al., 2005). However it has only been shown to have a mild therapeutic effect on the management of PD when used alone (Katzung, 2001).	Amantadine, an antiviral agent, was found by chance to be effective in PD. Studies regarding the current use of this agent have shown that it is particularly effective in reducing dyskinesias. These effects are thought to be mediated by its anti-glutamate action (Stoof et al., 1992). Amantadine is thought to either promote the release, prevent the reuptake or have an influence on the synthesis of DA. Its exact mechanism is however still unclear. However, amantadine has the potential to have an extremely detrimental effect on cardiovascular diseases and even induce seizures in susceptible patients (Factor and Molho, 1999). Its CNS effects include restlessness, depression, confusion and hallucinations (Katzung, 2001). Due to the nature of PD the patients that are more susceptible to the disease i.e. mainly the elderly, find these side effects to be intolerable. Its main disadvantages lies in the fact that it is less potent than levodopa and its benefits may work only briefly in some patients who have mild symptoms of the disease (Factor and Molho, 1999).	Anticholinergic medications, such as trihexyphenidyl or benztropine, are specifically effective against tremor. In a recent review from the Cochrane database, studies do not strongly support that a anticholinergic agents have a potentially better effect on tremor than on other outcome measures (Katzenschlager et al., 2003). In addition, these agents have little influence on reducing bradykinesia or akinesia (Comella and Tanner, 1995) in patients. The adverse effects of these medications often limits their dosing. Adverse effects such as fatigue, drowsiness, confusion, agitation and hallucinations, particularly in elderly PD patients are common (Katzung, 2001). Other side effects such as postural hypotension, dry mouth, blurred vision, urinary retention, nausea and vomiting, constipation, palpitations and cardiac arrhythmias may also occur. Effects on memory have also been documented as well as an increased sensitivity to dementia (Comella and Tanner, 1995). Furthermore, abrupt withdrawal leads to precipitation of acute parkinsonian symptoms.	DA receptor agonists can be divided in two main classes: the ergot derivatives like bromocriptine, pergolide, lisuride, cabergoline and the non-ergot derivatives like ropinirole, pramipexole, apomorphine or piribedil. They may be used alone to delay the need for levodopa, or may be used with levodopa to increase its effectiveness. Some studies have suggested a neuroprotective effect exhibited by these agents (Schapira, 2002a; 2002b; Schapira and Olanow, 2003; Schapira, 2003). Although these agents do demonstrate effectiveness in managing symptoms when used alone, they are riddled with side effects for the patient. While the ergot derivatives have the potential to cause psychiatric disturbances and CVS problems that can progress in certain instances to a myocardial infarction and subsequent death. Even when administered at lower doses patients experience orthostatic hypotension, constipation, dyskinesias, confusion and insomnia (Katzung, 2001; Wong et al.; .2003). The efficacy of DA agonists used as monotherapy in early stage of PD has been demonstrated in numerous studies (Clarke and Guttmen, 2002). However, as disease progresses, it becomes essential to add levodopa, to achieve a better therapeutic effect (Wong et al., 2003).	COMT inhibitors are used mainly in combination with levodopa. Examples of COMT inhibitors include entacapone and tolcapone. Once again the side effect profile cannot be dismissed. The incidence of sleep disturbances, orthostatic hypotension, dyskinesias, confusion and insomnia are common. Although tolcapone is efficacious in the control of motor fluctuations (Rajput et al., 1997), there have been increasing concerns about its safety, and in particular its potential hepatotoxicity (Assal et al., 1998) and due to this its use has been restricted in many countries. In contrast, entacapone has not been associated with changes in liver function. Entacapone in particular, provides a valuable therapeutic tool for the management of PD patients with motor fluctuations (Gershanik et al., 2003; Schrag, 2005). It is also believed that co-administration of levodopa with a COMT inhibitor in early PD patients may delay the onset of wearing off phenomenon by limiting any abrupt fluctuations in plasma levodopa levels (Gershanik et al., 2003; Schrag, 2005).

1.3 Neuroprotection as a Treatment Strategy for the Management of PD

It is estimated that the loss of dopaminergic neurons in the substantia nigra pars compacta are as much as 70-80% by the time diagnosis is made. Given this prolonged course of progressive neuronal loss, strategies aimed at reducing the rate of neuronal loss or dysfunction (i.e. clinical neuroprotection or disease-modification) are particularly important in this disorder. Effective clinical neuroprotection would importantly reduce PD-related disability for thousands of patients. In 2001, this prompted the National Institute of Neurological Disorders and Stroke (NINDS) at the National Institute of Health (NIH) in the United States of America to establish the Committee to Identify Neuroprotective Agents for Parkinson's disease or (CINAPS). This committee is aimed at identifying and conducting clinical trials of such agents that can slow the progression or prevent the onset of PD. In a review by Ravina and colleagues (2003), the authors sought to identify potential neuroprotective agents for testing in such clinical trials. They collaborated with scientist and clinicians from academia and industry as well as various patient and foundation groups in various countries to establish a broad list of potentially appropriate agents. After systematic reviews using the specified criteria they found 12 compounds to be attractive candidates for further clinical trials in PD (Table 1.2). The criteria employed during the systematic pharmacological assessment of each agent are as follows:

1. Scientific rationale
2. Evidence of blood-brain barrier penetration
3. Adequate safety and tolerability data
4. Efficacy in animal models of the disease and/or preliminary efficacy data in humans or human clinical studies

Table 1.2: Agents selected by CINAPS as potential neuroprotective agents for assessment in clinical trials for the treatment/prevention of PD.

Neuroprotective Agent	References
Caffeine	(Chen et al., 2001; Ross and Petrovitch, 2001; Checkoway et al., 2002)
Coenzyme Q10*	(Beal et al., 1998; Shults et al., 2002; Beal, 2004)
Creatine*	(Matthews et al., 1999; Tarnopolsky et al., 2001)
Estrogen	(Leranth et al., 2000; Shepherd, 2001; Sawanda and Shimohama, 2003; Morale et al., 2006)
GM-1 ganglioside*	(Schneider et al., 1998)
Minocycline*	(Du et al., 2001; Tomas-Camardiel et al., 2004)
Nicotine	(Maggio et al., 1998; Checkoway et al., 2002; Bordia et al., 2006; Quik et al., 2006)
Neuro-immunophilin A	(Gold and Nutt, 2002)
Selegiline (Deprenyl) and rasagiline	(The Parkinson Study Group, 2002; Maruyama et al., 2000; Maruyama et al., 2002; Tatton et al., 2003)
Ropinorole and pramipexole	(Schapira, 2002)

**these four compounds have been selected by CINAPS to evaluate in larger, Phase III Clinical Trials. Coenzyme Q10 has been under investigation since February 2005 (www.ninds.nih.gov/funding/research/parkinsonsweb/drug_summaries).*

While many of the discussed treatment options still remain in the primary stages of their evaluation, they all hold an immense potential to revolutionize PD therapy. The identification of several compounds with neuroprotective activity in numerous animal and human studies has lead

the progression of PD research towards the development of drug delivery systems that can deliver these agents via mechanisms that can minimize side effects for patients and optimise compliance. The therapeutic potential for the development of such drug delivery systems for neurodegenerative diseases has been emphasized in a review by Popovic and Brundin (2006). They have particularly emphasized the need to develop systems that can provide controlled delivery in a site-specific manner to the brain. Particular attention has been directed at biodegradable polymeric systems. The review provides significant insight into the importance of the site of administration as an essential factor dictating the efficacy of the intended system.

One of these 12 neuroprotective agents selected by CINAPS is the tobacco alkaloid nicotine (Table 1.2). For the purposes of our study it was selected as the model neuroprotectant agent to incorporate into the proposed drug delivery system. It represents a unique challenge to incorporate into a drug delivery system intended for prolonged release due to its hydrophilicity and low molecular weight.

1.4 Nicotine as a Neuroprotectant for PD

The potential application of the principal alkaloid in tobacco, nicotine as a neuroprotectant in PD was demonstrated as far back as 1926 (Moll, 1926). More recent studies have also shown that it plays a role in the prevention of age-related dementias. PD has been one of the diseases given much attention (Morens et al., 1995; Tzourio et al., 1997; Tanner et al., 2002). The results have shown that nicotine does indeed have a positive impact in preventing the degeneration of neurons involved in PD (Gorell et al., 1999; Rusted et al., 2000; Quik, 2004). Studies have demonstrated a

marked reduction in cortical nicotinic receptor binding that parallels the degree of dementia in PD (Newhouse and Kelton, 2000; Newhouse et al., 2004). Nicotine, a nicotinic receptor stimulator evokes the release of DA from the striatum and therefore protects the nigrostriatal neurons from degeneration (Rusted et al., 2000). The mode of its addiction is also a possible identification of this mechanism. A study conducted by Clarke and colleagues (1988) demonstrated that nicotine's ability to activate dopaminergic release in the mesolimbic cortical neurons, that mediates its reward effects, produces a dependant locomotor (possibly striatal) stimulation. Furthermore, it has also been shown that nicotine is able to act as a free radical scavenger (Quik and Kulak, 2002; Obata et al., 2002) and participate in iron complexation (Soto-Otero et al., 2002; Bridge et al., 2004) thus prevent lipid peroxidation and subsequent neuronal degeneration. Studies have shown a significant improvement in the patient's mental attentiveness, body control in walking and the use of hands, and reducing anxiety shortly after initiating therapy (Prasad et al., 1994; White and Levine, 1999; Quik and Kulak, 2004). Schneider and co-workers (1998) conducted a study in non-human primates, which demonstrated that the co-administration of a nicotinic agonist with a lower levodopa dosage resulted in an improvement in parkinsonism similar to that seen with a higher levodopa dosage, although it led to a decline in motor complications such as dyskinesias.

The mechanism of its action is under much debate and investigation. Studies have indicated that this action of nicotine is mediated by the activation of presynaptic nicotinic $\alpha_4\beta_2$ and α_7 receptors located on the dopaminergic nerve terminals in the corpus striatum (Quik and Jeyarasasingam, 2000; Belluardo et al., 2000; Matsubayashi et al., 2004; McCullam et al., 2005; Quik and McIntosh, 2005; Bordia et al., 2006; Quik et al., 2006). It has been proposed that it acts on the mRNA subunits within the dopaminergic terminals in the substantia nigra pars compacta (Visanji

et al., 2005). It has also been shown that nicotine directly induces the neuroprotection of dopaminergic neurons in the substantia nigra by stimulating the release of the neurotrophic fibroblast growth factor-2 (FGF-2) (Maggio et al., 1998). The additional effects of nicotine in the brain, such as its ability to selectively stimulate glucose utilization in cerebral neurons (that in turn stimulates striatal, cortical and mesolimbic activity) (London, 1990), inhibit brain MAO-A enzymes (Fowler et al., 1998) as well as its ability to enhance the production of pituitary hormones, of particular significance, ACTH, which stimulates cortisone production (Fuxe et al., 1990) may also shed light on its mechanism of action.

However, this does not justify patients to smoke in order to prevent the disease. Any benefits from nicotine in cigarettes or other tobacco products are far outweighed by the proven harm of using such products. Hence, the approach taken to deliver nicotine to the patient is consequently vital and must be addressed. Despite the fact that the research supporting the neuroprotective effects of nicotine is overwhelming, designing a novel system for its modulated delivery may have many merits. Thus far no such system has been developed.

Although transdermal patches have been effective for smoking cessation, some studies have shown contradictory findings regarding their use in PD. Patients often fail to comply with this treatment due to the unwanted side-effects, primarily nausea and gastrointestinal disturbances. The low tolerability may be related to a lack of specificity of nicotine, which would directly stimulate the autonomic nervous system (Lemay et al., 2003; Lemay et al., 2004). Nicotine gums and sprays also have benefits; however are accompanied by similar side-effects as the patch. While the patch and gum are unaesthetic, nasal sprays often lead to nasal congestion and rhinorrhea. The patch also has

a notorious reputation for causing severe skin irritation indicated by reddening, pruritis and oedema in the area of application (Gourlay et al., 1999).

Figure 1.4 summarizes the possible mechanisms by which nicotine may elicit its neuroprotective effects in the brain for the prevention of PD.

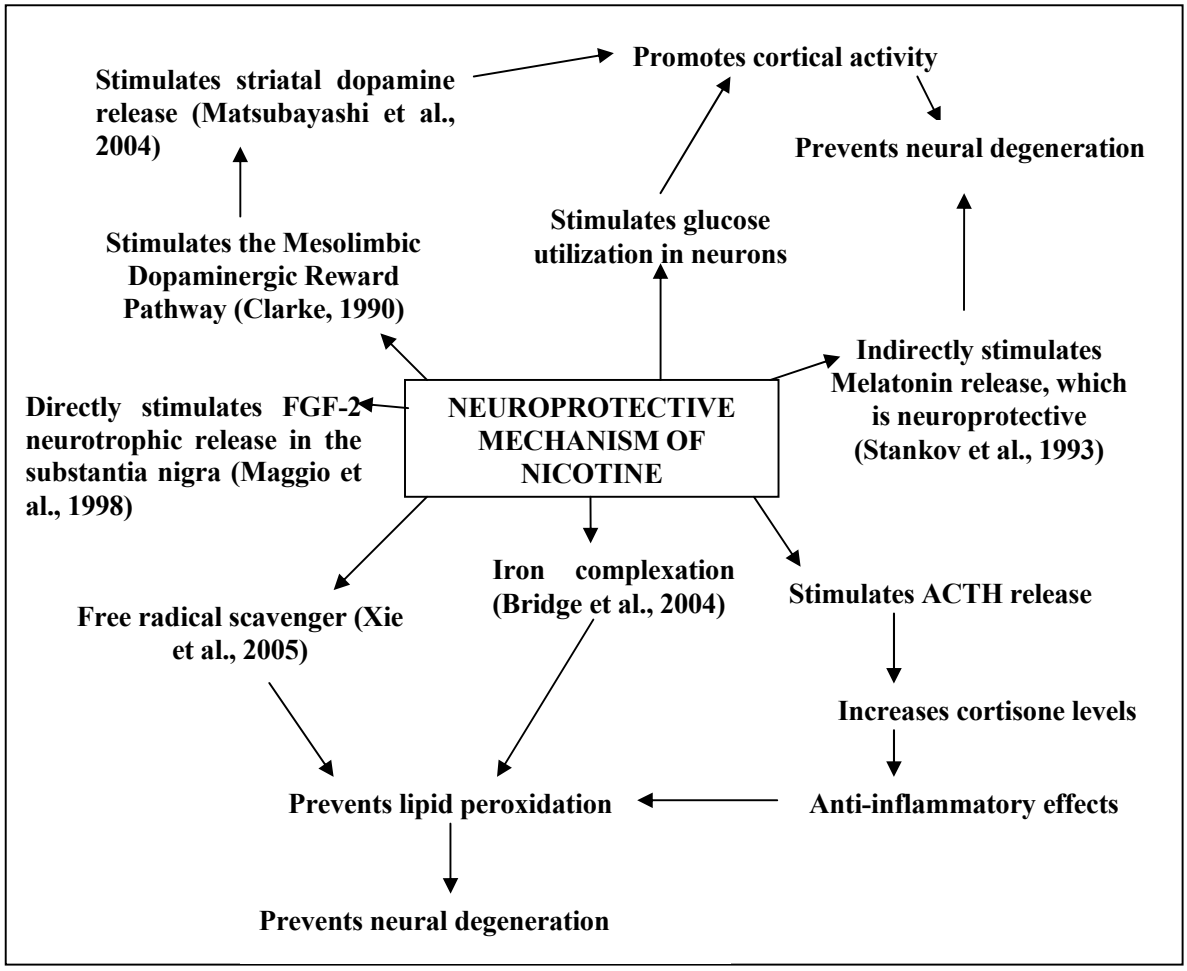

Figure 1.4: Proposed neuroprotective mechanisms of nicotine in the brain involved in preventing the onset and progression of PD.

For the purposes of this study nicotine has been considered as the model neuroprotectant to be delivered through a novel reinforced crosslinked multi-polymeric multi-unit drug delivery device.

To date, no such device exists for application in PD. Current means of delivering nicotine in pilot studies have demonstrated poor compliance due to the unwanted peripheral side effects (Lemay et al., 2003; Lemay et al., 2004). Thus site-specific delivery would enable elimination or attenuation of the aforementioned side-effects if nicotine is restricted to its site of action, the CNS.

1.5 Challenges Associated with Drug Delivery to the Brain

Despite the fact that knowledge regarding the molecular biology and cellular physiology of the brain has advanced at a rapid pace, much remains to be learned about delivering drugs and pharmaceuticals for the diagnosis and treatment of central nervous system (CNS) diseases. Neural activity in the brain requires precise regulation of the neural microenvironment as well as basic physiological processes including, delivery of nutrients, removal of waste, protection from toxic substances circulating in the blood and maintenance and repair processes. Sites where blood comes into contact with neural tissue are crucial interfaces known as the blood-brain barrier (BBB) and are important in creating the optimal environment for efficient neural activity through a variety of barrier mechanisms (summarized in Table 1.3). The BBB creates the largest 'barrier interface' with respect to its surface area (12–20 m^2/1.3 kg brain) in the body and has the most significant impact on drug delivery of neuroactive agents to the brain (Abbot et al., 2006).

Table 1.3: Properties of the BBB which limits delivery of neuroactive agents to the CNS (Source: Adapted from Abbot et al., 2006).

Blood Brain Barrier	Properties
Tight junctional structure	Tight junctions are a physical barrier. The tightness of the BBB appears not only from the physical complexity of its junctional structure, but also from the numerous transmembrane particles which, create an astomising dense network. Transmembrane proteins known as claudins, assist in sealing the intercellular spaces and enforce selectivity. The claudins function within a complex network of other transmembrane and cytoskeletal proteins linked to the actin cytoskeleton, which imposes adhesion between the junctions thus provides additional structural strength to the BBB. The result is a strong and restricting inter-cellular connecting region that extends around the endothelial cell margin severely restricting penetration of polar hydrophilic molecules through this paracellular pathway. Thus molecules employ a transcellular pathway across the brain endothelium to enter the BBB.
The nature of the endothelial cell membrane	The endothelial cell membrane influences passive drug permeability. Like all cells, the brain endothelium possesses an outer cell membrane composed of a lipid bilayer with embedded proteins. Small gaseous molecules such as oxygen and carbon dioxide can diffuse freely through the membrane, enabling oxidative metabolism of the brain and facilitating its pH regulation. The majority of drugs used to treat the CNS are lipophilic and thus easily diffuse through the endothelial membranes. Lipid analysis of the brain endothelium shows a high cholesterol content. The apparent average optimum molecular weights are approximately < 280Da and lipophilicity Log$P_{octanol}$ < 2.0. However these values can vary depending on the therapeutic activity of the neuroactive agent.
Uptake transporters	The paracellular pathway for small molecules between the blood and brain in comparison to peripheral vasculature is severely restricted. Thus, where transfer is required, it must be assisted by specific transport systems known as uptake transporters which are located in the endothelial membranes. Many BBB transporters facilitate transfer without requiring energy by allowing solute to move down an electrochemical gradient, while others require energy to transport against a gradient, either actively derived from ATP or through coupling mechanisms to develop favourable concentration gradients. Some transporters are located on both the luminal and brain-facing membranes of the endothelium (bidirectional), while others are localised predominantly to one or other membrane, allowing directional (vector-mediated) transport to occur.
Transcytosis	This can either be receptor- or adsorptive-mediated. As stated previously, some uptake transporters on the brain endothelium may function bidirectionally, thus also permit efflux. However, in addition, several families of transporters have been identified that are capable of actively transporting solutes out of the brain endothelial cells (often with the consumption of ATP). They restrict the CNS entry of a number of potentially harmful or toxic agents circulating in the blood, and are thought to have other housekeeping functions. They have a particular significance for drug delivery, since they can effectively block or reduce entry of lipophilic drug molecules.
Efflux transporters	Most membrane transporters are able to transport only small molecules (< 1000Da) due to the spatial and energetic requirements of the substrate-to-transporter docking sites and transfer mechanism. Larger molecules such as polypeptides and proteins can be transported across the BBB through vesicular routes. Of the two mechanisms that have been identified, one requires specific interaction with a membrane receptors followed by endocytosis and receptor-mediated transcytosis. The other is less specific, by which cationic molecules can bind to the surface negative charges of the endothelial glycocalyx and be internalised and transferred: adsorptive-mediated transcytosis.
The enzymatic barrier	Further metabolism, particularly in the cells of the BBB, specifically the brain endothelium and the choroid plexus significantly affect pharmacokinetics and bioavailability of neuroactive agents. Both sites express a range of Phase I, II and III enzymes. Due to the selectivity of the reactions, the influence of brain endothelial enzymes has to be considered exclusively for each potential neuroactive agent.

The ability to deliver these molecules systemically to the brain is impeded by several factors including their degradation and metabolism, either by relative short half-lives of the molecules, or metabolic degradation by the liver prior to reaching the CNS as a target site. Furthermore, the near-impermeable BBB presents as a protective cellular barrier and is the chief site regulating molecular transfer between the blood and brain (Table 1.3). It is made up of tightly bound brain endothelium, has low passive permeability combined with a highly selective transport system, and therefore poses a significant obstacle for the delivery of many neuroactive factors. A number of strategies have been developed to circumvent the selective BBB. Some of the techniques currently available for the delivery of neuroactive factors to the brain for PD include:

1. Trans-cranial brain delivery
    a. Direct infusion with stereotactic guidance
    b. Osmotic pumps
    c. Controlled- and/or sustained-release polymer systems
2. Trans-nasal brain delivery
3. Disruption of the BBB
    a. Carrier- or receptor-mediated transcytosis
    b. Osmotic opening
4. Small molecule lipidization

However, depending on the intended application, the systems offer various advantages and disadvantages with their use (Bodor 1992; Lossinsky et al., 1995; Tamai and Tsuji, 2000; Bodor and Buchwald, 2003; Guerin et al., 2004; Begley, 2004; Huynh et al., 2006; Siepmann, 2006; Popovic and Brundin, 2006; Pardridge**,** 2007).

In recent years, biopolymer based systems for the delivery of bioactive agents have gained considerable attention due to their established biodegradability and biocompatibility, excellent mechanical strength and controlled release profiles.

Furthermore, controlled release systems remain in direct and sustained contact with the tissues, and some of them degrade *in situ*. In such a case, both the polymeric material itself as well as its degradation products must be free from toxicity. For devices implanted into the body, the classical retaliatory tissue response to a foreign material (e.g. an implant) leads to its encapsulation. This may impede diffusion of the drug to the surrounding tissue and result in failure of the device. This tissue response depends on different factors, in particular, on the implantation site (Fournier et al., 2003).

1.6 Implantable Therapeutic Systems

Historically the first implantable devices formulated for therapeutic use to deliver medicaments for sustained and controlled release were developed by Lafarge in 1861 (Chien, 1987). Subsequently systems have been developed to release a variety of drugs. The development of biopolymer based implantable pharmacotherapeutic systems however is as recent as the late 1960s with the discovery of lipophilic silicone-capsules (Chien, 1987). Among the factors that were modulated to control drug release included the thickness and surface area of the silicone-capsules as well as the polarity of the entrapped medicament. This research has led to the formulation of numerous commercial products to provide a mechanism to administer drugs in a controlled and long-term manner. Gaginella and Bass (1974) employed the abovementioned silicone capsules to provide chronic

administration of nicotine *in vivo*. However, the primary disadvantage of such a system is that this modified silicone capsule is not biodegradable. This implies that following implantation, a second surgery is required to remove the device from the body. Furthermore, mechanical damage to the device or the empty (devoid of drug after its release) capsule can result in the accumulation of potentially toxic particles in the body. The development of biocompatible biodegradable polymers for sustained release implantable systems therefore has received significant focus.

Among the various advantages described in a review by Langer (1983), implantable polymeric devices have the capacity to optimise drug therapy and offer the following benefits to patients:

1. Plasma drug levels are consistently maintained within the therapeutic window;
2. Site-specific administration which can eliminate or attenuate peripheral adverse effects;
3. Prolonged-release systems improve patient compliance by allowing a significant reduction in dosing frequency;
4. They allow for the administration of drugs with short *in vivo* half-lives and the achievement of sustained plasma levels with minimum fluctuation, predictable and reproducible release rates for extended durations;
5. Implantable systems are more cost-effective long-term;
6. They allow for dose reduction since the drug can be administered to the site of action to regions in the body that are poorly perfused, such as the CNS;

Several advances in this area of research have been made to develop systems that display the ability to deliver drugs in a site-specific manner to tissues that can be activated by a variety of mechanisms including magnetic and electrical fields (Hsieh et al., 1981; Edelman et al., 1985;

Kwon et al., 1991; Furukawa et al., 2003; Zebli et al., 2005), vapour and osmotic pressure (Alzet® Osmotic Pump), pH (Siegel et al., 1988), enzymes (Fischel-Ghodsian et al., 1988), ultrasound (Kost et al., 1989; Kost, 1993), light (Mathiowitz and Cohen, 1989) and temperature (Hoffman et al., 1986; Bae et al., 1987; Furukawa et al., 2003; Lendlein et al., 2005; Ohya et al., 2005).

1.7 Rationale and Motivation for Study

To date PD remains an incurable disease, afflicting growing numbers of individuals. Organizations such as CINAPS have realised the importance of preventative treatments in the form of neuroprotective agents in the field of PD therapy and have devoted due attention to their potential role as future treatments for the disease. It is recognised that patient compliance with regards to drug therapy; particularly with neurodegenerative diseases is a significant concern for treatment success with the elderly (Grosset et al., 2005). This study aimed to develop a novel drug delivery system with the intent to bridge the discrepancy associated with optimising drug therapy and patient compliance for chronic neurodegenerative diseases such as PD. This study focused on the elucidation of the *in vitro* pharmaceutical benefits of developing a prolonged drug delivery system for neuroprotective agents. Nicotine was selected as the model neuroprotective agent to be delivered in the formulated system. A novel delivery system of this nature has thus far not been developed. It must be emphasised here that the device was intended to be versatile to deliver a range of neuroprotective molecules. Nicotine, being a small molecule with appreciable water solubility was a challenge to confine within the system to achieve the desired zero-order sustained release characteristics, hence displayed the potential that the device demonstrated for the delivery of other neuroprotective agents.

A device providing prolonged modulated release will allow patients to have as little exposure to dose-dependent adverse effects based on the attainment of steady-state blood levels and minimizing the fluctuations in plasma concentration through zero-order drug release kinetics. Developing a system with the capacity to provide site-specific delivery into the substantia nigra pars compacta in the brain would minimise peripheral accumulation of therapeutic agents and thus prevent unnecessary side-effects. The device would be developed employing biodegradable polymers so that only a single surgical minimally invasive procedure would be required.

The polymeric system would need to have the capacity to deliver small molecular compounds such as the proposed neuroprotective agent; nicotine over a period of a 1-2 months hence necessitated the investigation of a unique combination of polymers reinforced with crosslinking agents to develop a compact network which would disintegrate gradually *in situ* when exposed to cerebrospinal fluid (CSF) in order to release nicotine. This involved an investigation and understanding of the following factors:

1. The factors influencing the ability of the reinforced polymeric system to entrap drug (drug entrapment efficiency) and modulate drug release
2. The physicomechanical properties and viscoelastic behaviour of the device when exposed to simulated CSF and the mechanics of its degradation.

This study is the first to develop a reinforced crosslinked multi-polymeric multiple-unit device for the delivery of nicotine for PD therapy.

1.8 Aim and Objectives of This Study

The aim of this study was to focus on the *in vitro* development and evaluation of a novel prolonged release system for newly researched neuroprotective agents. As mentioned previously, the device was intended to be one that provides zero-order prolonged release of nicotine over a period of 1-2 months. The device was formulated such that its design was in keeping with the potential for implantation into the substantia nigra pars compacta in order to provide site-specific drug delivery. In order to do so, polymers with biocompatible and bioerodable characteristics were selected to entrap the drug within a reinforced crosslinked matrix.

In order to accomplish this aim the following objectives were outlined:

(i) Selection of an appropriate polymer combination based on the evaluation of the physicochemical and physicomechanical properties.

(ii) Application of ionotropic gelification in accordance with Design of Experiments approach to assimilate a multiple-unit polymeric structure reinforced with a suitable polymer(s) and crosslinking agents.

(iii) *In vitro* evaluation of the polymeric device in terms of its textural rigidity, gelation mechanism, erosional capacity and dissolution behaviour.

(iv) Elucidation of the molecular assemblage through enthalpic techniques and Fourier transform infrared (FTIR) spectroscopy.

(v) Kinetic modelling of drug release.

1.9 Synopsis of Dissertation

This dissertation is structured such that it provides a logical approach to present the research conducted in keeping with the aforementioned aims and objectives, while highlighting the various avenues investigated to modify nicotine release during the study.

The First Chapter provides an overview of Parkinson's disease, the lack of any effective treatments for the disease and the limitations of currently prescribed therapies. Studies being conducted on newer treatment options such as the use of neuroprotective agents are also discussed. Particular emphasis has been placed on the role of the alkaloid nicotine, which was employed as the model neuroprotectant for the proposed drug delivery system. An overview of the challenges associated with drug delivery to the brain elaborated on the hurdles that were considered when developing the reinforced crosslinked multi-unit device. Implantable devices previously and currently developed for site-specific delivery of neuroactive agents highlighted the rationale for the proposed study. The chapter summarizes the aims and objectives of the study which were achieved.

Chapter Two discusses the properties of alginate, the biopolymer selected to develop the drug delivery system. The influence of various formulation parameters on the physicomechanical and physiochemical properties of ionotropically crosslinked alginate spheres (gelispheres) were evaluated employing textural analysis. The influence of monomeric ratios within the copolymer and crosslinking agents, namely, zinc, calcium and barium was evaluated to select the appropriate alginate grade to incorporate nicotine.

Chapter Three presents the three phase approach adopted for the development and optimisation of the reinforced multi-polymeric gelispheres. An overview of the two polymers, hydroxyethylcellulose (HEC) and polyacrylic acid (PAA) which were incorporated into the alginate gelispheres as reinforcing agents is provided. Three crosslinked agates are discussed, namely zinc, calcium and barium. Studies demonstrated that zinc-crosslinked gelispheres generated formulations which disintegrated easily following exposure to simulated cerebrospinal fluid (CSF) (0.1M PBS; pH 7.4; 37ºC; 50rpm), hence it was not employed for the second phase of the study. The first phase elaborates on the role of the aforementioned crosslinked agents and the influence of post-curing exposure to dilute hydrochloric acid (HCl) on the erosional properties of the multi-polymeric gelispheres. The second phase involved adoption of a Design of Experiments approach through a Plackett-Burman screening design to elucidate the influence of 5 independent formulation variables, namely the concentrations of the three polymers; alginate, HEC and PAA and the crosslinking agents, barium (primary crosslinker) and calcium on the drug entrapment efficiencies and drug release behaviour of the gelispheres. The final phase involved conducting optimisation studies of the multi-polymeric gelispheres following which the optimised system was exposed to dilute HCl post-curing in order to attenuate the rate and extent of gelisphere swelling and erosion following exposure to simulated CSF. FTIR and enthalpic techniques were employed to elucidate the interactions between the polymers and nicotine on a molecular level. While the multi-polymeric barium-calcium-crosslinked system developed exhibited characteristics whereby it retained its integrity for durations which, far exceeded the native alginate gelispheres studied in Chapter Two, zero-order release was not achieved. Thus approaches to further prolong drug release were investigated.

Chapter Four investigates the incorporation of the optimised gelispheres from Chapter Three into compressed external polymeric matrices (discs). Three polymers were selected to formulate the discs, namely hydroxypropylmethylcellulose (HPMC), polyethylene oxide (PEO) and poly(lactic-co-glycolic) acid (PLGA). Various polymer blends were formulated to elucidate the degradation and erosional behaviour of the compressed discs following exposure to simulated CSF. Drug release studies demonstrated zero-order release for 50 days from PLGA discs incorporating optimised gelispheres. Finally, kinetic analysis of drug release from the multi-units was undertaken employing FDA-recommended f_1 and f_2 similarity and difference factors.

Chapter Five presents the results for the study which investigated the first alternative approach employed to modify nicotine release. This involved formulating PLGA-coated compressed polymeric discs, which incorporated calcium-crosslinked alginate-HEC gelispheres.

Chapter Six investigates the role of crosslinked alginate and pectin gelispheres as a means to deliver a polylactic acid (PLA) and PLGA microparticulate system incorporating nicotine. A Box-Behnken statistical design was employed to formulate the microparticles through an oil-in-oil (O/O) phase separation process. Three factors were evaluated, namely polymer type, stirring time and concentration of the surfactant, Span 80. Artificial Neural Networks (ANN) was also employed using a Generalized Feed Forward algorithm, as a simultaneous optimisation technique. Optimised microparticles were incorporated into alginate-pectinate gelispheres (double entrapment) to formulate a polyspheric crosslinked system.

The concluding chapter emphasises significant parameters regarding the multi-polymeric multi-unit systems developed and provides recommendations for future studies in terms of the versatile means of adapting the developed system for alternative neuroprotectant agents.

1.10 Potential Benefits of This Study

The development of the proposed reinforced crosslinked multi-unit device providing prolonged site-specific delivery of neuroprotectants such as nicotine will enable PD patients to receive preventative treatments through a means that will provide the various benefits. The most significant advantages of the system include enhanced patient compliance and improved therapeutic success. Elderly patients form the majority of those afflicted with the disease. It has been widely established that compliance to treatments in this patient group is a significant hurdle with regard to therapeutic success (Dipiro, 1999). Through the use of a prolonged release device we can provide patients with administration at extended intervals and enable them to achieve the optimal benefits of the treatment. Furthermore the attainment of sustained drug levels of the administered neuroprotectants will enable improved therapeutic success, since it will maintain drug concentrations at the site of action (the brain) within the therapeutic window. This translates into better product tolerability and minimization of unnecessary peripheral adverse effects.

Developing the proposed device also enables the formulation of a unique polymeric drug delivery system and the formulation of technology that is entirely novel in this field. This study allows the elucidation of new mechanisms of interaction between a composite crosslinked multi-unit multi-polymeric device and biodegradable matrix reinforcers. The developed system serves as a platform

for the future development of and formulation of novel crosslinked prolonged release implant for the encapsulation of newly studied and/or developed neuroprotectants. Finally due to the fact that the proposed system seeks to employ simple formulation procedures which expose the incorporated molecules to minimal degradative factors, such as extremes of temperature and pH implies that a variety of bioactive molecules or entities (such as proteins and cells) can be delivered through the proposed system. Such a versatile platform can provide a means of delivering bioactives through ideal zero-order release.

Chapter 2

Elucidation of the Properties of Crosslinked Alginate Gelispheres as a Platform for Drug Delivery through Physicomechanical Analysis

2.1 Introduction

The polyanionic algal polysaccharide alginate was employed to formulate the proposed drug delivery system. Alginate is a biocompatible and biodegradable glycosidic copolymer which undergoes instantaneous crosslinking in the presence of divalent cations by a process known as ionotropic gelation. This process has been widely used commercially since the conditions under which gelispheres are formulated are mild, usually conducted at room temperature and in an aqueous medium. This rapidly occurring process is both simple and cost-effective, therefore allows for easy scale-up and large-scale manufacture. Crosslinked alginate spheres, referred to as gelispheres, have found wide application in the field of pharmaceutical drug delivery. The term 'gelisphere' was coined by Pillay and coworkers (2002). It refers to an ionically crosslinked polymeric spherical matrix, prepared by ionotropic gelation. Such an entity has the capacity to undergo a process known as gelation, which involves the polysaccharide polymer imbibing water from a surrounding hydrating medium (e.g. physiological fluid or buffers) swelling, and undergoing polymeric disentanglement and resulting in subsequent matrix degradation.

Alginate is a natural polysaccharide extracted from a variety of brown seaweed, each of which produces a variant of the copolymer with specific characteristics dependant on its monomeric

constituents. Alginates differ in terms of their viscosity and the ratio of monomeric units, namely the 1,4-linked sugars, β-D-mannuronic acid (M) and its C-5 epimer α-L-guluronic acid (G). These units are arranged in homopolymeric blocks (GG and MM) interspersed with regions where the monomers alternate (MG) (Smidsrød and Draget, 1996; Draget et al., 2002). The chemical structures of the polymer and its constituent monomers are represented in Figure 2.1.

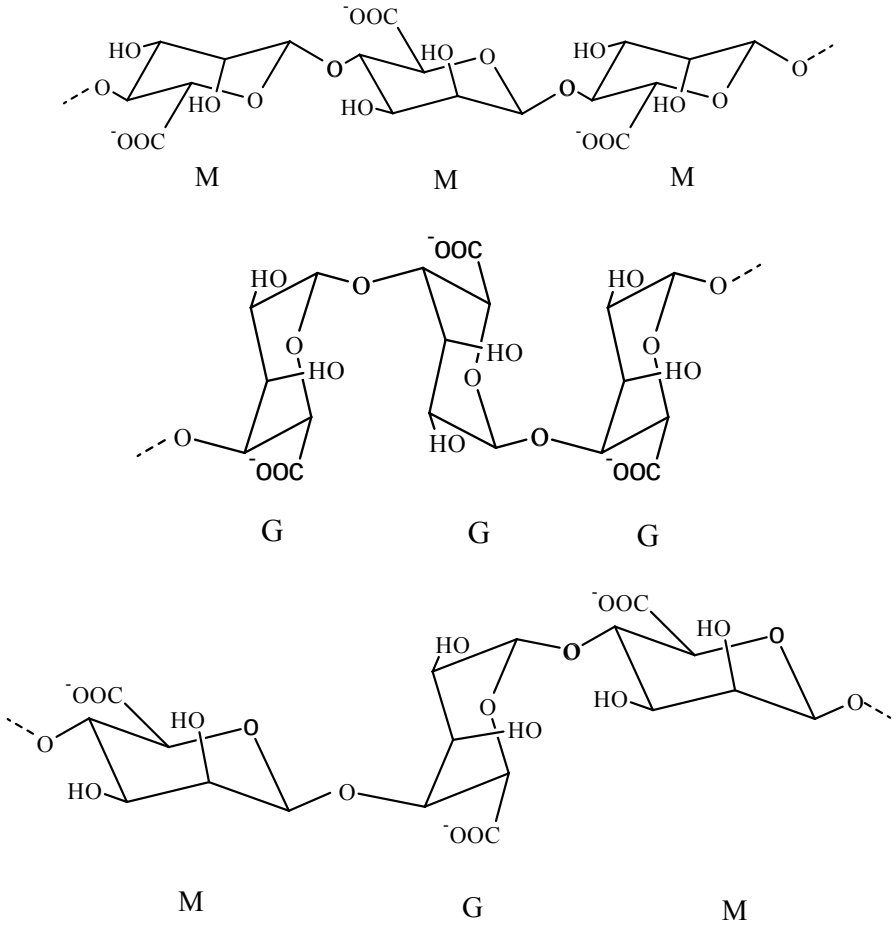

Figure 2.1: Chemical structure of alginate and its monomers mannuronic acid (M) and guluronic acid (G). (Source: Draget et al., 2003).

Alginate undergoes instantaneous crosslinking in the presence of divalent cations such as calcium and zinc (Yotsuyanagi et al., 1987), but not with magnesium or other monovalent cations

(Sutherland, 1991). The resultant matrix represents a hydrogel i.e. a polymeric network capable of absorbing, swelling and retaining large quantities of water within their hydrated matrices without rapid dissolution or loss of their three-dimensional networks (Hoffman, 2002). Gelling induced by specific cations is indicative of an interaction between the crosslinking ions that produces a conformational change in the polymer. G-units exist as associated crystalline aggregates in the form of a two-dimensional ribbon-like structure. The 'ribbon' contains electronegative cavities, which when interacting with divalent cations, entrap them within the cavities in an 'egg-box' arrangement (Grant et al., 1973) (Figure 2.2). This association allows for the formation of a three-dimensional gel network with intra-polymeric bonding occurring in conjunction with cation stabilization of G-chains.

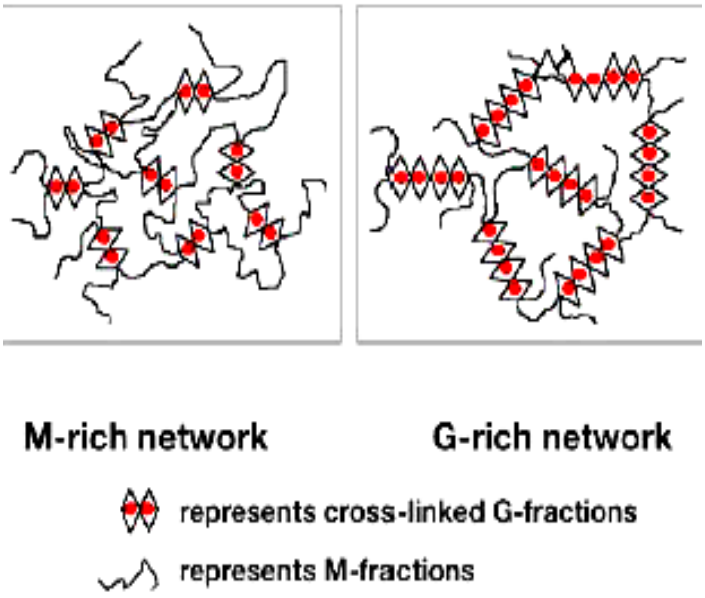

Figure 2.2: Chemical structure of alginate and its monomers guluronic acid (G) and mannuronic acid (M) in an 'egg-box' arrangement when crosslinked with divalent cations (depicted by the red circles in the diagram) (Source: FMC BioPolymer Novamatrix, CRS Conference, 2005).

M-units have a unique mechanism of interaction between their carboxyl groups and the divalent crosslinking cations; however they produce weaker bonds (Draget et al., 2003). The physical properties of the developed hydrogel are consequently a direct function of factors such as the monomeric composition, sequential structure, molecular mass, nature of crosslinking agent, the presence of chelating agents that bind with crosslinking ions, concentration of non-gelling ions and the presence of a strengthening polycationic coat (Kong and Mooney, 2003). Studies have indicated that a general trend of superior mechanical strength is demonstrated by G-rich alginates due to preferential binding of divalent crosslinking cations such as calcium to these monomeric units (Smidsrød and Skjåk-Bræk, 1990; Kuo and Ma, 2001). The GG-block exhibits a high selectivity for crosslinking cations depending on the structural orientation of the GG-blocks in the polymeric substrate which in its stereo-chemical orientation provides a cavity like space for cations to sit in easily in a thermodynamically stable stereo-orientation. The cations and water molecules utilize the area in accordance with the fast developing crosslinking polymeric matrix and determine the final stereo-chemical orientation of the resultant filled cavity (Draget et al., 2003). This is illustrated in Figure 2.3. The larger size of the crosslinking cation generates a smaller space for hydrated ion clusters and therefore fewer water molecules can be accommodated within the filled cavity (Draget et al., 2003). Thus it provides more stability to the polymeric backbone. This is discussed in greater detail in later sections.

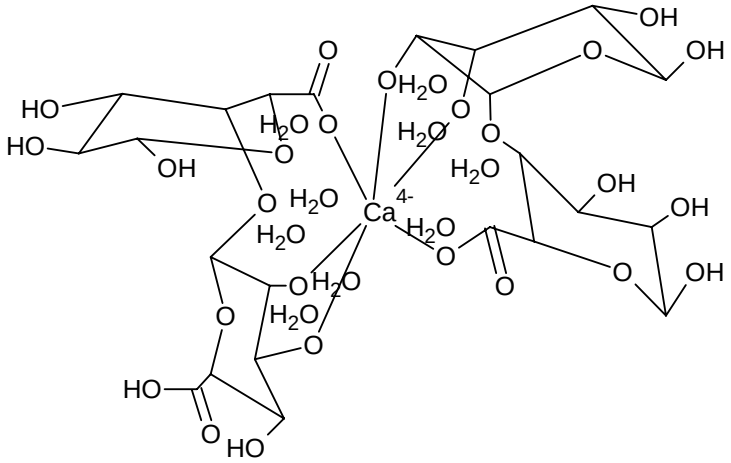

Figure 2.3: A calcium ion packed in a GG pocket between two alginate strands. Crosslinking between the carboxyl ends of the saccharide units alters the stereochemistry of the two approaching pockets considerably. (Source: Adapted from Al Musa et al., 1999).

The development of novel crosslinked gelisphere systems of alginate has been viewed as a possible means to deliver a variety of pharmaceuticals (Gombotz and Wee, 1998). Alginates are an ideal medium for pharmaceutical delivery. In particular site-specific delivery to mucosal tissue for localized action is a possibility due to the fact that alginates are bioadhesive. Commercially available preparations of alginate films and fibres have exploited this characteristic and have found extensive application as protective surgical wound dressings (Gilchrist and Martin, 1983). Moreover, it is biocompatible, biodegradable and freely permeable to small molecules, such as oxygen, nutrients and small proteins (Gombotz and Wee, 1998; Leonard et al., 2004) which is an ideal environment to entrap and deliver among other pharmaceutical products, viable cells (Gombotz and Wee, 1998; Krasaekoopt et al., 2004). Other commercial uses of alginates are listed in Table 2.1.

Table 2.1: Commercial uses of alginates. (Source: Whistler et al., 1953).

Commercial Use	Examples of Applications in Field
Medical	Sulphonated alginic acid is an anticoagulant, pharmaceutical drug delivery, surgical uses, dental impression material
Cosmetics	Water soluble colloids in lotions, toothpastes and 'grease-free' creams
Food	Ice cream stabilizer, cheeses, whipping cream, thicken soups and sauces etc.
Other	Used to remove small quantities of metals from solution. This property allows it to be used to soften water

Furthermore, the conditions under which gelispheres are formulated are mild, usually conducted at room temperature and in an aqueous medium. This rapidly occurring process is both simple and cost-effective. It has been successfully employed for the delivery of sensitive drugs (Badwan et al., 1983; Hari et al., 1996; Tonnesen and Karlsen, 2002; Ueng et al., 2005), proteins (Kim and Lee, 1992; Xing et al., 2003; Leonard et al., 2004), DNA (Smith, 1994; Alexakis et al., 1995), living cells (Smidsrød and Skjak-Braek, 1990; Orive et al., 2002; Koch et al., 2003; Serp et al., 2005), spermatozoa (Torre et al., 2000) and genes (You and Peng, 2005).

Drug release from alginate gelispheres is directly related to matrix pore size if present and the rate at which matrix degradation occurs when the system is exposed to hydration. The mechanical transformation incurred by the polymeric matrix following exposure to hydration further determines the rate at which drug release occurs over time. Such data allows for the prediction of the duration for which the gelispheres will be intact within the body subsequent to administration (Bajpai and Tankhiwale, 2006).

While most alginate delivery systems have focused their attention on employing zinc and calcium as a biocompatible crosslinking agents that can adequately interact with the polymer; more recent studies have demonstrated the potential offered by agents such as barium on controlling drug delivery through its unique mechanism of interaction with the polymer (Bajpai and Sharma, 2003). While the choice may seem controversial due to potential biocompatibility problems, as has been pointed out in a study conducted by Bajpai and Sharma (2003), the barium released from alginate matrices (a process known as sequestration which occurs through an exchange with sodium ions in buffer/physiological fluids such as cerebrospinal fluid (CSF) which, discussed in the following chapter), when exposed to physiological environments, it immediately interacts with phosphate ions to form barium phosphate, thus preventing any interaction with body tissues. This study aimed to establish the influence of barium, calcium and zinc on the physicomechanical properties of crosslinked alginate gelispheres in their unhydrated and hydrated states in order to elicit their potential role in pharmaceutical delivery systems.

The influence of hydration on the swelling behaviour and subsequent degradation of the gelispheres is a direct function of their mechanical strength. Since our aim was to develop a system that has prolonged release kinetics, we sought to establish the most thermodynamically stable stereo-orientation possible within the crosslinked system by employing a range of crosslinking ions and varying monomeric ratios. The influence of the crosslinking agents, namely barium, calcium, zinc and various combinations of these three cations on the mechanical properties of alginate gelispheres were assessed in both the hydrated and unhydrated states.

The following sections detail the study conducted to evaluate the physicomechanical and physiochemical properties of native ionotropically crosslinked alginate gelispheres following exposure to hydration. This study investigates the influence of the monomeric constitution of the polymer (G/M ratio) and crosslinking agents, namely barium, calcium and zinc on the textural and erosional properties of the matrix.

2.2 Materials and Methods

2.2.1 Materials

Six different grades of sodium alginate with varying G/M-ratios were analysed in this study. These included TIC Pretested® TICA-algin™ 200 powder, TICA-algin™ 400, TICA-algin™ HG-400, TICA-algin™ 900 which were donated by TIC Gums (Belcamp, MD, USA), Protanal® LF 10/60 were donated by FMC BioPolymer (Haugesund, Norway) and ISP Manugel® DMB (ISP Corporation, CA, USA). The constituent ratios of monomeric units are detailed in Table 2.2.

Table 2.2: Alginates of varying G/M-ratios.

Alginate Designation	Commercial Alginate	Guluronic acid (%)	Mannuronic acid (%)
A1	TICA-algin™ 200	45	55
A2	TICA-algin™ 400	45	55
A3	TICA-algin™ HG 400	60-65	35-40
A4	TICA-algin™ 900	45	55
A5	Protanal® LF 10/60	65-75	25-35
A6	Manugel® DMB	69	31

The crosslinking agents employed included barium chloride, calcium chloride and zinc gluconate which were purchased from Rochelle Chemicals (Gauteng, South Africa).

2.2.2 Preparation of Alginate Gelispheres

Ionotropic gelation was employed to formulate the gelispheres. Briefly a $1\%^{w}/_{v}$ solution of alginate dispersion was prepared in 100mL double deionized water (Millipore® filter with pore size 0.22μm). The crosslinking solution was composed of either $2\%^{w}/_{v}$ barium chloride, calcium chloride, zinc gluconate or binary combinations ($2\%^{w}/_{v}$ each) of the salts prepared in 200mL double deionized water. A 23-gauge syringe was employed to titrate the alginate solution dropwise into the gently vortexed crosslinking solution. A 24-hour curing period was employed following which the gelispheres were removed and washed with 3x500mL deionized water. The gelispheres were subsequently dried in ambient conditions under an extractor for 48 hours. The dried gelispheres were then analysed for their mechanical properties.

2.2.3 Textural Analysis of Unhydrated Gelispheres

A Texture Analyser (TA*XT.plus* Stable Micro Systems®, Surrey, UK) was employed to conduct textural analysis on the gelispheres. Data acquisition was performed at 200 points per second. Resilience, matrix hardness (deformability modulus) and matrix fracture energy of the crosslinked gelispheres were assessed according to their G and M content. The association of the monomers, i.e. GG, GM, MM blocks and their interaction with the crosslinking cations on the mechanical properties was also examined. Samples with an identical G/M ratio were compared according to differences in viscosity. Typical parameters are listed in Table 2.3.

Table 2.3: Parameter settings for measurement of the physicomechanical properties of gelispheres.

Test Parameter	Fracture Energy and Deformability Modulus	Matrix Resilience
Pre-test speed	1.0 mm/s	1.0 mm/s
Test speed	0.5 mm/s	0.5 mm/s
Post-test speed	1.0 mm/s	1.0 mm/s
Target mode	Force	50% Strain
Target force	40 N	-
Trigger force	0.5 N	0.5 N
Load cell	5 kg	5 kg

The force-time profile was employed for the determination of matrix resilience. This refers to the ability of a gelisphere to recover upon application of deforming stress to its original state of equilibrium. This was calculated as the ratio of the areas under the compression and decompression curve (Figure 2.4a). A force-distance profile generated for the gelispheres was employed to obtain the area under the curve (AUC) which enabled the evaluation of the energy needed to rupture the gelisphere matrix, i.e. the fracture energy (Nm) (Figure 2.4b) while the gradient to the peak force, known as the deformability modulus (N/mm) (Figure 2.4c) corresponds to the hardness of the gelisphere matrix.

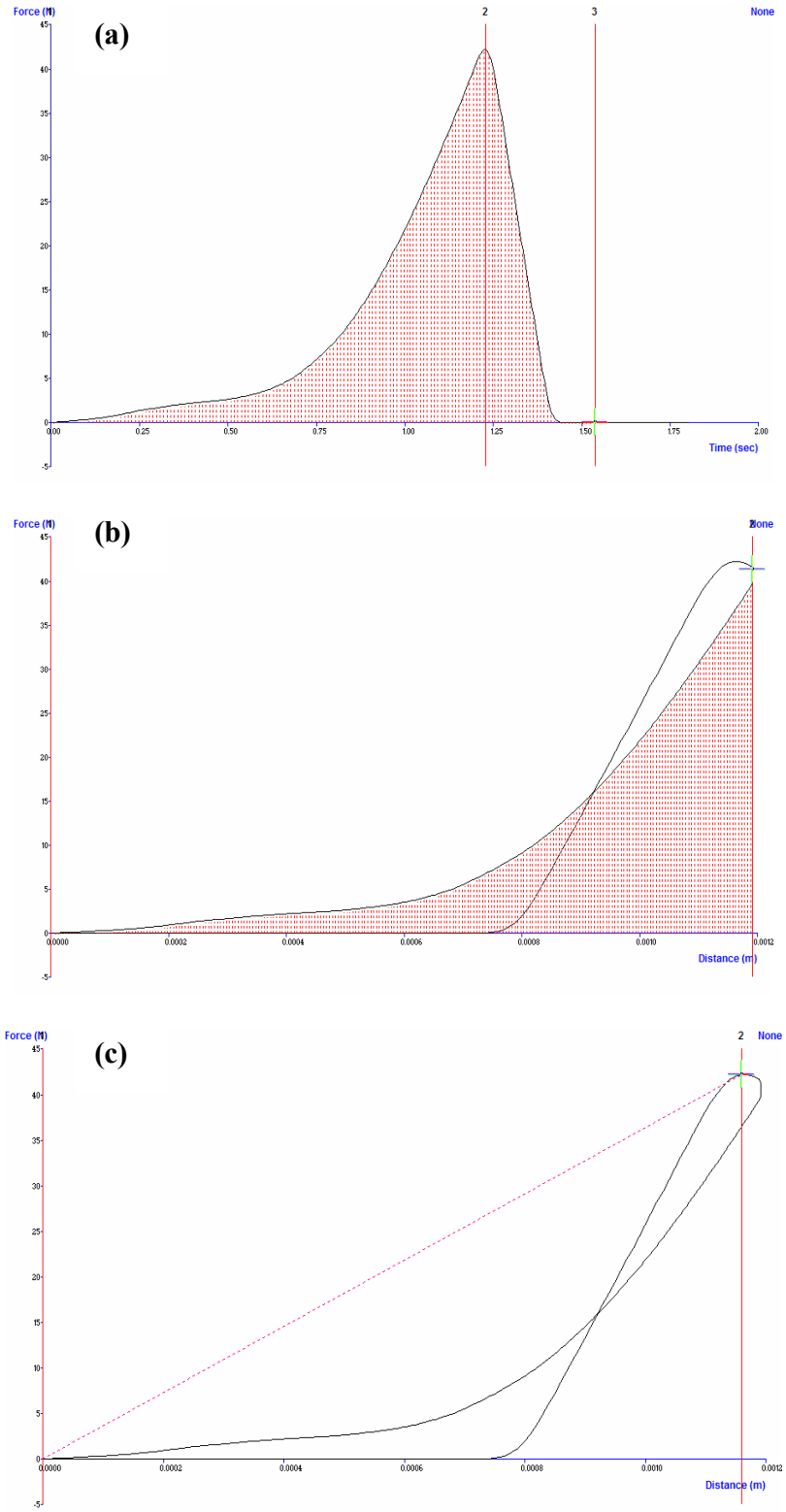

Figure 2.4: Typical textural profiles generated for crosslinked alginate gelisphere matrices (a) matrix resilience (%); (b) fracture energy (Nm) and (c) deformability modulus (N/mm).

2.2.4 Textural Analysis of Hydrated Alginate Gelispheres

Gelispheres were immersed in 15mL double deionised water in glass vials and agitated at 50rpm in a shaker bath (Labline® Instruments, IL, USA) maintained at 37°C. Samples (N=10) were removed and analysed for four 24 hours intervals and evaluated for the above stated parameters (Table 2.3) employing a texture analyser. Texture Exponent® for Windows Version 3.2 (Stable Micro Systems®, UK) was used to facilitate fully integrated data acquisition.

2.2.5 Analysis of Alginate Gelisphere Erosion

Gelispheres of known weight were immersed in 15mL deionized water maintained at 37°C and agitated at 50rpm in a shaker bath (Labline® Instruments, IL, USA). At predetermined periods of times samples were extracted and dried in ambient conditions under an extractor for 48 hours to allow complete removal of water from the matrix. Samples were then re-weighed and the loss of matrix was computed. Studies were conducted in triplicate. The % of the gelisphere matrix eroded after hydration was calculated employing Equation 2.1.

$$ME_t = \frac{(W_0 - W_t)}{W_0} \times 100 \qquad \text{Equation 2.1}$$

Where:

ME_t = Matrix erosion at time t hours (%);

W_t = Mean weight of gelispheres after t hours of exposure to hydration; and

W_0 = Mean weight of gelispheres at time t_0

2.3 Results and Discussion

2.3.1 Textural Analysis of Unhydrated Alginate Gelispheres

Textural analysis demonstrated that the both the G/M-ratio and nature of crosslinking agent had a significant impact on the robustness of unhydrated gelispheres. It is important to define the implication of the terms compact and porous with respect to the crosslinked matrices here. Compact refers to the formation of a matrix which is densely networked. They are resistant to applied mechanical stress, thus display high fracture energy and deformability moduli. Such a network has the capacity to entrap a significant amount of drug (discussed further in Chapter 3) and contain it for longer durations of time following exposure to hydrating medium. Thus the formation of such a matrix is beneficial for generating gelispheres capable to providing sustained drug release, which is the intended purpose of the drug delivery device for the study. A porous matrix on the other hand has a patent structure, hence demonstrates the ability to recover more easily after an applied mechanical stress, which confers to a high matrix resilience. These matrices are not suitable for entrapping drug molecules of a small molecular weight, since it permits ready entry of water molecules in the matrix, allowing the entrapped drug to be rapidly released.

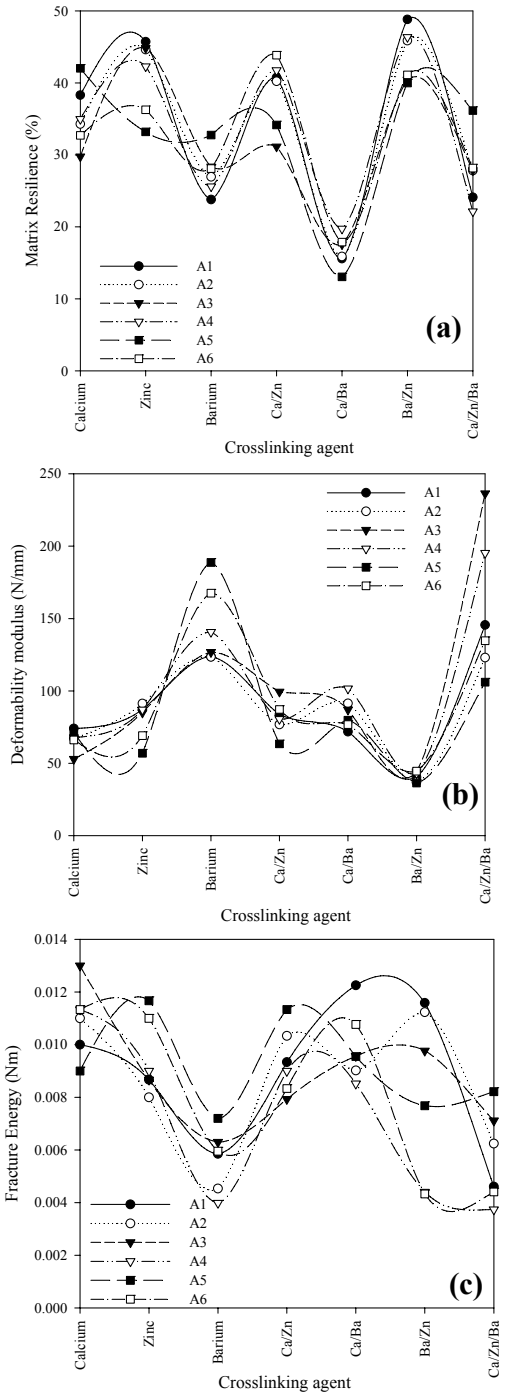

Figure 2.5: Profiles depicting the relationship between, (a) matrix resilience (%) (SD<1.23%), (b) deformability modulus (N/mm) (SD<3.45N/mm) and (c) fracture energy (Nm) (SD<0.0004) of unhydrated gelispheres crosslinked with zinc, calcium, barium and various binary combinations of the cations (N=5).

2.3.1.1 Influence of G/M-Ratio on the Textural Properties of Unhydrated Alginate Gelispheres

G-rich alginates employing calcium as a crosslinking agent produced more robust gelispheres in comparison to zinc-crosslinked gelispheres. This was due to the fact that calcium selectively has a greater affinity for G-units in alginate (McDowell, 1977; Aslani and Kennedy, 1996). Hence, G-rich gelispheres crosslinked with calcium demonstrated higher fracture energies. However their resilience and deformability modulus were lower than the corresponding zinc-crosslinked gelispheres. For instance, A5 demonstrated a deformability modulus of 71.42N/mm for calcium-crosslinked matrices, while this value declined to 56.96N/mm with zinc-crosslinked matrices.

Alginates with lower G/M-ratios demonstrated that zinc ions were less selective with regard to their affinity for the monomeric units within the polymer. They produced more robust gelispheres due to more extensive crosslinking within the polymer network. For example A2 has a deformability modulus of 91.23N/mm when crosslinked with zinc ions whereas a significantly lower modulus of 67.17N/mm was obtained for calcium-crosslinked matrices. However, zinc-crosslinked G-rich alginate gelispheres (i.e. A5 and A6) demonstrated significantly lower resilience, deformability moduli and fracture energy than their calcium-crosslinked counterparts (Figure 2.5a-c). This was due to the weaker bonds produced between the small cation and G-units. Barium also demonstrated selective binding with G-rich alginates A5 and A6, thus generating gelispheres which displayed high deformability moduli, 188.76N/mm and 167.50N/mm respectively. This is discussed further in the next section.

2.3.1.2 Influence of Crosslinking Agent on the Textural Properties of Unhydrated Alginate Gelispheres

Divalent calcium ions have an ionic radius of 114pm with an atomic volume of 29.9cm^3/mol, while divalent zinc ions have smaller ionic radii of 88pm with, an atomic volume of 9.2cm^3/mol (Ionic Information of Calcium, 2004; Ionic Information of Zinc, 2004). Thus they prove to be a greater challenge to destabilize from within their highly stable crosslinked G-unit pockets. Hence the crystal structure of the zinc-crosslinked gelispheres succumbed to the pressure of applied mechanical stress more easily causing collapse of the matrix.

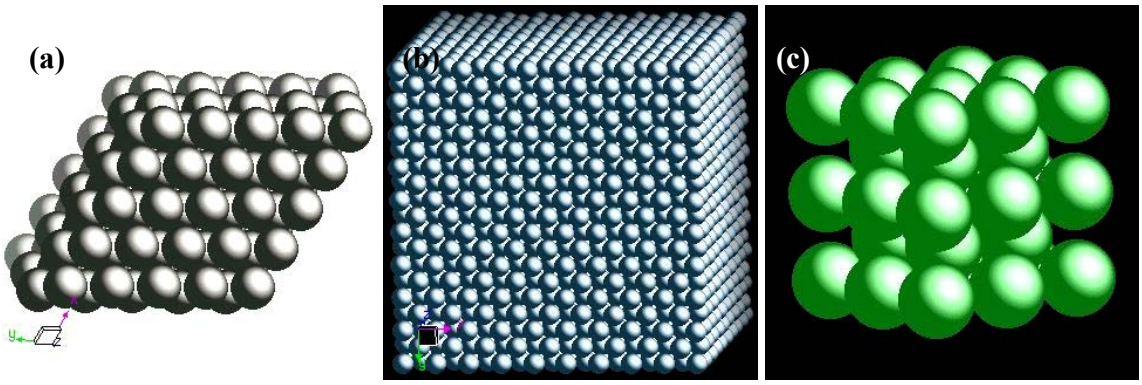

Figure 2.6: Spatial arrangement of (a) zinc (b) calcium and (c) barium ions.
(Source: http://www.scescape.net/~woods/elements/zinc.html 2004;
http://www.scescape.net/~woods/elements/calcium.html 2004;
http://www.scescape.net/~woods/elements/barium.html 2004).

Calcium ions in their divalent states are present as an ordered rigid hexagonally close-packed shape (Figure 2.6). The zinc ions in comparison are arranged in a distorted hexagonally close-packed shape (Ionic Information of Calcium, 2004; Ionic Information of Zinc, 2004). This implies that zinc due to its smaller atomic radius (almost a third of that of divalent calcium ions) and distorted structure has the capacity to insert itself into sites where the larger calcium ions cannot. Divalent barium ions have an even larger ionic radius at 149pm and atomic volume of 39.24cm^3/mol (Ionic Information of Barium, 2004). These Ba^{2+} ions exist in a body centred cubic structure as a 6-

coordinate octahedron (Figure 2.7). Their observed interaction with alginate was thus very different from calcium and zinc ions. The chelated structure formed as result of the alginates' G-unit interaction with the cations was thermodynamically more favourable, since due to its larger ionic radius it produced a more compact arrangement with 'smaller voids' (Al Musa et al., 1999).

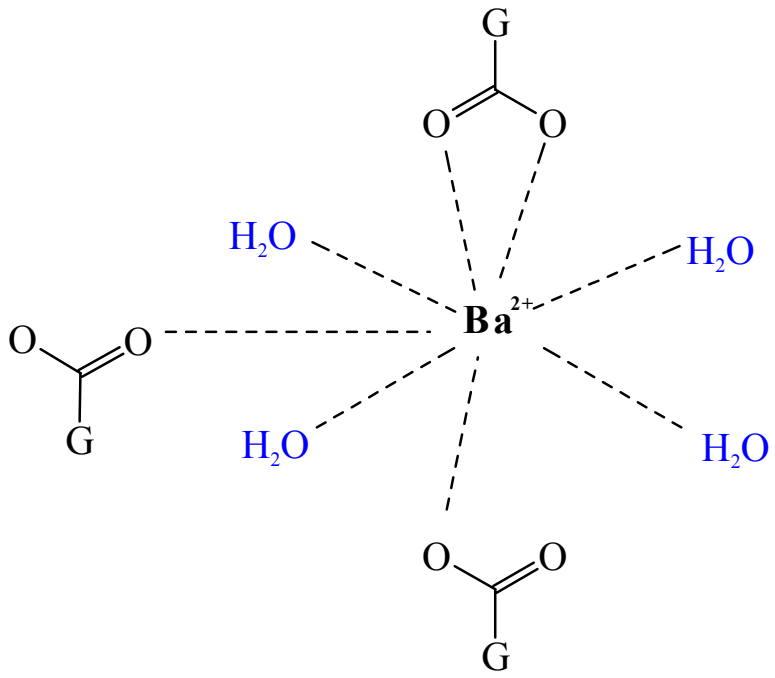

Figure 2.7: The interaction of divalent barium ions with carboxylic acid groups on alginate G-units and water molecules (octahedral arrangement) within the polymeric matrix. (Source: Adapted from Briceño et al., 2002).

The results demonstrated that there is an inverse relationship between matrix resilience (which confers to matrix porosity) and fracture energy (which confers to matrix hardness) for gelispheres crosslinked with calcium and zinc. It is postulated that this emerges from the fact that the application of a deforming force on the gelispheres compresses the loose matrices and thus indicated that a porous sponge-like matrix was present. Thus the fracture energy was in fact indicative of the energy needed to maximally compress the gelispheres which subsequently led to

rupture of the matrix. Barium-crosslinked gelispheres demonstrated low matrix resilience and fracture energy however their deformability moduli exceeded those of the calcium and zinc-crosslinked counterparts by between approximately 49-121N/mm and 36-102N/mm respectively for the various alginates. This indicated that barium-crosslinked gelispheres were brittle in nature, as opposed to the amorphous porous matrices of the calcium and zinc-crosslinked gelispheres. Gelispheres produced by a Ba/Ca combination were less porous than those produced by a Ba/Zn combination, indicated by the lower resilience and high fracture energies of Ba/Ca-crosslinked gelispheres. Conversely, Ba/Zn-crosslinked matrices demonstrated higher resilience and G/M ratio dependant behaviour on fracture energy, indicated by the lower fracture energies demonstrated by G-rich alginates, A5 and A6.

On the other hand, zinc imparted an amorphous character particularly to M-rich Ba/Zn-crosslinked gelispheres. For example, the M-rich alginate A1 had an unhydrated matrix resilience of 48.80% when crosslinked with Ba/Zn, while this value declined to 15.57% when crosslinked with the Ba/Ca combination. This occurred with Ca/Zn-crosslinked matrices also. While the calcium ions selectively bound with G-units; zinc ions could bind with both G- and M-units (McDowell, 1979). The zinc ions could not be displaced by the calcium ions from their stable locations within the polymeric network. The smaller atomic size of the divalent zinc ions implied that they could fit into smaller electronegative polymer pockets. However, this also implied that the resultant structure was more porous due to the presence of larger 'voids' between the polymeric chains. The resilience values for unhydrated M-rich alginates, i.e. A1-A4 were approximately 10-20% higher for zinc-crosslinked gelispheres, versus their calcium-crosslinked counterparts. With regards to the combination of Zn/Ca/Ba, a dominant effect of calcium and barium was observed.

2.3.2 Textural Analysis of Hydrated Alginate Gelispheres

The results generated for hydrated gelispheres over a period of 96 hours provided significant insight into the mechanism of hydration and subsequent disentanglement of the gelisphere matrices. The gelispheres eroded completely after 96 hours.

The hydrated gelisphere matrices underwent gelation when exposed to aqueous medium as a result of the polymeric network undergoing chain relaxation (Figure 2.8). This increased the viscoelastic properties of the gelispheres and resulted in a decrease in matrix rigidity and resilience. As the gelispheres become hydrated the matrix initially swelled to accommodate the water molecules diffusing into the gelispheres and adopted its new porous structure. Once water had penetrated the core of the gelispheres, the 'egg-box' structure broke and they began to lose weight and finally eroded. It has been postulated that dissociation of the crosslinking cations initially occurs at the site of M-unit binding (Al Musa et al., 1999). As mentioned earlier, the cations bind to the electronegatively charged carboxylic acid ($-COO^-$) groups of the M-units. Hence, once the cations were dissociated from these locations an electrostatic repulsive force was generated between the electronegative groups resulting in chain relaxation, increased water uptake and gel swelling.

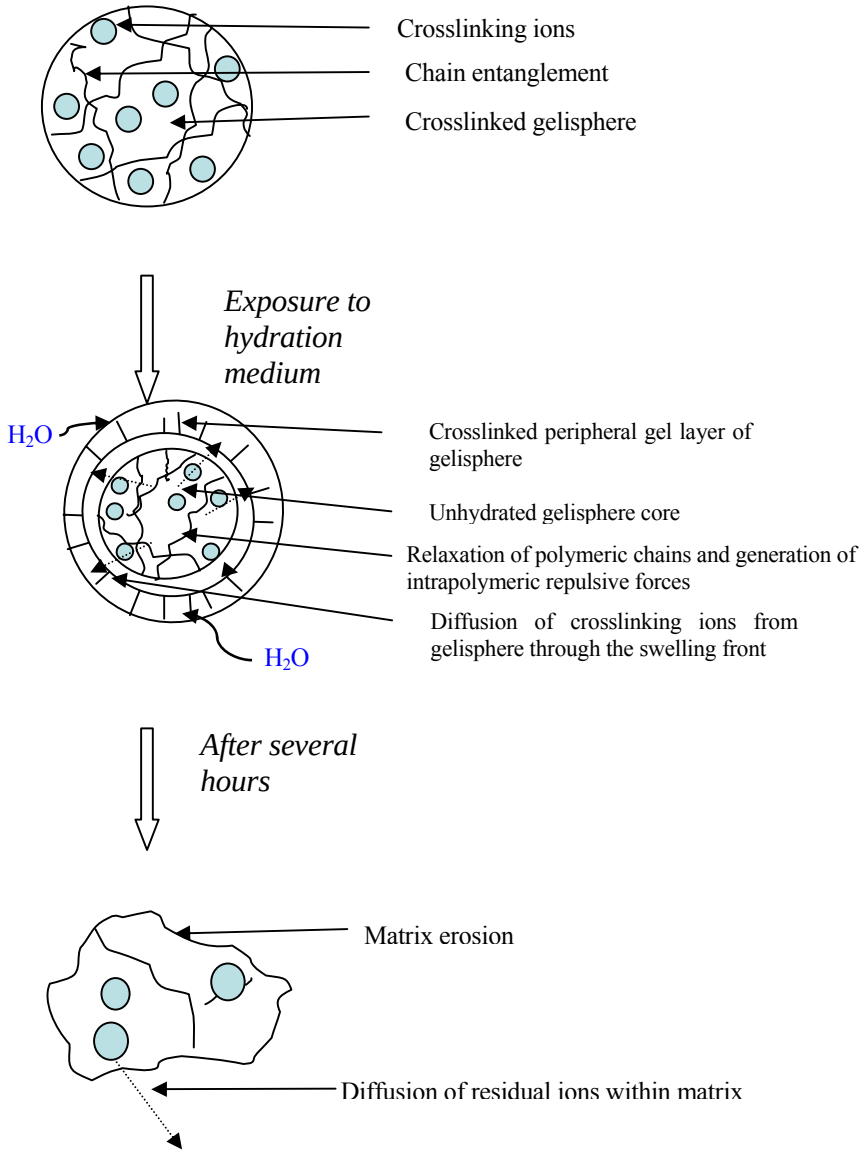

Figure 2.8: Schematic illustration of the hydration mechanism and erosion of ionically crosslinked gelispheres.

Apparent 'increases' in robustness (indicated by peaks in the resilience profiles) resulted due to the unique hydration mechanism of the gelispheres. The gelispheres absorbed water and sequentially formed peripheral layers of hydrated crosslinked polymer, while the central core remained unhydrated. As the peripheral layers reached maximal hydration and ruptured, the subsequent layer

became exposed to water molecules and in turn underwent hydration. Therefore hydration occurred in concentric layers within the gelispheres (Figure 2.9).

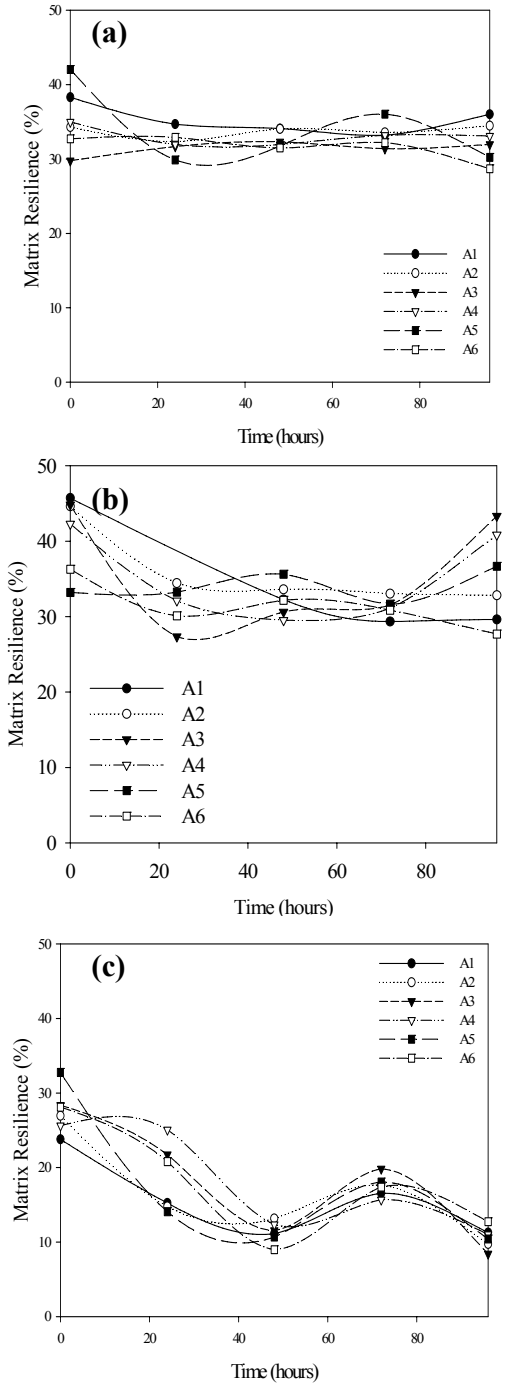

Figure 2.9: *Contd. on pg 75*

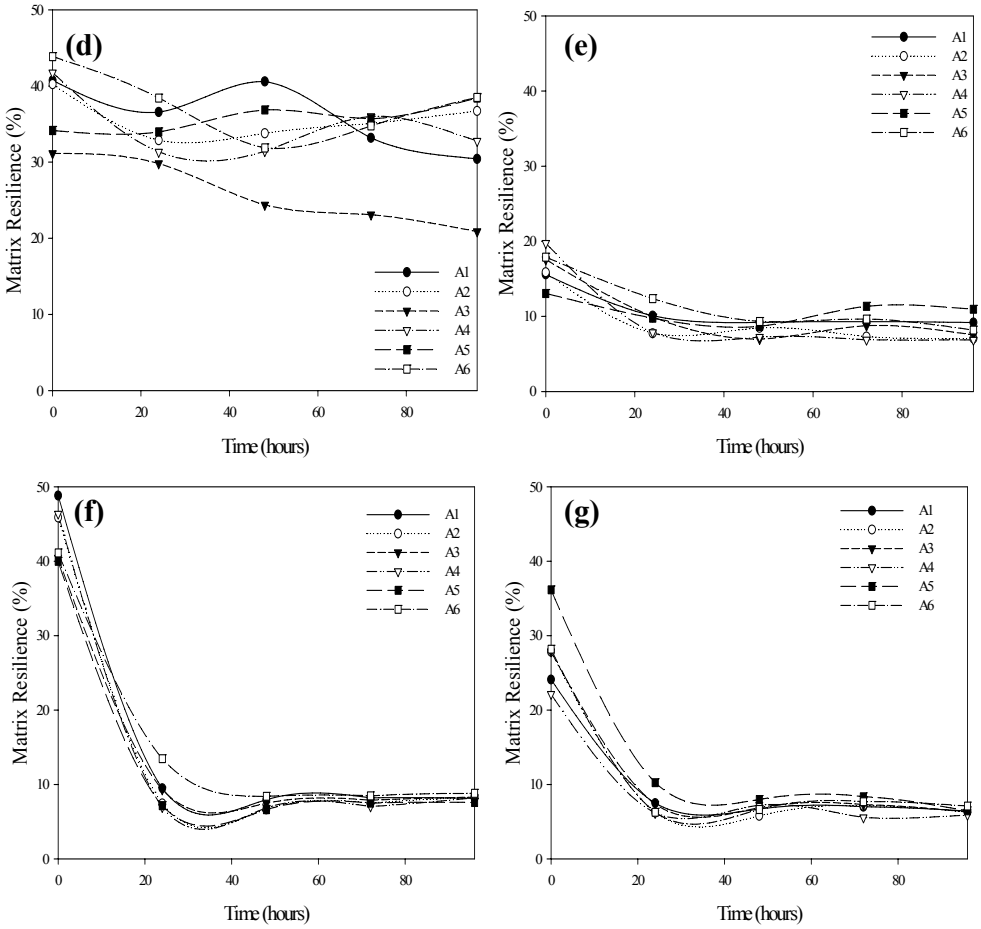

Figure 2.9: Matrix resilience (%) of hydrated alginate gelispheres crosslinked with (a) calcium, (b) zinc, (c) barium, (d) calcium and zinc, (e) calcium and barium, (f) barium and zinc, (g) calcium, barium and zinc over a period of 96 hours (N=3; SD<3.18%).

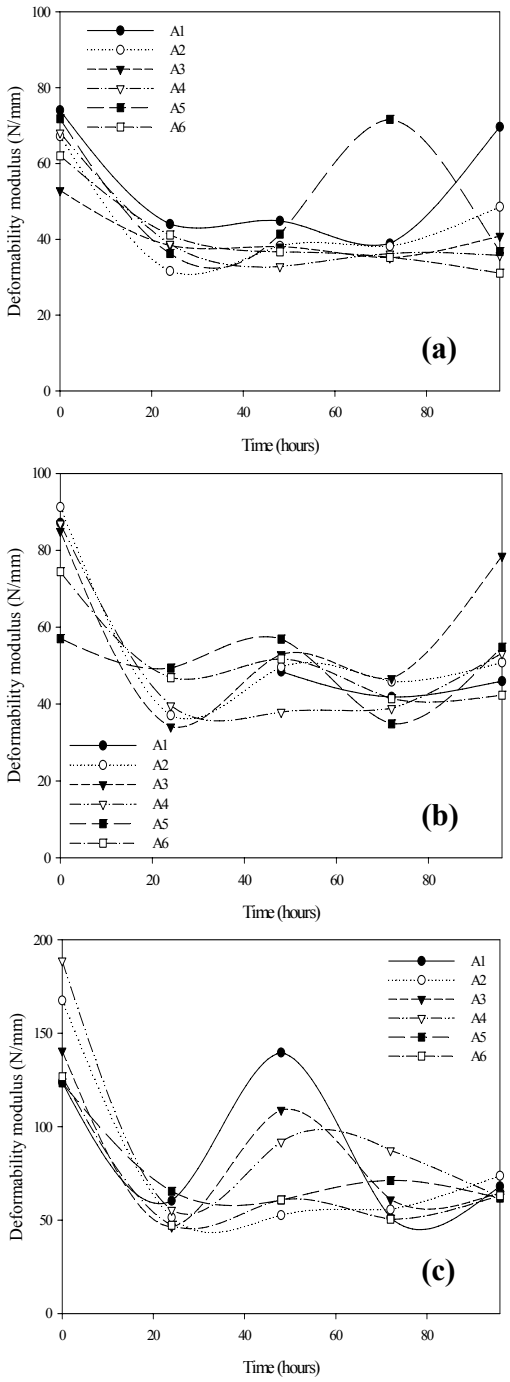

Figure 2.10: *Contd. on pg 77*

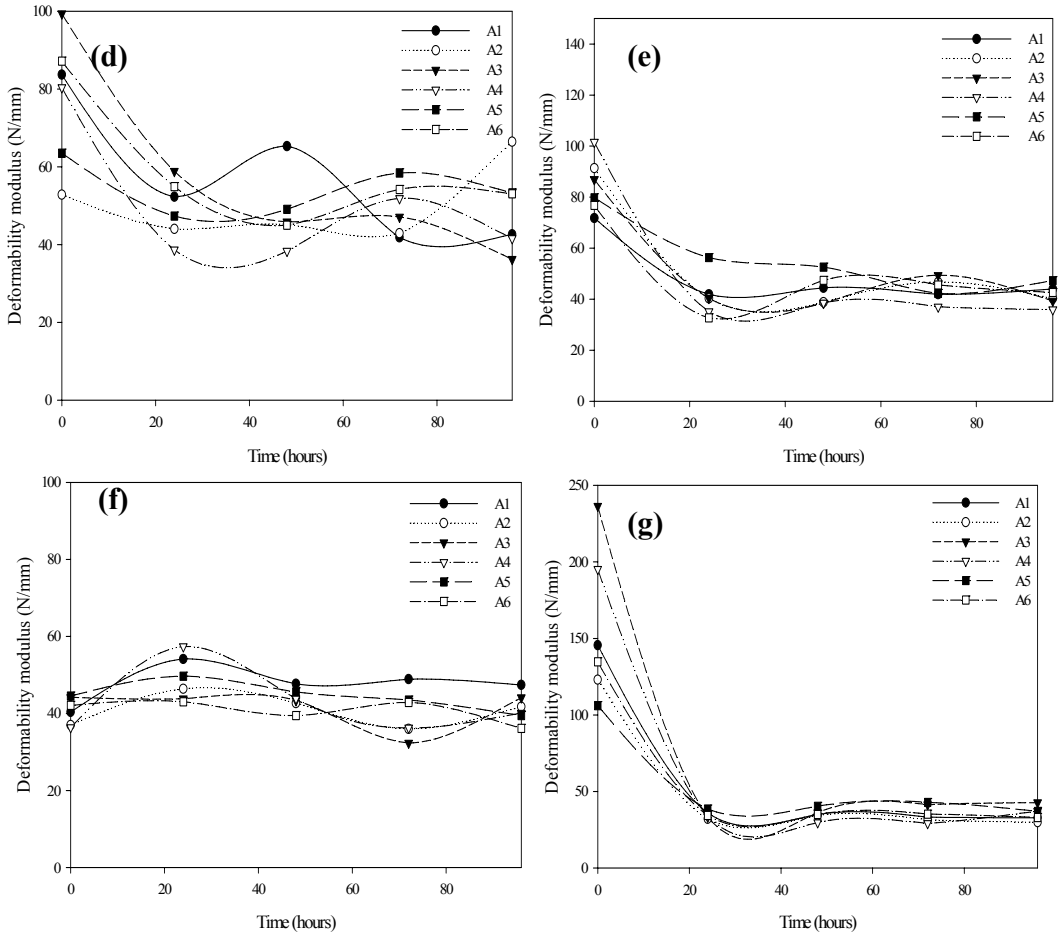

Figure 2.10: Deformability modulus (N/mm) of hydrated alginate gelispheres crosslinked with (a) calcium, (b) zinc, (c) barium, (d) calcium and zinc, (e) calcium and barium, (f) barium and zinc, (g) calcium, barium and zinc over a period of 96 hours (N=3; SD<5.42N/mm).

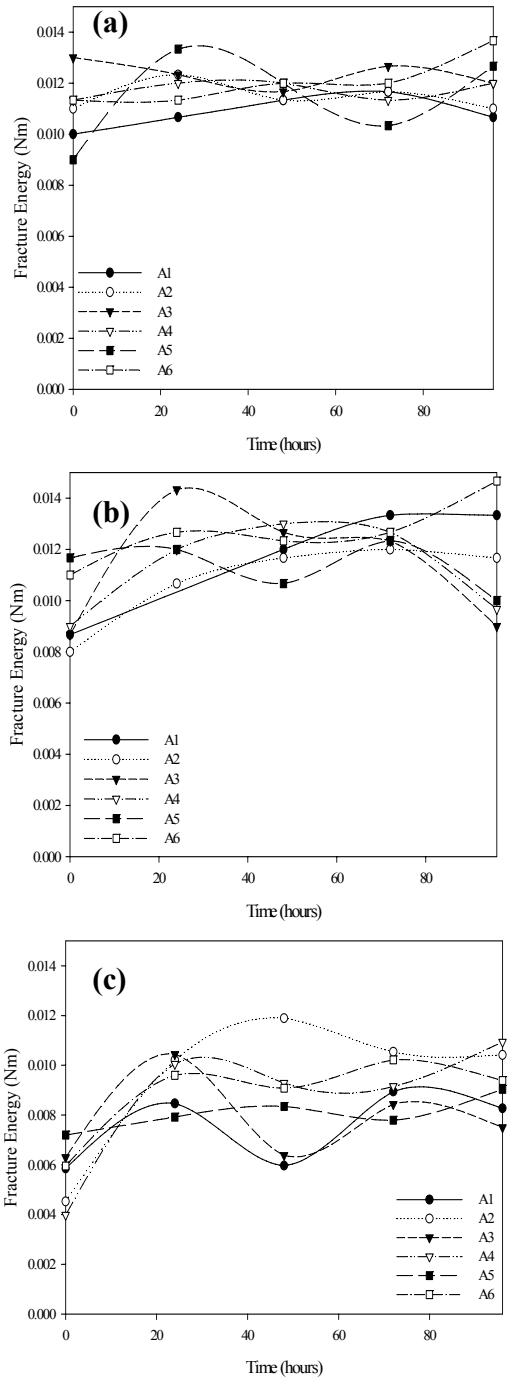

Figure 2.11: *Contd. on pg 79*

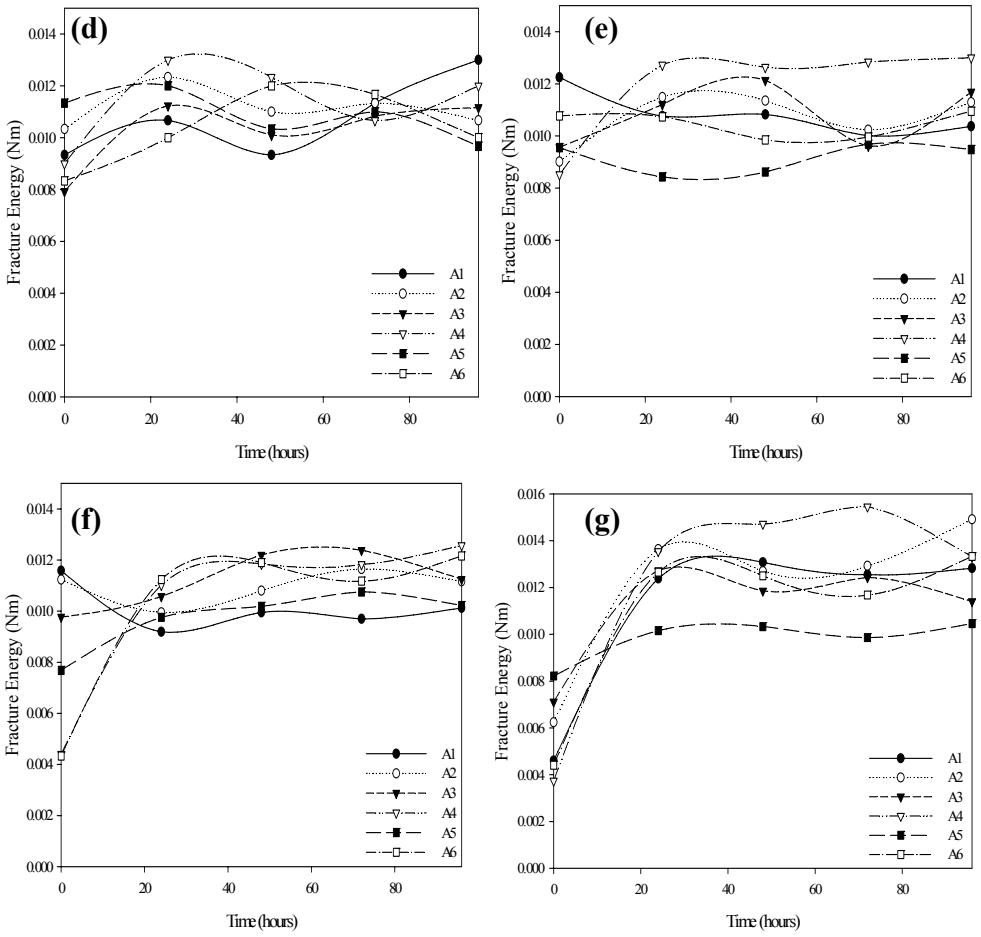

Figure 2.11: Fracture energy (Nm) on hydrated alginate gelispheres crosslinked with (a) calcium, (b) zinc, (c) barium, (d) calcium and zinc, (e) calcium and barium, (f) barium and zinc, (g) calcium, barium and zinc over a period of 96 hours (N=3; SD<0.0005).

2.3.2.1 Influence of the Co-ordination Number of Crosslinking Agent on Matrix Hydration

The rate and extent of chain relaxation and water uptake was markedly decreased as the degree of crosslinking increased. This was reflected in the physicomechanical properties undergoing a generalized decline over time when exposed to hydration. When exposed to hydration zinc-crosslinked gelispheres demonstrated slower rates of chain relaxation and matrix degradation. This was due to the fact that water penetrated these gelispheres more slowly and to a lesser degree over time in comparison to the calcium-crosslinked spheres. Upon hydration, calcium ions have a

greater propensity to attract oxygen atoms in water molecules due to the fact that they possess higher co-ordination numbers (7-9) in the crystal structure (Cambridge Structural Database, Version 5.25, 2004). Zinc ions bind with lower co-ordination numbers (4-6) in the crystal state (Cambridge Structural Database, Version 5.25, 2004) and therefore do not have as significant a water attracting power as calcium. Hence when exposed to water the crystal lattice of the zinc-crosslinked matrix underwent chain relaxation and subsequent degradation more slowly. Furthermore, due to the more extensive polymeric binding with zinc ions, the matrix did not collapse when it was dissociated from G-unit bound sites, as was the case with calcium-crosslinked matrices. Over time zinc-crosslinked gelispheres also indicated overall higher initial deformability moduli than their calcium-crosslinked counterparts. Unhydrated zinc-crosslinked gelispheres had deformability moduli 10-30N/mm higher than calcium-crosslinked gelispheres. Upon hydration, the corresponding values for zinc-crosslinked gelispheres at any given point in time were higher by approximately 2-20N/mm than hydrated calcium-crosslinked gelispheres.

2.3.2.2 Influence of G/M-Ratio on Matrix Hydration

The degree of chain relaxation over time varied with the different grades of alginates, such that some alginates (e.g. M-rich A4) underwent polymeric relaxation to the core almost immediately, while others (e.g. G-rich A5) retained an unhydrated core up to 24-72 hours. The G-rich alginate A5 crosslinked with calcium had an unhydrated deformability modulus of 71.78N/mm, which declined to 36.23N/mm after 24 hours exposure to hydration. However, after 72 hours exposure to hydration however, it ‘increased’ to 71.60N/mm. This indicated that although hydration of the peripheral layers of the gelisphere did occur, the unhydrated core was not exposed to water until 72 hours, where-after hydration of the core occurred rapidly when the deformability modulus declined

to 36.75N/mm. Correspondingly apparent 'increases' in the observed fracture energy required to rupture gelispheres were greater at 24 and 48 hours following hydration due to swelling of the gelispheres. Thus anomalous results were obtained as the probes broke through the hydrated layers of the gelispheres and approached the rigid crosslinked unhydrated core.

Zinc-crosslinked alginates with low G/M-ratios allowed the formation of more rigid gels upon hydration. This can be explained in terms of the fact they possess a greater capacity for interaction with the zinc cation. The unhydrated gelispheres formulated with alginates the low G/M-ratio alginates A1-A4 crosslinked with zinc, possessed initial deformability moduli in the region of 85.00-91.23N/mm. Upon hydration, relatively M-rich alginates such as A3 and A4 crosslinked with zinc retained an unhydrated core until 96 hours. Hence although an initial decline (approximately 10%) in resilience could be seen after 72 hours, at t=96 hours the resilience 'increased' by approximately 9% to reveal the unhydrated rigid zinc-crosslinked core.

2.3.2.3 The Influence of G-Unit Selectivity for Crosslinking Agents on Matrix Hydration

Gelispheres prepared by employing a Ca/Zn combination of crosslinking agents demonstrated results that were a direct function of G-ratio and polymer molecular weight. While for relatively M-rich alginates such as A1, the effect was that the combined crosslinking resulted in a weakening of the unhydrated matrix in comparison to gelispheres prepared with only zinc as the crosslinking agent. Upon subsequent hydration the matrix of the Ca/Zn combination gelisphere remained more robust through the 96 hours. At the 96th hour when the unhydrated core was exposed to hydration, the deformability moduli for calcium, zinc and Ca/Zn combination were observed to be 48.55N/mm, 50.82N/mm and 66.44N/mm respectively. This phenomenon can be explained in

terms of the combined effects of thermodynamically more stable binding of calcium ions with electronegative cavities of G-units with the extensive binding within the matrix provided by zinc ions and M-units. Water molecules therefore not only had to dissociate stable zinc-M-unit bonds, but also destabilize the large calcium ions from their G-bound cavities in the matrix. When unhydrated Ca/Zn-crosslinked gelispheres were exposed to hydration, a rearrangement of crosslinking cations within the polymeric cavities allowed the matrix to acquire a thermodynamically stable arrangement that was more compact than the individually crosslinked matrices. For G-rich alginate A6 this phenomenon was clearly synergistic. The deformability moduli of the unhydrated spheres crosslinked with a Ca/Zn combination of cations was greater (87.15N/mm) than either calcium or zinc-crosslinked gelispheres (62.02N/mm and 74.43N/mm respectively). Furthermore, it was observed to be the larger value (53.03N/mm) (more robust gelisphere) of the three over the 96 hours subsequent to hydration (31.05N/mm and 42.29N/mm for calcium and zinc-crosslinked gelispheres respectively).

2.3.2.4 Barium as a Matrix Re-inforcer for G-rich Alginates

It was observed that barium had a significant impact on the hydration dynamic of the polymeric matrices. As mentioned earlier, barium imparted a brittle character to the matrices due to its more compact binding mechanism with the polymer. The gelispheres were therefore less resilient and demonstrated higher deformability moduli. The interaction of Ba/Ca combination-crosslinked gelispheres with water molecules was similar to that shown by barium-crosslinked gelispheres. However the interaction with zinc ions produced an interesting phenomenon. Resilience underwent a sharp decline in the first 24 hours following which it stabilized for the next 72 hours. The average decline in resilience of Ba/Zn combination-crosslinked gelispheres observed in the first 24 hours

was 34.79% (SD<5%). This decline was not as large when all three cations are employed to crosslink the matrix. For the first 24 hours the decline was 20.42% (SD<4%). This phenomenon was also seen in the deformability modulus values for the respective gelispheres. Sharp declines were observed, in particular over the first 24 hours. While high values were prevalent for all unhydrated gelispheres which had barium as one of the crosslinking agents, the initial decline after exposure to hydration was significant. Fracture energy indicated a notable deviation. Following hydration, the abovementioned gelispheres demonstrated higher fracture energies. This can be explained in terms of the fact that zinc within matrices could easily be displaced from M-bound units with penetrating water molecules. The selectively G-unit-bound barium ions proved to be greater challenge to displace. The brittle Ba/Zn crosslinked gelispheres therefore demonstrate low deformability moduli (in the region of 57.36-32.32 N/mm) throughout the study.

2.3.3 Erodibility of the Crosslinked Alginate Gelispheres

Crosslinked water-soluble polymeric matrices such as those generated in this study undergo erosion through a very unique mechanism. The generation of water-soluble entities from the initial water-insoluble matrix that leads to the eventual degradation of the matrix involves a stepwise process. Theoretically it has been stated that ‘as long as the crosslinks (within the three-dimensional polymeric network) remain intact, it is insoluble, and, when placed in an aqueous medium it can swell only to the extent allowed by the crosslink density’ (Heller, 1987). Thus the process of matrix erosion is dependant upon two mechanisms, namely:

1. Cleavage of the crosslinks;
2. Cleavage of the water-soluble polymeric backbone.

Cleavage of polymeric bonds within such a matrix results in chain disentanglement and the formation of pores in the structure. These 'pores' hold the penetrating water, causing the matrix to swell. This swelling allows the influx of more quantities of water and results in the ionisation of the polymer causing subsequent dissolution into the aqueous medium. The process culminates in the loss of the integrity of the matrix and its degradation.

2.3.3.1 Influence of G/M Ratio and Crosslinking Agent on Matrix Erosion

Results indicated that matrix erosion over time was maximally observed with calcium-crosslinked gelispheres (approximately 39.90 - 59.17% gelisphere mass was lost within 48 hours of exposure to hydration). Zinc and barium-crosslinked matrices remained comparatively more intact for a longer period of time. In comparison, at 48 hours zinc-crosslinked gelispheres underwent between 11.87 - 24.89% matrix erosion, while barium-crosslinked gelispheres underwent only 20.81 - 28.40% erosion. As stated previously, the slower rates of hydration of the central core of the gelispheres with these matrices implied that the matrix remained intact for a longer duration. The various combination-crosslinked matrices demonstrated a general trend of slower rates of hydration over the first 24 hours after which the rate of matrix degradation increased exponentially. This was due to the destabilizing effect of calcium ions on the matrix and their greater affinity for water molecules that caused the gelispheres to swell and lose their integrity at a faster rate. Observed differences between the various M-rich alginates of varying molecular weight were not significantly vast. However, gelispheres crosslinked with only calcium indicated that the rate of matrix degradation and erosion was a function of G-ratio in the polymer. Although barium ions possess a greater water-attracting potential (due to its higher coordination number), it formed

chelates with the alginate G-units which were less porous. This implied that water molecules had greater difficulty penetrating the matrix and to force chain disentanglement. Thus the profile of barium-crosslinked gelispheres imitated that of zinc. The compact barium-crosslinked alginate structure retained its integrity for a longer duration of time.

Table 2.4 indicates the range of matrix erosion for the various alginates crosslinked with combinations of cations were as follows.

Table 2.4: Range of matrix erosion for the various alginate gelispheres crosslinked with various combinations of divalent cations after 24 hours of exposure to hydration.

Crosslinking Cations	Mean Matrix Erosion (%) (t=24 hours)	Standard Deviation for Matrix Erosion (%) (t=24 hours)
Ca/Zn	13.42	4.50
Ba/Ca	56.76	3.39
Ba/Zn	52.71	2.95
Ba/Ca/Zn	55.35	3.06

The differences between the rates of matrix erosion of gelispheres crosslinked with various combinations of the three cations were not vast. The exception to this rule was Ca/Zn combination-crosslinked gelispheres. The Ca/Zn-crosslinked gelispheres underwent an exponential rise in matrix erosion after 24 hours. By the 96^{th} hour, gelisphere matrices were between 38.12 - 65.86% eroded. In comparison, at 96 hours, the other gelispheres underwent little, if any change following their initial 24 hour degradation. This can be explained in terms of the fact that once zinc was initially removed from its M-unit chelated sites, the matrix became significantly more porous and open to the entry of water molecules. Thus following the first 24 hours exposure to hydration, subsequent entry of water molecules into the matrix and degradation was much more rapid. The

presence of barium imparted a significant degree of robustness to the alginate matrices. Barium-crosslinked matrices retained their integrity for a prolonged period of time. Initially the matrix eroded rapidly due to the ions rapid displacement from weakly bound M-unit bound regions. Subsequent disintegration is prevented due to tightly bound G-unit bound components of the matrix, which were difficult to displace.

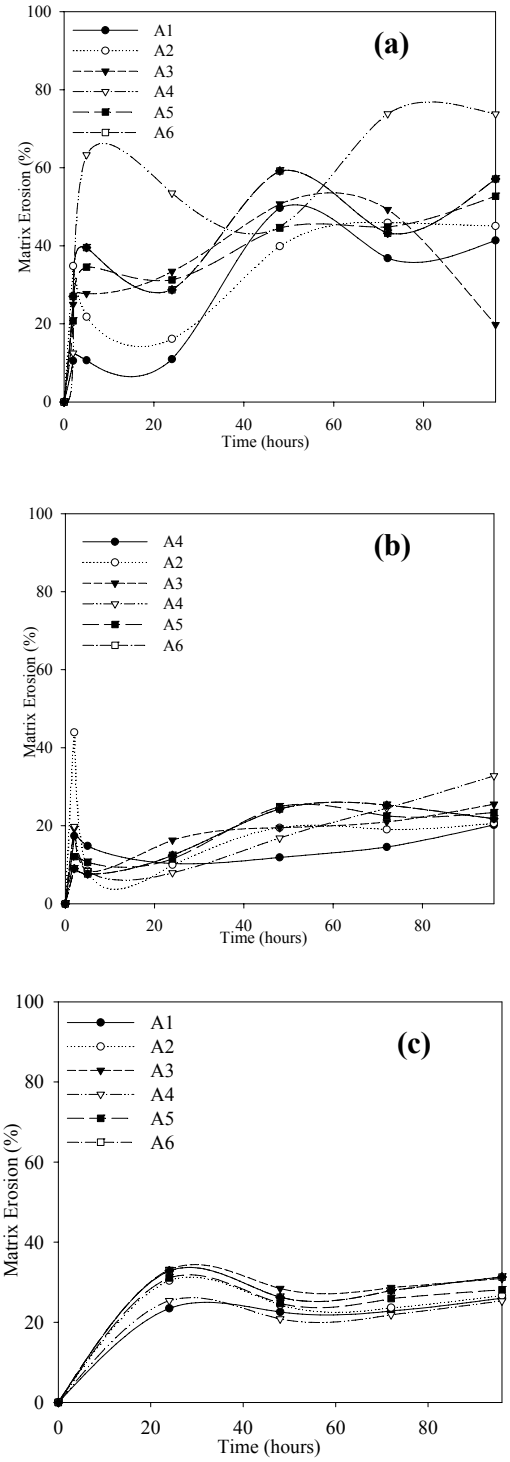

Figure 2.12: *Contd. on pg 88*

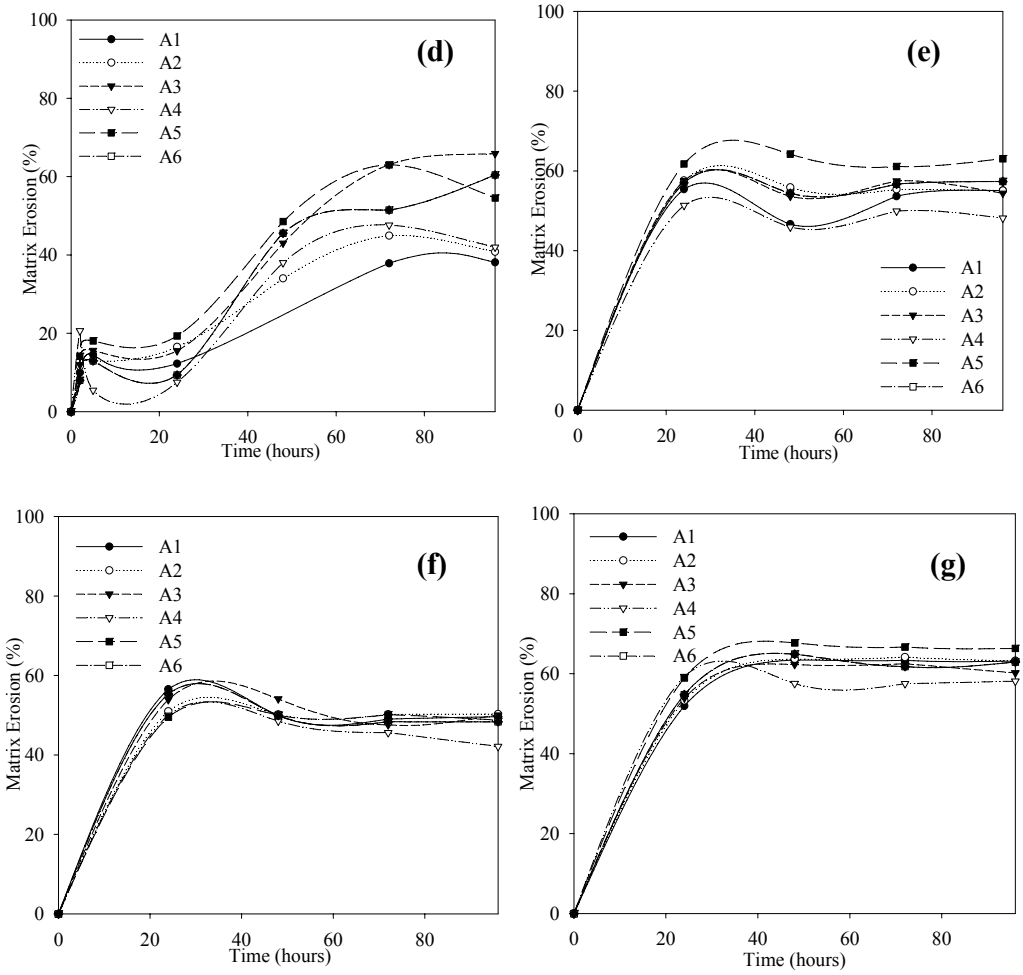

Figure 2.12: Matrix erosion (%) of gelispheres following hydration crosslinked with (a) calcium, (b) zinc, (c) barium, (d) calcium and zinc, (e) calcium and barium, (f) barium and zinc, (g) calcium, barium and zinc over a period of 96 hours (N=3; SD<4.52%).

2.4 Concluding Remarks

The results indicated that the different crosslinking agents interacted with varying intensity with monomeric units of the polymer, thereby generated gelispheres with significantly different mechanical characteristics. The study demonstrated that the relative monomeric (G/M) ratio within the alginates significantly influenced the degree of crosslinking and subsequently the physicomechanical behaviour of formulated gelispheres. Textural analysis of the different matrices indicated that that the robustness of crosslinked matrices declined over time when exposed to

hydration through a gradual process of concentric hydration whereby the peripheral layers of the matrix become hydrated first.

Overall textural analysis of the crosslinked gelisphere matrices indicated that incorporation of barium imparted a brittle character to the crosslinked matrices due to the formation of densely compact crosslinked polymeric networks. The presence of zinc in crosslinked matrices produced porous and therefore resilient gelispheres which interacted more significantly with the M-rich alginates. Zinc-crosslinked gelispheres possessed porous networks that demonstrated little change in matrix resilience despite indicating a slight decline in matrix hardness following exposure to hydration over time due to dislocation from M-unit bound sites within the polymeric network. The calcium matrices demonstrated intermediate mechanical characteristics and imparted greater robustness to gelispheres with high G/M-ratios due to their preferred chemical affinity for G-units within alginate networks. In terms of matrix erosion it was observed that zinc-crosslinked gelispheres demonstrated the most rapid rates of erosion due to the formation of porous matrices that allowed easier entry of water molecules into the polymeric networks. Calcium and barium in particular demonstrated selectivity for G-rich alginates, imparting them with significantly more compact crosslinked matrices. Matrix erosion occurred least significantly with zinc and barium-crosslinked matrices. Calcium-crosslinked gelispheres remained most intact over time following hydration. It was also observed that the most significant degradation of gelisphere matrices occurred within the first 24 hours of exposure to hydration.

In view of the rapid matrix erosion rates, it was established that in order for the system to survive simulated CSF, the system required further reinforcement. This was achieved by the addition of

further polymers into the gelisphere matrix (discussed in the following chapter). Barium-crosslinked gelispheres demonstrated beneficial properties in terms of their capacity to generate denser compact matrices which allowed minimal penetration of hydrating media and indicated slower rates of degradation. These compact matrices are ideal for entrapping small molecules such as nicotine, the proposed model neuroprotectant into their cavities and preventing rapid drug release.

Chapter 3

Evaluating the Role of Hydroxyethylcellulose and Polyacrylic Acid on the Modifying Drug Release Rates of Crosslinked Alginate Gelispheres

---

'……scientific research was much like prospecting: you went out and you hunted, armed with your maps and your instruments, but in the end your preparation did not matter, or even your intuition. You needed your luck, and whatever benefits accrued to the diligent through sheer, grinding hard work.'

- The Andromeda Experiment, Michael Crichton, 1969.

3.1 Introduction

Advances in producing high-performance polymer-based compositions is predominately the utilization of new mixtures of polymers and mixtures of polymers with reinforcing components, rather than from new polymer compositions. Multi-polymeric systems resulting from the combination of two or more miscible polymers can under certain circumstances result in the development of systems that have superior properties than either system alone. The development of strong interfacial adhesion, either though the development of covalent bonds or secondary bonds, such as dipole interactions or the significantly stronger hydrogen bonds may result in a system with properties demonstrating synergy between the components to bring about superior mechanical strength, easier processability and wider commercial applicability.

As outlined in Chapter 2, the ability of alginate to react with crosslinking cations is a direct function of the average length of G-units within the polymer. During initial studies the combination of a high G-content alginate (A5 from Chapter 2) with numerous biodegradable

polymers was evaluated to produce a polymeric system that had superior robustness and delayed degradation kinetics than the conventional calcium-crosslinked alginate systems currently employed for drug delivery.

The following polymers were evaluated as reinforcing agents for the crosslinked alginate gelispheres during preformulation:

- Cellulosic ethers including hydroxyethylcellulose (HEC), hydroxypropylcellulose (HPC); and hydroxypropylmethylcellulose (HPMC);
- Polyesters including polylactic acid (PLA) and poly(lactic-co-glycolic) acid (PLGA) of varying viscosities;
- Poly(acrylic acid) (PAA);
- Pectin with varying degrees of methoxylation; and
- Polyvinyl alcohol (PVA) of various molecular weights

Results demonstrated that although gelispheres generated by ionotropic gelation as discussed in Chapter 2 employing various polymer blends, none were able to retard nicotine release sufficiently beyond 2 hours when exposed to simulated cerebrospinal fluid (CSF). Furthermore, being a polyanionic polymer, alginate is known to degrade in the presence of an alkaline pH (physiological pH 7.4) due to interactions between carboxylic acid groups in the polymer and the surrounding alkaline medium that induces ionization of the polymer (which confers to enhanced solubility) and subsequently polymer degradation. Hence it was concluded that induction of an interaction between the free carboxylic acid groups, particularly those of the M-units (since G-units have a

significant and selective interaction with crosslinking ions employed in gelation) with another species, degradation could be retarded.

The polymer that demonstrated the most promising results was the cellulosic ether, hydroxyethylcellulose (HEC). This hydroxylated cellulosic ether is a non-ionic water-soluble polymer. Its physiochemical properties are discussed in more detail in the following sections.

Cellulose is the most abundant naturally occurring polysaccharide. Being a polysaccharide it is a biodegradable and biocompatible polymer composed of polymerised sugar monomers. It is arranged predominately as linear 1,4-β-D'-glycosidic linked β-D-glucospyranose units that have the capacity to arrange themselves in closely formed arrangements through the formation of strong secondary hydrogen bonds and numerous other primary and secondary valence attachments. The resulting huge molecular structure is one that is rigid and poorly water soluble. It forms the main constituent of structural components in plants. Celluloses have very high molecular masses and due to their size and strong associative forces demonstrate poor water solubility.

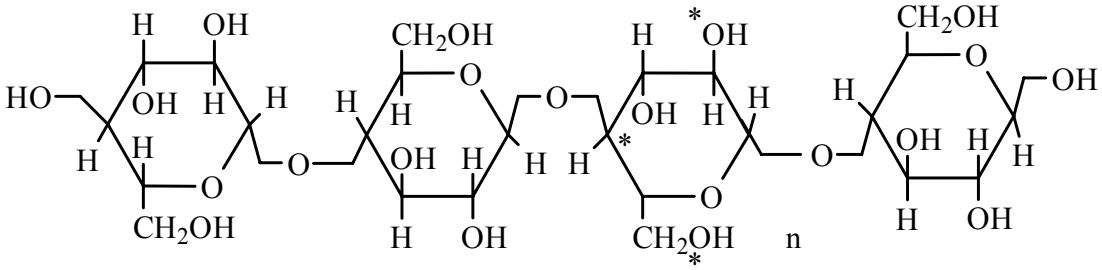

Figure 3.1: The chemical structure of cellulose composed of linear 1,4-β-D'-glycosidically-linked β-D-glucospyranose units. (Source: Ludwig, 2005).

Each anhydroglucose unit in the cellulose molecule has three reactive hydroxyl groups (depicted by (*) in Figure 3.1). Cellulosic ethers such as hydroxyethylcellulose (HEC) (Figure 3.2) are prepared by the action of ethylene oxide or ethylene chlorhydrin on alkali cellulose (cellulose treated with sodium hydroxide). This reaction occurs in two steps first, whereby ethylene oxide reacts at the hydroxyls (*) in the cellulose chain and subsequently ethylene oxide polymerizes to form a side chain. The polymer employed in this study has two units of ethylene oxide groups and a degree of substitution of 1.5, i.e. two units of hydroxyls substitutes in two units of ethylene oxide. These polymers are more soluble in water and alkaline solutions than native cellulose and insoluble in organic solvents. The hydroxyl groups attached to the ethyl groups imply that the polymeric chains are branched hence, do not associate as significantly as native cellulose (Whistler et al., 1953). Its application in the pharmaceutical industry includes formulation of controlled-release dosage forms (Alvarez-Fuentes et al., 2004; Andrews and Jones, 2006), as a binder and coating agent in tablets (Wade and Weller, 1994), and as a bioadhesive in muco-adhesive patches and implants (Dayal et al., 2005; Andrews and Jones, 2006).

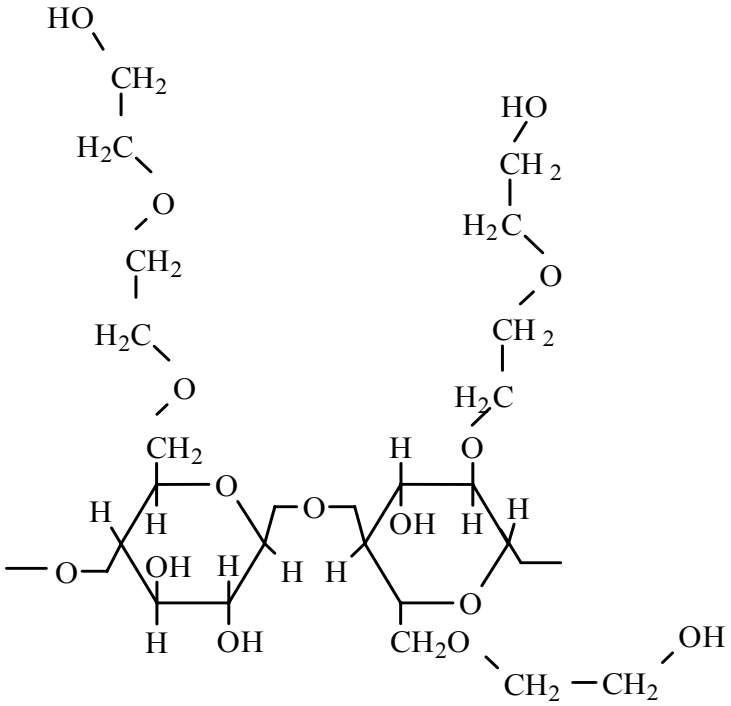

Figure 3.2: The chemical structure of the cellulosic ether hydroxyethylcellulose (HEC). (Source: Ludwig, 2005).

Initial studies indicated that the interaction between alginate and various celluloses and polyesters indicated extremely rapid matrix degradation and drug release rates. The interaction occurring between alginate and HEC was however exceedingly promising in this regard.

Recent studies employing combinations of the alginate and HEC to develop membranes have indicated concurring results of the presence of a synergistic interaction between the polymers (Naidu et al., 2005; Kalyani et al., 2006). The membranes developed have been applied in the field of chemical, petrochemical and the pharmaceutical industry. However no study thus far has employed the alginate-HEC combination in a crosslinked gelisphere matrix for the purpose of achieving sustained drug release.

Alginate salts such as sodium alginate undergoes gelation below a pH of 3 to form alginic acid. This fibrous precipitate of alginic acid demonstrates some significant physicochemical and physicomechanical properties which differ from its predecessor (Stanford, 1883; 1884; 1885; 1886). According to typical X-ray diffraction (XRD) profiles (Figure 3.3), it is observed that sodium alginate is not a flat molecule, like most celluloses, which have a typical fibre period of 10.0Å (Whistler et al., 1953). Alginate is an amorphous polymer with a fibre period of approximately 15.0Å. Alginic acid and sodium alginate have polymeric arrangements that differ in the skew symmetry and the conformation of the pyranose rings that lead to different physiochemical properties. Alginic acid has a fibre period of 8.7Å (Whistler et al., 1953), indicating that it is superiorly three-dimensional with a significantly greater negative rotation within the molecule. It demonstrates greater stability to hydration in comparison to its salt but is capable of absorbing approximately 200 to 300 times its weight of water and salts to the extent of 60% of its own weight (Hoagland and Lieb, 1915). It is insoluble in cold water and only mildly soluble in hot water and is significantly resistant to acidic degradation, however degrades in hot alkaline solutions after several days (Stanford, 1883; Percival and McDowell, 1967). In the unhydrated state it is rigid and extremely resistant to the action of solvents. As a colloid alginic acid may be considered an irreversible gel.

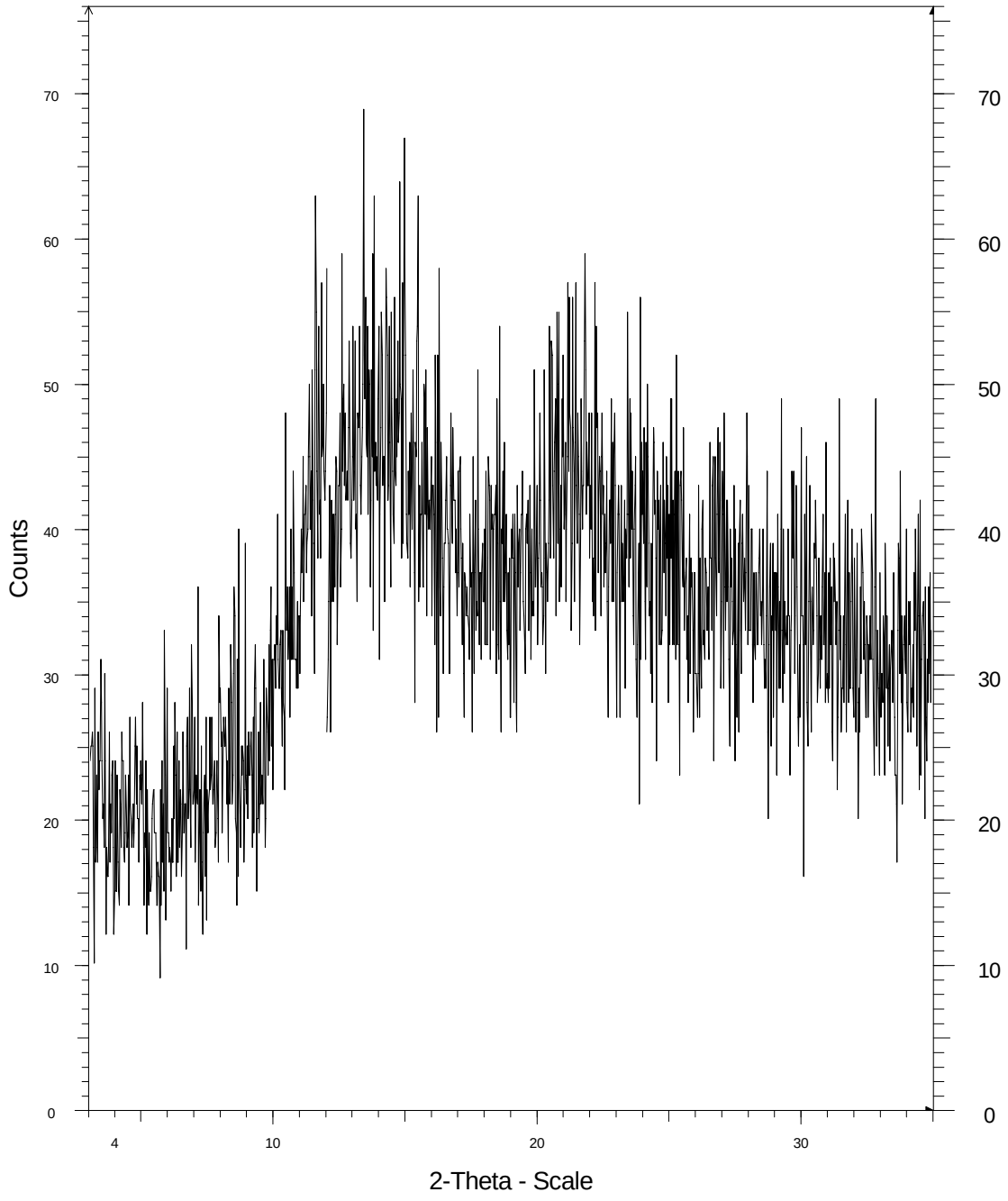

Figure 3.3: X-ray diffraction (XRD) profile observed for the G-rich sodium alginate (FMC BioPolymer) selected for further studies.

Polyacrylic acid (PAA) is also called a polyelectrolyte since each monomeric unit has an ionizable carboxylic acid group (Figure 3.4). PAA has the unique ability to absorb significant amounts of water significantly exceeding its own weight. For this study the PAA Carbopol® 934 was employed to coat the reinforced gelispheres. It is a lightly crosslinked branched chain polymer of polyacrylic acid. It has a high molecular weight of approximately 3 MDa and a pK_a between 5.35 and 7.2 (Mortazvi and Smart, 1995; Riley et al., 2001). At a low pH, the degree of dissociation of the carboxylic acid groups is low and the polymer adopts a coiled conformation, while at a high pH, the chain expands as a result of intra-polymeric electrostatic repulsions. The polymer appears more hydrophobic when the chain is in a compact conformation. It has been employed in the field of pharmaceutical drug delivery due to its unique muco- and bioadhesive properties (Cuña et al., 2001; Baloğlu et al., 2003).

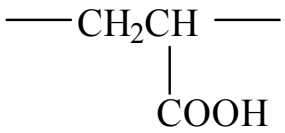

Figure 3.4: The chemical representation of the monomer in Carbopol® 934; the covalently crosslinked branched chain polymer employed to coat the crosslinked reinforced alginate gelispheres. (Source: Ludwig, 2005).

Its equilibrium swelling is highly affected by various factors including pH and ionic strength of the hydrating medium. In aqueous media with a physiological pH of 7.4, Carbopol® 934 exists as swollen gel particles. Inter-particulate contact is a prerequisite for gel formation. In the presence of cations the negatively charged carboxylic groups are shielded, resulting in less repulsion between the polymer chains. Polyacrylic acids appear to have an especially strong affinity for divalent cations such as zinc and calcium (Kriwet and Kissel, 1996; Lueßen et al., 1996). Complexation of the divalent cations with the polymer is dependant on the accessibility (which corresponds to the

degree of pH dependant ionisation) of carboxylic acid groups. It has also been suggested that divalent ions such as calcium may bridge adjacent carboxylic acid groups in the polymer (Kriwet and Kissel, 1996), which would influence the rheological properties by permitting the formation of more entangled networks within the hydrated gels.

Crosslinked systems have received much focus as a means of achieving prolonged release in drug delivery. The phenomenon of crosslinking or the formation of covalent bonds between individual, often heterogeneous polymeric chains allows the formation of macro-networks (illustrated in Figure 3.5) that have significantly greater dimensional stability, increased thermal and chemical resistance than either of the individual polymer systems (Rosen, 1993; Painter and Coleman, 1997). Thus their capacity to retard and significantly prolong drug release confers them suited for controlled release. The degree of crosslinking is a function of numerous factors, including the type of crosslinking agent employed, the concentration, crosslinking reaction time, polymer viscosity and molecular mass and concentration of the polymers (Al Musa et al., 1999).

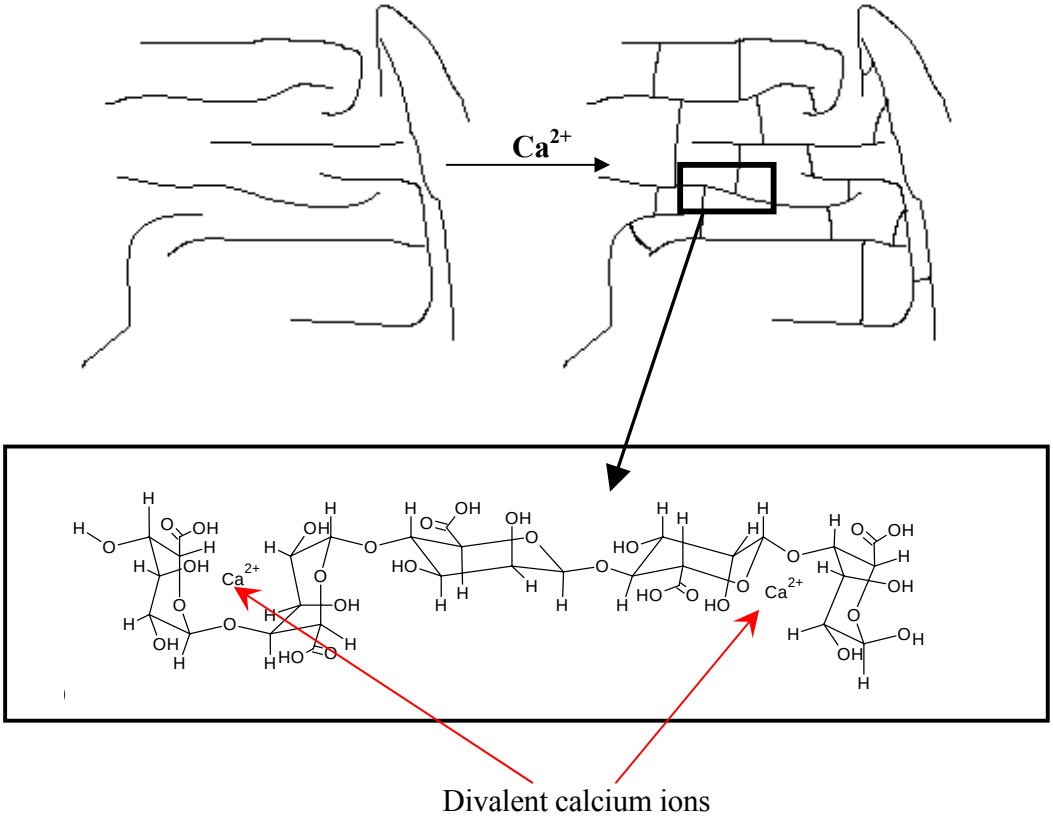

Figure 3.5: Schematic illustrating the mechanism of crosslinking of alginate G-units with divalent calcium ions.

Previous studies have focused on employing divalent and trivalent ions as crosslinking agents for hydrophilic polymers. In terms of drug delivery, this interaction has been evaluated in particular between the pectins and alginates (Cohen et al., 1997; Pillay and Fassihi, 1998; Miyazaki et al., 2000; Nokhodchi and Tailor, 2004; Pillay et al., 2005). The formation of crosslinks within the polymeric matrices leads to the formation of covalent bonds which causes precipitation of the insoluble hydrogel. Such crosslinking processes increase the rigidity of the polymer and reduce their swelling in solvents. This generally causes it to have a reduced permeability and release of incorporated drugs from polymeric matrices (Badwan et al., 1983, Al Musa et al., 1999).

The following sections discuss the physiochemical properties of the model neuroprotectant nicotine employed for the study. The three phase approach (discussed in detail further on) adopted for the formulation and optimisation of the multi-polymeric ionotropically crosslinked gelispheres is presented. Formulations are evaluated employing a combination of textural analysis, drug release studies, drug entrapment efficiency, enthalpic techniques and FTIR to elucidate the factors that mediated their physicomechanical behaviour on a molecular level.

3.2 Materials and Methods

Nicotine ((-)-1-methyl-2-(3-pyridyl)-pyrolidine) was purchased from Sigma Pharmaceuticals (Sigma Pharmaceutical Group; MA, USA). The polymers that the gelispheres comprised of included: Sodium alginate which was donated by FMC BioPolymer (Drammen, Norway) and hydroxyethylcellulose (HEC), which was donated by Hercules Inc., Natrosol® Pharm (Wilmington, DE, USA). The crosslinking agents employed were zinc sulphate, calcium chloride and barium chloride which were donated by UniLab, Saarchem (Pty.) Ltd. (Krugersdorp, Republic of South Africa).

3.2.1 Physiochemical Properties of Nicotine

Nicotine or (-)-1-methyl-2-(3-pyridyl)-pyrolidine is a bicyclic alkaloid with a pyridine ring and a pyrrolidine ring. The molecule possesses a chiral carbon (depicted in Figure 3.6), therefore exists in two enantiomeric forms. In nature, nicotine only exists in the S-enantiomer, which is levo-rotatory.

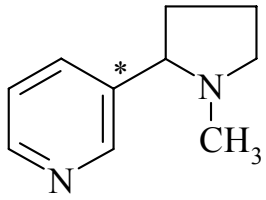

3-(1-Methyl-pyrrolidin-2-yl)-pyridine

Figure 3.6: The 2-dimensional representation of the S-enantiomer of nicotine. The (*) indicates the location of the chiral carbon. (Source: Armstrong et al., 1998).

It is a weak base with a pK_a of 8.0 and is soluble in both lipids and water. Native nicotine exists as a pale yellow pungent liquid. At physiological pH of 7.4, 31% of nicotine exists in the unionized form, hence can readily diffuse through biological membranes, including the BBB. The chemical properties of nicotine are briefly summarized in Table 3.1.

Table 3.1: The chemical properties of nicotine. (Source: CRC Handbook, 2004).

Property	Nicotine
Formula	$C_{10}H_{14}N_2$
Molecular weight	162,234 $g.mol^{-1}$
Melting point	-7.9°C
Boiling point	247°C
Basicity (pKa)	8.0
Ionization (pH 7.4)	69%
Aqueous solubility of tartarate salt (21ºC)	50mg/mL

A typical Fourier Transform Infrared (FTIR) spectrum of nicotine (Figure 3.7) indicates the following peaks that characterize its various chemical groups:

- Between 2700 and 2390 cm^{-1} indicates C-H stretching.
- The peak at 1647 cm^{-1} indicates an aromatic C=N double bond stretching.
- The peak at 1691 cm^{-1} aromatic C=C double bond stretching.
- The peaks at 717 cm^{-1} and 896 cm^{-1} correspond to the out of plane bending

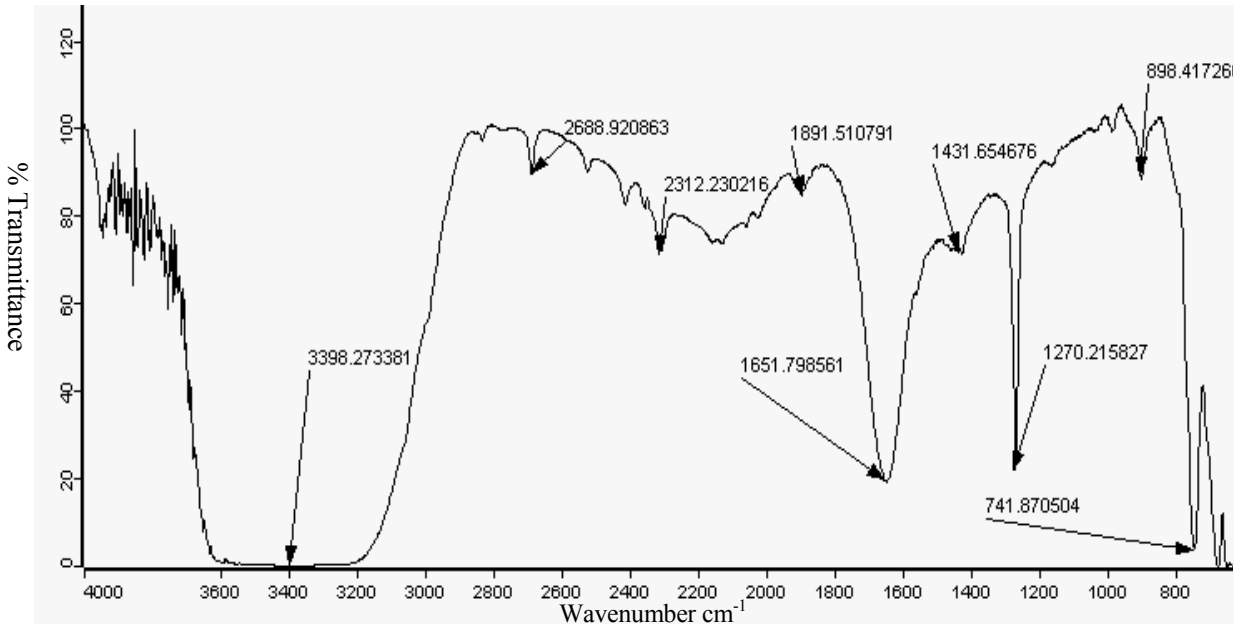

Figure 3.7: FTIR spectra of nicotine.

The hydrogen tartarate salt of nicotine (nicotine hydrogen tartarate or NHT), was employed for this study. It is a crystalline substance and is an extremely stable substance compared to the nicotine base, which is known to be highly unstable (Place et al., 1992). Upon exposure to aqueous medium, NHT dissociates to form tartrate ions and nicotine (Place et al., 1992). Figure 3.8a depicts the typical DSC profile obtained. The first distinct endothermic peak observed at 91.54ºC corresponds to the heat of fusion of the solid crystalline powder of the tartarate salt of nicotine. The second peak observed at 183.60ºC corresponds to the point when it is liberated from its salt and exists as pure nicotine in the liquid form. The peak seen at 207.09ºC corresponds to the temperature beyond which the liquid nicotine loses its crystalline properties and becomes an isotropic liquid.

A typical X-ray diffraction profile (XRD) (Figure 3.8b) indicates the presence of a significant peak at an angle of 17.95 2-Theta degrees which it is proposed corresponds to the pyrrolidine

ring. Smaller peaks observed at 22.49 and 27.08 2-Theta degrees correlate to the pyridine ring and methyl group respectively.

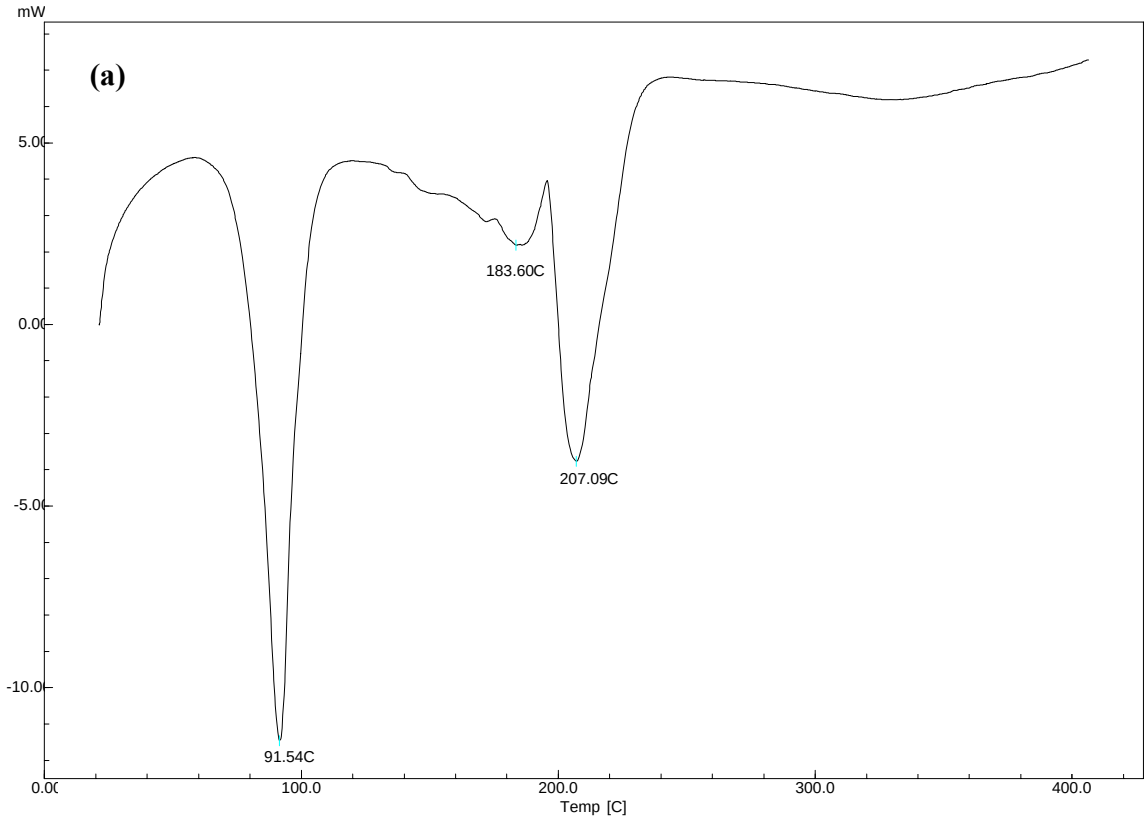

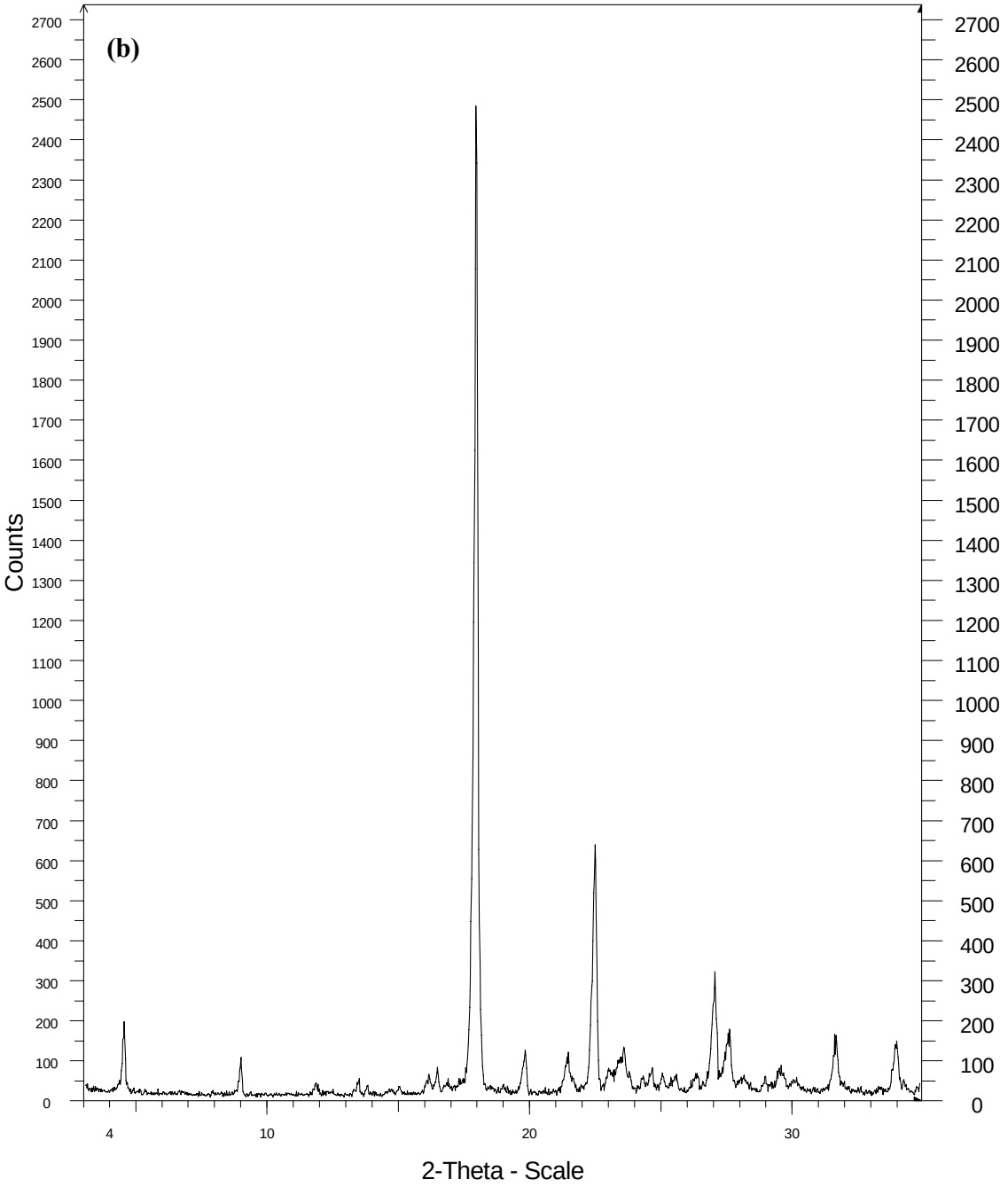

Figure 3.8: Typical (a) DSC and (b) X-ray diffraction (XRD) profile observed for the model neuroprotectant nicotine.

3.2.2 Standard Curve for Nicotine

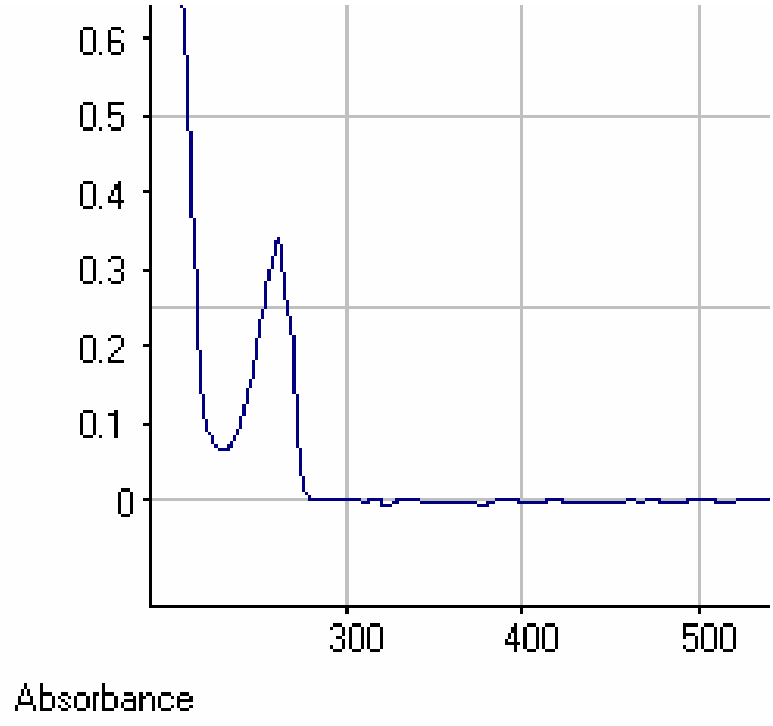

Figure 3.9: UV spectrum for nicotine (WinASPECT, Version 1.6.13.0, 2002, Analytik Jena AG, Germany).

The maximum UV absorption of nicotine occurs at a wavelength of 261nm (Figure 3.9). To generate the standard curve for nicotine three dilutions of nicotine were prepared in 0.1M PBS with a pH of 7.4 (Figure 3.10).

It was observed that the polymers employed to formulate the gelispheres, namely alginate and HEC, absorbed at a wavelength of 261nm. Since this interfered with an evaluation of nicotine absorbance at the same wavelength an alternative one was selected where the absorbance of nicotine was sufficiently significant but would not invite the same interference from the polymers. Hence samples were evaluated at 245nm to avoid interference from the constituent polymers with

nicotine UV absorption. Figure 3.10 indicates the calibration curve generated for nicotine at a wavelength of 245nm.

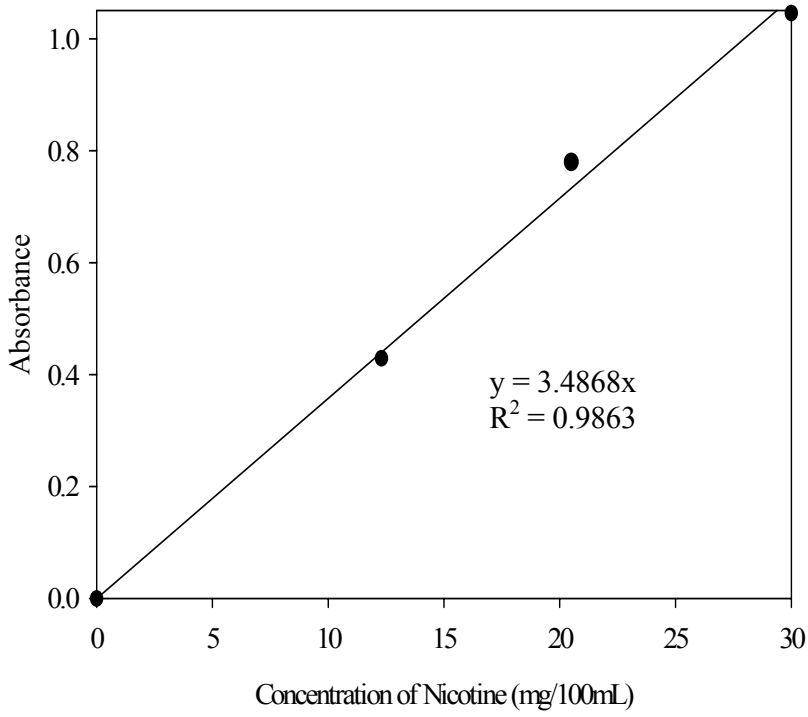

Figure 3.10: Standard curve for nicotine at a wavelength of 245nm in 0.1M PBS at pH 7.4.

Three Phase Approach Employed to Develop and Optimise the Crosslinked Multi-Polymeric Gelispheres

The study was divided into three phases. Phase I comprised of 12 formulations. Six of these formulations contained drug, while the remaining did not. Two polymers were employed, alginate and HEC in a fixed concentration ratio of $2\%^{w}/_{v}$:$1\%^{w}/_{v}$. These were denoted as the Alg-HEC gelispheres. These gelispheres were crosslinked with three cations namely, zinc, calcium and barium. Half of each set of formulations was exposed to dilute hydrochloric acid (HCl) to establish its effect on the swelling and drug release kinetics of the gelispheres. Based on the results, it was concluded that barium and calcium would be employed for further study, due to rapid degradation observed for zinc-crosslinked gelispheres. Phase II comprised a Plackett-Burman screening design

to identify the influence of 5 independent formulation variables, namely, the concentrations of the three polymers, alginate, HEC and PAA and crosslinking agents, barium (primary crosslinker) and calcium on the dependant factors, drug entrapment and drug release from the gelispheres (Alg-HEC-PAA gelispheres). Based on these findings, Phase III sought to optimise the crosslinked system based on the abovementioned parameters and expose the optimised system to dilute HCl. Within the distinct phases, studies were conducted to establish the scientific rationale which resulted in the observed physicomechanical behaviour of the developed systems.

3.2.3 PHASE I: Elucidating the Effect of Crosslinking Agent and Post-Curing Exposure to Dilute HCl on Multi-Polymeric Reinforced Gelispheres

3.2.3.1 Formulation of Crosslinked Reinforced Alg-HEC Gelispheres

Ionotropic gelation was employed to formulate the gelispheres. A dispersion comprising 2%$^{w}/_{v}$ alginate and 1%$^{w}/_{v}$ HEC (the reinforcing agent) in their native forms were prepared in double de-ionised water (Millipore® filter; pore size 0.22μm) and subsequently homogenized employing a vortex mixer (Lab Mixer-Emulsifier®, England). The dispersion employed the stated concentrations based on the fact that this resulted in a dispersion which was viscous enough to permit the generation of suitable gelispheres with adequate robustness. 1%$^{w}/_{v}$ nicotine was incorporated into the polymeric solution. Drug-free formulations were also prepared. The polymeric solution was titrated at a rate of 5mL/minute through a 23-gauge hypodermic syringe into a gently vortexed (VELP® Scientifica Microstirrer, Germany) crosslinking solution comprising either of 2%$^{w}/_{v}$ barium chloride, calcium chloride or zinc sulphate. The crosslinked alginate-HEC (Alg-HEC) gelispheres were gently agitated for an additional 30 minutes in the crosslinking solution and thereafter washed with 3x500mL de-ionized water. Formulations were

then exposed to dilute HCl subsequent to curing (Stanford, 1883; Bajpai and Sharma, 2004) to evaluate the effect of precipitating alginic acid in the crosslinked system on the swelling and hydration dynamics of the gelispheres.

Briefly, the gelispheres were immersed in 300mL of a gently vortexed (VELP® Scientifica Microstirrer, Germany) solution of 2M HCl for 15 minutes. Formulations were allowed to dry under an extractor at ambient conditions (21ºC) for 72 hours. The gelispheres were subsequently stored in a refrigerator at -5°C until further analysis. Table 3.2 summarizes the various formulations prepared during Phase I to evaluate the role of crosslinking agent and exposure to dilute HCl post-curing on drug entrapment efficiency, drug release and gelisphere erosion.

Table 3.2: Crosslinked Alg-HEC gelispheres prepared for Phase I.

Formulation Number	Crosslinking Solution	Post-curing Treatment
1	Barium chloride ($2\%^{w}/_{v}$)	-
2	Barium chloride ($2\%^{w}/_{v}$)	Exposed to HCl
3	Calcium chloride ($2\%^{w}/_{v}$)	-
4	Calcium chloride ($2\%^{w}/_{v}$)	Exposed to HCl
5	Zinc sulphate ($2\%^{w}/_{v}$)	-
6	Zinc sulphate ($2\%^{w}/_{v}$)	Exposed to HCl

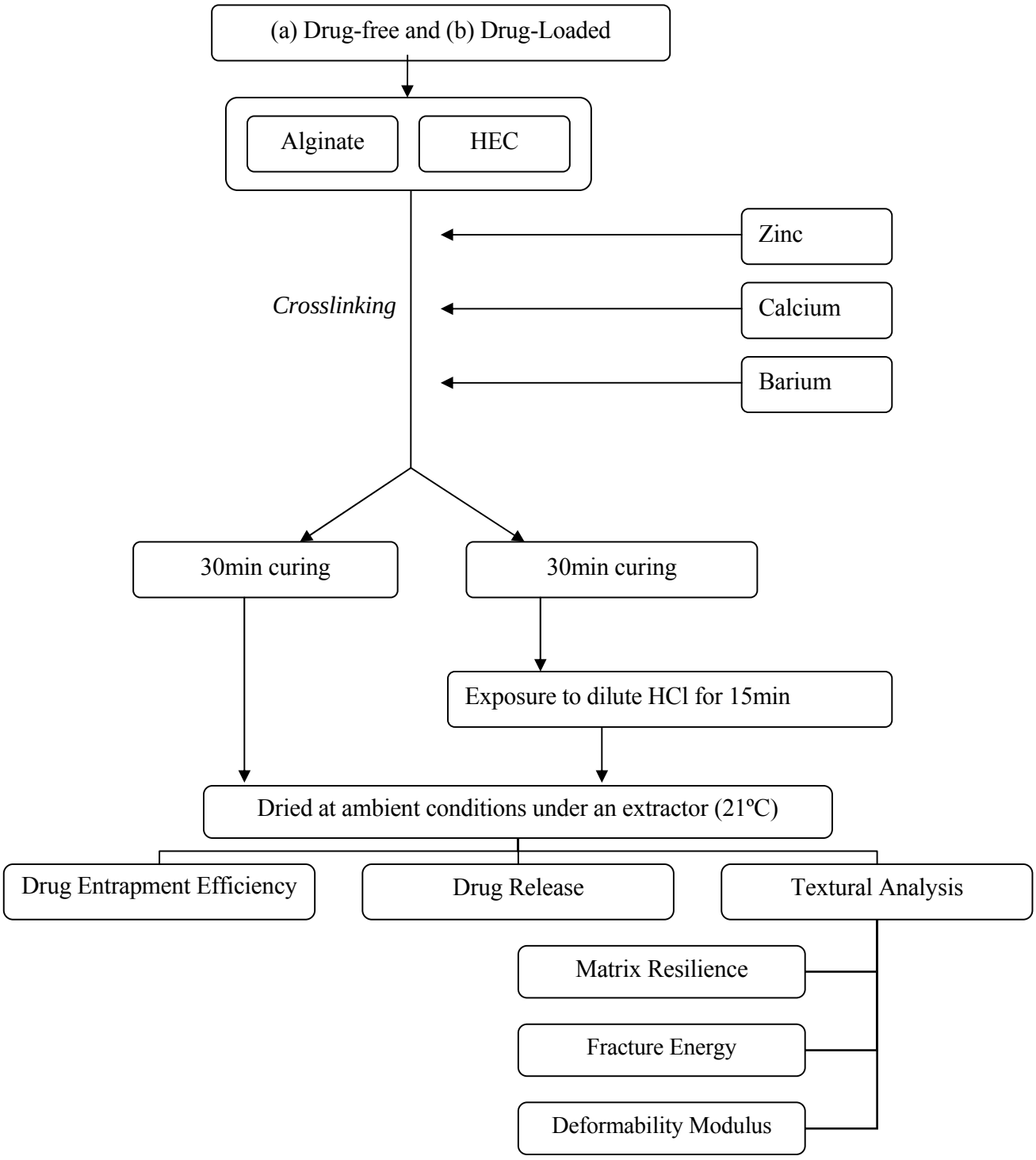

Figure 3.11: Schematic illustrating the methodology employed to formulate and analyse the Alg-HEC gelispheres.

3.2.3 PHASE II: Formulation and Evaluation of Reinforced Multi-Polymeric Gelispheres Employing a Design of Experiments Approach

3.2.4.1 Formulation of Alg-HEC-PAA Gelispheres in Accordance with a Plackett-Burman Screening Design

The study aimed to elucidate new mechanisms of interaction between the various components of the developed reinforced crosslinked multi-polymeric device (Chapter 1). In order to understand the influence of various processing factors on the properties of the nicotine-loaded crosslinked gelispheres a Design of Experiments approach was adopted. This entailed the use of the Plackett-Burman screening design (Plackett and Burman, 1946). The formulation variables evaluated included, evaluation of the influence of the concentrations of alginate, the reinforcing agent HEC, and the crosslinking ions barium and calcium. The influence of a third biodegradable hydrophilic polymer PAA on the properties of the matrix was also evaluated. PAA was included in the crosslinking solution, and not in the polymer dispersion. The responses of these factors were evaluated on both the physicochemical and physicomechanical level. Equation 3.1 was employed to screen responses in accordance with this statistical design.

$$\text{Response} = b_0 + b_1[\text{Alginate}] + b_2[\text{HEC}] + b_3[\text{PAA}] + b_4[CaCl_2] + b_5[BaCl_2]$$

Equation 3.1

Where, $b_1 – b_5$ represent the coefficient constants for the concentrations of Alginate, HEC, PAA, $CaCl_2$ and $BaCl_2$ respectively.

Nicotine-loaded multi-polymeric gelispheres were formulated according to a Plackett-Burman (PB) statistical design template (Table 3.3) that allowed various combinations and permutations of polymers and crosslinking agents to be formulated employing ionotropic gelation as described previously in Section 3.3.4.1. These gelispheres are referred to as the Alg-HEC-PAA gelispheres.

Table 3.3: The Plackett-Burman design template employed to optimise drug-loaded Alg-HEC-PAA gelispheres indicating the various combinations and permutations of polymers (alginate, HEC and PAA) and crosslinking agents (calcium and barium) that were employed.

Formulation Number	Alginate ($\%^{w}/_{v}$)	HEC ($\%^{w}/_{v}$)	PAA ($\%^{w}/_{v}$)	$CaCl_2$ ($\%^{w}/_{v}$)	$BaCl_2$ ($\%^{w}/_{v}$)
1	2.5	1.00	0.5	2	2.00
2*	2.0	0.75	1.0	1	1.25
3	2.5	0.50	1.5	0	0.50
4	1.5	0.50	0.5	0	0.50
5	1.5	1.00	1.5	0	2.00
6	2.5	1.00	1.5	0	2.00
7	1.5	0.50	0.5	2	2.00
8	2.5	0.50	0.5	0	2.00
9	1.5	0.50	1.5	2	2.00
10	1.5	1.00	1.5	2	0.50
11	2.5	1.00	0.5	2	0.50
12	2.5	0.50	1.5	2	0.50
13*	2.0	0.75	1.0	1	1.25
14	1.5	1.00	0.5	0	0.50

* *centrepoints*

3.2.4 Determination of Drug Entrapment Efficiency

Evaluation of the drug entrapment efficiency (DEE) was conducted in triplicate on 200mg of nicotine-loaded gelispheres. The gelispheres were agitated with the aid of a homogenizer (VELP® Scientifica Microstirrer, Germany) in 500mL PBS (0.1M; pH 7.4) for 72 hours under ambient conditions. A 5mL aliquot was removed and centrifuged (Minor® Centrifuge, MSE, England) for 15 minutes at 5000rpm. The clear supernatant was subsequently filtered through a Millipore® filter (0.45μm pore size) in order to remove any contaminants or residual polymer. Thereafter they were analysed by UV spectroscopy (WinASPECT, Version 1.6.13.0, 2002, Analytik Jena AG, Germany), at a wavelength of 245nm employing a Beckman® DU 650 Ultraviolet Spectrophotometer (Germany).

Equation 3.2 was employed to determine the DEE of the gelispheres.

$$\% \text{ DEE} = \frac{\text{(Actual Drug Entrapment)}}{\text{(Theoretical Drug Entrapment)}} \times 100 \qquad \text{Equation 3.2}$$

The theoretical drug entrapment was calculated as a ratio of the amount of nicotine incorporated into the polymeric dispersion and the combined amount of drug and polymers in the dispersion.

3.2.5 Evaluating *In Vitro* Drug Release Characteristics of Alg-HEC and Alg-HEC-PAA Gelispheres

In vitro drug release studies were performed in triplicate on 100mg of nicotine-loaded crosslinked Alg-HEC and Alg-HEC-PAA gelispheres. An environment which simulated CSF was provided to conduct drug release studies. In order to achieve this, the gelispheres were immersed in 100mL 0.1M phosphate buffered saline (PBS) of pH 7.4, maintained at 37°C in sealed 100mL glass jars that were placed in a shaker bath (Labex, Stuart SBS40®, South Africa) and agitated at 50rpm. At 3 hour intervals 5mL samples of the solution were removed, following which they were centrifuged (Minor® Centrifuge, MSE, England) for 15 minutes at 5000rpm. The clear supernatant was subsequently filtered through a Millipore® filter (0.45μm pore size) in order to remove any contaminants or residual polymer. Samples were analysed by UV spectroscopy at a wavelength of 245nm. An equal volume of drug-free PBS was replaced into the glass bottles to maintain sink conditions.

3.2.6 Textural Analysis of Hydrated of Alg-HEC and Alg-HEC-PAA Gelispheres

The Texture Analyser (TA*XT.plus,* Stable Micro Systems®, Surrey, UK) was employed to conduct textural analysis of the gelispheres (N=5). The texture analyser was fitted with a 10mm cylindrical steel probe and a 40kg load cell was used. Matrix resilience, deformability modulus and fracture energy of the crosslinked Alg-HEC gelispheres were assessed in both the unhydrated and hydrated state. Typical test parameters are indicated in Section 2.2.3 (Chapter 2). Data acquisition was performed at 200 points per second.

In order to determine the effect of hydration, the gelispheres were immersed in 100mL simulated CSF (PBS 0.1M; pH 7.4 37°C; 50rpm) in a shaker bath (Labex, Stuart SBS40®, South Africa). Samples were analysed at 1, 2, 3, 6, 9 and 12 hours. Studies were conducted in triplicate.

3.2.7 Analysis of Gelisphere Volume Changes following Hydration

An Olympus Stereo Microscope, Model SZX-D2-200, equipped with an Olympus SZX-TR30 camera (Tokyo, Japan) was used to evaluate changes in the surface morphology and volume of the gelispheres over time following exposure to hydration. AnalySIS Version 3.2 (Soft Imaging Systems, Japan) was employed to evaluate the images. The mean of three mutually perpendicular diameters of the gelispheres were measured and sphere volume (V_s) calculated employing Equation 3.3.

$$V_s = \frac{4}{3}\pi r^3 \qquad \text{Equation 3.3}$$

Where, r is the radius of the gelispheres (mm).

The change in gelispheres diameter following exposure to hydration was evaluated to establish the degree of swelling and the mechanism of matrix degradation. Studies were conducted in triplicate.

3.2.8 Thermal Analysis of Alg-HEC and Alg-HEC-PAA Gelispheres

Thermal analysis of the Alg-HEC gelispheres was performed employing differential scanning calorimetry (DSC). Differential scanning calorimetry is a technique employed to evaluate the influence of applied heat and analyze thermal transitions of polymeric systems. A linear temperature gradient at a rate of 5˚C per minute was used from 25 - 400˚C (Perkin Elmer Pyris-1). Approximately 5mg of the samples were placed within crimped aluminium pans and subjected to analyses.

3.2.9 Analysis of Polymer-Polymer and Drug-Polymer Interactions Employing FTIR Spectroscopy

Fourier Transform Infrared (FTIR) studies were conducted on pure nicotine and the native polymers, namely Alginate and HEC and the crosslinked multi-polymeric gelispheres at 21°C (Nicolet Impact 400D; Nicolet Instrument Corporation, Oreland, Pennsylvania, USA). Samples of 20mg were mixed with 2g of potassium bromide and triturated. From this mixture, 150mg was compressed with 8 tons force in a Beckman® Hydraulic Press (Beckman Instruments, Inc., Fullerton, USA) to produce transparent discs. The discs were inserted into the spectrophotometer cell and transmittance profiles generated.

3.2.10 Analysis of Changes in Surface Morphology of Hydrated Alg-HEC-PAA Gelispheres

An Olympus® Stereo Microscope (Model SZX-D2-200) fitted with an Olympus® SZX-TR30 camera (Tokyo, Japan) was employed to evaluate transitions in surface morphology of the Alg-HEC-PAA gelispheres over 50 hours following exposure to simulated CSF as described in Section 3.2.6.

Scanning Electron Microscopy (SEM) was also employed to view changes in surface morphology of the Alg-HEC-PAA gelispheres at an enhanced magnification. Dried samples of the gelispheres were coated with a thin layer of colloidal graphite. Thereafter they were mounted onto aluminium stubs and coated with a thin layer of gold-palladium under an electrical potential of 20keV. Samples were viewed in the FE-SEM (JEOL JSM-840, Tokyo, Japan) at various magnifications employing probe currents between 60-30 nanoamps.

3.2.12 PHASE III: Formulation Optimisation Studies

3.2.12.1 Statistical Optimisation of Alg-HEC-PAA Gelispheres

Drug release profiles generated from formulations from the PB Design indicated first-order kinetics with a burst effect. Optimisation was carried out through the application of a Design of Experiments response optimiser function employing Minitab Software (Release 14, Minitab Inc., USA) that allows simultaneous optimisation of responses. Optimised formulations were maximized for DEE and minimized for drug release at t=1 hour to achieve a minimal burst effect.

3.2.12.2 Precipitating Alginic Acid in Optimised Formulations as a Means to Retard Gelisphere Swelling

As discussed in the previously, exposure of gelispheres to dilute HCl resulted in matrices that swelled at a slower rate and therefore retarded drug release effectively. The optimised formulation from the PB template was exposed to 300mL 2M HCl post-curing as discussed in Section 3.2.2 and analysed for drug release, drug entrapment and swelling behaviour.

3.3 Results and Discussion

3.3.1 PHASE I: Elucidating the Effect of Crosslinking Agent and Post-Curing Exposure to Dilute HCl on Multi-Polymeric Reinforced Gelispheres

3.3.1.1 Analysis of Physicomechanical Properties of Drug-free Alg-HEC Gelispheres

Evaluating the physicomechanical properties of drug-free formulations provided insight into the nature and possible mechanism of inter-polymeric interactions as well as elucidation of the influence of the crosslinking ions on the robustness of the gelisphere matrices.

The stereomicrographs in Figure 3.13 depict the changes within the matrices following hydration.

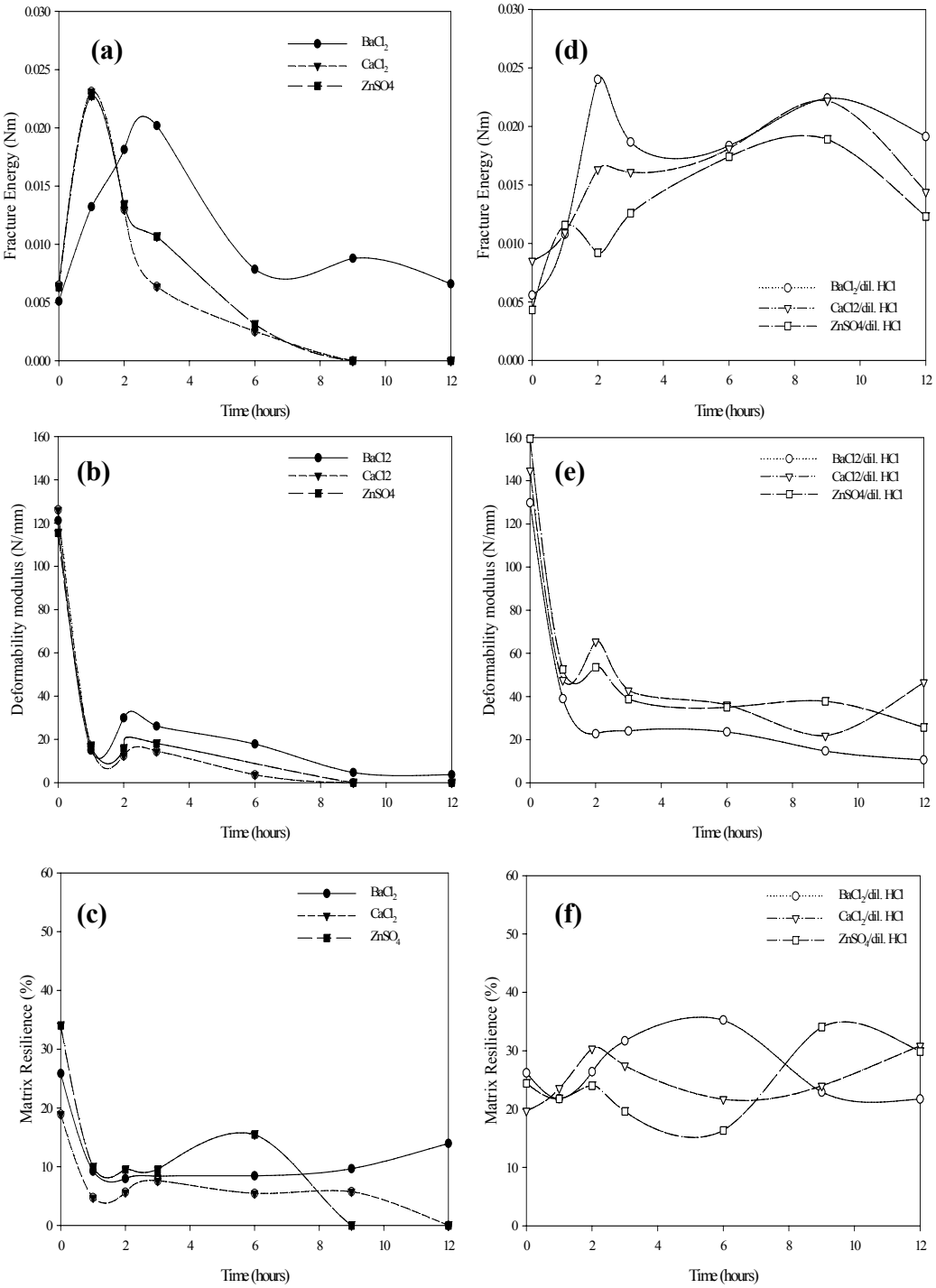

Figure 3.12: (a) Fracture energy (Nm) (SD<0.001Nm), (b) Deformability modulus (N/mm) (SD<7.11N/mm) and (c) Matrix resilience (%) (SD<0.54%) of drug-free unexposed Alg-HEC gelispheres and (d) Fracture energy (Nm) (SD<0.0014Nm), (e) Deformability modulus (N/mm) (SD<4.334N/mm) and (f) Matrix resilience (%) (SD<1.40%) of drug-free HCl-exposed Alg-HEC gelispheres, over a period of 12 hours following exposure to simulated CSF (N=5).

Upon exposure to PBS the gelispheres undergo typical 'concentric-hydration' that results in the transient increases in fracture energy of the gelispheres (discussed in Chapter 2). This phenomenon was particularly evident with matrices exposed to dilute HCl post-curing. While unexposed zinc and calcium-crosslinked matrices virtually disintegrated by the 9^{th} hour to PBS exposure (indicated by the negligible fracture energies at t=9 hours), those crosslinked with barium remain significantly more intact (fracture energy at t=9 hours was approximately 8.80 x 10^{-3} Nm). HCl-exposed matrices remain unchanged from their initial state of equilibrium achieved within the first hour of exposure to PBS. As expected the deformability moduli for all formulations declined following exposure to PBS, with the most significant change occurred within the first hour of exposure. Unexposed matrices experienced a decline in the deformability modulus (hardness) after the first hour of exposure to PBS of between 87.64 - 85.19%, while the decline observed for HCl-exposed matrices was smaller, between 67.03 - 69.96%.

With regards to the porosity of the matrices, HCl-exposed matrices did not indicate any significant change following the decline observed within the first 3 hours of exposure to PBS. The matrix resilience of unexposed gelispheres declined by approximately 18.30% within the first hour of exposure to PBS, while that of HCl-exposed matrices declined by only 2.65% and 4.42% for zinc and barium-crosslinked matrices respectively. For calcium-crosslinked matrices, this increased by 3.87% within the same period of time (t=3 hours). This may be due to the capacity of divalent calcium ions to attract and accommodate more water molecules within crosslinked G-units due to their higher co-ordination number (Chapter 2, Section 2.3.2). Barium ions, on the other hand did not offer sufficient space within the crosslinked pockets due to their large atomic size, despite comparative water attracting capacity. Zinc ions were too small to develop sufficiently crosslinked

pockets within the polymer, hence allowed the matrix to unravel more rapidly following initial water penetration.

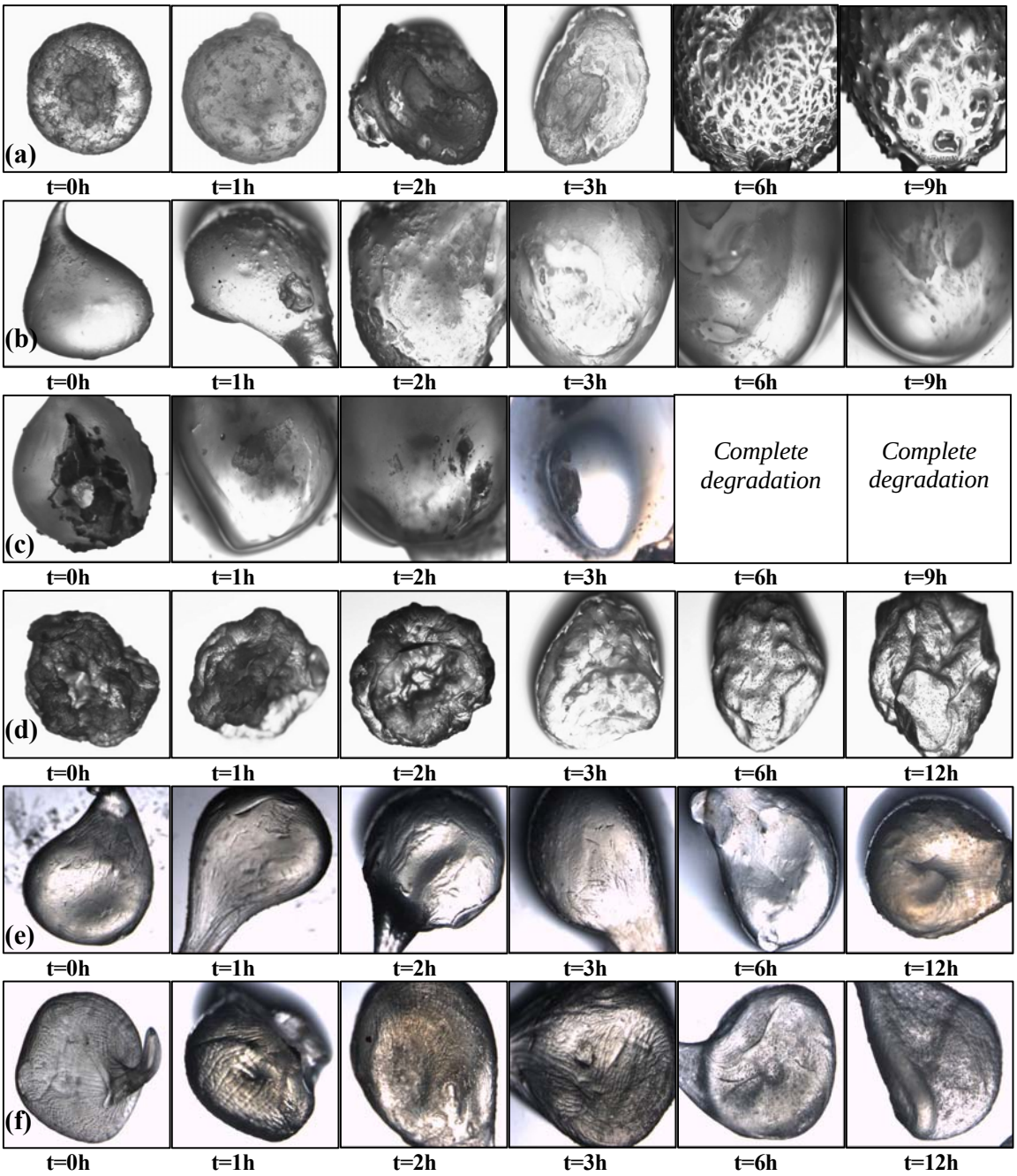

Figure 3.13: Stereomicrographs (Magnification x16) indicating changes in surface morphology of drug-free Alg-HEC gelispheres crosslinked with (a) $BaCl_2$, (b) $CaCl_2$, (c) $ZnSO_4$, (d) $BaCl_2$/dil. HCl, (e) $CaCl_2$/dil. HCl, and (f) $ZnSO_4$/dil. HCl, following exposure to simulated CSF over a period of 12 hours.

3.3.1.2 Analysis of Physicomechanical Properties of Drug-loaded Alg-HEC Gelispheres

3.3.1.2.1 Unhydrated Drug-loaded Alg-HEC Gelispheres

The unhydrated gelispheres revealed the nature of the drug-loaded matrices prior to exposure to simulated CSF (0.1M PBS; pH 7.4; 37ºC; 50rpm). Textural analysis indicated a general trend of higher matrix robustness among gelispheres exposed to dilute HCl (Figure 3.14a-c). Calcium and barium-crosslinked matrices were robust and compact, while zinc-crosslinked matrices were porous.

(a)

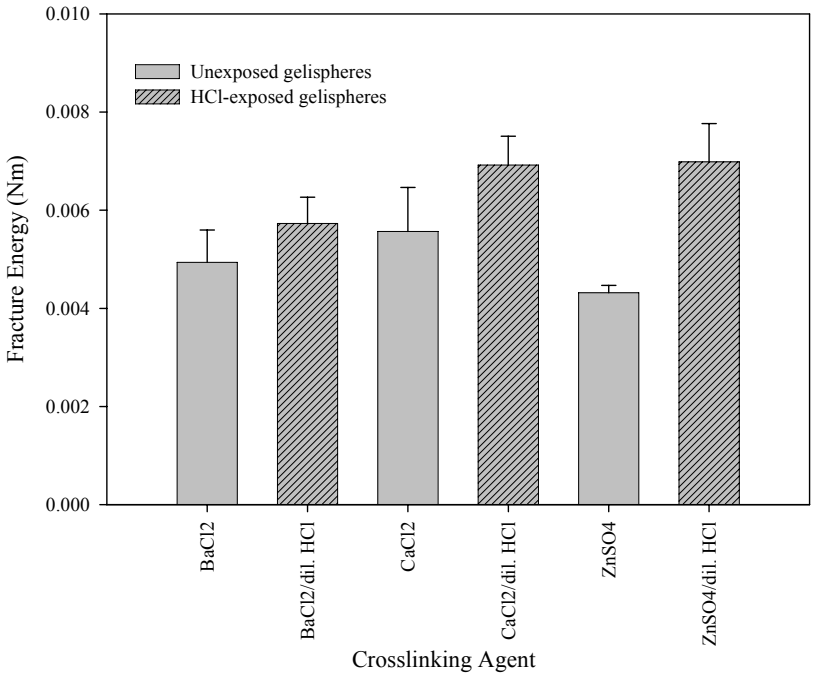

(b)

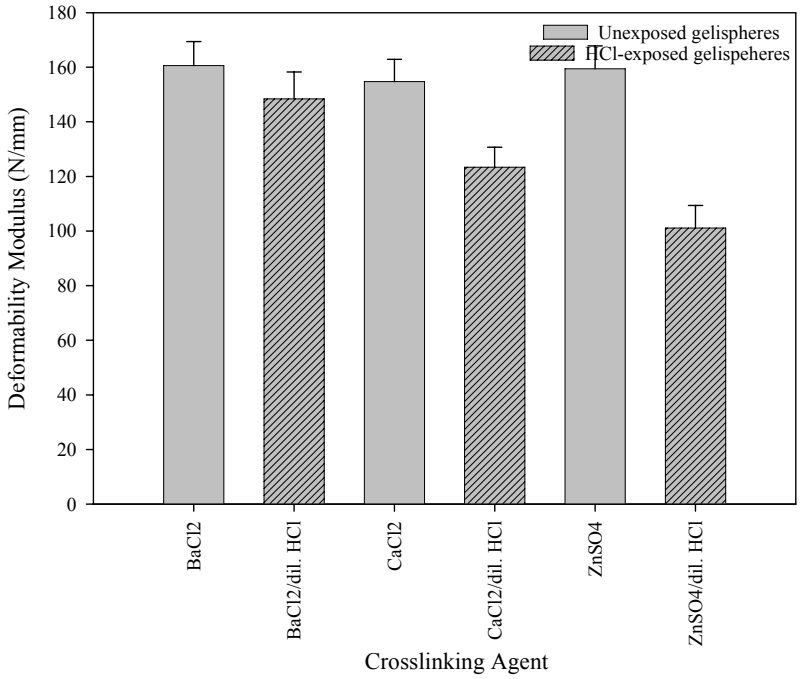

(c)

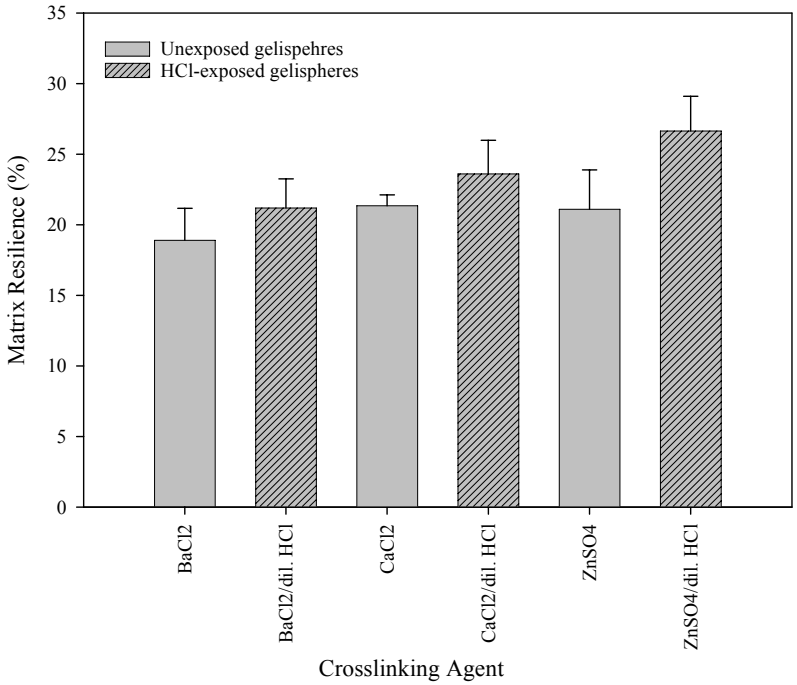

Figure 3.14: Textural analysis indicating the (a) Fracture energy (Nm) (SD<0.0001Nm), (b) Deformability modulus (N/mm) (SD<3.15N/mm) and (c) Matrix resilience (%) (SD<1.96%) of unhydrated drug-loaded Alg-HEC gelispheres crosslinked with various crosslinking agents (N=5).

Results were congruent with those obtained in Chapter 2, however it is essential to indicate here that a general trend of lower matrix resilience, higher deformability modulus and fracture energy were observed for the corresponding matrices that employed only A5 (G-rich alginate, Chapter 2) as the polymeric framework of the gelispheres, in comparison to the multi-polymeric system developed in this study. Furthermore, all formulations exposed to dilute HCl post-curing demonstrated correspondingly higher values for fracture energy and matrix resilience and lower values for deformability modulus. This conferred to greater robustness of the gelispheres, which in turn had a positive impact on retarding matrix degradation and drug release kinetics.

With regards to matrix porosity, matrix resilience of HCl-exposed gelispheres was higher by approximately 2.30% - 5.55% than their unexposed counterparts. This implied that the porosity of the unexposed matrices decreased when dried following curing. The nature of water loss with HCl-exposed gelispheres occurred through an alternative mechanism, such that it lead to a contraction of the matrix and thus resulted in a lower matrix porosity. The HCl-exposed matrices were significantly brittle in comparison to the unexposed gelispheres. Fracture energies were higher by 7.94 - 26.69 x 10^{-4} Nm. The deformability moduli declined by 12.24 - 58.36N/mm following exposure to dilute HCl post-curing.

As discussed in Chapter 2 the crosslinking ions with larger ionic radii, such as barium, enabled a greater degree of 'networking' of the polymeric matrix and therefore permitted the matrices to be more compact. The adjacent polymeric strands within the matrix were drawn closer together due to the larger cationic radii. Thus the order of matrix compactness

was as follows: Zinc<Calcium<Barium. This phenomenon was observed to concur for all matrices regardless of exposure to dilute HCl. Following exposure, the variation between the robustness was most significant with zinc-crosslinked matrices. The hardness of zinc-crosslinked matrices increased by 58.44N/mm. In comparison, the difference between barium-crosslinked matrices exposed to dilute HCl and the unexposed was 12.24N/mm.

3.3.1.2.2 Textural Analysis of Hydrated Drug-loaded Alg-HEC Gelispheres

Textural analysis of nicotine-loaded gelispheres indicated the presence of more compact matrices entrapping the drug that eroded at a slower rate from drug-free gelispheres. It is proposed that the presence of secondary dipole-dipole interactions between lone pairs of nitrogen ions in the heterocyclic rings in nicotine may interact with carboxylic acid and hydroxyl groups of the polymers, thus generating a superiorly compact network which was more resistant to degradation.

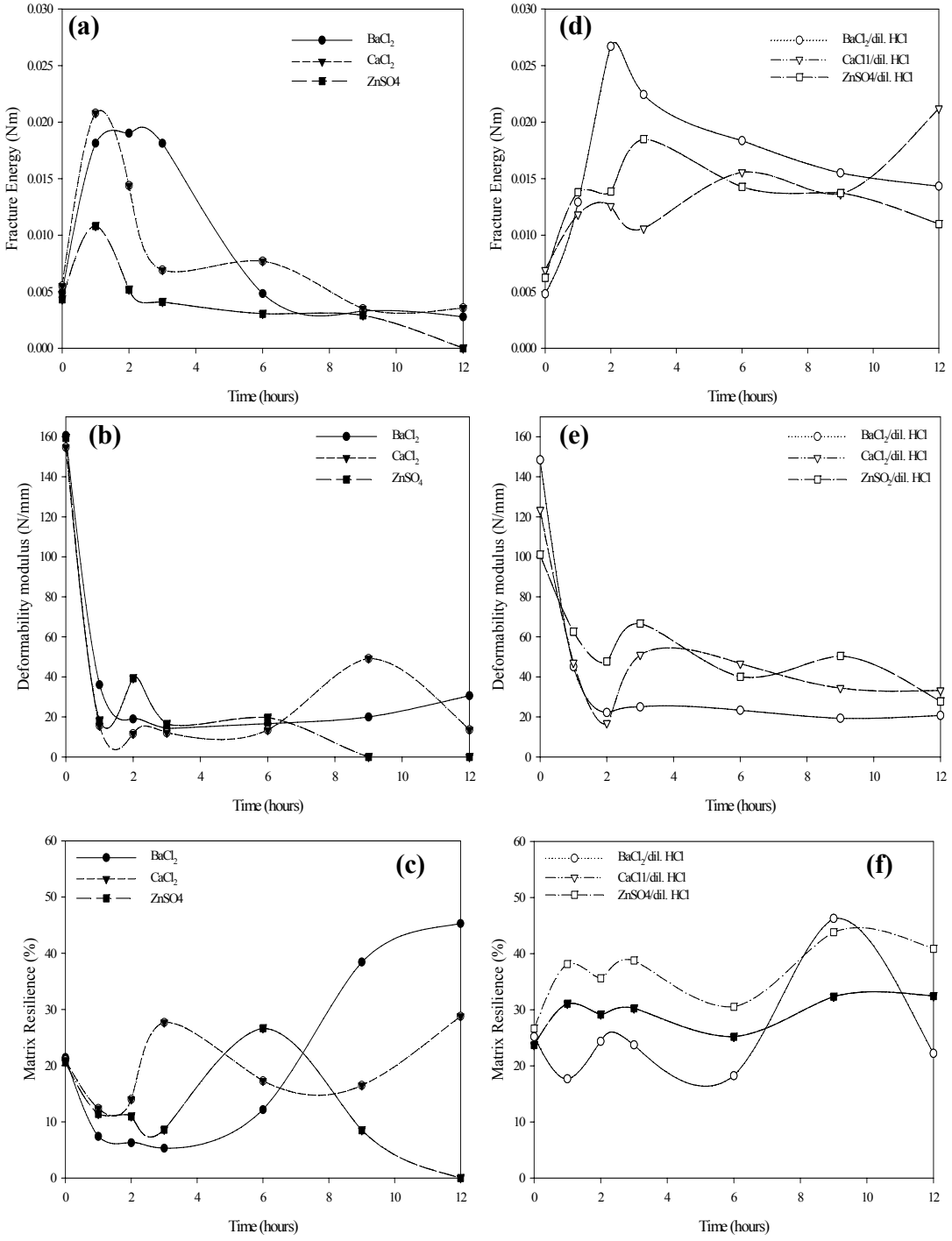

Figure 3.15: Changes in the physicomechanical properties observed in the (a) Fracture energy (Nm) (SD<0.0006Nm), (b) Deformability modulus (N/mm) (SD<9.87N/mm) and (c) Matrix resilience (%) (SD<3.4%) of drug-loaded Alg-HEC gelispheres and (d) Fracture energy (Nm) (SD<0.0004Nm), (e) Deformability modulus (N/mm) (SD<10.32N/mm) and (f) Matrix resilience (%) (SD<1.27%) of drug-free HCl-exposed Alg-HEC gelispheres, following exposure to simulated CSF, to over a period of 12 hours (N=3).

Results demonstrated that when nicotine was incorporated into the polymeric matrix, the behaviour of the gelispheres concurred with drug-free formulations. Following hydration, the gelispheres attracted solvent molecules into the matrix thus allowing water molecules to enter the crosslinked pockets within the network. Hence the gelispheres exhibited a greater fracture energy value since, energy was accommodated within the voids of the matrix. With the exception of barium-crosslinked gelispheres the fracture energies of hydrated gelispheres declined appreciably after t=3 hours of exposure to PBS. Barium-crosslinked gelispheres retained higher fracture energies up to t=6 hours before any significant decline was observed. Transient increases in fracture energy and deformability moduli demonstrated the typical concentric mechanism of matrix degradation discussed in Chapter 2. HCl-exposed matrices demonstrated a significantly greater and sustained fracture energy for the corresponding crosslinking ions verses unexposed formulations. HCl-exposed barium-crosslinked demonstrated the highest fracture energies over time. This indicated the presence of significant interaction between the two polymers and the large divalent barium ions that enabled the generation of formulations significantly resistant to degradation, which correlated with the rate of drug release observed (discussed further in Section 3.3.1.7).

Deformability moduli declined appreciably within the first hour of exposure to simulated CSF. The most appreciable decline was observed in unexposed zinc-crosslinked matrices. In contrast the HCl-exposed zinc-crosslinked matrices demonstrated the least decline in matrix hardness i.e. deformability modulus. This discrepancy was approximately 44.41N/mm, and the most significant among the gelispheres. This phenomenon was

interesting since the initial (unhydrated) deformability moduli for the unexposed gelispheres was greater, while following hydration, the decline experienced was also significant. Thus it was observed that exposure of the gelispheres to PBS resulted in a rapid influx of water and ion exchange into the matrix that allowed an increased rate of degradation. In contrast, the rate of water penetration and ion exchange (sequestration) for the HCl-exposed matrices was retarded by the reduced interaction between water molecules and the unionized alginate (alginic acid).

Initially observed higher values for matrix resilience were sustained for the HCl-exposed matrices throughout the hydration study. However, the porosity of the HCl-exposed matrices was found to be a function of the nature of crosslinking agent employed. As observed previously, zinc-crosslinked matrices generated more porous matrices, followed by calcium and then barium. With regards to unexposed matrices, barium demonstrated significantly increased porosity following t=6 hours of exposure to PBS. When combined with the high values for fracture energy and deformability modulus at the same time, it was concluded that this was primarily due to an increased uptake in water i.e. gelispheric swelling (Figure 3.15 and 3.16) and not due to matrix degradation. Unexposed zinc-crosslinked matrices appeared to disintegrate appreciably by t=9 hours of exposure to PBS, indicating that ions had a very minimal interaction with the polymers and were unable to retain the structural properties of the matrix for a sustained period of time.

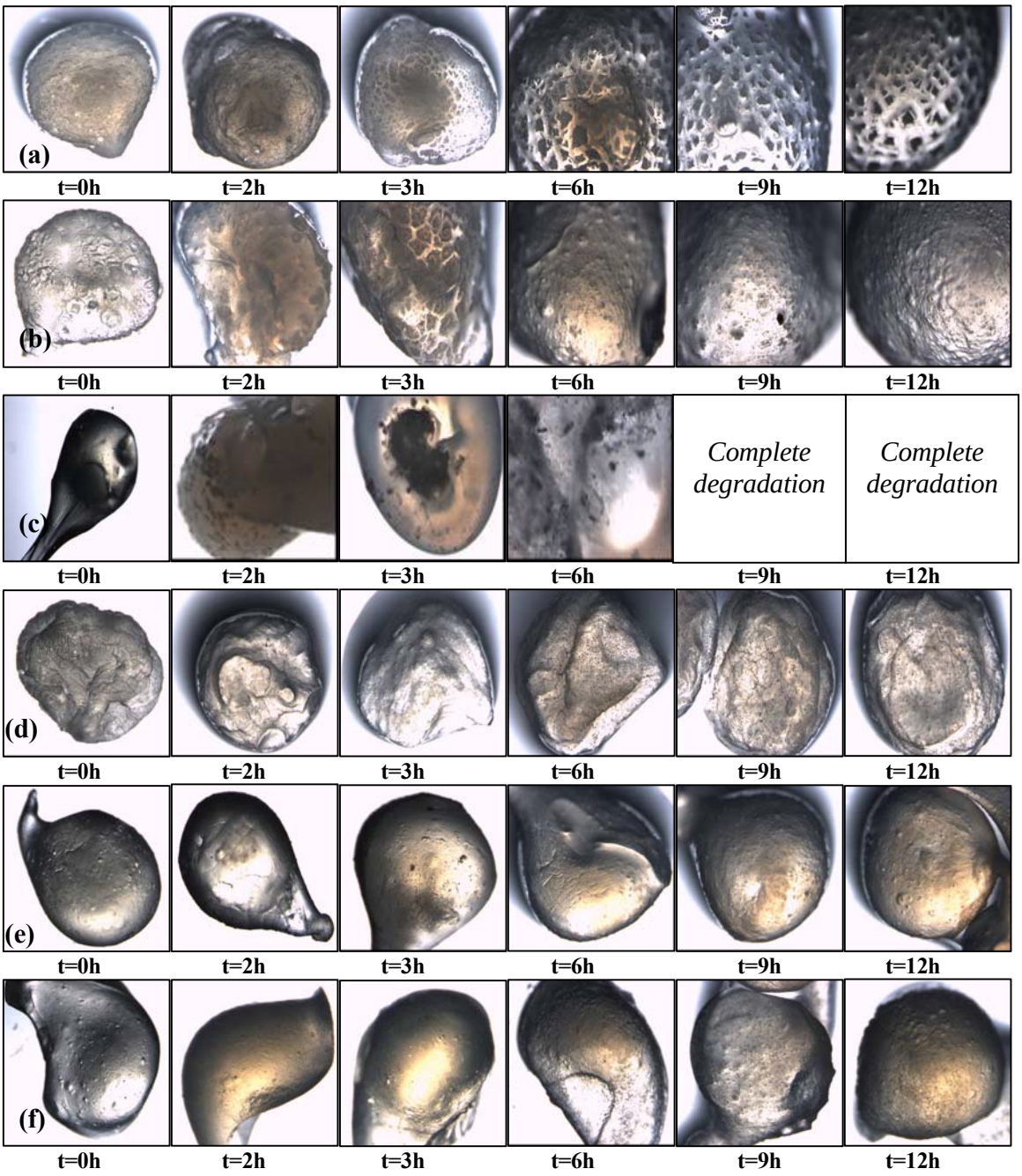

Figure 3.16: Stereomicrographs (Magnification x16) indicating changes in surface morphology of nicotine-loaded Alg-HEC gelispheres crosslinked with (a) $BaCl_2$, (b) $CaCl_2$, (c) $ZnSO_4$, (d) $BaCl_2$/dil. HCl, (e) $CaCl_2$/dil. HCl, and (f) $ZnSO_4$/dil. HCl, following exposure to simulated CSF, to over a period of 12 hours.

3.3.1.3 Swelling Behaviour of Hydrated Alg-HEC Gelispheres

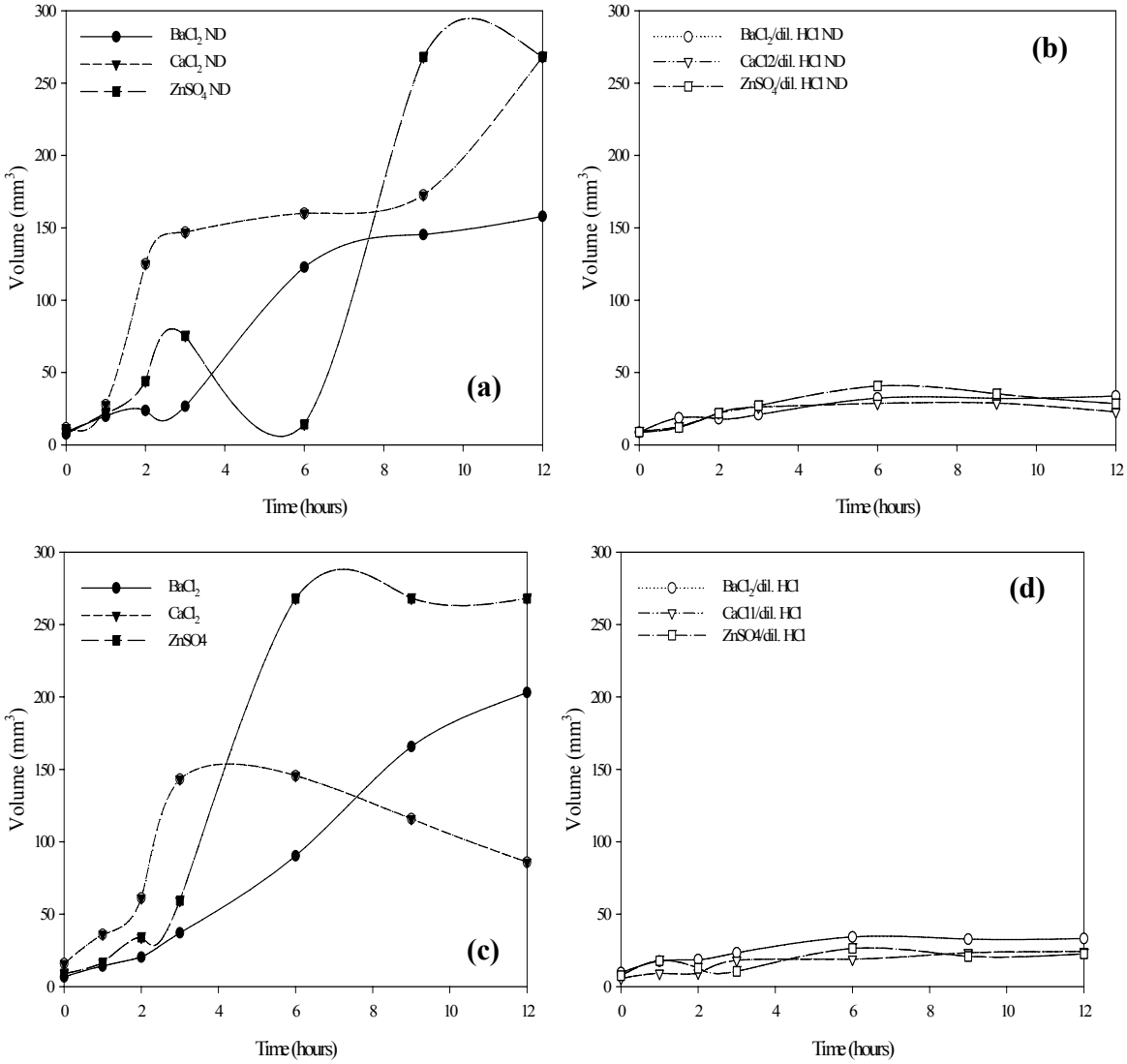

Figure 3.17: Change in volume (mm^3) of hydrated crosslinked Alg-HEC gelispheres drug-free (ND) (a) unexposed to dilute HCl and (b) exposed to dilute HCl and drug-loaded gelispheres (c) unexposed to dilute HCl and (d) exposed to dilute HCl following exposure to simulated CSF, over a period of 12 hours (N=3; SD<5.34%).

Since both alginate and HEC are hydrogels, they have the capacity to take up water when exposed to hydration. When exposed to simulated CSF, the gelispheres undergo sequestration and gradually

expanded in gelisphere volume until sufficient polymeric relaxation occurs to cause the matrix to erode and disintegrate. Exposure to dilute acid prevented the uptake of water and subsequent matrix degradation significantly. The matrices imbibed sufficient water that allowed for a 201.15% - 329.14% increase in volume, following which an 'equilibrium hydrated gelisphere volume' was maintained for the remainder of the 50 hours. Due to the nature of the alginate employed, i.e. G-rich, the selectivity of the polymer for the crosslinking ions had a significant impact on the degree of crosslinking in the polymer. As observed from textural analysis, the greater affinity of the G-units towards calcium and barium ions resulted in the formation of more compact matrices. An increase in the degree of crosslinking had a predictable effect on the swelling behaviour. With such a large degree of physical restriction in the hydrogel network, water uptake decreased markedly, and the swelling rate also decreased. In general unexposed zinc-crosslinked gelispheres increased in volume to the greatest degree over the 50 hours. Barium-crosslinked gelispheres generally indicated slower rates of water uptake and matrix swelling over the 12 hours. The decline in volume for calcium-crosslinked gelispheres with drug after t=6 hours indicated that matrix erosion occurred.

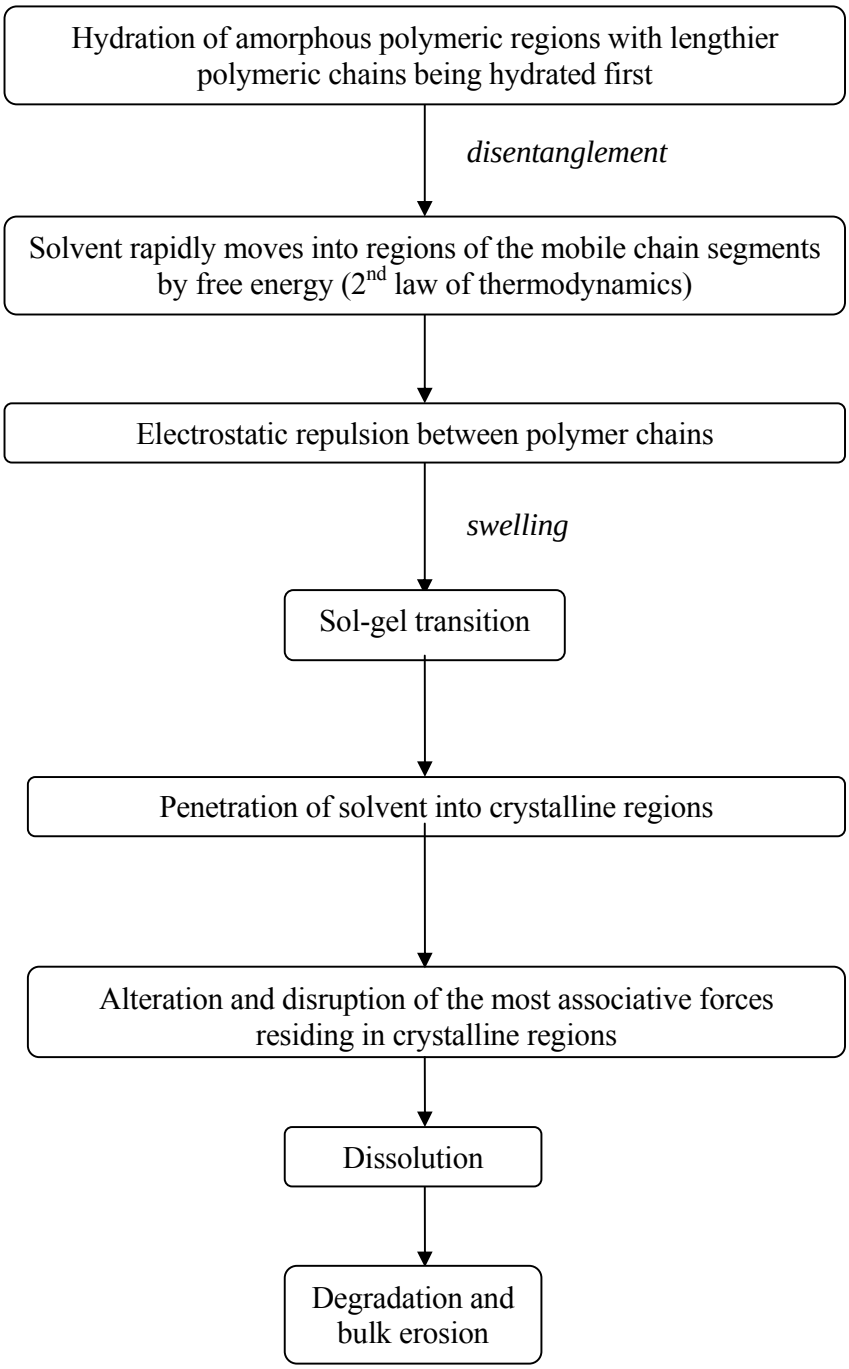

Figure 3.18: Flowchart illustrating the process of hydration and subsequent chain disentanglement following hydration of the polymeric matrix.

3.3.1.4 Evaluation of Drug-Polymer Interactions Employing FTIR Spectra

FTIR spectra of nicotine, sodium alginate, nicotine/alginate, calcium/alginate; with and without nicotine are shown in Figure 3.19a-c. FTIR spectrum of sodium alginate revealed various distinct peaks of alginate: hydroxyl at 3364.03cm^{-1}, carbonyl at 1627.34cm^{-1}, and carboxyl and carboxylate at about 800 to 1400cm^{-1} (Figure 3.19a). However, the physical mixture of nicotine and sodium alginate showed the peaks attributable to both nicotine and sodium alginate. The distinct peak at 1255.54cm^{-1} (Figure 3.19b) indicates the aromatic N-H stretching in the nicotine molecule. The broad peak observed at 1426.76cm^{-1} (Figure 3.19b) corresponds to O-H bending in the alginate molecule. It is proposed that hydroxyl groups in the alginate monomers, most likely in the G-pockets housing the nicotine molecules, interact with lone pairs on the nitrogen atoms which form part of the nicotine pyridine aromatic ring. This confirms the interaction of nicotine with alginate at the molecular level (Figure 3.20). With the addition of calcium to the dispersion, more distinct peaks were observed between 2700 and 230cm^{-1} (Figure 3.19c) (which confer to C-H stretching) indicate a possible ionic interaction with nicotine molecules within the crosslinked G-pockets. Boarder peaks at in the region of 1380 - 1500cm^{-1} indicated enhanced bending of hydroxyl groups in alginate, corresponding to interactions with interactions of the carboxylic acid groups with divalent calcium ions.

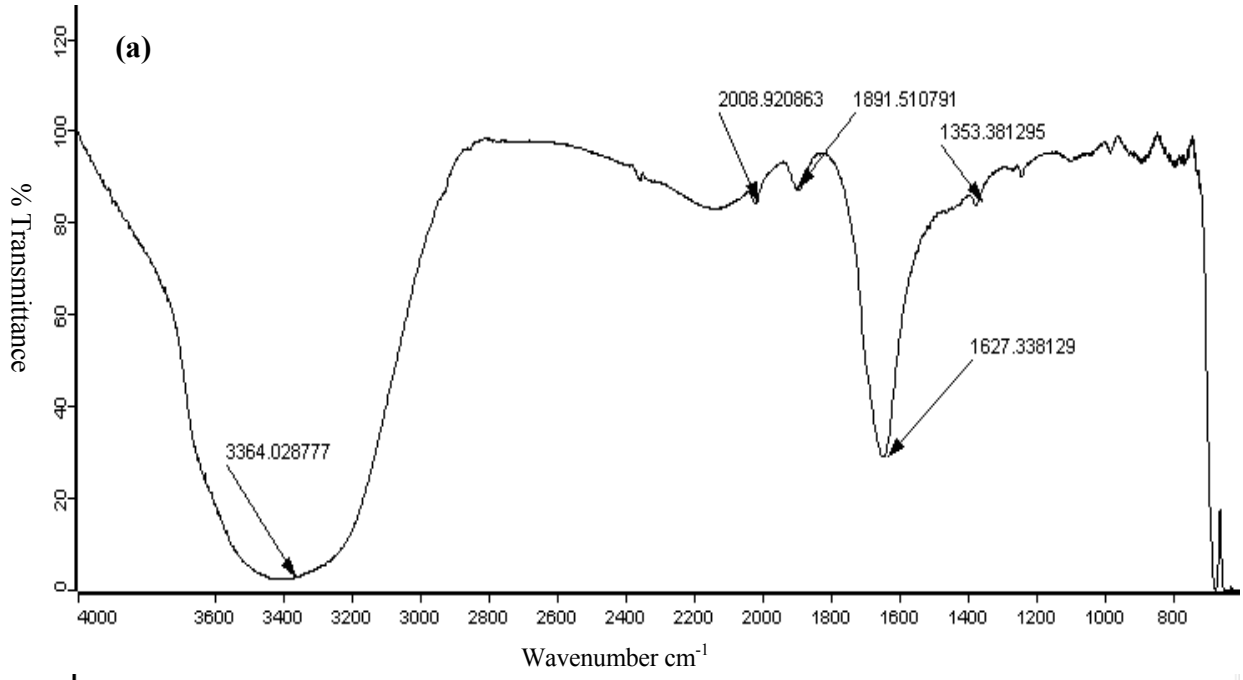
(a)
2008.920863
1891.510791
1353.381295
1627.338129
3364.028777
% Transmittance
Wavenumber cm-1

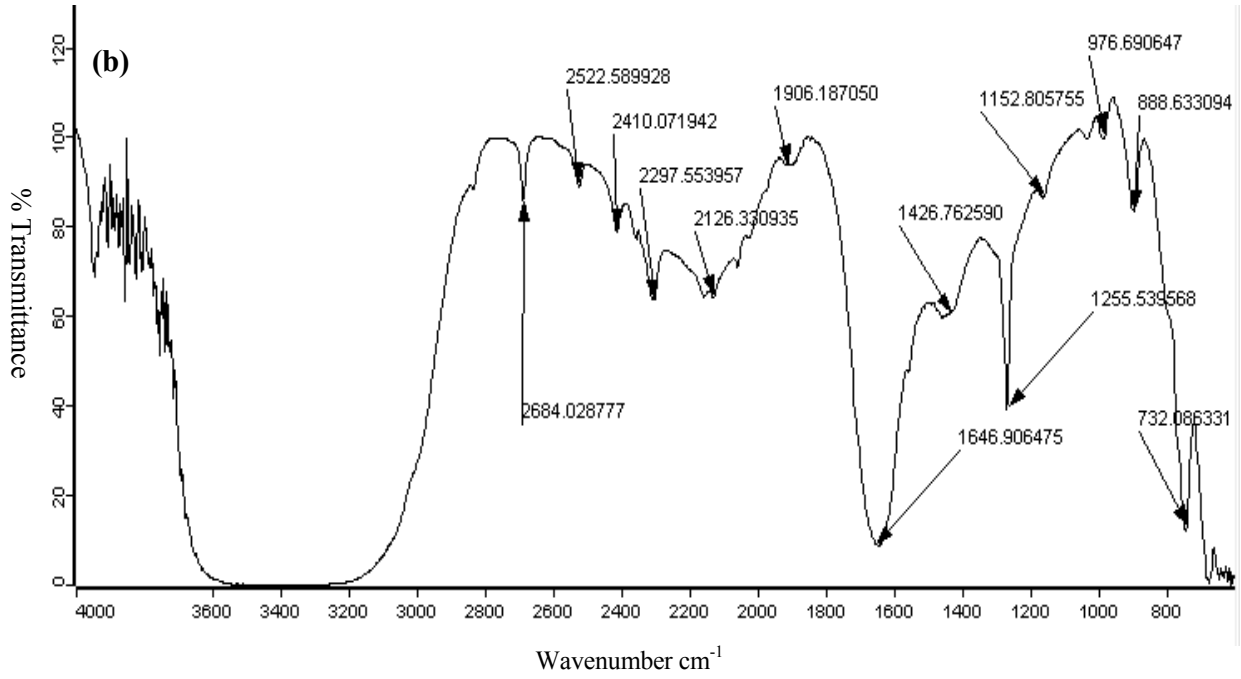
(b)
976.690647
2522.589928
1906.187050
1152.805755
888.633094
2410.071942
2297.553957
2126.330935
1426.762590
1255.539568
2684.028777
1646.906475
732.086331
% Transmittance
Wavenumber cm-1

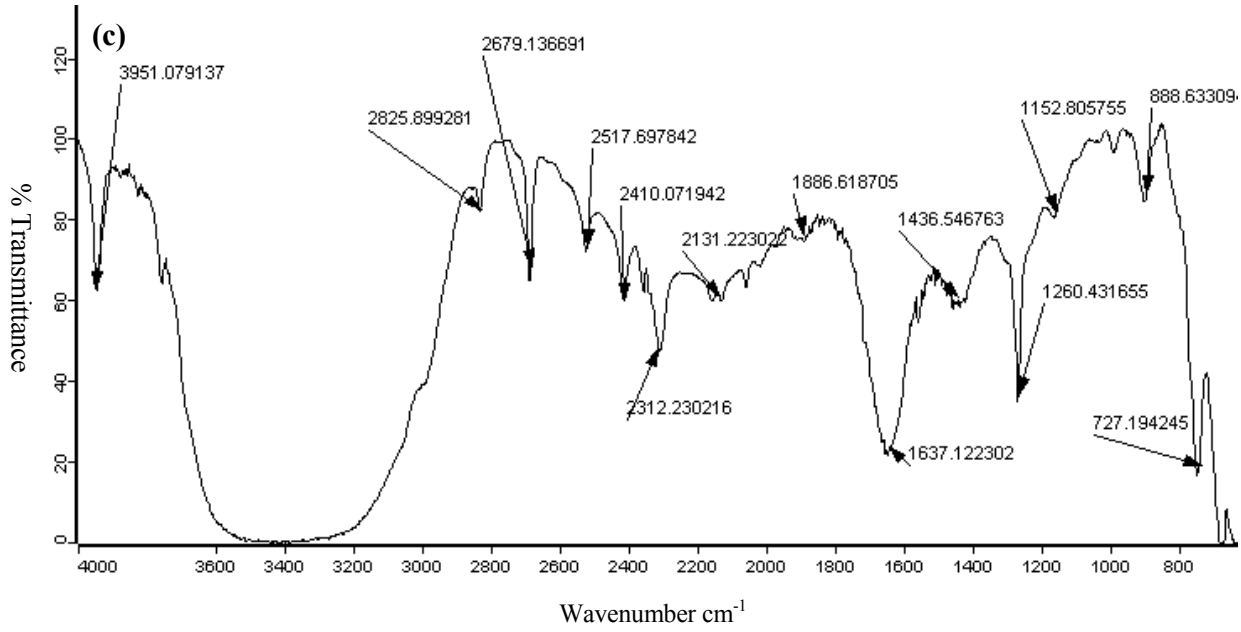

Figure 3.19: FTIR spectra for (a) native alginate, (b) alginate/nicotine and (c) calcium-crosslinked alginate incorporating nicotine indicating the interactions between the alginate, calcium and nicotine.

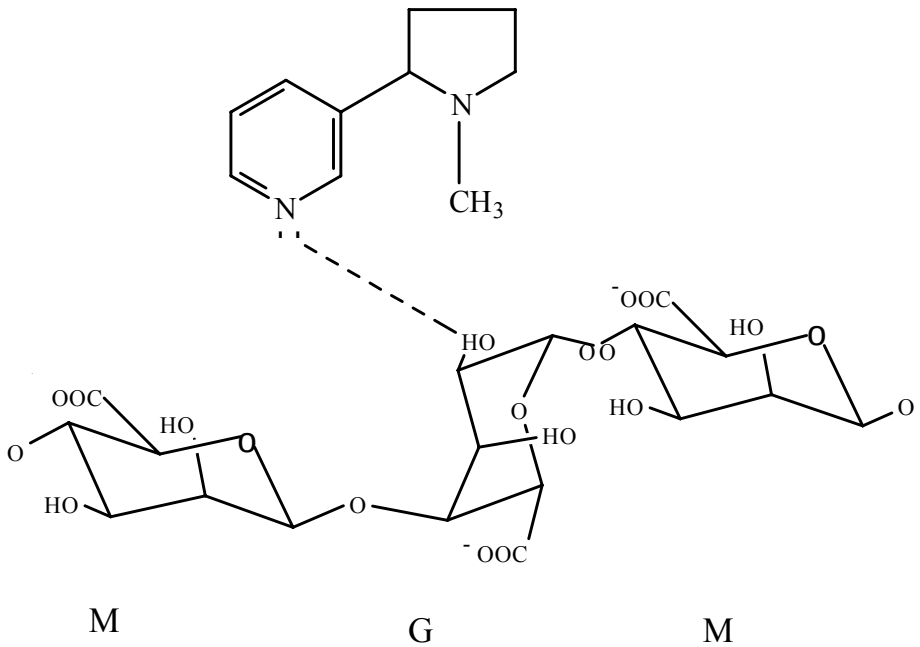

Figure 3.20: Proposed mechanism of interaction of nicotine with alginate monomers at a molecular level.

3.3.1.5 Evaluating Changes in Surface Morphology of Unexposed and HCl-Exposed Gelispheres following Hydration

The scanning electron micrographs (SEM) indicated the changes in surface morphology of unexposed and HCl-exposed gelispheres following exposure to simulated CSF.

Unhydrated unexposed gelispheres possessed diameters approximately in the range of 2-3mm and demonstrated spherical to elongated morphology. Their surface indicated the presence of pores on the surface in the region of approximately 0.5 - 10μm (Figure 3.21a). Their surface appears generally smooth and indicated the presence of small rectangular crystalline structures, possibly due to the presence of residual crosslinking salts on the surface. Following hydration, the gelispheres underwent polymeric disentanglement and degradation. Hence the dried gelispheres indicated a significantly smaller diameter between 0.7 - 1.5mm. A porous surface was observed, which conferred with matrix degradation and increased matrix resilience following hydration (Figure 3.21b). Pores appeared enlarged and 'clogged' with crystalline structures. It was proposed that crystalline structures observed on their surface were as a result of sequestered crosslinking ions. These crystals were smaller in size. This porous matrix permitted the small nicotine molecules to rapidly diffuse out of the matrices and conferred to the rapid drug release rates observed (Figure 3.21b).

Unhydrated HCl-exposed gelispheres possessed diameters of approximately 3mm. Their surfaces appeared irregular and coarse (Figure 3.21c). Minute crystalline particles (residual crosslinking salts) were also observed on the surface. The gelispheres were approximately spherical. Surfaces also appeared porous and undulated. SEMs indicated that precipitation of alginic acid had occurred throughout the matrix, due to the homogeneity of the matrix. This is expected, since hydrogen ions

are sufficiently small to rapidly penetrate the entire crosslinked matrix during the 15 minute period for which the gelispheres are exposed to dilute HCl post-curing. Following exposure to simulated CSF, the pores enlarged and the matrix underwent degradation in a manner similar to that previously observed with unexposed gelispheres however, the matrix appeared to remain more intact and less porous. This conferred to the slower rates of drug release observed for HCl-exposed gelispheres.

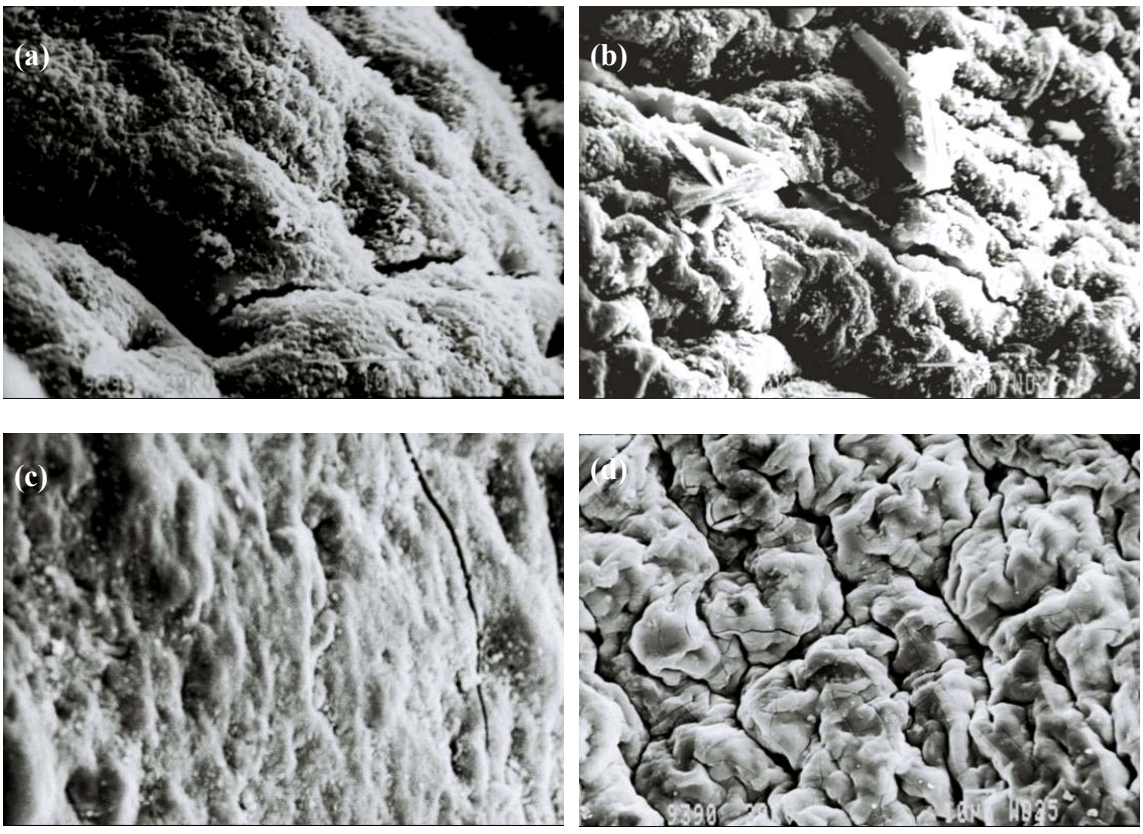

Figure 3.21: Scanning electron micrographs of unhydrated drug-loaded (a) unexposed barium-crosslinked (Magnification 1300x; 30 nanoamps) and (b) HCl-exposed barium-crosslinked gelispheres and hydrated (Magnification 300x; 30 nanoamps) (c) unexposed barium-crosslinked and (Magnification 1300x; 30 nanoamps) (d) HCl-exposed barium-crosslinked (Magnification 6500x; 30 nanoamps) gelispheres following exposure to simulated after 50 hours.

3.3.1.6 Evaluation of the Drug Entrapment Efficiency of Alg-HEC Gelispheres

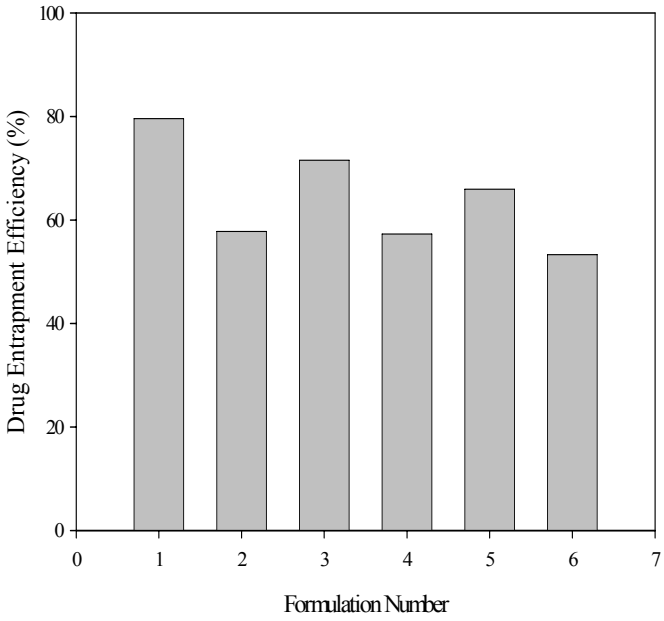

Figure 3.22: Drug entrapment efficiency (%) (where, Formulation 1:$BaCl_2$, 2:$BaCl_2$/dil. HCl, 3:$CaCl_2$, 4:$CaCl_2$/dil. HCl, 5:$ZnSO_4$, 6:$ZnSO_4$/dil. HCl) of nicotine within crosslinked Alg-HEC gelispheres following exposure to simulated CSF over a period of 50 hours (N=3; SD<2.89%).

Initial studies indicated that approximately 29% - 38% of the incorporated nicotine was lost into the crosslinking solution during the 30 minute curing period. This is due to the extremely high aqueous solubility of nicotine (50mg/mL, 21ºC) and combined with the fact that it is significantly ionised at a pH of 7.4 (approximately 69%). This 'leaching' phenomenon observed implied that the curing time had to be kept to a minimum. The DEE for matrices exposed for an additional 15 minutes to aqueous dilute HCl solution permitted further 'leaching' of nicotine into the medium and resulted in an approximate 21.82% - 12.64% loss of nicotine indicated by the lower DEE (Figure 3.22). For HCl-exposed formulations, maximal loss is observed with formulations crosslinked with barium and least with zinc-crosslinked gelispheres. However it is interesting to note that unexposed barium-crosslinked matrices demonstrated the highest DEE values. It is

proposed that this is due to the fact that while the barium ions significantly crosslink the matrices to entrap a substantial quantity of nicotine, since drug release was primarily controlled by diffusion, according to Fick's Law, the concentration gradient was greater, which resulted in a greater efflux post-curing.

3.3.1.7 Elucidation of *In Vitro* Drug Release from Crosslinked Alg-HEC Gelispheres

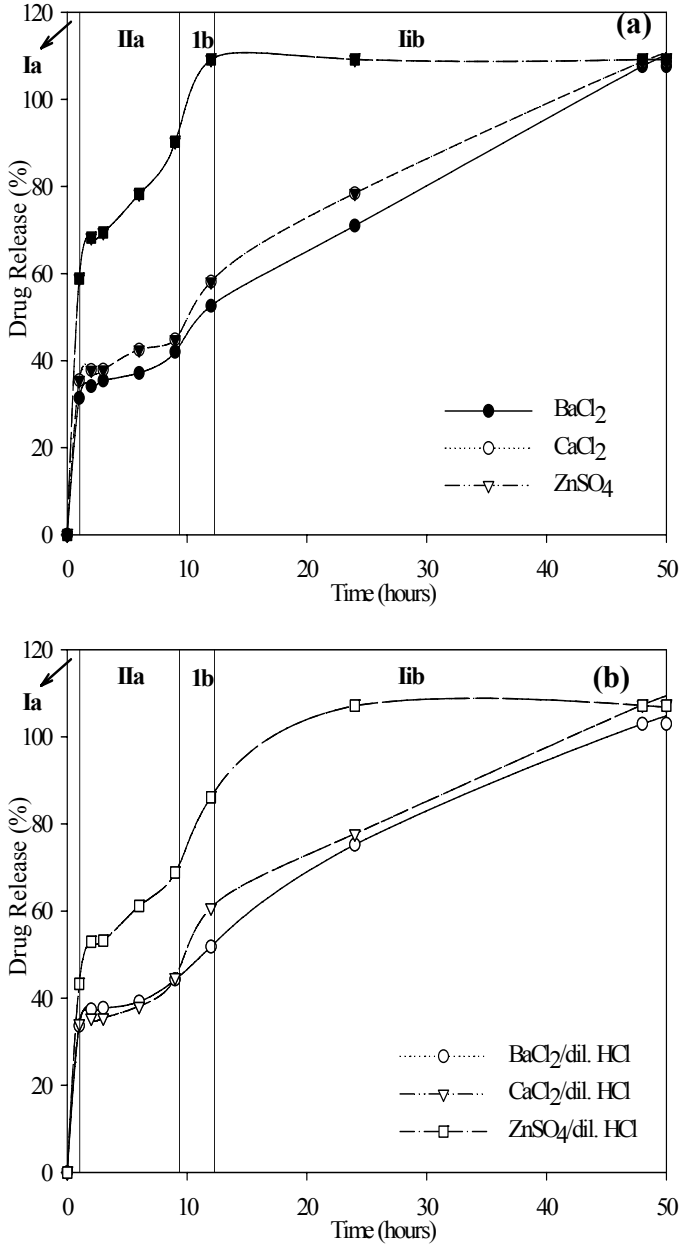

Figure 3.23: % Drug release profile of nicotine from (a) unexposed Alg-HEC gelispheres crosslinked with zinc, calcium and barium and (b) Alg-HEC gelispheres exposed to dilute HCl following curing, over a period of 50 hours in simulated CSF. The four phases (Ia, IIa, Ib and IIb) of release are also depicted (N=5; SD<0.96%).

Polymers such as alginate and HEC are significantly amorphous in nature (indicated by XRD profiles, Figure 3.4) hence the rate of drug dissolution is expected to follow this swelling process. The presence of crosslinking within the polymeric matrix imparts a significant degree of entanglement and retards the rate of solvent penetration (Heller, 1987).

The presence of secondary inter-polymeric hydrogen bonds between the constituent polymers allows for a more densely entangled network thus the movement of an incorporated drug is hindered significantly. Due to the nature of the hydrophilic polymers employed to generate the matrix, it is expected that the process of matrix degradation will primarily consist of bulk erosion i.e. the process of hydrolysis throughout the polymeric matrix, the phenomenon of 'concentric hydration' as was observed in Chapter 2 indicated the presence of a second mechanism, that of surface erosion. Prolonging the phase of surface erosion and retarding bulk erosion kinetics may allow for the development of a reservoir-like system that could delay the rate of drug release. However, nicotine being highly hydrophilic compound with a small molecular weight (162.23 $g.mol^{-1}$) diffused rapidly out of polymeric matrices as soon as it was exposed to hydrating medium. It has an aqueous solubility of approximately 50 mg per millilitre of water (21ºC), which is enhanced at physiological temperature. Correlating this with mechanism of matrix erosion for crosslinked water-soluble polymers incorporating a drug within a three-dimensional framework such as the one generated, as described in Chapter 2, Section 2.3.3, compounds such as nicotine rapidly move out of these polymeric matrices, independent of the rate of matrix erosion (Heller, 1987).

Nicotine appeared to have the least affinity for zinc-crosslinked matrices. Both the HCl-exposed and unexposed zinc-crosslinked gelispheres allowed for rapid first-order release of nicotine (Figure 3.23). Approximately 58.85% of entrapped nicotine was leached within the first hour of exposure to simulated CSF from unexposed while, 43.29% was leached from HCl-exposed zinc-crosslinked gelispheres. There was little variation between the drug-release profiles of barium and calcium-crosslinked gelispheres, regardless of exposure to dilute HCl. All formulations demonstrated typical release profiles that had four distinct phases of drug release (Figure 3.23). The first phase was the initial burst effect (Ia), which resulted in drug release between the range of 31.43% - 58.85% of entrapped drug being released within the first hour of exposure to PBS. This is followed by a second phase (IIb) of zero-order kinetics, where a linear phase of drug release is observed. This was followed by a second phase of burst release (Ib) after 12 hours of exposure to simulated CSF. Finally, a second phase of zero-order release allows the remainder of drug to be released from the matrices (IIb).

From a mechanistic point of view, the schematic illustrates the phenomenon of 'sequestration' (Figure 3.24). This is described by an exchange between monovalent sodium ions in the simulated CSF and the divalent ions that crosslink the polymeric matrix. This exchange of ions leads to chain disentanglement and an influx of water molecules. This caused the matrix to swell and subsequently caused matrix degradation into smaller non-toxic water-soluble entities.

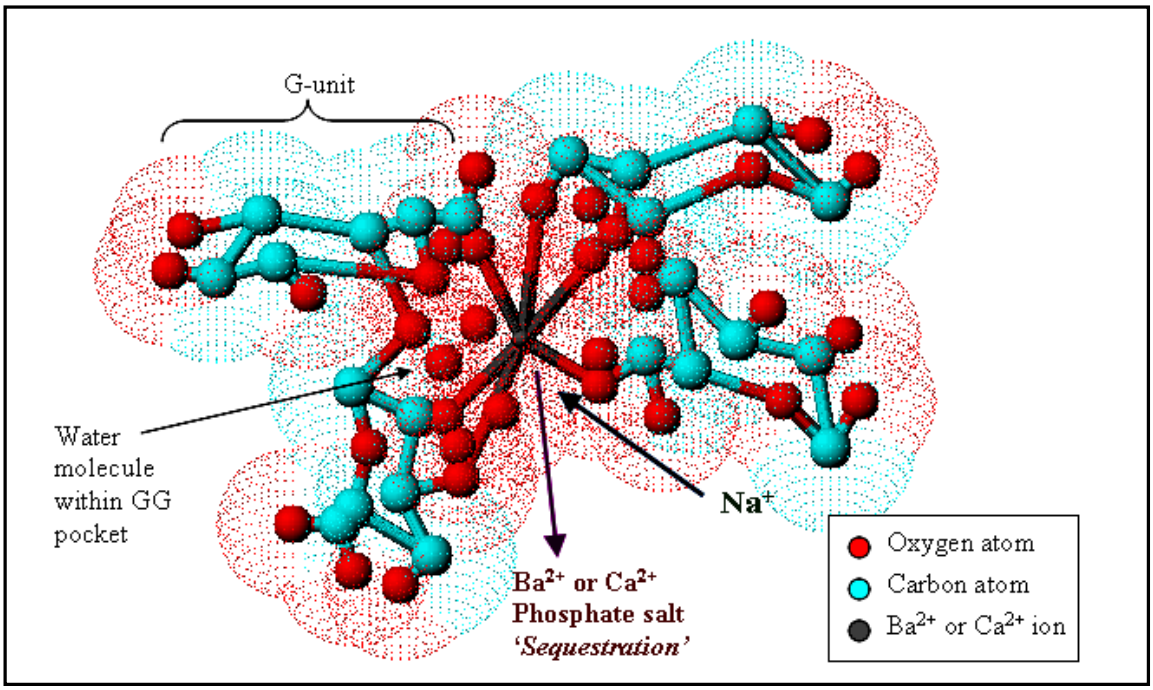

Figure 3.24: Schematic illustrating the mechanism of sequestration.

This phenomenon related to drug release as the influx of water molecules dissolves the entrapped nicotine, which is a very hydrophilic and small molecule. Hence, as soon as this occurred the encapsulated nicotine rapidly diffused out of the matrix. It was observed that matrices crosslinked with a greater ratio of calcium allowed this process to occur more rapidly.

3.3.1.8 Elucidation of Polymer-Polymer Interactions Employing FTIR Studies

FTIR spectra of HEC indicated the presence of -OH, -COOH and –CH groups. The presence of an interaction occurring between the two polymers and divalent cations guluronic acid residues forming the hydrogen bonds and bond stretching is evident due to the shifts observed in absorption peaks of –OH and –COOH groups, indicated by the broad band observed between 1550 - 1720cm^{-1} and the peak at 1886.26cm^{-1}.

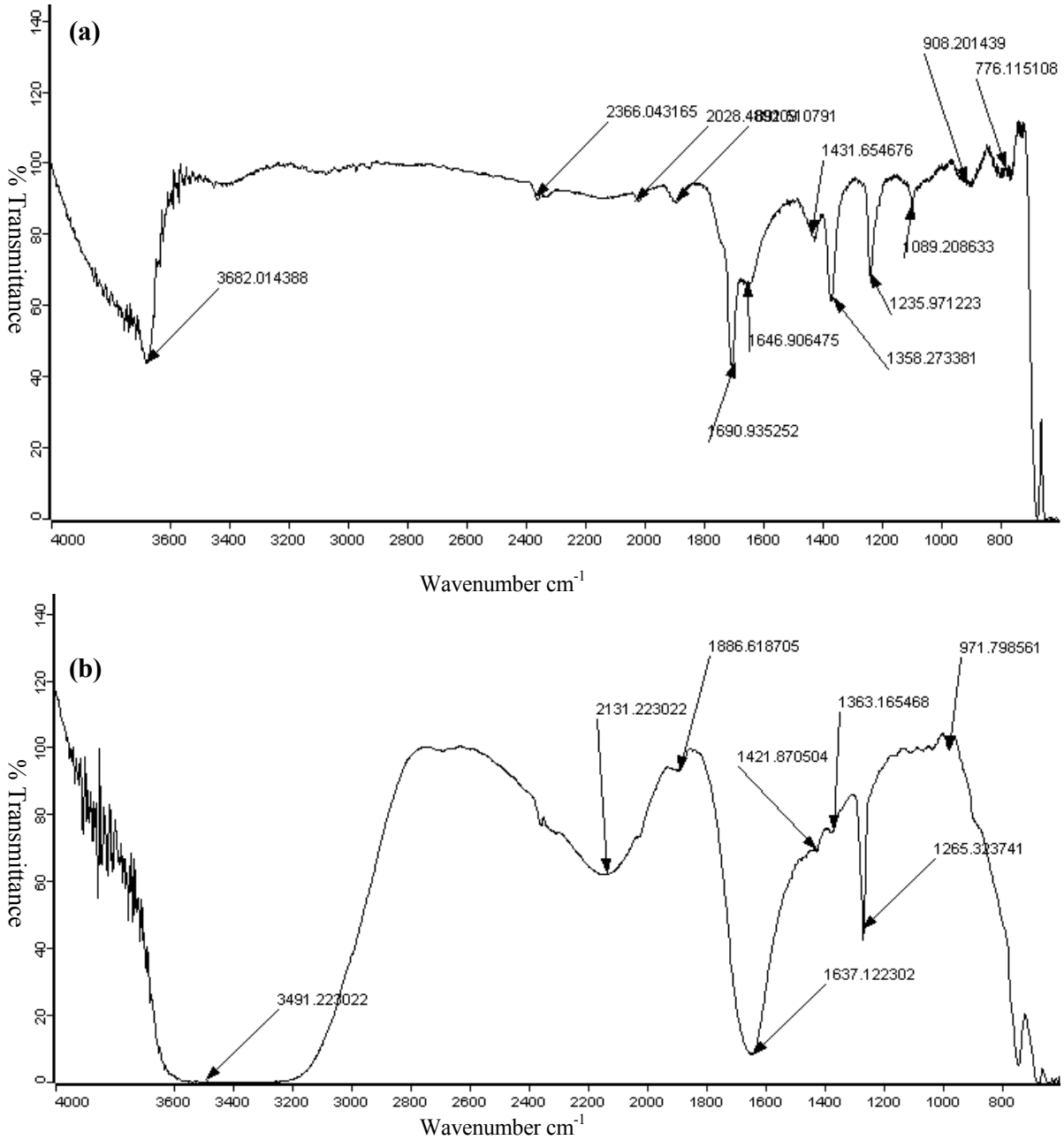

Figure 3.25: FTIR spectra of (a) HEC and (b) HEC and alginate.

The formation of secondary hydrogen bonding between the hydroxyl groups on HEC and carboxylic acid groups (illustrated in Figure 3.25), whether in the ionized or unionised state results in strong inter-polymeric bonds that were resistant to degradation. The presence of fewer sites

within the polymer to interact with interpenetrating water molecules prevented accelerated degradation. The presence of unionised carboxylic acid groups, as in the case of precipitated alginic acid, (resulting from exposure to dilute HCl post-curing) further prevented interaction between the polymer and water molecules. It is proposed that this interaction occurred more significantly between the carboxylic acid groups on the M-units in alginate and HEC due to the fact that the crosslinking divalent actions employed have selectivity for G-units. The fact that drug release was observed to be more rapid from zinc-crosslinked gelispheres can be explained in these terms. As observed from Chapter 2, due to its smaller ionic size, zinc is the least selective for G-units of the three ions employed. This implies that zinc ions interacted with comparatively more M-units within the polymeric matrix. These M-units therefore were unable to form significant hydrogen bonds with HEC. Thus it was postulated that the degree to which the matrix was reinforced was not as significant as for Ba^{2+} and Ca^{2+}. Hence the relative rate of degradation and consequent translation to drug release kinetics was more rapid for zinc-crosslinked matrices.

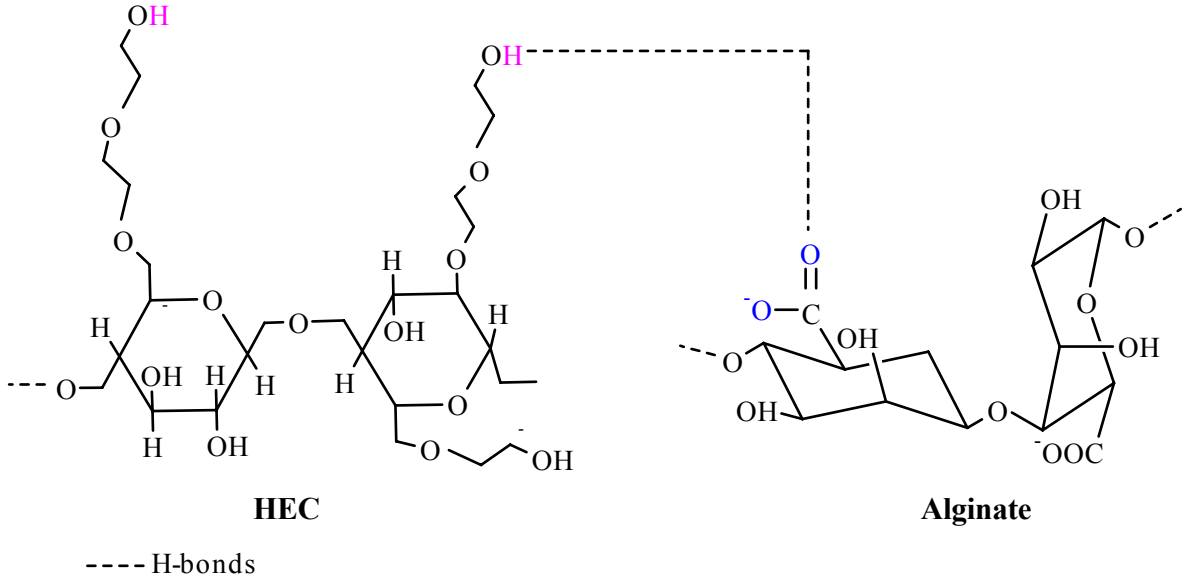

Figure 3.26: Schematic illustrating the proposed mechanism of hydrogen bonding (H-bonds) forming between alginate M-units and HEC resulting in a reinforced gelisphere matrix.

3.3.1.9 Analysis of Native and Crosslinked Polymer Thermal Transitions Employing Differential Scanning Calorimetry

The glass transition temperature (TG) for the polymers was calculated employing Differential Scanning Calorimetry (DSC). The G-rich alginate was dehydrated at approximately 98.93ºC indicated by the endothermic peak in the DSC profile (Figure 3.27a). Endothermic peaks at approximately, followed by an exothermic peak indicating decomposition of the biopolymer between 230ºC - 270ºC. This resulted in the formation of Na_2CO_3 and a carbonized residue. Decomposition of the carbonaceous material occurred above 300°C.

The DSC profile for HEC (Figure 3.27b) indicated two distinct endothermic peaks. The first peak between 40°C - 115°C indicated a phase of water loss (dehydration) from the polymer. This temperature range was smaller in magnitude which indicated that dry HEC possessed a smaller water content than alginate. The second endothermic peak corresponded to the thermal transition relating to polymer melting.

The crosslinked gelispheres indicated four distinct phases of thermal transition (Figure 3.27c). It is proposed that that the first endothermic peak between 50°C - 74°C corresponded to dehydration of the matrix. The second endothermic peak between 170°C - 250°C corresponded to the phase whereby alginate and HEC break the secondary hydrogen bonds binding them. The second phase corresponded to endothermic peaks between 250°C - 310°C which correlated with dissociation of crosslinking ions from guluronic and mannuronic acid residues within the alginate molecule. The final endothermic peak corresponded with melting and matrix decomposition.

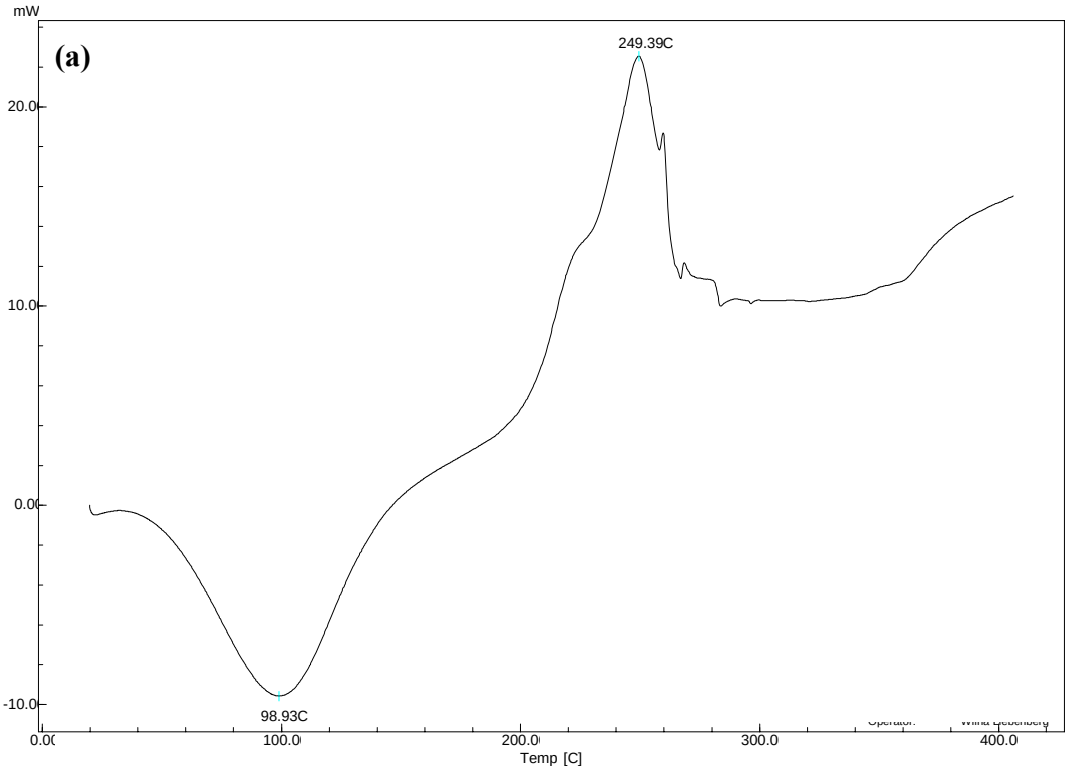
mW
(a)
249.39C
20.0
10.0
0.0
-10.0
98.93C
0.0
100.0
200.0
300.0
400.0
Temp [C]

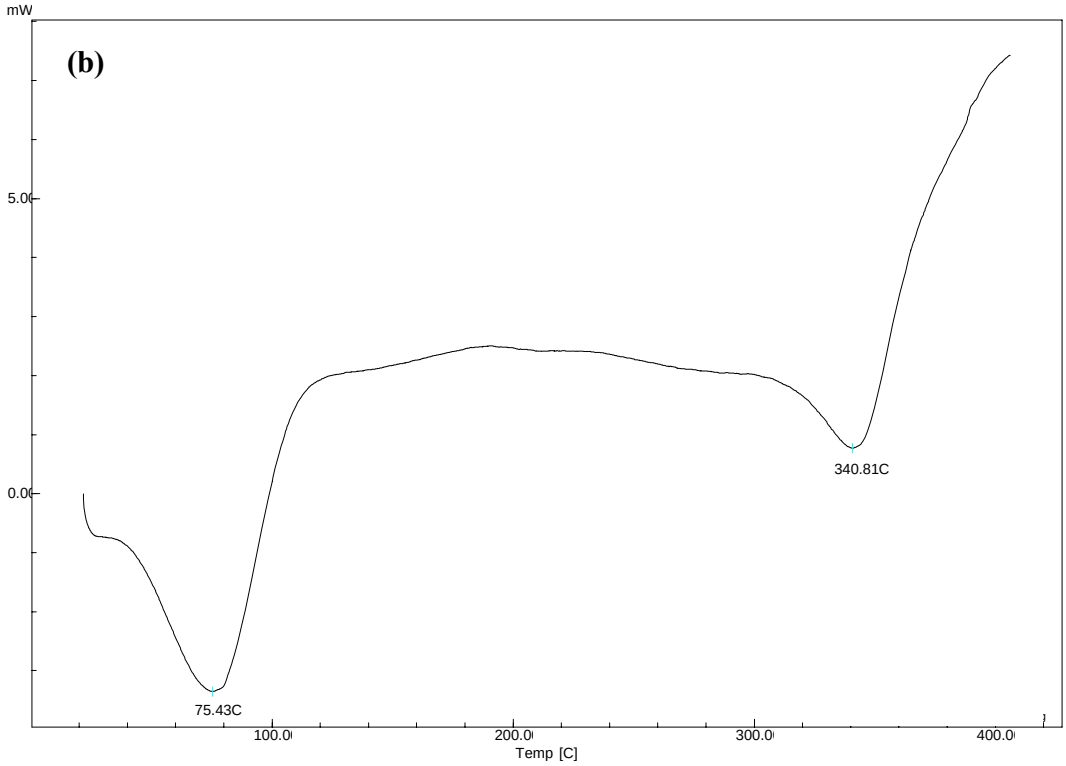
mW
(b)
5.0
0.0
340.81C
75.43C
100.0
200.0
300.0
400.0
Temp [C]

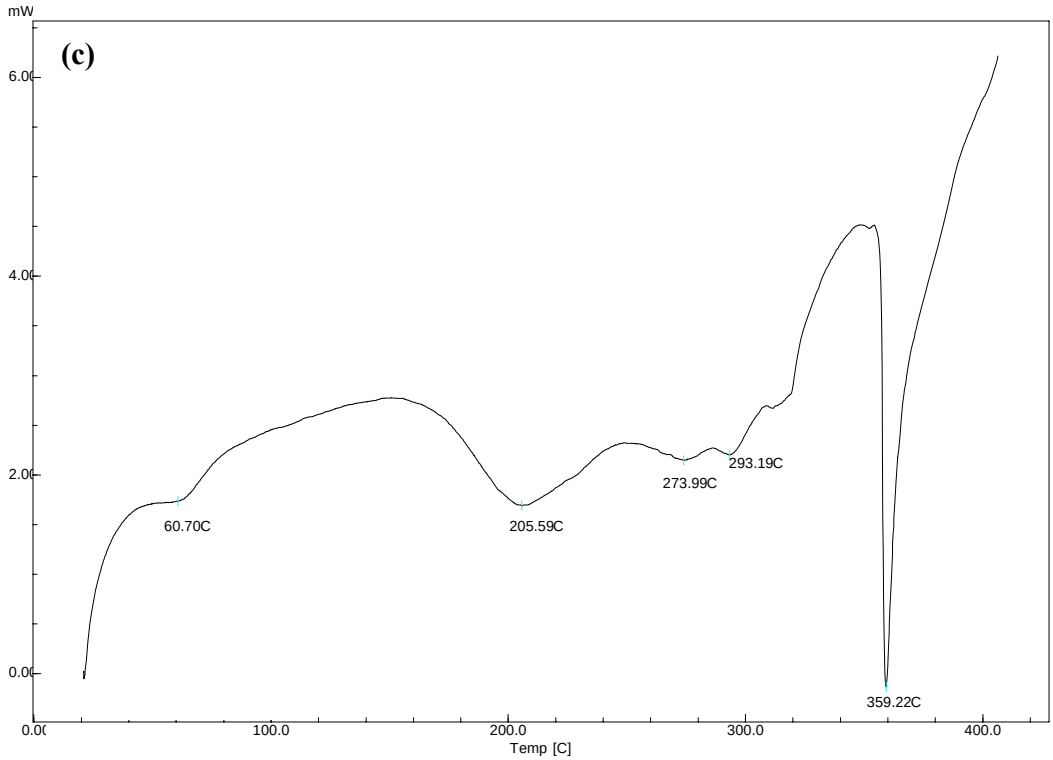

Figure 3.27: Typical DSC profiles obtained for the G-rich Alginate (FMC BioPolymer) and (b) HEC (Hercules Inc., Natrosol® Pharm) selected for formulating the proposed drug delivery system and (c) the unexposed calcium-crosslinked Alg-HEC gelispheres.

3.3.2 PHASE II: Formulation and Evaluation of Reinforced Multi-Polymeric Gelispheres Employing a Design of Experiments Approach

3.3.2.1 Alg-HEC-PAA Gelisphere Yield – Evaluation of Reaction Efficiency

The efficiency of a reaction can be measured in numerous ways. The most common method employed is though the calculation of the percentage yield. No reaction proceeds with 100% yield efficiency due to factors such as the formation of by products, incomplete conversion of the starting materials, loss upon formulation of the reaction mixture, and upon isolation and purification of the desired end product. The % gelisphere yield was calculated employing Equation 3.5 to establish the influence of formulation parameters on the efficiency of the crosslinking reaction.

$$\% \text{ Gelisphere Yield} = \frac{\text{(Actual Gelisphere Yield)}}{\text{(Theoretical Gelisphere Yield)}} \times 100 \qquad \text{Equation 3.5}$$

Results indicated that larger polymeric concentrations (both alginate and HEC) resulted in higher gelisphere yield (Table 3.4). The presence of calcium in the formulation also enhanced % gelisphere yield.

Table 3.4: Gelisphere yield efficiency ($\%^{w}/_{w}$) for the Alg-HEC-PAA formulations.

Formulation Number	Gelisphere Yield Efficiency ($\%^{w}/_{w}$)
1	74.67
2*	98.42
3	73.70
4	63.52
5	57.46
6	67.75
7	71.49
8	68.12
9	72.66
10	76.62
11	76.97
12	78.92
13*	98.42
14	80.29

**centerpoints*

3.3.2.2 Evaluation of the Drug Entrapment Efficiency (DEE) of Alg-HEC-PAA Gelispheres

DEE for the Alg-HEC-PAA gelispheres ranged between 18.75% - 53.67% (Table 3.5). Higher entrapment efficiencies were observed with formulations composed of a higher alginate and HEC concentration and both crosslinking ions produced compact matrices. This was due to the fact that the greater degree of polymer interaction and crosslinking that occurred within the gelisphere resulted in an increased restriction for nicotine molecules from leaching out of the matrix during formulation. An increased concentration of the polymers allowed the formation of more secondary hydrogen bonds, resulting in a denser crosslinked polymeric network. The presence of both barium and calcium ions increased the degree of crosslinking within the matrix, accentuating the density of the gelisphere. The final system was therefore one that could effectively retain the incorporated nicotine and achieve higher DEE.

A higher concentration of PAA resulted in gelispheres with higher nicotine entrapped within their matrices due to the fact that the polymer formed a mechanical barrier around the crosslinked gelispheres, and thus prevented 'nicotine-leaching' during curing.

According to statistical analysis (discussed further under Section 3.4.6) the concentration of alginate in the formulation had the most significant impact on DEE in comparison to all other factors. There was a direct correlation between the quantity of nicotine entrapped within the matrices and the $\%^{w}/_{v}$ of alginate employed in the formulation. This is due to the fact that alginate is the polymer that undergoes crosslinking with the cations resulting in the development of the network that restricts nicotine within the matrix. Hence, the greater the quantity of polymer

(alginate) to undergo crosslinking, the denser the developed crosslinked matrix, and the greater the degree of nicotine entrapment.

Table 3.5: Response outcomes for the Alg-HEC-PAA formulations (N=3).

Formulation Number	Drug Entrapment Efficiency (%)	Drug Release (%) at 1 hour
1	40.73	50.51
2*	40.03	65.05
3	53.67	56.46
4	34.03	90.22
5	29.01	74.43
6	47.37	52.60
7	38.68	34.05
8	26.14	84.29
9	18.75	73.29
10	30.75	58.01
11	41.23	51.78
12	32.91	61.61
13*	40.03	65.05
14	24.91	88.35

**centerpoints*

3.3.2.3 Elucidation of *In Vitro* Drug Release from Alg-HEC-PAA Gelispheres

All formulations demonstrated first-order drug release kinetics. The concentration of both polymeric constituents had a synergistic and significant effect on retarding drug release. Higher concentrations of both polymers allowed for an attenuated burst-effect (Figure 3.28). Formulations prepared with lower alginate and HEC concentrations demonstrated drug release exceeding 90% within the first hour (Figure 3.28). In comparison, formulations with higher alginate HEC concentrations were able to retard drug release in the first hour to 34%. This indicated significant interaction between the polymeric components in determining matrix integrity, which impeded drug release. The matrices generated thereof possessed a greater degree of polymeric chain

entanglement assisted by the formation of inter-polymeric secondary hydrogen bonds. This in turn impeded the movement of water molecules into the matrices, which resulted in polymeric relaxation and subsequent matrix degradation and nicotine release.

Higher concentrations of PAA were observed to have a mildly positive effect on retarding drug release (discussed further in Section 3.4.6). This was due to the formation of a mechanical barrier around the gelispheres that prevented the ready interaction and subsequent penetration of water molecules in the surrounding medium with the polymeric matrix.

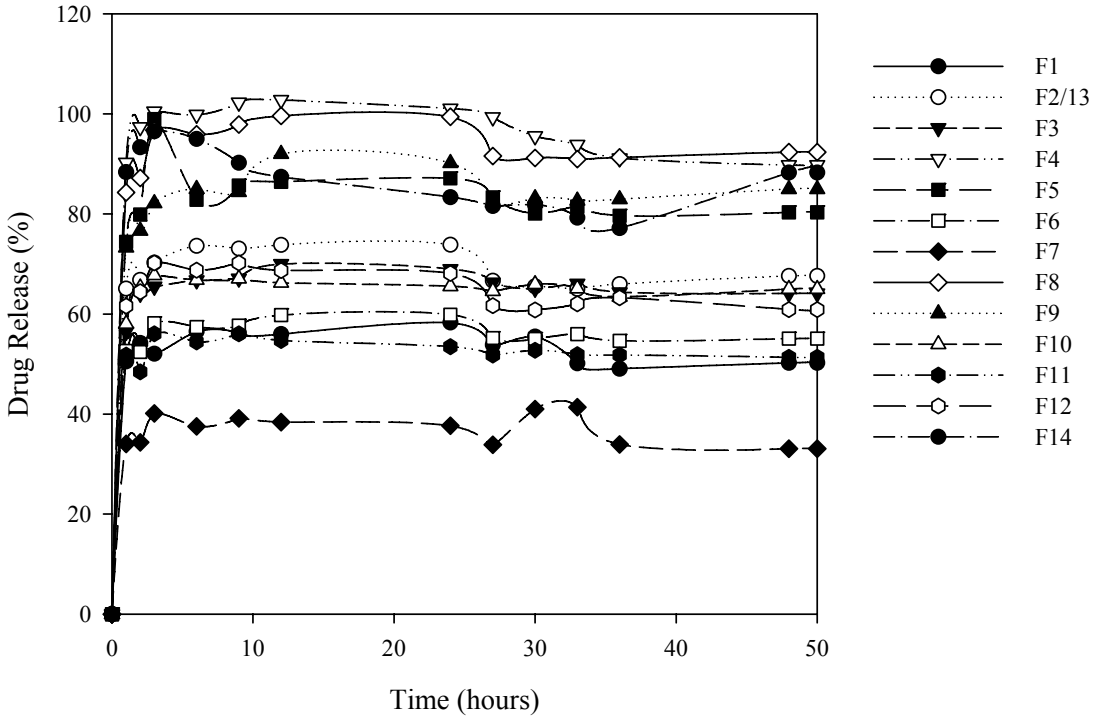

Figure 3.28: % Drug released over a period of 50 hours from the Alg-HEC-PAA gelispheres following exposure to simulated (N=3; SD<3.55%).

3.3.2.4 Thermal Analysis of Alg-HEC-PAA Gelispheres

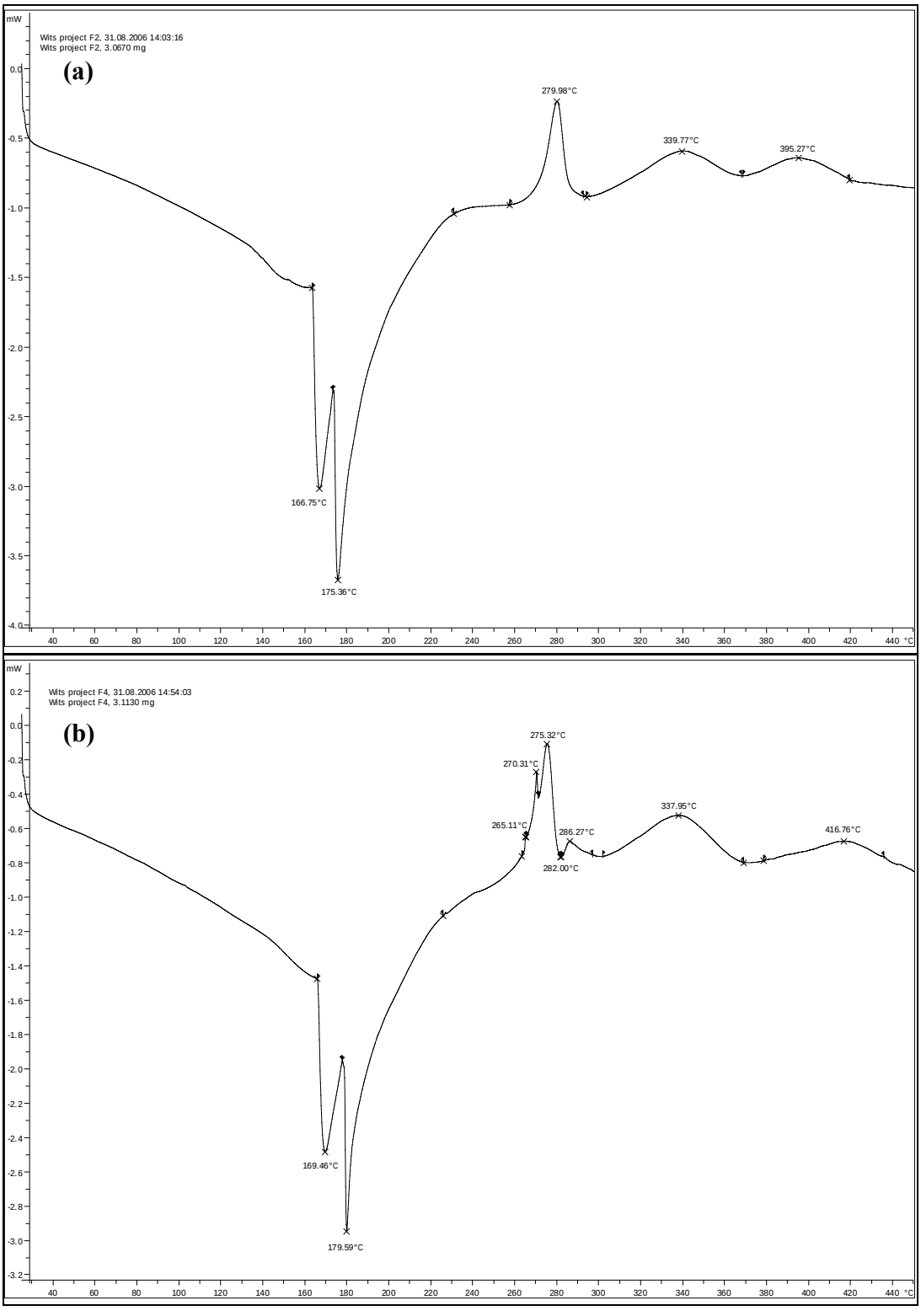

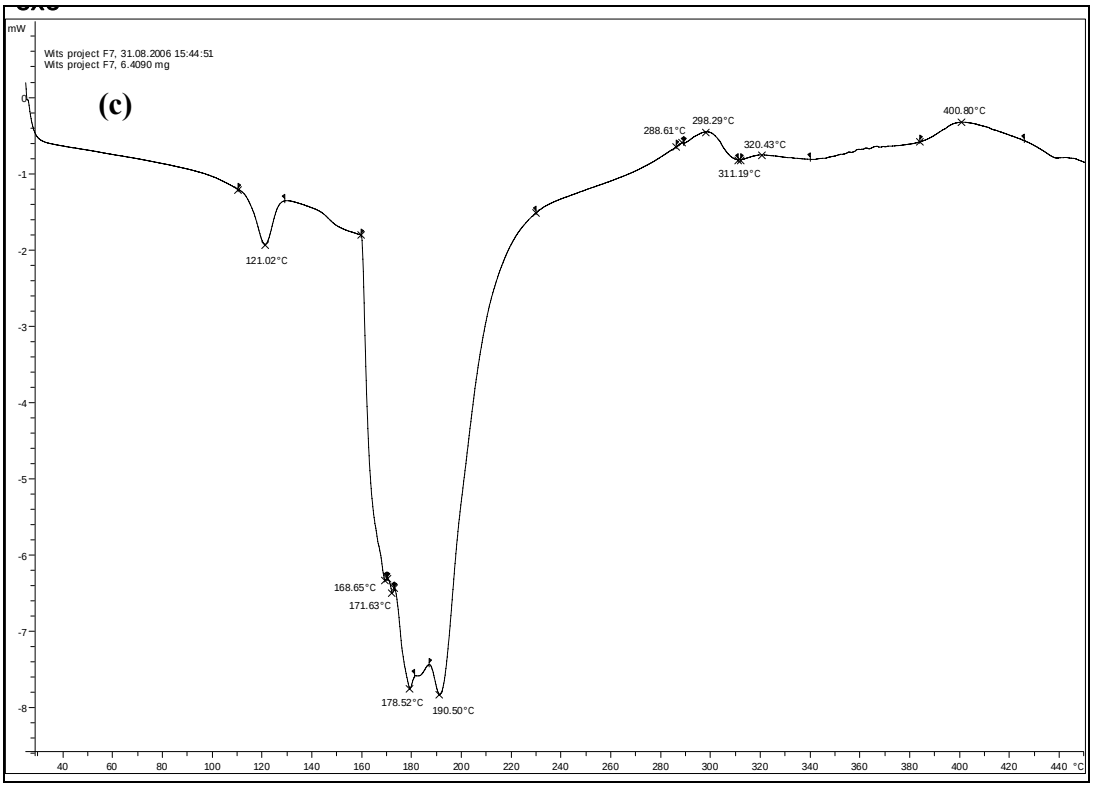

Figure 3.29: Typical differential scanning calorimetry (DSC) profiles of (a) Formulation 2, (b) Formulation 4 and (c) Formulation 7.

Three formulations were selected to conduct DSC analyses. Selection was based on concentration of polymers and crosslinking ions, so that a variety of combinations could be observed. Typical DSC profiles for the Alg-HEC-PAA gelispheres indicated an enhanced endothermic peak in the region of 160ºC - 180ºC indicating complex de-polymerization, primarily of alginate. The schematic in Figure 3.26 illustrated the possible chemical groups that result in the abovementioned interaction causing the enhanced thermodynamic stabilisation of the multi-polymeric entity. This stabilisation contributed towards the reduced degradation of the gelispheres. Figure 3.29 indicates the DSC profiles obtained for three formulations with sufficiently different compositions to illustrate the influence of formulation parameters on the thermal stability of the gelispheres. For

Formulation 2 (2%$^{w}/_{v}$ Alginate, 0.75%$^{w}/_{v}$ HEC; 1%$^{w}/_{v}$ PAA, 1%$^{w}/_{v}$ $CaCl_2$ and 1.25%$^{w}/_{v}$ $BaCl_2$) (centerpoint), two distinct endothermic peaks are observed at 166.75ºC and 175.36ºC (Figure 3.29a). It is postulated that these corresponded to loss of water molecules from the matrix and the breaking of secondary hydrogen bonds between alginate and HEC. These endothermic peaks were shifted higher in Formulation 4 (1.5%$^{w}/_{v}$ Alginate, 0.5%$^{w}/_{v}$ HEC; 0.5%$^{w}/_{v}$ PAA, 0%$^{w}/_{v}$ $CaCl_2$ and 0.5%$^{w}/_{v}$ $BaCl_2$) to 169.46ºC and 179.56ºC (Figure 3.29b). Hence an enhanced interaction, as is observed when a greater of crosslinking occurred due to the presence of higher concentrations of both crosslinking ions as in Formulation 7 (1.5%$^{w}/_{v}$ Alginate, 0.5%$^{w}/_{v}$ HEC; 0.5%$^{w}/_{v}$ PAA, 2%$^{w}/_{v}$ $CaCl_2$ and 2%$^{w}/_{v}$ $BaCl_2$) (Figure 3.29c) to generate the matrix, allowed for enhanced stabilisation. This is further validated by the reduced burst effect observed when these formulations are exposed to simulated CSF (Figure 3.28). Exothermic peaks between the region of 250ºC – 350ºC indicate polymeric relaxation.

3.3.2.4 Evaluation of Physicomechanical Properties of Alg-HEC-PAA Gelispheres

Alginate and Ba^{2+} concentrations had the most significant impact on the formation of compact and robust gelispheres. Textural analysis indicated that matrix resilience and therefore the porosity of the Alg-HEC-PAA gelispheres gradually increases over time. Formulations generated with higher concentrations of alginate and barium demonstrated minimal changes in matrix resilience (porosity) over time hence remained intact for a longer duration of time following hydration. The porosity of the matrices correlates directly with the surface area available for the matrix to interact with solvent molecules which promotes matrix degradation and drug release. Hence lower and sustained matrix resilience indicates an increased capacity to maintain the integrity of the matrix and retard nicotine release.

The results indicated that the gelispheres swelled in concentric layers with the peripheral layers becoming hydrated first. This demonstrated a deviation from the expected bulk hydration kinetics expected with hydrophilic polymers employed to generate the matrices. Instead it was observed that surface hydration and erosion preceded bulk erosion. It was observed that a transition occurred in the basic physicochemical nature of the matrices which was adequate to significantly affect its degradation behaviour. The profiles for fracture energy confirmed this phenomenon by indicating transient increases in fracture energy when the texture analyser probe came in contact with the central unhydrated crosslinked core of the matrix (Figure 3.30b).

With regard to deformability moduli, there is a general decline of between 69.97% - 92.58% following exposure to hydration as water penetrated the matrix and resulted swelling (Figure 3.30c). Thereafter, a thermodynamic equilibrium was achieved and stabilized the system until complete matrix degradation occurred.

As mentioned previously, HEC functioned as a matrix reinforcer by forming strong secondary hydrogen bonds with alginate (discussed further on). This interaction was sufficiently significant to enhance matrix robustness, retard drug release and decrease the matrix porosity (indicated by smaller resilience following exposure to simulated CSF) (Figure 3.30a). Upon hydration HEC aided the maintenance of the matrix and prevented water penetration, therefore delaying matrix degradation.

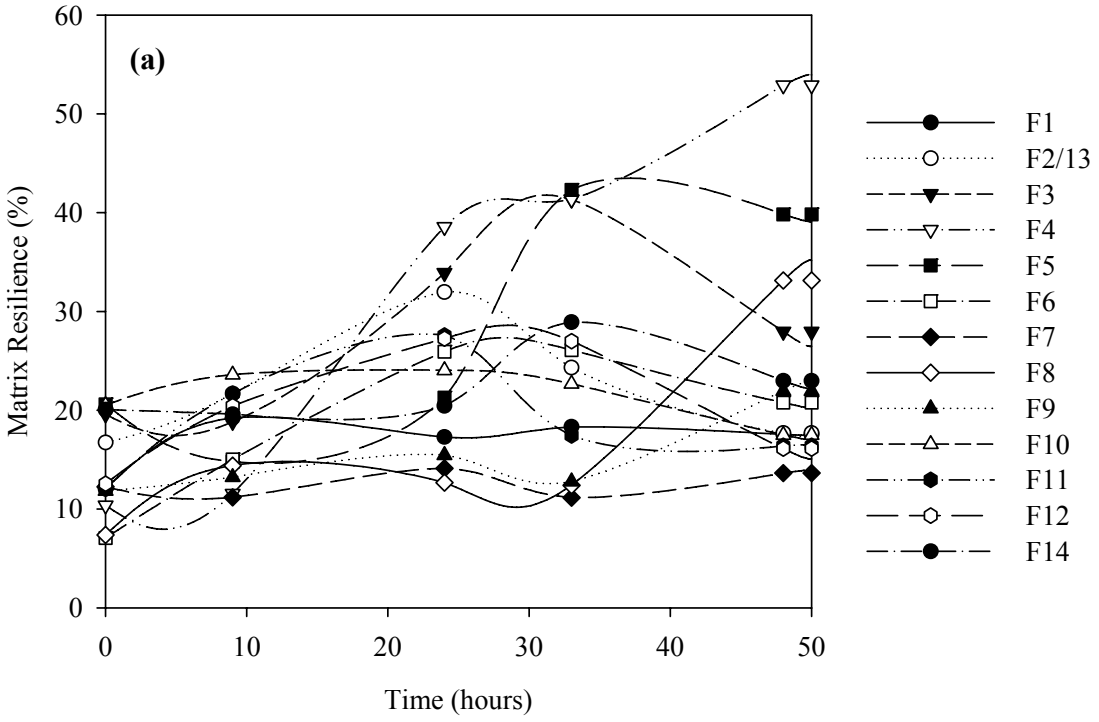
(a)
Matrix Resilience (%)
Time (hours)
F1
F2/13
F3
F4
F5
F6
F7
F8
F9
F10
F11
F12
F14

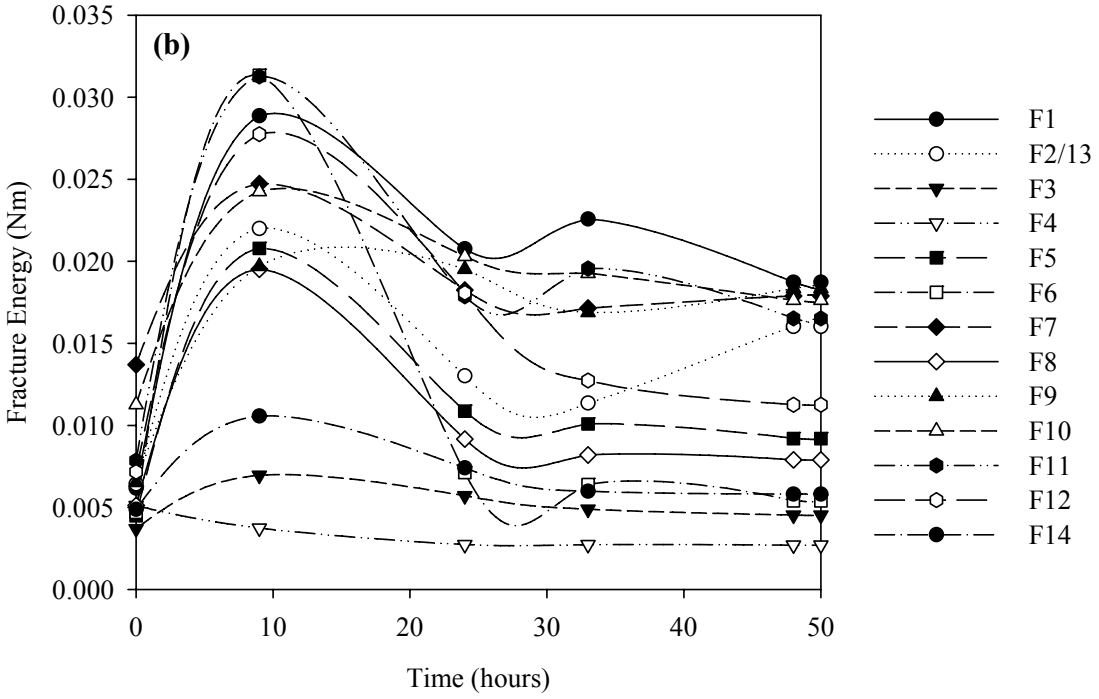
(b)
Fracture Energy (Nm)
Time (hours)
F1
F2/13
F3
F4
F5
F6
F7
F8
F9
F10
F11
F12
F14

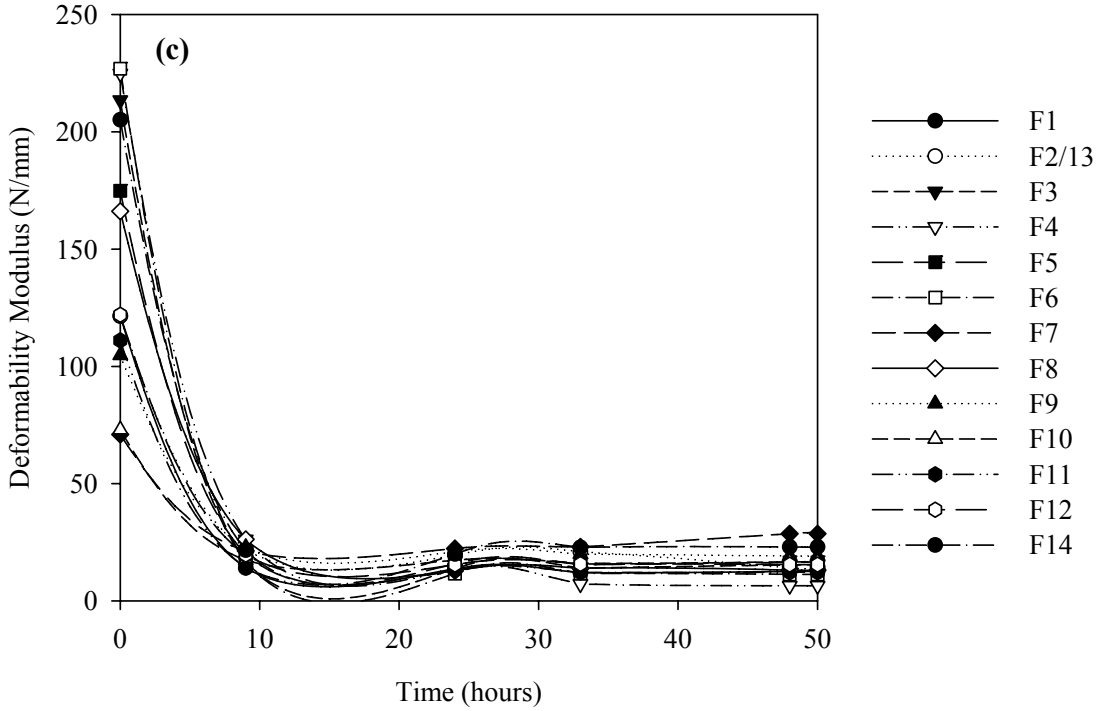

Figure 3.30: Changes observed in the (a) Matrix resilience (%) (SD<0.72%) (b) Fracture energy (Nm) (SD<0.0001Nm) and (c) Deformability modulus (N/mm) (SD<11.67N/mm) of Alg-HEC-PAA gelispheres over 50 hours following exposure to simulated CSF (N=3).

Table 3.6: Response Outcomes for Textural Analysis of unhydrated (t=0hr) and hydrated (after 9 hours of exposure to simulated CSF gelispheres of the Alg-HEC-PAA Formulations.

Formulation Number	Matrix Resilience (%)		Deformability Modulus (N/mm)		Fracture Energy (Nm) (10^{-2})	
	t=0hr	t=9hr	t=0hr	t=9hr	t=0hr	t=9hr
1	12.05	20.13	15.04	121.47	0.617	2.89
2*	16.73	18.43	13.89	121.48	0.643	2.20
3	19.58	28.37	12.93	213.48	0.370	6.96
4	10.37	41.66	29.17	224.84	0.510	3.73
5	20.60	22.84	19.03	174.83	0.450	2.08
6	7.08	3.54	17.78	226.90	0.470	3.13
7	12.25	8.17	71.88	70.98	1.370	2.47
8	7.38	88.86	23.25	166.10	0.511	1.95
9	11.83	16.39	28.47	104.76	0.652	1.97
10	20.52	17.19	16.70	73.01	1.130	2.42
11	12.06	16.41	14.56	111.05	0.785	3.13
12	12.56	13.44	18.23	205.13	0.717	2.77
13*	10.37	18.39	13.89	121.48	0.489	2.20
14	20.05	18.08	19.73	121.97	0.617	1.06

3.3.3 PHASE III: Formulation Optimisation Studies

3.3.3.1 Statistical Analysis of the Alg-HEC-PAA Gelispheres

Main effects plots are employed in conjunction with an analysis of variance. A main effect occurs when the mean response to a defined outcome changes across the levels of an input parameter. These plots are employed to examine the level means for each parameter and compare them to level means for other parameters. They are also employed to evaluate the comparative influence of several parameters on the responses. The response mean is plotted along the x-axis against the overall mean effect of the parameter on the response. Significant (vertical) deviation from the response mean i.e. upon varying the level of a given parameter indicates the presence of a greater magnitude of the main effect. The gradient of the response provides an indication of the magnitude, since it relates to its distance from the mean response.

Interaction plots are also employed in conjunction main effects plots to display the two-way interactions input parameters and to evaluate the relative potency of effects across parameters. An interaction occurs when the change in response of an input parameter from the one level of another differs from the change in response at the same two levels of a second parameter. That is, the effect of one factor is dependent upon a second factor. Parallel lines indicate an absence of interactions, conversely deviation from such a presentation indicates the presence and magnitude of interaction between the parameters.

The PB design was analysed in terms of two responses, DEE, and % drug release (DR) occurring at t=1 hour.

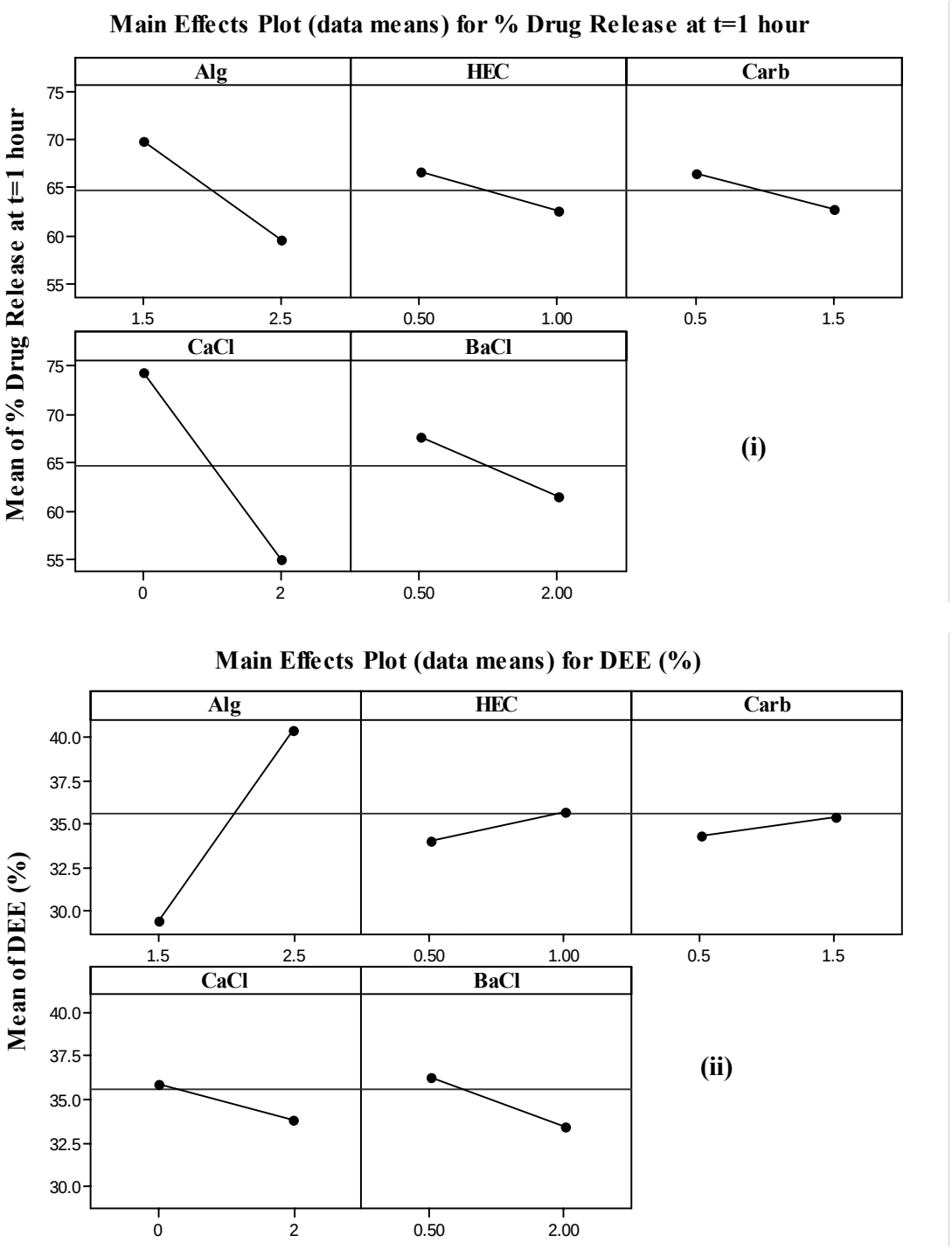

Figure 3.31a: Main effects plots indicating the influence of input parameters on (i) % drug release t=1 hour (i.e. the burst effect) and (ii) % DEE (where, Carb refers to PAA).

(iii)

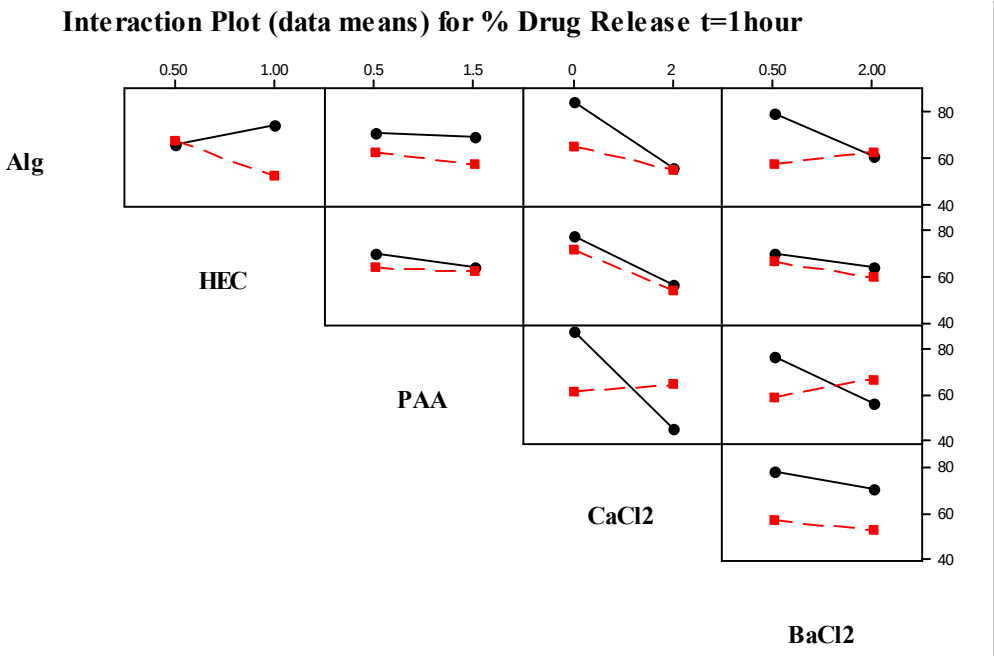

(iv)

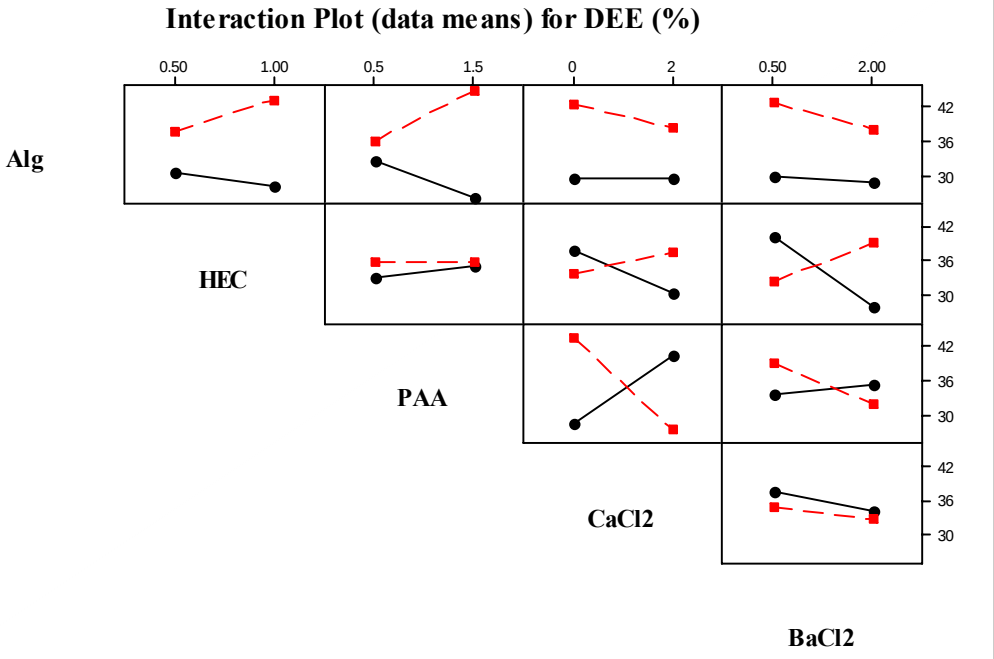

Figure 3.31b: Interaction plots correlating the pair-wise influence of input parameters (iii) % drug release t=1 hour and (iv) % DEE. The red lines indicate the upper limits of the parameters, while the black lines indicate the lower limits.

The concentration of alginate had the most significant impact on drug release from the crosslinked formulations. Higher concentrations of alginate had a dramatic impact in permitting slower rates of drug release, indicated by a minimal burst effect within the 1st hour of exposure to simulated CSF, and matrix degradation following hydration, as well as % DEE (Figure 3.33a-c).

High concentrations of calcium in the gelispheres also had a very significant impact on retarding drug release. The smaller cations interpenetrated the crosslinked polymer network during formulation and resulted in a denser system in the central portions of the matrix thus, allowing the formation of a more homogenously crosslinked matrix. It did not however influence % DEE substantially.

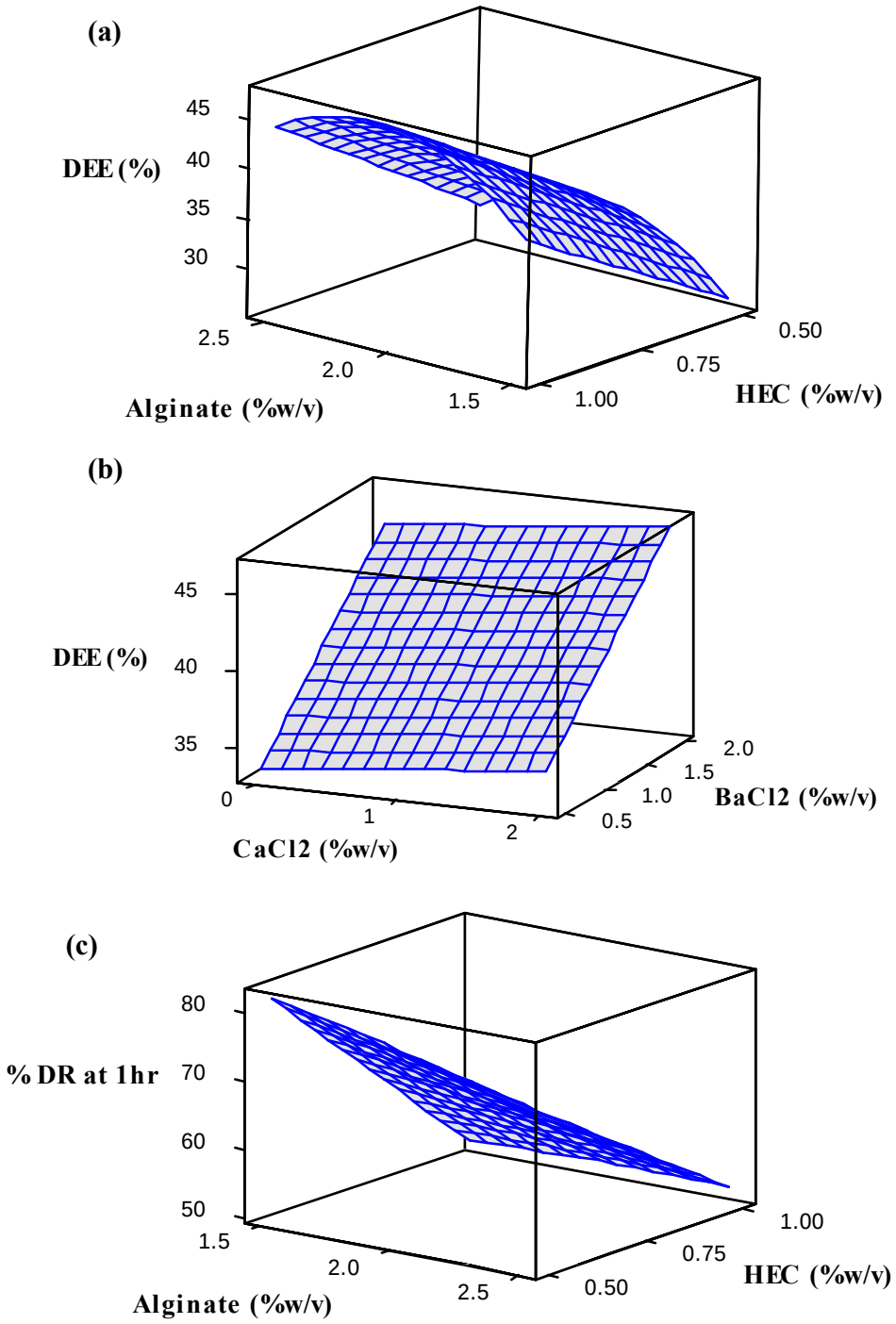

Figure 3.32: Response surface plots correlating % drug entrapment efficiency (DEE) and the influence of (a) polymer concentration (alginate and HEC) and (b) the concentration of crosslinking ions, barium and calcium and (c) % drug release (DR) at t=1 hour (i.e. the burst effect) and the influence of alginate and HEC concentration.

PAA provided a mechanical barrier to hydration by coating the gelispheres, hence retarded drug release and matrix degradation when employed in higher concentrations. It is proposed that due to its high molecular weight (3 MDa), it did not penetrate the crosslinked matrix during formulation, hence it did not form part of the matrix. Furthermore, it prevented nicotine leaching from the matrices during curing, allowing for a greater entrapment efficiency. It indicated the presence of an interaction with both crosslinking agents in the formation of compact matrices capable of entrapping a significant amount of nicotine and retarding drug release (Figure 3.32c-d).

Table 3.7: Summary of results for % drug release (DR) t=1 hour (i.e. the observed burst effect) and drug entrapment efficiency (DEE) for Alg-HEC-PAA gelispheres.

Parameter	% DR at t=1 hour	% DEE
|R|	0.847	0.747
R^2	0.717	0.558
R^2 adjusted	0.540	0.282
Standard Error	10.88	7.922
R^2 for Prediction	0.008	0.132
Durbin-Watson d	2.908	1.267
First Order Autocorrelation	-0.466	0.357
Coefficient of Variation	16.813	22.260

Results indicated that only the concentration of alginate in the formulation was significant in determining burst effect drug release (%DR at t=1 hour) and % DEE, since it demonstrated p-values which were less than 0.005.

Table 3.8: Summary of results for % drug release (DR) t=1 hour (i.e. the observed burst effect) for Alg-HEC-PAA gelispheres.

Analysis of Variance for % DR at t=1 hour						
Source	*SS*	*SS%*	*MS*	*F*	*F Signif*	*df*
Regression	2393.4	72	478.68	4.046	0.03962	5
Residual	946.45	28	118.31			8
LOF Error	945.23	28(100)	135.03	111.2593	0.07287	7
Pure Error	1.214	0(0)	1.214			1
Total	3339.8	100				13

% DR 1hr = b0 + b1*[Alginate] + b2*[HEC] + b3*[PAA] + b4*[$CaCl_2$]+ b5*[$BaCl_2$]						
Parameter	Coefficient	P value	Std Error	-95%	95%	t Stat
b0	95.26	0.001	18.21	53.27	137.26	5.231
Alginate	-25.52	0.000	6.280	-40.01	-11.04	-4.065
HEC	17.63	0.198	12.56	-11.33	46.59	1.404
PAA	1.954	0.764	6.280	-12.53	16.43	0.311
$CaCl_2$	-1.132	0.728	3.140	-8.373	6.108	-0.361
$BaCl_2$	5.147	0.254	4.187	-4.507	14.80	1.229

Table 3.9: Summary of results for % DEE for Alg-HEC-PAA gelispheres.

Analysis of Variance for % DEE						
Source	*SS*	*SS%*	*MS*	*F*	*F Signif*	*df*
Regression	633.96	56	126.79	2.020	0.180	5
Residual	502.07	44	62.76			8
LOF Error	239.56	21(48)	34.22	0.1304	0.972	7
Pure Error	262.51	23(52)	262.51			1
Total	1136.0	100				13

% DEE = b0 + b1*[Alginate] + b2*[HEC] + b3*[PAA] + b4*[$CaCl_2$]+ b5*[$BaCl_2$]						
Parameter	Coefficient	P value	Std Error	-95%	95%	t Stat
b0	11.05	0.429	13.26	-19.53	41.64	0.833
Alginate	13.72	0.01708	4.574	3.173	24.27	3.000
HEC	4.149	0.662	9.148	-16.95	25.24	0.454
PAA	-3.261	0.496	4.574	-13.81	7.286	-0.713
$CaCl_2$	-0.864	0.715	2.287	-6.138	4.409	-0.378
$BaCl_2$	-1.513	0.633	3.049	-8.544	5.519	-0.496

3.3.3.2 Formulation and Evaluation of Optimised Gelispheres

Two formulations were generated from optimising the formulations by maximizing % DEE and minimizing drug release at t=1 hour (burst effect). The formulations were identical and employed high concentrations of alginate, HEC and PAA as well as calcium and differed only in the concentration of barium employed to crosslink the matrices (Table 3.10).

Table 3.10: Optimised formulations developed.

Optimised Formulation Number	Alginate ($\%^{w}/_{v}$)	HEC ($\%^{w}/_{v}$)	PAA ($\%^{w}/_{v}$)	$CaCl_2$ ($\%^{w}/_{v}$)	$BaCl_2$ ($\%^{w}/_{v}$)
1	2.5	1.00	1.5	2	**2.00**
2	2.5	1.00	1.5	2	**0.50**

As observed previously, greater concentrations of barium employed to crosslink the matrix negatively impacted on DEE, however resulted in a reduced burst effect of drug release from the matrices.

Results indicated that the formulation crosslinked with a greater concentration of barium (Formulation 1), resulted in a moderately compromised DEE (Table 3.11), due to the fact that barium ions occupied greater space within G-pockets of the alginate molecule. The presence of higher quantities of alginate and HEC conferred to superior DEE due to extensive crosslinking.

Table 3.11: Drug entrapment efficiency (%) for optimised formulations (N=3; SD<0.08%).

Optimised Formulation Number	Drug Entrapment Efficiency (%)
1	50.13
2	52.22

Drug release kinetics demonstrated minimal difference, however as observed from previous results, reduced burst effects were observed for Formulation 1, which employed a higher concentration of barium to crosslink the matrices. The more compact matrices demonstrated desirable DEE and were selected to be exposed to dilute HCl in order to reduce the degree of matrix swelling with the intention to further attenuate the burst effect.

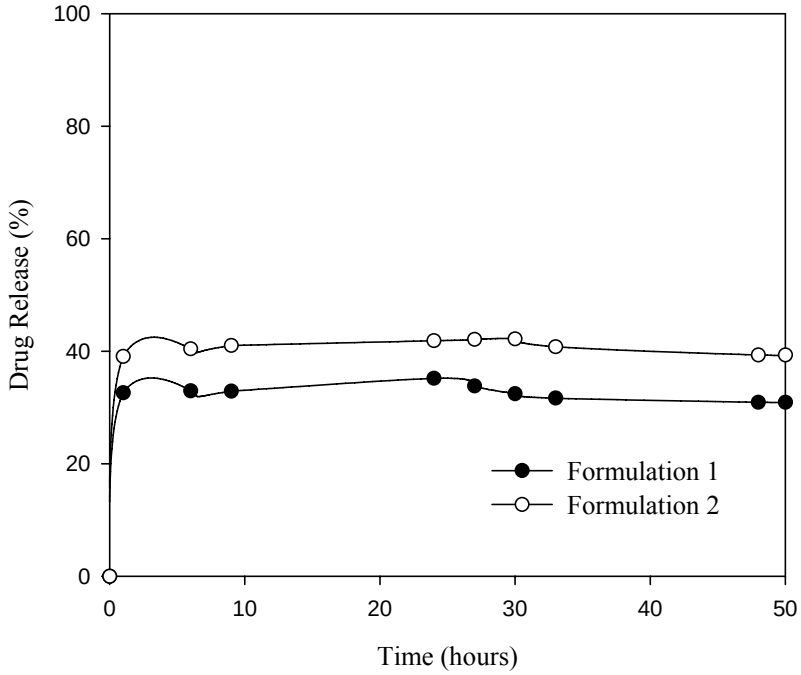

Figure 3.33: % Drug release from optimised formulations exposed to simulated CSF over 50 hours (N=3; SD<2.06%).

3.3.3.3 Elucidating the Effect of Precipitating Alginic Acid on Optimised Gelispheres

As observed previously, the influence of exposure of gelispheres to dilute HCl caused the precipitation of alginic acid within the crosslinked polymeric structure. Thus significantly retarded the rate at which the matrices swelled and underwent erosion and directly impacted the rate of drug release from the gelispheres. Reducing the extent of the burst effect was the primary goal of this

study. The optimised Formulation 1 from Section 3.4.3.2 was exposed to dilute HCl to reduce the extent of matrix swelling and erosion as observed previously during preliminary studies (Section 3.3). The formulations were subsequently evaluated for drug release and DEE.

As expected the resulting formulation, demonstrated a significant reduction of approximately 8.07% in DEE (Table 3.12). This correlates with the prolonged period of exposure of the gelispheres to an aqueous environment beyond the 30 minute curing time that permits drug 'leaching'.

Table 3.12: Drug entrapment efficiency (%) for unexposed optimised formulation 1 and HCl-exposed optimised formulation (N=3; SD<1.15%).

Formulation	Drug Entrapment Efficiency (%)
Unexposed optimised gelispheres	50.13
HCl-exposed optimised gelispheres	41.16

In this instance drug release studies were conducted over a period of 120 hours to assess the behaviour of the gelispheres over a prolonged period of time. It was observed that drug release kinetics were more sustained in comparison to those generated in previously, where it was observed that almost 100% of the entrapped drug was released from zinc-crosslinked gelispheres within 12 hours.

Results indicated that the release profile for gelispheres exposed to dilute HCl followed first-order kinetics, with a minimal burst effect (it declined by approximately 3.76%). Over the following 50 hours, the release profiles have minimal variation, an average of 3.26% lower drug release was observed for HCl-exposed optimised gelispheres (Figure 3.34). After 50 hours, the unexposed

gelispheres underwent a significant degree of matrix erosion that caused a surge in drug release. The HCl-exposed optimised gelispheres however, maintained their steady state of drug release even after 50 hours.

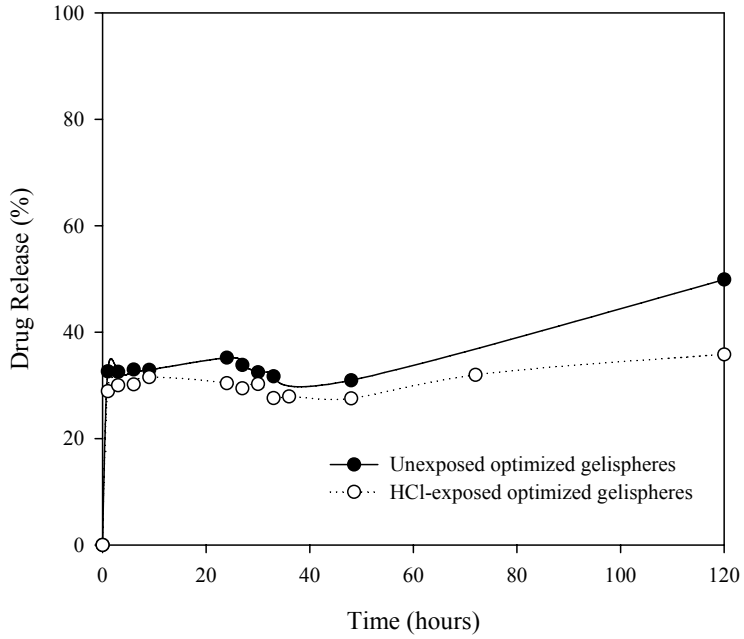

Figure 3.34: % Drug release from unexposed optimised formulation and HCl-exposed optimised formulation to over 120 hours to simulated CSF (N=3; SD<0.83).

3.4 Concluding Remarks

The most significant revelation from this study was the effect of exposure to dilute HCl precipitated alginic acid within the crosslinked matrices and significantly retarded gelisphere water uptake (swelling) (due to lower ionisation of the polymer and thus, lower aqueous solubility) and drug release rates. HCl-exposed gelispheres also displayed significantly greater robustness i.e. higher fracture energies, deformability moduli and resilience versus unexposed gelispheres. The influence of crosslinking agents in order of that which imparted greatest robustness over the 12 hour testing period was barium>calcium>zinc. The rates of drug release observed in formulations

crosslinked with the various cations were in the order, barium<calcium<zinc, and inversely correlated with the swelling behaviour of gelispheres. The initial 12 hours demonstrated first-order release and was followed by a second phase of zero-order release. Drug entrapment efficiency was found to be in the order barium>calcium>zinc and declined by approximately 21.81% - 12.64% upon exposure to dilute HCl post-curing due to 'leaching' of nicotine into solution.

While results demonstrated lower DEE for HCl-exposed gelispheres, the most significant findings indicated that HCl-exposed gelispheres underwent a significantly lower degree of matrix swelling and released nicotine at a slower rate in comparison to unexposed matrices. This property was significantly beneficial and the discrepancies sufficient to warrant it being an approach that may have potential in developing compact gelispheric matrices that underwent minimal expansion following exposure to CSF. Both barium and calcium demonstrated significantly robust matrices that retained their structure following exposure to hydration for longer durations of time. Their selectivity for the guluronic acid monomer resulted in the development of matrices that were significantly more compact than their zinc-crosslinked counterparts.

Statistical optimisation of the generated multi-polymeric Alg-HEC gelispheres employing barium as the primary crosslinking agent system indicated that the interaction between alginate and HEC is significantly synergistic in producing a highly compact gelisphere matrix when crosslinked with both barium and calcium ions. This interaction is unique and demonstrated superior drug entrapment and release kinetics than conventional alginate calcium-crosslinked systems. Exposure to dilute HCl post-curing further retarded drug release, but more importantly reduced the rate of swelling and degradation of the gelispheres. Although these results were exceedingly promising,

there was still a need to further retard drug release and alter the release kinetics to achieve zero-order release. In order to achieve this, the HCl-exposed optimised gelispheres were incorporated into an external polymeric matrix formulated as a prolonged release drug delivery system. Optimisation and evaluation of the parameters of formulation of these novel multi-unit compressed polymeric discs is discussed in the Chapters 4 and 5.

Chapter 4

Modulation of Nicotine Release via Formulation of a Compressed External Polymeric Matrix Incorporating Crosslinked Gelispheres

4.1 Introduction

Chapter 3 revealed that a significant modulation of drug release kinetics could be achieved from calcium-barium crosslinked alginate gelispheres when the reinforcing polymers, HEC and PAA were incorporated into the matrix. Exposure of the gelispheres to dilute HCl post-curing led to a further attenuation of drug release rates as well as matrix swelling. However, drug release was rapid and followed first-order release. This Chapter explicates the studies conducted to further modify the release of nicotine. The optimised gelispheres were incorporated into an external polymeric matrix formulated as compressed polymeric discs with the aim of modulating drug release to achieve prolonged zero-order release. Optimising formulation variables of the compressed polymeric discs through a variety of mechanisms was explored. The following sections discuss properties of the polymers selected to develop the proposed system and evaluate the studies that have been conducted in recent times in the arena of site-specific drug delivery via compressed biodegradable polymeric discs with particular emphasis on prolonged release systems.

Three polymeric materials with sufficient compressibility and adequate safety data regarding biocompatibility and safety were selected to develop the external compressed matrices incorporating the crosslinked gelispheres developed in Chapter 3. They were:

- Hydroxypropylmethylcellulose (HPMC)
- Polyethylene oxide (PEO) and
- Poly(lactic-co-glycolic) acid (PLGA)

Generally, parenteral prolonged zero-order release systems have the capacity to minimize dose-related side-effects by achieving constant and sustained plasma-levels. This is particularly important for drugs with narrow therapeutic indices. A dose reduction resulting from the avoidance of fluctuations in plasma drug levels, as well as the enhancement of patient compliance by reducing the frequency of administration, are further potential benefits (Pillay and Fassihi 1999).

The use of compressed hydrophilic polymeric discs are among the most popular means of achieving controlled drug release due to the simplicity and cost-effectiveness of their formulation and manufacturing and versatile applicability to deliver compounds with range of solubilities (Williams et al., 2002; Durig and Fassihi, 2002; Jamzad et al., 2005). Numerous factors influence the rate of drug release from such matrices. The most significant factor being the properties of the polymer employed to generate the matrices (Jamzad and Fassihi, 2006). The simplest form is known as a monolithic system that is formulated by simply incorporating the pharmaceutical active into a hydrophilic polymer (Li et al., 1989; Durig and Fassihi, 2002).

HPMC and PEO (FDA approved) are both hydrophilic biopolymers that undergo simultaneous swelling and dissolution when exposed to hydration. Both polymers have been used extensively to formulate controlled-release drug delivery systems (Maggi et al., 2000; Jamzad and Fassihi, 2006).

Depending on the solubility of entrapped of incorporated drugs within monolithic matrices of such polymers, the actives diffuse out into the bulk medium preceding or following erosion of the polymer (Ju et al., 1995; Skoug et al., 1993; Tahara et al., 1995). The mechanisms relating to the swelling of hydrophilic polymeric matrices has been the subject of significant research (Doelker, 1993; Gao et al., 1996; Narasimhan and Peppas, 1997; Colombo et al., 1999). In particular, there have been several studies which have attempted to relate molecular characteristics of the swelling process including aspects such as polymeric chain extension, disentanglement and solvent accommodation to macroscopic characteristics such as drug release (Peppas, 1983; Kim and Fassihi, 1997; Pillay and Fassihi, 1999). Other formulation factors which influence the drug release rate from hydrophilic matrices include the quantity of drug loading, drug-polymer ratio, drug particle size and molecular mass, polymer viscosity and molecular weight, presence and nature of formulation excipients and release modulators (Pillay and Fassihi, 1999; Pillay and Fassihi, 2000; Jamzad et al., 2005). In a study conducted by Maggi and colleagues (2000), high molecular weight hydrophilic polymers were employed to formulate compressed polymeric matrices. Their study demonstrated that the degree of water uptake significantly impacted the rate of matrix degradation and erosion. This directly influenced the rate of drug (diltiazem hydrochloride) release. As was anticipated, higher viscosity grades of each polymer displayed slower hydration rates by demonstrating a greater degree of resistance to erosion verses the corresponding lower viscosity polymers. The rate of drug release was significantly dependant on the rate and extent of polymer gelation and swelling over time.

(a)

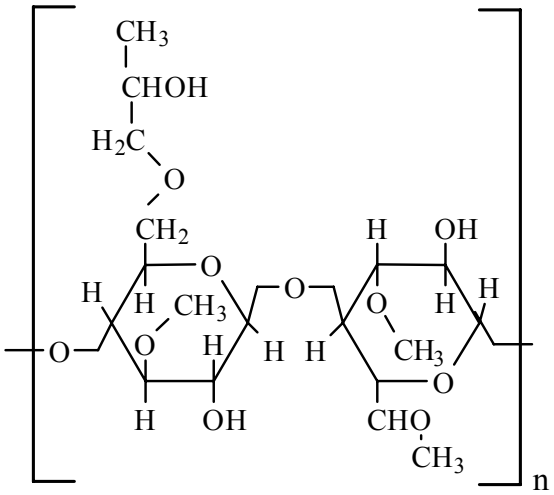

(b)

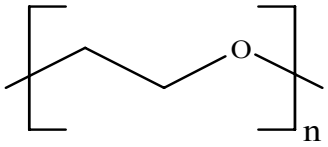

(c)

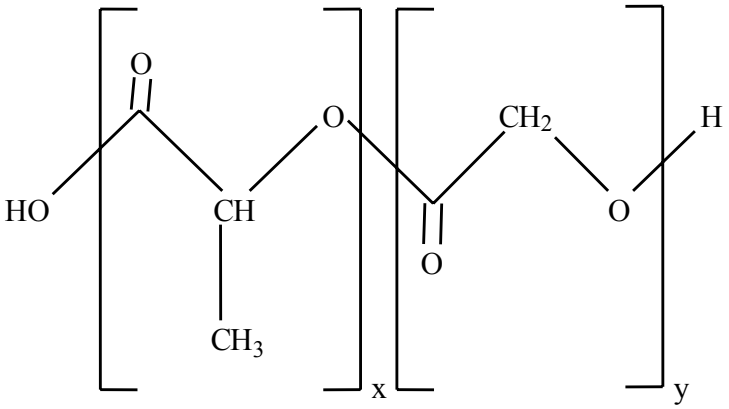

x = number of lactic acid units
y = number of glycolic acid units

Figure 4.1: The chemical structures of (a) hydroxypropylmethylcellulose (HPMC), (b) polyethylene oxide (PEO) and (c) poly(lactic-co-glycolic acid) (PLGA). (Source: Ludwig, 2005).

Yoo et al. (2004) evaluated the role of the biodegradable polyester poly(lactic-co-glycolic acid) or PLGA as a carrier to administer a prolonged release formulation for site-specific delivery of the antibiotic gentamicin sulphate for the prevention of osteomyelitis in the form of compressed discs for controlled delivery. The system had the advantages of being only moderately aqueous soluble for controlled drug diffusion, being biocompatible as well as non-toxic and biodegradable. The FDA approved polymer is naturally biodegraded to glycolic acid and lactic acid (both components of Krebs cycle) *in vitro* and *in vivo* (Bhardwaj and Blanchard, 1998; Choi et al., 2002). Consequently, no surgical intervention or procedures are required for their removal following implantation. Other studies have employed compressed PLGA controlled release discs for delivery of a variety of pharmaceutical agents (Wang et al., 2002; Choonara et al., 2006). Biocompatibility studies performed indicated that it is considerably well tolerated when implanted into the CNS (Fournier et al., 2003). A review by Fournier et al. (2003) established that regardless of the drug carrier shape (whether it is on the form of a rod, microspheres, or granules) or the implantation site, the CNS tissue response to implanted PLGA drug delivery devices is only a moderate and non-specific inflammatory reaction due to the mechanical trauma of implantation. The biodegradable polyanhydride, poly(bis(p-carboxyphenoxy)propane-sebacic acid) (pCPP:SA) has been widely studied as a means to deliver anti-neoplastic agents to the brain in the form of compressed discs (Brem et al., 1994; Walter et al., 1994; Williams et al., 1997; Yuan et al., 1999a, Yuan et al., 1999b; Yuan et al., 1999c; Pradilla et al., 2005). Recent studies (Storm et al., 2002; Frazier et al., 2003) have investigated the release, biodistribution, and efficacy of anti-neoplastic agents from these compressed discs implanted intracranially *in vivo* in rat models. Results have been extremely promising displaying that the systems permitted site-specific drug

release and resulted in a therapeutic effect with little or no systemic toxicity, and prolonged survival in the rat models.

The subsequent sections present the study conducted to establish the pertinent aspects involved in the development and evaluation of the properties of an external polymeric matrix (disc) for incorporating the optimised gelispheres from the previous chapter in order to achieve attenuated drug release. The properties of the three polymers, namely HPMC, PEO and PLGA are evaluated in their powdered and compressed forms. The degradation and erosional behaviour of the discs following exposure to simulated CSF are also conducted to elucidate their influence on drug release. Finally kinetic modelling is undertaken to understand the predominant mechanisms involved in controlling drug release.

4.2 Materials and Methods

Low molecular weight (50/50) polylactic-co-glycolic acid (PLGA) with an inherent viscosity of 0.32-0.44dL/g in $CHCl_3$ at 30°C (Resomer® L 503) was donated by Birmingham Polymers Inc. (Bioabsorbable Polymers, MA, USA), hydroxypropylmethylcellulose (HPMC) USP 2208 (Methocel™ K4M, M_W ~ 86,000 Da; methoxyl 23%, hydroxypropoxyl 8.4%, with an average moisture content of 3.4%$^w/_w$) was donated by Dow Chemical Company and polyethylene oxide (PEO) Polyox™ WSR 303 (M_W ~7 MDa and average moisture content of 0.22%$^w/_w$) was donated by Union Carbide (USA).

4.2.1 Evaluation of Powder Flow Properties and Compressibility of Polymers

For highly soluble compounds, diffusion is the primary mechanism of drug release from polymeric matrices. Hence, drug release is a function of the porosity of a compressed polymeric disc can be modulated by a variety of factors including compression force, the size, shape and adhesion between the powder particles (van Veen et al., 2005). Modulating these characteristics can allow for the development of entities which have the capacity to undergo controlled bioerosion with prolonged release capability (Wise, 1984).

The rheological properties of powders can be evaluated employing a range of tests that provide an indication of the nature of forces present between the surfaces of solid particles.

4.2.1.1 Carr's Compressibility Index (CCI) of Polymers Employed to Formulate External Compressed Matrices

Carr (1965) evaluated inter-particulate cohesive properties with angle of repose measurements and studied the effects of packing geometry of solids with bulk and tap density measurements. He established that the density of a powder is dependant upon the degree of particle packing and that the powder density changes as the powder consolidates. The degree of consolidation is unique to the powder and ratio of these densities is related to inter-particulate friction. Carr's Compressibility Index (CCI) (Equation 4.3) is employed to measure the underlying phenomena of inter-particle interactions between powders. The higher the CCI for any given powder after the application of mechanical stress, the lower its bulk density. The application of mechanical stress (tapping) allows for the expulsion of entrapped air within the powder and indicates good compressibility, or more accurately, consolidation characteristics.

Samples of accurately weighed powder (3g) were loaded into a 20mL graduated glass measuring cylinder. The initial volume (V_0) was recorded. The contents were tapped and powder volume recorded following 2, 8, 16, 30 and 60 taps (V_t). The fluff and apparent density was calculated employing Equation 4.1 and 4.2 respectively.

$$\text{Fluff Density} = W/V_0 \ \text{g/mL} \qquad \text{Equation 4.1}$$

$$\text{Tapped Density} = W/V_t \ \text{g/mL} \qquad \text{Equation 4.2}$$

Where, W (g) is the weight of powder employed to conduct the test.

Carr's Compressibility Index (CCI) (%) was calculated employing Equation 4.3.

$$\%\ \text{CCI} = (\text{Tapped Density} - \text{Fluff Density})/\text{Tapped Density} \times 100 \qquad \text{Equation 4.3}$$

4.2.1.2 Evaluation of Angle of Repose (ϕ) of Polymers Employed to Formulate External Compressed Matrices

A static heap of powder, when only gravity acts upon it, will tend to form a conical mould. The angle to the horizontal cannot exceed a certain value. This is known as the angle of repose (ϕ) (AR). If any particle temporarily lies outside this 'limiting' angle, it will slide down the adjacent surface under the influence of gravity until the gravitational pull is equated by the friction caused by inter-particulate forces. A higher value for AR indicates poor flowability and indicates high inter-particle interaction.

To evaluate the angle of repose (ϕ) an adapted fixed-funnel and free-cone method was employed (Carr, 1965). This involved attaching a conical funnel to a retort stand with the bottom orifice (diameter 7mm) at 10cm height above the surface. A sample of powder (3g) was placed into the funnel while keeping the orifice closed. The centerpoint and a graduated set of axes was marked on a piece of paper and placed beneath the funnel. The contents of the funnel were allowed to flow out of the orifice and the angle that the side of the conical heap made with the horizontal plane was recorded as the angle of repose (ϕ) and calculated employing Equation 4.4:

$$\tan \phi = 2h/D \qquad \text{Equation 4.4}$$

Where,

h = powder height at centerpoint (mm) and

D = diameter of powder bed (mm)

4.2.2 Formulation of Compressed Polymeric Discs Incorporating Gelispheres

Briefly, 500mg of the dry polymer mixture comprising either HPMC, PEO or PLGA, and various binary combinations and gelispheres equivalent to 20mg of entrapped nicotine (approximately 100mg gelispheres) and subsequently compressed into discs using a Beckman® Hydraulic Press (Beckman Instruments, Inc., Fullerton, USA) applying a pressure of 8 tons. Flat-faced punches with a diameter of 10mm were employed to compress the discs. Table 4.1 summarizes the investigated disc compositions.

Table 4.1: Investigated polymer compositions for the external matrix.

Formulation Number	HPMC (mg)	PEO (mg)	PLGA (mg)
F1	500	-	-
F2	-	500	-
F3	-	-	500
F4	250	250	-
F5	250	-	250
F6	-	250	250
F7	166	166	166

4.2.3 Evaluation of *In Vitro* Drug Release Characteristics of the Compressed Polymeric Discs Incorporating Gelispheres

In vitro drug studies were performed in triplicate as described in Chapter 3, Section 3.3.8 over a period of 50 days for each disc.

4.2.4 Evaluation of Friability of External Polymeric Matrices

Friability analysis evaluated the ability of the compressed polymeric discs to withstand mechanical damage. The friability of the discs was measured employing a Roche® Friabilator (Hoffman la Roche, Basel, Switzerland). The discs were accurately weighed prior to being placed into the friabilator (N=3). A rotation time of 4 minutes and 20 minutes at 25rpm was used. Discs were removed and loose particles brushed off the surface and re-weighed. The percentage weight loss was calculated (Equation 2.1, Chapter 2).

4.2.5 Textural Analysis: Evaluation of Brinell Hardness Number (BHN) of Compressed Polymeric Discs

The change in the mechanical properties of the discs following exposure to simulated CSF was assessed by measuring the Brinell Hardness Number (BHN). The BHN is an indication of the force required to indent the surface of the disc and is a measure of the hardness of the surface of the compressed polymeric discs.

The TA.*XTplus* Texture Analyser (TA) (Stable Micro Systems®, Surrey, UK) was employed to generate a force-distance profile for discs exposed to simulated CSF (0.1M PBS; pH 7.4; 37°C; 50rpm) at predetermined time intervals. The input parameters employed are listed in Table 4.2.

Table 4.2: Typical test parameters employed for analysis of the Brinell Hardness Number (BHN) of compressed polymeric matrices exposed to simulated CSF.

Test Parameter	BHN (N/mm^2)
Pre-test speed	1.0 mm/s
Test speed	0.5 mm/s
Post-test speed	1.0 mm/s
Target mode	Distance
Trigger type	Auto (force)
Trigger force	0.5 N
Load cell	5 kg

The textural analyzer was fitted with a 3.175mm ball-tipped steel probe and inserted into the discs the probe was inserted into the discs to a depth of 0.25mm at a speed of 0.5mm per second and removed as indicated by the test parameters listed in Table 4.2. BHN (N/mm^2) was calculated employing the following equation,

$$BHN = \frac{2F}{\pi D[\, D - (D^2 - d^2)^{1/2}\,]} \qquad \text{Equation 4.5}$$

Where,

D = Diameter of ball probe (3.175mm)

d = Depth of indentation (0.25mm)

F = Force (Newtons), measured from the generated distance-time profile.

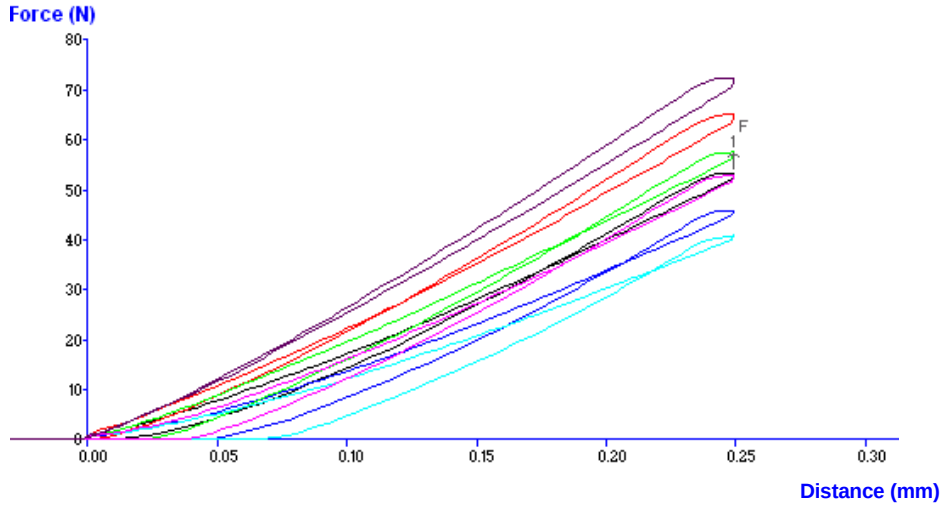

Figure 4.2: Typical force-distance profile obtained for the calculation of BHN for the compressed polymeric discs exposed to simulated CSF.

4.2.6 Evaluation of Conductivity Changes Following Disc Gelation

An OAKTON® TDS Testr™ Kit (Model WD-35661-70) (Solon, OH, USA) was employed to measure the conductivity of the PBS (0.1M; pH 7.4) solution containing the polymeric discs at predetermined intervals of time over a period of 30 days. Samples were extracted from the solutions and diluted 1:10 in double deionised water. The electrode was immersed in the diluted polymer-PBS solution and conductivity (μSiemens) was read.

4.2.7 Evaluation of Matrix Erosion of Compressed Polymeric Discs Following Hydration

Pre-weighed hydrated discs were removed from simulated CSF at predetermined intervals and dried under ambient conditions (21ºC) for 7 days. The dried discs were re-weighed and the percentage weight loss (% WL) calculated employing Equation 2.1 (Chapter 2).

4.2.8 Evaluation of Changes in Disc Porosity Following Hydration

Scanning Electron Microscopy (SEM) was employed to assess the changes in the porosity of the polymer matrices following hydration. Dried samples of the discs were cross-sectioned and coated with a thin layer of colloidal graphite. Thereafter they were mounted onto aluminium stubs and coated with a thin layer of gold-palladium under an electrical potential of 20keV. Samples were viewed in the FE-SEM (JEOL JSM-840, Tokyo, Japan) at magnification of 65 and probe current of 30 nanoamps.

4.2.9 Kinetic Modelling of Release Kinetics from Compressed Polymeric Discs

Kinetic models represent the molecular interactions that occur when chemical bonds are broken and reformed into new chemical compounds. Such kinetic models are sometimes referred to as micro-kinetic models. A reaction mechanism consists of a set of reaction pathways, rate coefficients for each reaction pathway and either reverse rate coefficients or the thermodynamic properties necessary for calculating reverse rate coefficients. FDA-recommended f_1 and f_2 similarity and difference factors were employed to compare profiles generated from drug release studies. This approach has been shown to be superior to conventional statistical methods such as

the t-test or the ANOVA, due to its ability to account for pharmaceutical variability rather than statistical 'over-sensitivity' (FDA guidelines, 1997).

The Power Law equation (Equation 4.6) is employed to describe drug release from polymeric systems.

$M_t/M_\infty = k_1 t^n$ Equation 4.6

Here, M_t and M_∞ are the absolute cumulative amount of drug released at time t and overall drug released, during the study respectively; k is a constant incorporating structural and the geometric dimensions of the device, and n is the release exponent, indicative of the mechanism of drug release. It is an equation which assumes that the two apparently independent mechanisms of drug transport namely, Fickian diffusion and Case II transport occur simultaneously. Thus it describes the dynamic interaction between the swelling of and drug release from glassy polymers. It is independent of the form of the constitutive equation and the nature of coupling of polymeric relaxation and drug diffusion. However it must be noted that the classic equation stated above is applicable primarily for 'moderately swellable systems' (in other words, the equilibrium swelling ratio (ratio between the hydrated and unhydrated polymeric matrix) of the polymeric system does not exceed 1.33) (Pillay and Fassihi, 1999).

Thus Equation 4.6 has two distinct physical implications, when n=0.5, this indicates the occurrence of diffusion-controlled drug release or Fickian release kinetics, while, when n=1.0, it indicates swelling-controlled drug release, or Case II transport kinetics. Values of n which lie between 0.5 and 1.0 are regarded as an indicator for the occurrence of anomalous transport kinetics (superposition of both phenomena). From Equation 4.6 it can be observed that when the value of

the exponent n = 1.0, the rate of drug release from the polymeric matrix is independent of time. This corresponds to zero-order release kinetics. For slabs, the mechanism that creates the zero-order release is known as Case II transport. Here the relaxation process of the macromolecules occurring upon water imbibed into the system is the rate-controlling step. Water acts as a plasticizer and decreases the glass transition temperature (T_g) of the polymer, which allows the polymeric chains to undergo the transformation from glassy to the rubbery state, with increasing mobility of the macromolecules and volume expansion (i.e. swelling and subsequent polymeric disentanglement).

Peppas and Sahlin (1989) developed the following geometry-independent equation (Equation 4.7) which consolidates the contributions of both Fickian and Case II transport mechanisms in drug release kinetics:

$$M_t/M_\infty = k_1 t^n + k_2 t^{2n} \qquad \text{Equation 4.7}$$

Here, k_1 is the Fickian kinetic constant and k_2 is the relaxational/dissolution rate constant (i.e. anomalous transport).

The Hopfenberg equation (Hopfenberg, 1976) is employed to compare the release rates of a drug within different batches produced under different conditions (Equation 4.9).

$$M_t/M_\infty = 1-[1- k_1 t]^n \qquad \text{Equation 4.9}$$

Where, k_1 is the overall erosion rate constant and n is dependant on the geometry of the polymeric matrix i.e. it is a geometry-dependent equation. Hopfenberg proposed a model applicable to either a slab, cylinder or sphere showing heterogeneous erosion (Table 4.3). The model assumes that drug

release is not influenced by internal or external time-dependent resistance to diffusion in the eroding polymeric matrix (Pillay and Fassihi, 1999). It takes into account the fact that the surface area of the polymeric matrices change over time as a result of polymeric erosion and degradation. It correlates drug release with the change in surface area of the matrix (Pillay and Fassihi, 1999; Pillay and Fassihi, 2000).

Table 4.3: The relationship between the geometry of the polymeric matrix and mechanism of drug release. (Source: Siepmann and Peppas, 2001).

Exponent 'n'			**Drug Release Mechanism**
Slab	*Cylinder*	*Sphere*	
0.5	0.45	0.43	Fickian Diffusion
0.5<n<1	0.4<n<0.81	0.43<n<0.85	Anomalous Transport
1	0.89	0.85	Case II Transport

This model was designed specifically for evaluating drug release from a planar surface of for instance, a tablet which follows zero-order kinetics from an erodible device maintaining constant surface area over a period of time. This model assumes heterogeneous erosion with a kinetic constant,

$k_1=k_0/C_0r_0$ Equation 4.8

Where,

k_0 is the erosion rate constant,

C_0 is the uniform initial concentration of drug in matrix and

r_0 is the initial radius.

When numerous parameters are being evaluated when conducting time series analysis, it is possible to generate several widely different models. Thus objective criteria such as the Akaike Information Criterion (AIC) and the Schwartz's Bayesian Criterion (SBC) can be employed to attenuate this pitfall (Akaike, 1974; Schwarz, 1978). Both are a measure of the goodness of fit of a particular model based on the maximum likelihood. For a given mode, the lower the AIC and SBC scores, the better the model. Furthermore, correlation between the predicted and experimental dissolution data is an additional tool which was employed to establish the reliability of the mathematical model. Superior correlation is suggested when the value of correlation approaches one.

In a review by Siepmann and Peppas (2001) a comprehensive discussion on various theories based on drug release from a cylindrical geometry is given, whereby mass transfer is considered in three dimensions. However it was established that while, in most cases, simple empirical models are adequate to establish the basic mechanism(s) of drug release kinetics from a compressed polymeric matrix. However, when more reliable and detailed information is required, more complex, mechanistic theories need be applied and/or developed. For the purposes of our study the validity ('goodness of fit') of the abovementioned theories was evaluated for the optimised systems developed.

4.3 Results and Discussion

4.3.1 Powder Flow and Compressibility of Polymers Employed to Formulate Compressed Discs

4.3.1.1 Carr's Compressibility Index (CCI) of Polymers Employed to Formulate Compressed Discs: Evaluating Powder Compressibility

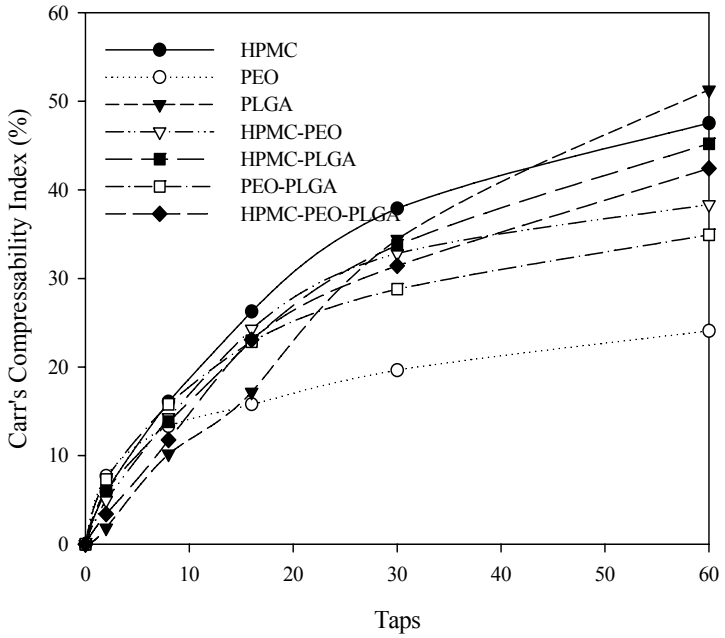

Figure 4.3: Carr's Compressibility Index (%) of polymers employed to formulate compressed discs.

The porosity and apparent density of a powder are inversely proportional (Hui et al., 1989). PLGA demonstrated the most significant degree of compressibility. After the first 6 taps, PEO achieved an equilibrium tapped density and little change was observed upon the application of further mechanical stress. Powders such as HPMC and PLGA demonstrated that the small size of their particles (in comparison to those of PEO, which had a slightly more granular texture) indicated that application of further mechanical stress increased the propensity for particles to be in contact with

one another and thus form inter-particle bonds i.e. increased cohesion (Führer, 1996). Furthermore, the smaller particle size implied a higher surface area for contact between adjacent particles. Thus they demonstrated significantly enhanced compressibility characteristics. The incorporation of HPMC with PLGA demonstrated excellent compressibility and subsequently allowed for the formulation of compact discs. The relevance of these results indicated the degree to which the compressibility of the polymers and thus indicated their ability to prevent solvent penetration to their core containing drug-loaded gelispheres. This data allowed us to predict that polymers, such as PLGA with superior compression characteristics would generate more dense matrices that demonstrated greater endurance to the influence of the surrounding aqueous medium.

4.3.1.2 Angle of Repose (ϕ) of Polymers Employed to Formulate Compressed External Matrices: Evaluating Powder Flowability

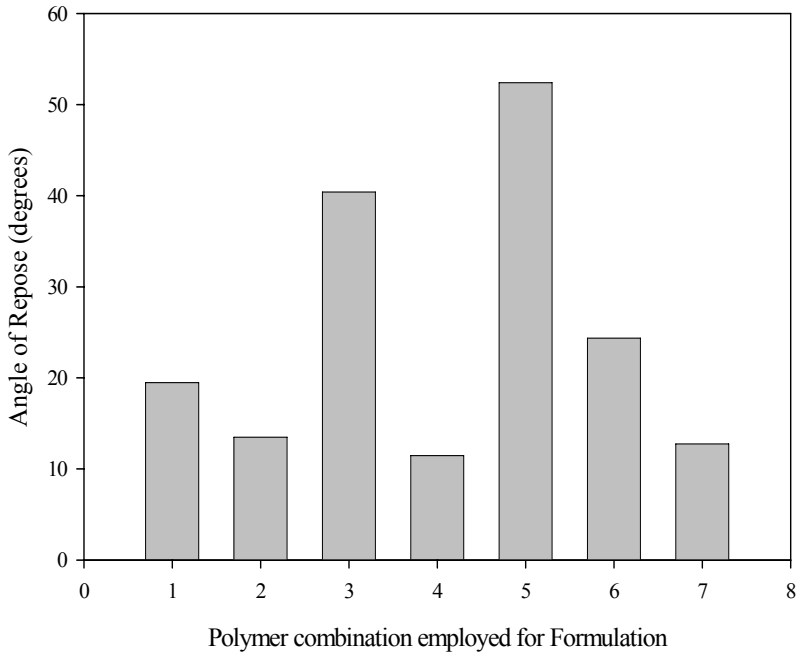

Figure 4.4: Angle of Repose (degrees) of polymers employed to formulate compressed discs.

The results (Figure 4.4) indicated that PLGA had the greatest degree of inter-particle interaction (cohesion). Hence it's high angle of repose (AR) (40.40º) indicated that it had poor flow properties. When combined with HPMC, their mutually attractive interaction was indicated by the highest AR of 52.41º which implies that the combination had the potential for producing highly dense compressed discs. PEO on the other hand indicated excellent flow properties, as it demonstrated a lower AR of 13.49º. This can be explained in terms of the fact that it was predominately composed of spherical granular particles. These particles had a smaller surface area per particle to interact with each other, as compared to PLGA and HPMC. Its incorporation with PLGA and HPMC resulted in a significant decline in AR (11.46º and 12.74º respectively) and improved overall flowability, thus it negatively impacted on the cohesive tendency of the particles, which implied

that matrices generated with the aforementioned combinations would generate less compact matrices. From a manufacturing process point of view, improved flowability permits easier processing conditions. However this implies that additional substances (such as binders) may need to be added to enhance powder compressibility to generate discs.

4.3.2 Evaluation of *In Vitro* Drug Release from Optimised Alg-HEC-PAA Gelispheres Incorporated within Compressed Polymeric Discs

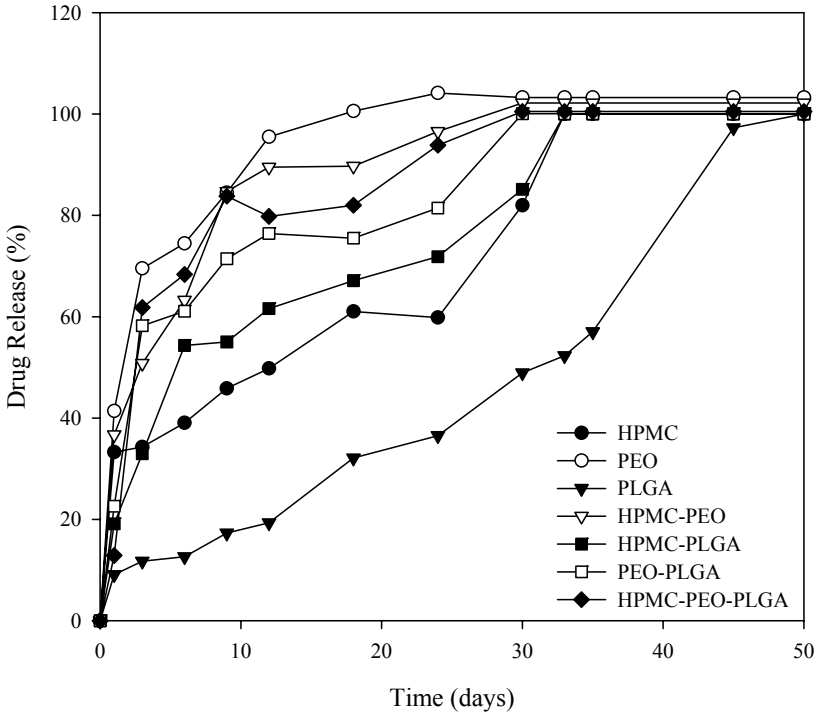

Figure 4.5: % Drug released from optimised gelispheres (Chapter 3) compressed into polymeric discs following exposure to simulated CSF over a period of 50 days (N = 3; SD<0.59%).

In vitro drug release studies in simulated CSF indicated that optimised gelispheres incorporated into PLGA discs demonstrated zero-order release kinetic, that were able to provide controlled and prolonged release for approximately 50 days. Drug release kinetics indicated a rapid burst in drug

release after day 35, whereafter a first-order release profile was obtained. An additional 40% of entrapped nicotine was released between days 35 and 40. In retrospect it was observed that PLGA had the maximum cohesive tendency between its particles and has the ability to be most compressible. Being a hydrophobic polymer, its main degradative mechanisms are though the hydrolytic cleavage of its polymeric backbone. Consequently, these discs underwent minimal matrix degradation.

The rapid release rates observed from PEO and HPMC matrices allowed us to conclude that drug release occurred primarily by Fickian diffusion. The presence of PEO in matrices enhanced the rate of drug release from the compressed discs. Its hydrophilic character allowed rapid disentanglement and degradation of the compressed matrices. Its tendency was therefore to undergo comparatively rapid bulk erosion when it came in contact with the alkaline hydrating medium (Figure 4.5). HPMC is a hydrogel, hence it has the capacity to imbibe a significant amount of water before is begins to degrade. Furthermore, as observed from previous results, its particles were sufficiently cohesive to generate compact discs that are able to provide zero-order release following the achievement of an equilibrium hydrated state (discussed under later sections). Between days 3 and 18, a linear drug release profile was observed from HPMC discs. Prior to this a burst release was observed, whereby approximately 33.25% of the entrapped nicotine was released within the first 24 hours. Combining HPMC and PLGA had a unique effect on drug release. While in this case zero-order release was also observed, they exceeded those observed with the individual polymers. A burst effect was observed until day 6, by which time 54.31% of the drug had been released. Thereafter drug release followed a linear zero-order release profile until day 32. Release kinetics

for all other combinations exhibited rapid burst rates of drug release and predominately first-order release.

4.3.3 Friability of Compressed External Polymeric Matrices

According to the United States Pharmacopoeia (USP 23), conventional compressed tablets that incur a loss in weight after 100 revolutions (which is the equivalent of 4 minutes in the frabilator at 25rpm) in a friabilator of less than 0.5% - 1.0% are considered acceptable.

Table 4.4: Friability results for polymeric matrices expressed as % weight loss (% WL) after 4 and 20 minutes in a friabilator at a rotation 25rpm.

Formulation	% WL_4	% WL_{20}
HPMC	0.081428	0.306921
PEO	0.101458	0.133164
PLGA	0.000000	0.025974
HPMC-PEO	0.050232	0.106744
HPMC-PLGA	0.051463	0.064329
PEO-PLGA	0.038346	0.102256
HPMC-PEO-PLGA	0.025410	0.050819

The results indicated that the discs generated were well within the predetermined limits. PLGA discs were exceedingly well compressed and underwent negligible loss in weight following 500 revolutions (i.e. 20 minutes at 25rpm). Furthermore, the incorporation of PLGA with HPMC and PEO into the disc resulted in an enhanced robustness imparted into the matrix, while the addition of PEO has the reverse effect, indicated by the greater friability.

4.3.4 Changes in Brinell Hardness Number (BHN) of Compressed External Polymeric Matrices Following Hydration

Evaluating changes in the Brinell Hardness Number (BHN) of the discs allowed us to establish the rate at which water penetrated the surface of the discs and lead to their subsequent hydration and

erosion. The faster this occurred, the more quickly the incorporated gelispheres became exposed to the surrounding aqueous medium and released the entrapped nicotine.

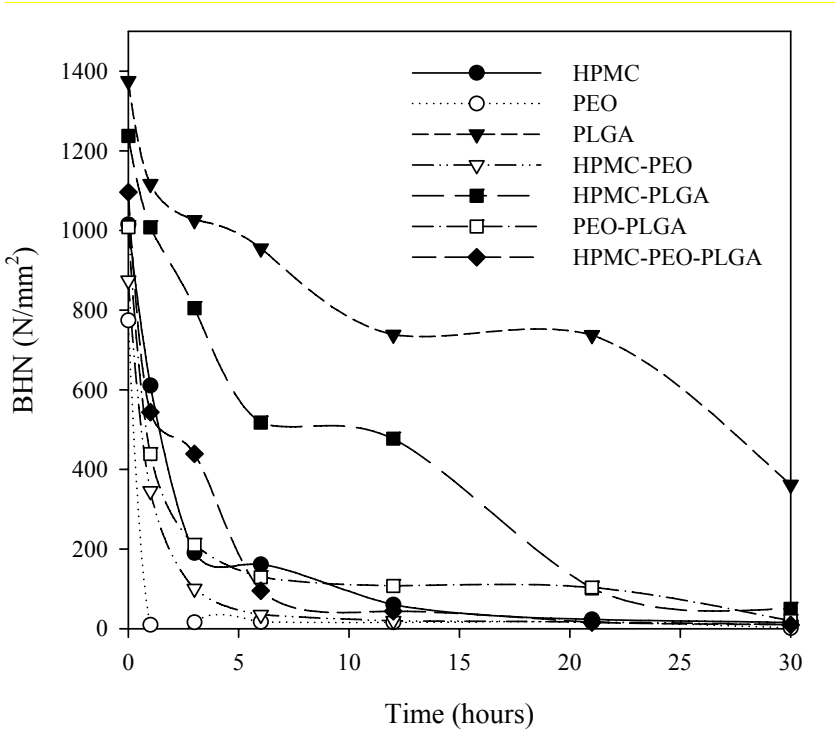

Figure 4.6: Changes in the Brinell Hardness Number (BHN) (N/mm^2) of compressed polymeric discs following exposure to simulated CSF over a period of 30 days (N=3; SD<23.67N/mm^2).

The results demonstrated that the most significant changes in BHN occurred within the first 1 day of exposure to simulated CSF. Discs composed of PEO in particular experienced a significant decline in BHN value within the first 24 hours. Due to the fact that both PEO and HPMC hydrogels imbibed and retained a substantial amount of water from the surrounding buffer media to become hydrated and subsequently undergo polymeric relaxation and generated a gel front on the surface of the disc. Subsequent to the initial 24 hour decline, the discs underwent gelation to the core of their compressed matrices rapidly. Furthermore, the presence of PEO impeded cohesion between the HPMC and PLGA powder particles it consequently generated matrices that were more prone to degradation upon exposure to hydration and mechanical stress. Due to the more complex

nature of the HPMC polymer in comparison to PEO, it did not undergo polymeric relaxation as rapidly. Thus the BHN value for HPMC declined most significantly between days 1-6. PLGA proved to be the exception to this rule. It demonstrated a steady decline in BHN over the 30 days. The combination of PLGA-HPMC also depicted a gradual, albeit more rapid decline in BHN indicating that the presence of PLGA with the HPMC generated sufficient cohesion between the polymers to restrict the diffusion of water molecules into the compressed polymeric matrix.

4.3.5 Evaluation of Erosion of Compressed External Polymeric Matrix

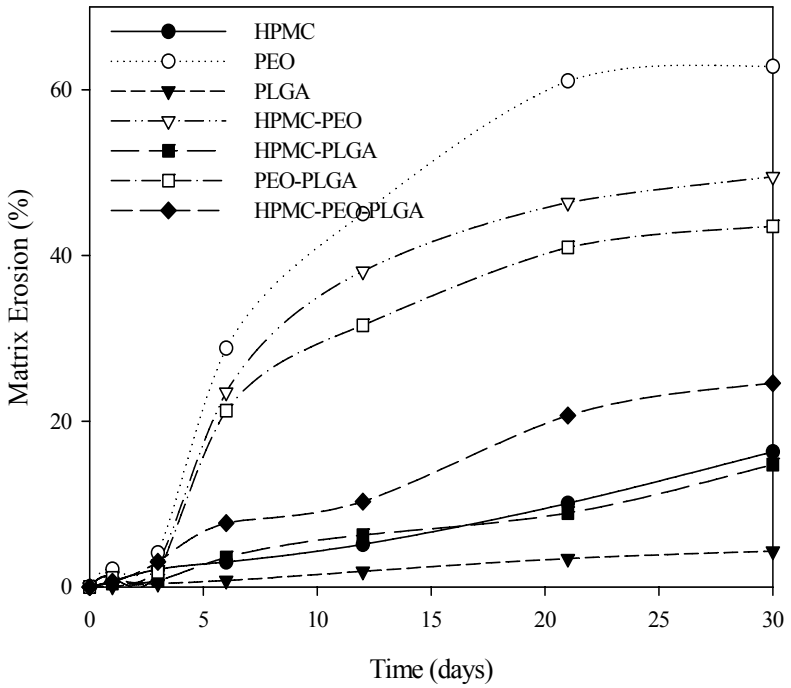

Figure 4.7: Matrix erosion (%) of compressed polymeric discs following exposure to simulated CSF over a period of 30 days. (N=3; SD<0.05%).

When hydrophilic polymers such as HPMC and PEO come in contact with dissolution medium (in this case simulated CSF) they can either swell and generate a continuous gel layer or undergo erosion or undergo combination of the two processes. Their swelling behaviour is controlled by their rate of hydration in the dissolution medium (Wan et al., 1993). 'The extent of polymer

swelling, relative mobilities of dissolution medium and drug, and matrix erosion dictate the kinetics as well as mechanism of drug release from the polymeric matrices.' (Roy and Rohera, 2002).

As indicated by previous results, PEO discs demonstrated lower gel strength, greater water uptake, and therefore demonstrated greater matrix erosion. HPMC discs on the other hand demonstrated greater matrix swelling with negligible matrix erosion. However, from the results it was observed that the rate of drug release by far superseded the rate of matrix degradation; hence it was concluded that the rate of drug release in this case was predominately as a result of the diffusion of the drug from the matrices.

As mentioned previously, PLGA is a hydrophobic bioerodible polymer. Thus the mechanics of polymeric degradation and matrix erosion therefore occur via two main mechanisms, namely bulk erosion and surface erosion (Heller, 1987). The degradation of such polymers is based on the conversion of the macromolecule into its water soluble monomers via the hydrolytic cleavage of the ester bonds that constitute the backbone of the polymer. While bulk erosion does occur, a second mechanism that of surface erosion also takes place concurrently. This refers to the occurrence of hydrolytic breakdown of the polymer confined to the surface of the polymeric matrix. This was reflected by the steady decline in its BHN value over time following hydration. Drug release was therefore involves complex combination of both the drug diffusion from the surface and as a result of bulk erosion. This is discussed further under Section 4.3.7 which evaluates the results obtained for kinetic modelling of drug release data.

Scanning electron micrographs of the discs demonstrated the progression of pore formation and enlargement, formation of a trabeculated network of channels within the structure followed by erosion, and loss of integrity (Figure 4.8). PLGA discs demonstrated the most intact matrices in comparison to other systems. Figure 4.8a indicates the formation of a porous structure within the matrix at day 21 following exposure to simulated CSF. Larger pores (diameter of approximately 300μm) were limited to the periphery of the discs, while the core of the matrix was relatively intact (where pores have a diameter of approximately 50μm). This matrix did not expand significantly, nor did it undergo any significant erosion. In contrast by day 21, HPMC-PLGA discs (Figure 4.8b) had a significantly more patent network, with pore sizes in the core of the matrix having comparatively larger diameters. The disc expanded in width and cross-sectional diameter due to the tendency of HPMC to 'swell'. PEO-PLGA discs (Figure 4.8c) demonstrated a significant degree of erosion within the matrix while simultaneously indicating a greater degree of swelling and erosion. By day 21, the entire network, including the core of the matrix was extremely patent and highly trabeculated. The majority of the matrix appeared to be composed of PLGA.

(a)

(b)

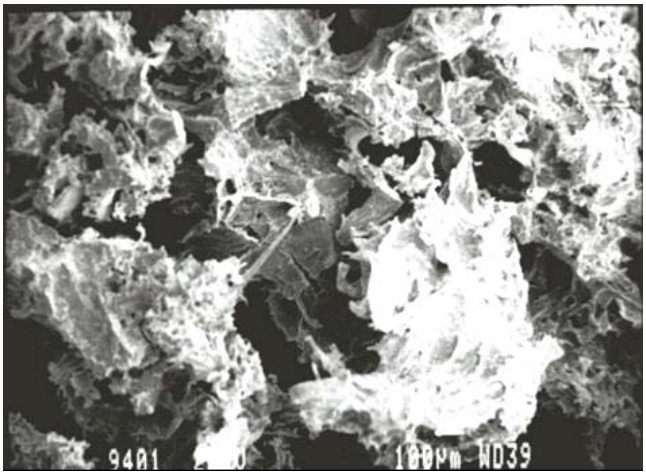

(c)

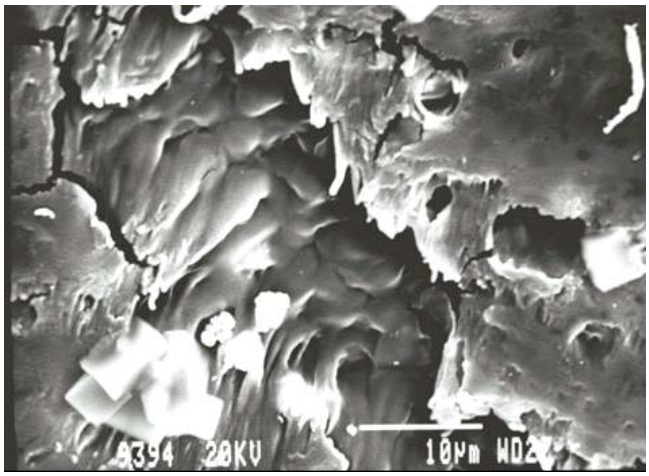

Figure 4.8: Scanning electron micrographs (Magnification 65x) of compressed (a) PLGA, (b) HPMC-PLGA and (c) PEO-PLGA discs following exposure to simulated CSF after 21 days.

4.3.6 Changes in Conductivity of Compressed External Polymeric Matrices Following Hydration

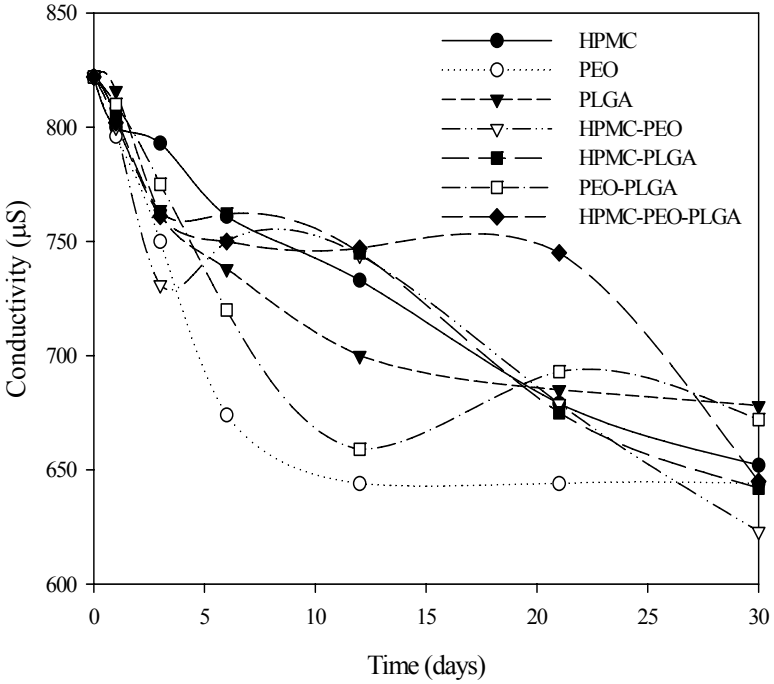

Figure 4.9: Changes in conductivity (µSiemens) of compressed polymeric discs following exposure to simulated CSF over a period of 30 days. (N=3; SD<16.34µS).

These results inversely correlated with those observed for matrix erosion (Section 4.4.6) i.e. the greater the matrix erosion, the lower the observed conductivity of the solution. This indicated a greater degree of interaction between the untangling polymeric chains and the ions in solution. As greater quantities of the polymer unravelled from the disc i.e. matrix eroded, it ionized and interacted with ions in the surrounding PBS. Hence we observed a decline in the conductivity of the solution over the 30 days. The greatest decline was observed for PEO, not surprisingly since it undergoes the most rapid rates of matrix degradation. Since the most significant phase of degradation of the PEO discs occurred within the first 12 days of exposure to simulated CSF, conductivity declines exponentially until this point, after which equilibrium was attained. HPMC demonstrated a steady, almost linear decline in conductivity until day 21 after which a significant

amount of the matrix had degraded to interact with surrounding counter-ionic species. As expected, PLGA expressed the least change in electrical conductivity, since it demonstrated the minimal change in weight (matrix erosion) over time following hydration.

4.3.7 Kinetic Modelling of Release Kinetics from Compressed Polymeric Discs

From model fitting, using WinNonlin Professional Edition, Version 5 (Pharsight, USA), the following data was generated from drug release data obtained for PLGA compressed polymeric discs incorporating optimised gelispheres. As observed previously from Figure 4.5, PLGA discs incorporating optimised gelispheres demonstrated zero-order release.

Table 4.5: Release kinetics obtained from the various diffusion, relaxation and erosion models for compressed PLGA discs incorporating optimised gelispheres (Chapter 3).

Model M_t/M_∞=	**k_1**	**k_2**	**n**	**[2]AIC**	**[3]SBC**	**[4]Correlation**
k_1t^n	0.33	-	0.91	47.97	37.76	0.91
$k_1t^n+k_2t^{2n}$	0.11	0.29	0.95	54.79	55.09	0.93
$1-[1- k_1t]^n$	0.41	-	2	19.21	19.85	0.96

[2]Akaike Information Criterion
[3]Schwartz's Bayesian Criterion
[4]Correlation between experimental and predicted dissolution data

Statistically, the large value of k_2 (0.29) indicates substantial polymeric relaxation for the PLGA discs as compared to the k_1 value (0.11) (Table 4.5) and only confirms that erosion is not the only release mechanism occurring when the formulation is exposed to simulated CSF. As mentioned previously, PLGA undergoes a combination of surface and bulk erosion (Section 4.3.5). The results obtained concur with this since it is demonstrated that drug release was a combination of diffusion (Fickian transport) and polymeric swelling and disentanglement (Case II transport).

High correlation and k_1 values obtained for the Hopfenberg equation indicated that matrix erosion predominated polymeric swelling. While PLGA discs imbibed water into the matrix, since they retained their integrity substantially over time following exposure to simulated CSF, since they are hydrophobic in their chemical constitution, they do not swell significantly (as discussed previously). Furthermore, the lower AIC and SBC values for this model (AIC = 19.21 and SBC = 19.85) indicated that this model most aptly described the mechanism of drug release kinetics from the system. The correlation for this model was also the highest (0.96). Hence it was concluded that drug release was a primary function of matrix erosion, rather than polymeric relaxation (matrix swelling).

4.4 Concluding Remarks

The intended drug delivery system this study sought to develop was one that could provide sustained zero-order release of a nicotine from a crosslinked polyspheric system. This would allow for the attainment of constant drug levels at the site of action and minimize adverse effects associated with fluctuating drug levels, as well as optimising patient therapy and compliance. PLGA matrices incorporating calcium-barium-crosslinked alginate-hydroxyethylcellulose (optimised system formulated) gelispheres offered minimal rates of matrix degradation and successfully retarded nicotine release which achieved zero-order release for 50 days following exposure to simulated CSF. Kinetic modelling demonstrated that drug release occurred primarily as a result of PLGA erosion following exposure to simulated CSF.

Two alternative approaches to further modify nicotine release from the proposed delivery system were also investigated. It was proposed that coating HPMC and HPMC-PEO compressed discs

with PLGA would be investigated to establish an alternative method to retard drug release. The results from the study conducted are discussed in Chapter 5. In Chapter 6, a polyspheric drug delivery system was developed to deliver PLA-PLGA microparticles incorporating nicotine.

Chapter 5

Alternative Approach to Modify Nicotine Release: (I) PLGA-Coated Polymeric Discs Incorporating Crosslinked Calcium-Alg-HEC Gelispheres

5.1 Introduction

Dissolution is often the rate limiting step for the rate of release of highly soluble drugs from compressed polymeric matrices. Sustained release of such medicaments can be achieved by a variety of means, one of which involves the coating of drug particles or granules with various materials. Drug release is generally a function of the solubility of the drug and the porosity and physiochemical properties of the coating membrane. Biopolymers such as celluloses, polyethylene glycol (PEG), various polysaccharides, fatty bases and waxes have been employed to coat numerous oral drug delivery systems with this goal. Release can be modulated to provide for site-specific, targeted and pH and/or enzymatic-controlled release systems through the use of various materials. The majority of these systems have been applied for controlled drug delivery in oral dosage forms (Conrad and Robinson, 1982). In fact reservoir devices employ polymeric coats as their primary means of restricting drug release. The various categories of coatings investigated are listed below with a brief summary of their properties.

Table 5.1: Various categories of coatings investigated are listed below with a brief summary of their properties (Source: Adapted from Hui et al., 1989).

Type of Coating	Properties
1. Barrier coating	This mechanism employs the use of various hydrophobic polymers and is applicable to provide film-coatings for tablets and granules as well as compressed tablets. Release mechanisms can be compromised due to disintegration and fracture during compression.
2. Embedment into a fatty coating	This applies to the formulation of a various compressed and multilayer tablets. Such formulations allow for modulated release such that portions of the medicament can be released more rapidly than others. However it is often difficult to control release since release is often pH and/or enzymatic hydrolysis dependant.
3. Repeat action coatings	While these are not regarded as 'true' sustained release forms and has the same limitations and properties of barrier coating.
4. Coated plastic matrix	The majority of the dosage forms employing this mechanism to retard drug release involves the use of non-biodegradable polymeric materials to formulate the device. Hence the plastic matrix after drug release must be eliminated or removed from the body.
5. Coated hydrophilic matrix	Drug release is significantly dependant on the nature of coating polymer employed. The rate of drug release is more dependant on the properties (primarily the solubility) of the drug entity delivered.

The entrapped drug partitions into the surrounding membrane prior to release. Depending on the nature of the coating material, the drug can be released either via diffusion or dissolution. For coats composed of hydrophilic polymers, release is dependant on the formation of a viscous gelatinous layer of polymer as it becomes hydrated and undergoes a transition between the glassy and rubbery phase. Hence release in such systems is controlled provided the hydrated gelatinous layer remains intact. On the other hand, for hydrophobic polymers, release is more dependant on the porosity of

the coating membrane developed. Drug release in such cases is expected to follow Fickian diffusion kinetics. Equation 5.1 describes Fick's First Law of diffusion from a plane surface, with a position-dependent diffusion coefficient is,

$$\frac{\delta c}{\delta t} = \frac{DA(Cs - Cb)}{q}$$

Equation 5.1

Where,

$\frac{\delta c}{\delta t}$ the rate of change in molar drug concentration (the equivalent of the rate of drug release

D the diffusion coefficient, a macroscopic measurable quantity

A the cross-sectional surface area of the polymeric matrix

Cs the aqueous saturation concentration of the drug

Cb the concentration of the drug in the bulk solution (this is usually neglected, due to the presence of sink conditions in the body)

q the thickness of the stagnant diffusion layer

Fick's Law describes the presence of a direct and linear relationship between the rate of drug release (diffusion) and the concentration gradient, the surface area, the diffusion coefficient of the drug molecule (a factor dependant upon the chemical nature molecule and its molecular weight) and an inverse relationship between the thickness of the stagnant diffusion layer, a region around the drug delivery systems that is saturated with dissolved drug (Burnette, 1987).

However if the coating materials are insoluble and non-biodegradable, this can result in problems regarding device elimination from the body. In the case of implants this scenario is not ideal as it

necessitates a second surgical procedure to remove the implant, resulting in great risk, inconvenience and expense to the patient.

Apart from the nature of the coating agents employed, the thickness of the coat is directly related to the degree of control on drug release kinetics. In other words, the thicker the coating, the greater the provision to achieve sustained drug release from the delivery system (Rosen, 1989).

From Chapter 4 it was observed that the presence of hydrophobic PLGA within the compressed polymeric matrices allowed for reduced rates of drug release. It was proposed that the presence of a hydrophobic coat of the polymer around HPMC and a combination of HPMC and PEO may also impact the rate of drug release.

Calcium-crosslinked Alg-HEC (Ca-Alg-HEC) gelispheres generated previously (Chapter 3) were incorporated into external polymeric discs coated with PLGA. A comparison was conducted on uncoated discs also to establish the degree to which drug release could be retarded.

The purpose of this study is to use the beneficial properties of coating to control the rate of drug release from the gelispheres. A biopolymeric barrier coating on compressed polymeric matrices is employed. From Chapter 4 it was observed that the porosity of PLGA matrices changed little over time, hence offer a suitable material for coating hydrophilic matrices. By employing high compression forces on this highly compressible hydrophobic polymer, we were able to employ a simple manufacturing strategy to develop a dense resistive coat around the matrices. The results from this study are presented in the following sections.

5.2 Materials and Methods

The materials employed to generate the Ca-Alg-HEC gelispheres were the same as previously stated in Chapter 3 and those employed to formulate the external polymeric matrices were as those stated in Chapter 4.

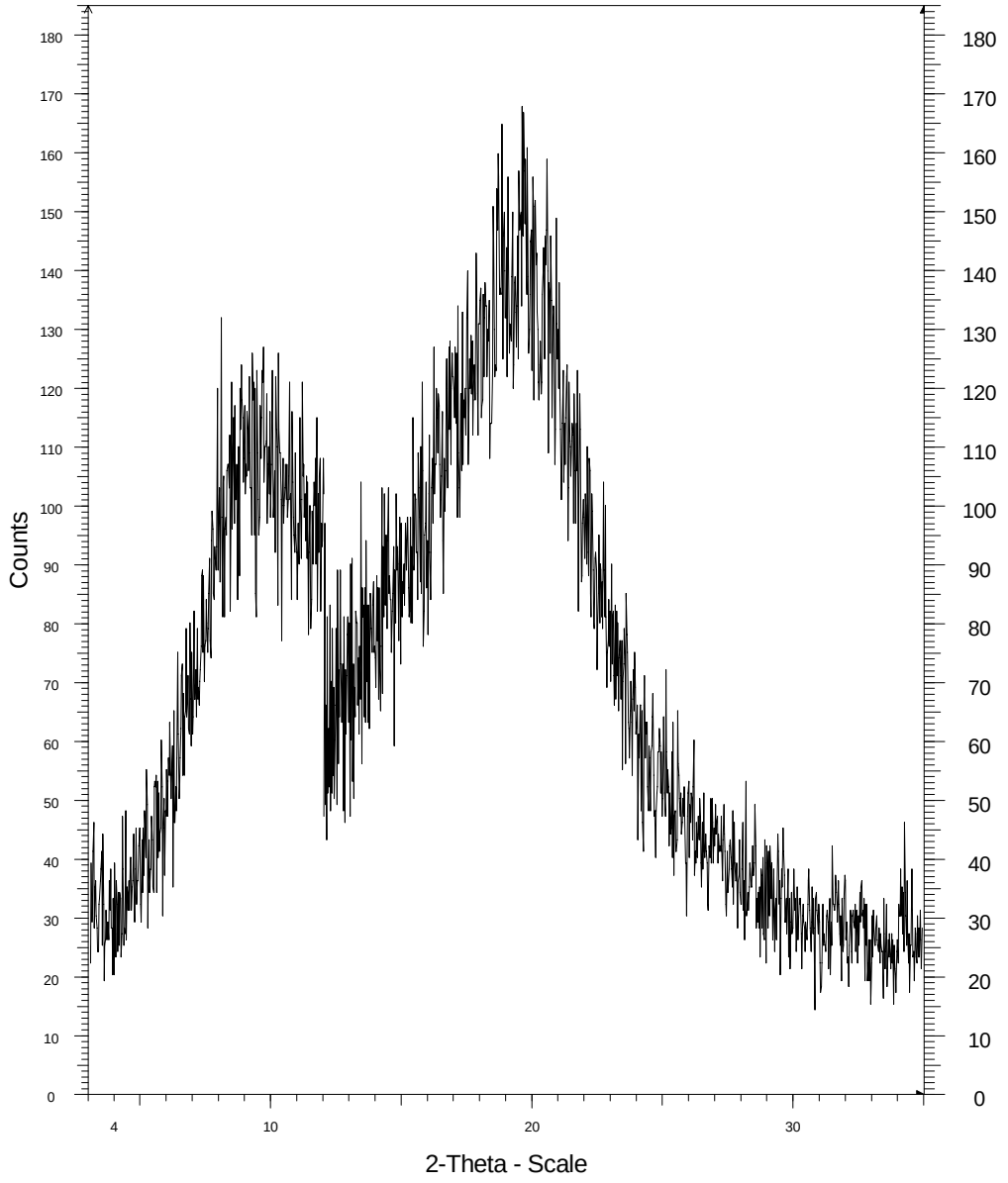

Figure 5.1: X-ray diffraction (XRD) profile observed for the calcium-crosslinked Alg-HEC gelispheres selected for incorporation into external polymeric discs coated with PLGA.

5.2.1 Formulation of PLGA-Coated (PC) Polymeric Matrices

Briefly, 500mg of the dry polymer(s) blended was mixed with the Ca-Alg-HEC 100mg gelispheres and subsequently compressed into discs using a Beckman® Hydraulic Press (Beckman Instruments, Inc., Fullerton, USA) applying a pressure of 8 tons. Flat-faced punches with a 10mm diameter were employed to compress the polymeric discs. The coated matrices were generated by compressing the discs with 100mg PLGA in a larger punch diameter (11.5mm in diameter) employing the same compression parameters as previously mentioned. Based on the results from Chapter 4, two formulations were selected for coating with a layer of PLGA to assess its effect on retarding drug release from these matrices. Table 5.2 summarizes the investigated disc compositions. In order to establish the impact of coating on drug release, native uncoated discs were also formulated.

Table 5.2: Investigated polymer compositions for the external compressed polymeric matrix incorporating Ca-Alg-HEC gelispheres.

Formulation Number	Polymer Composition
1	*PC-HPMC
2	*PC-HPMC-PEO
3	HPMC-PEO
4	HPMC
5	PLGA

*(*PC = PLGA-coated)*

5.2.2 Determination of *In Vitro* Drug Release Characteristics

In vitro drug release studies were performed in triplicate the discs formulated were as described in Chapter 3, Section 3.2.8 over a period of 21 days for each disc.

5.2.3 Kinetic Modelling of Drug Release from Compressed Polymeric Discs

In order to elucidate the kinetic mechanisms involved in nicotine release from the compressed polymeric matrices, drug release data was employed to generate mathematical models as discussed in Section 4.2.10 (Chapter 4).

5.3 Results and Discussion

5.3.1 Evaluating *In Vitro* Drug Release from PLGA-Coated (PC) Polymeric Matrices

A brief summary of the properties of the gelispheres highlights the rapid release rates observed for the system. Figure 5.2 and Table 5.3 indicate the release profile obtained for the Ca-Alg-HEC gelispheres selected for incorporation into external polymeric discs over a period of 50 hours, whereby 100% of the drug was released. Values exceeding 100% drug release after 50 hour indicated the presence of residual nicotine on the surface of the gelispheres following curing.

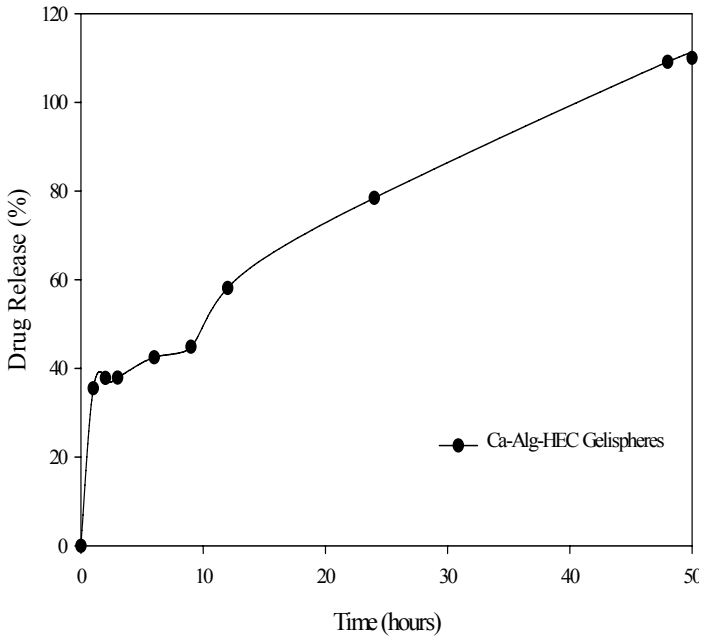

Figure 5.2: % Drug released from Ca-Alg-HEC gelispheres over a period of 50 hours after exposure to simulated CSF (N=3; SD<0.56%).

In comparison to the HCl-exposed Alg-HEC-PAA gelispheres incorporated into discs form the Chapter 4, it should be noted that there was a significant discrepancy between the rates of drug release from the two types of gelispheres. While drug release for Ca-Alg-HEC gelispheres was completed within 50 hours, the duration of release was far exceeded for HCL-exposed optimised gelispheres (Chapter 3). This therefore impacted upon the degree to which the external matrices retarded drug release.

Coating the hydrophilic compressed matrices with the hydrophobic PLGA significantly retarded drug release. In particular a substantial difference was observed for HPMC-PEO matrices, which demonstrated zero-order kinetics following approximately 15 days exposure to simulated CSF. PLGA demonstrated predictable release kinetics with phasic (or pulsatile) first and zero-order release that continued to release the drug past the 21 day test period. This was a dramatic improvement from the release profiles obtained from native Ca-Alg-HEC gelispheres prior to incorporation, which degraded to release the entrapped drug within a space of less than 50 hours.

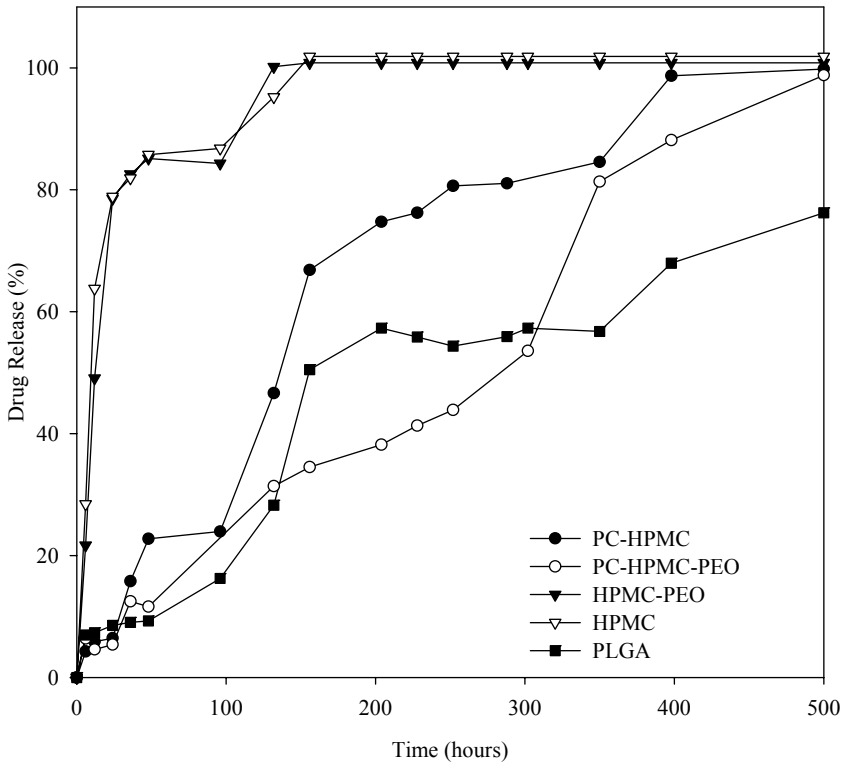

Figure 5.3: % Drug released over a period of 500 hours (or 21 days) from the gelispheres compressed into native PLGA and PLGA coated (PC) polymeric discs following exposure to simulated CSF (N=3; SD<3.10%).

Approximately 80% drug was released within the first 24 hours from uncoated HPMC and HPMC-PEO formulations, indicating a significant burst effect. Native PLGA discs had a significantly attenuated burst effect, whereby a mere 8.53% of the incorporated drug was released during the same period of time. The most promising results were obtained with the coated discs, whereby drug release was 6.44% and 5.40% for HPMC and HPMC-PEO coated discs, respectively within the first 24 hours. Approximately 100% of the drug was released from uncoated HPMC and HPMC-PEO discs by day 6. The PLGA coating provided a significant barrier to penetrating solvent molecules into the matrices. While initially when the PLGA coating is intact, drug release is controlled by diffusion, indicated by the pseudo-zero-order release, subsequent to PLGA hydrolysis, drug release more rapid.

5.3.2 Kinetic Modelling of Drug Release from PLGA-Coated Compressed Polymeric Discs

The results obtained from model fitting, (WinNonlin, Professional Edition, Version 5 (Pharsight, USA)) the following data was generated:

Table 5.3: Drug release kinetics obtained from the various diffusion, relaxation and erosion models for PLGA-coated compressed HPMC-PEO discs incorporating Ca-Alg-HEC gelispheres.

Model M_t/M_∞=	**k_1**	**k_2**	**n**	**[2]AIC**	**[3]SBC**	**[4]Correlation**
k_1t^n	0.92	-	0.90	47.16	38.98	0.89
$k_1t^n+k_2t^{2n}$	0.15	0.87	0.95	16.02	26.54	0.94
$1-[1- k_1t]^n$	0.55	-	2	39.96	59.08	0.87

[2]Akaike Information Criterion
[3]Schwartz's Bayesian Criterion
[4]Correlation between experimental and predicted dissolution data

A significantly large value for k_2 (0.87) was observed which, indicated that matrix swelling and polymeric disentanglement contributed substantially towards the drug release mechanism form the compressed polymeric discs. This is further proven by the significant correlation value (0.94) obtained for experimental and predicted dissolution data. From previous studies (Chapter 4) it was observed that the contribution of Fickian diffusion mediated drug release kinetics from native PLGA discs to a comparatively greater degree (where, k_1 = 0.11 and k_2 = 0.29) verses Case II transport. This implies that despite PLGA coating the HPMC-PEO compressed discs, the system as a whole experienced a significant degree of polymeric swelling in the interior of the matrix from the HPMC-PEO core when exposed to simulated CSF. It is proposed that Fickian diffusion predominates (indicated by the high k_1 value for Power Law) drug release kinetics, which may be as a result of a greater drug load in the Ca-Alg-HEC gelispheres (as opposed to the optimised system from Chapter 3, which was incorporated within native PLGA discs in Chapter 4).

Furthermore, gelisphere swelling cannot be ignored in this case, since these gelispheres were not exposed to dilute HCl post-curing, hence undergo substantial increase in volume subsequent to simulated CSF exposure. This theory is further supported by the low values obtained for AIC and SBC for this model (AIC = 16.02 and SBC = 26.54). The model also demonstrated the highest correlation value of 0.94.

5.4 Concluding Remarks

PLGA is a unique polymer with many properties that makes it an ideal agent for developing controlled and sustained release drug delivery devices. This study has demonstrated that it imparted a significant impact on the nature and kinetics of drug release. We achieved zero-order release from the developed gelispheric system by incorporating PLGA as an external matrix as well as a coating agent to hydrophilic polymer systems composed of HPMC and PEO.

Coating the HPMC-PEO matrices with PLGA significantly retarded drug release and allowed the achievement of constant zero-order release following 15 days exposure to simulated CSF. The presence of PLGA as a coating agent retarded the rate of drug release and allowed the achievement of phasic or pulsatile release.

Chapter 6

Alternative Approach to Modify Nicotine Release: (II) Application of Novel Crosslinked Alginate-Pectinate Double-Encapsulated Approach for Delivering a PLA-PLGA Microparticulate System

6.1 Introduction

The comparative merits of multiple-unit dosage forms (e.g., in terms of bioavailability, more consistent blood levels and greater product safety) over single-unit products are well established. Analysis of release data indicates that a zero-order mechanism can be obtained (Pillay and Fassihi, 1999; Efentakis and Koutlis, 2001). The dose dumping phenomenon that is a real risk factor with single-unit systems is a limitation that multiple-unit devices can very effectively overcome (Shivakumar et al., 2002). Failure of a single entity does not compromise the efficacy of the entire device.

The aim of the study was to formulate and to optimise a novel drug delivery system for nicotine through double entrapment, finally with the biodegradable hydrophobic polymers PLA-PLGA and then a crosslinked zinc-alginate-pectinate polyspheric matrix. The physiochemical and physicomechanical characteristics that would optimise this formulation for its use as a possible brain implant to prevent the progression of PD were evaluated.

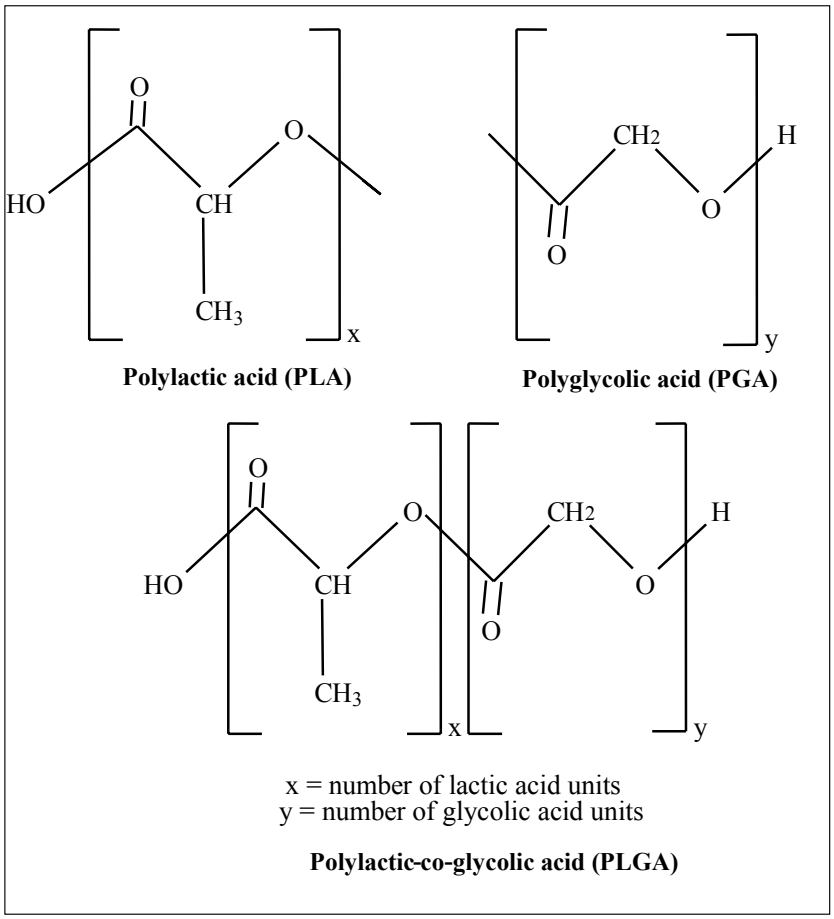

Figure 6.1: Chemical structure of polylactic acid (PLA), polyglycolic acid (PGA) and poly(lactic-co-glycolic) acid (PLGA).

Biodegradable polyesters, such as polylactic acid (PLA), polyglycolic acid (PGA), and poly(lactic-co-glycolic acid) (PLGA) (Figure 6.1), have been extensively studied for a variety of pharmaceutical and biomedical applications. They offer unique advantages by enabling controllable biodegradability, displaying excellent biocompatibility, and a high degree of safety. The general properties and typical applications of PGA, PLA, and PLGA are summarized in Table 6.1.

Table 6.1: General properties and typical applications of the biodegradable polyester polymers polyglycolic acid (PGA), polylactic acid (PLA) and their copolymer poly(lactic-co-glycolic) acid (PLGA).

Polyester	Crystallinity	Glass Transition Temperature (Tg) (ºC)	Degradation Rate	Typical Pharmaceutical and Biomedical Applications
PGA	Highly crystalline	35-40	2-3 months	Sutures
PLA	Semi-crystalline-Amorphous (depending on D/L ratio)	65-55	1-2 years	Fracture fixation, ligament augmentation and drug delivery systems
PLGA	Amorphous (depending on PLA/PGA ratio)	45-55	1-6 months	Fracture fixation, ligament augmentation, grafts, prosthetic devices and potentially implantable and oral drug delivery systems.

PGA is a highly crystalline polymer and the most hydrophilic among them. It has an extremely high melting point (224°C to 226°C), and a significantly prolonged degradation rate. During polymerization, successive monomeric units (of glycolic or lactic acid) are linked together in PLGA by ester linkages, thus yielding a linear, aliphatic polyester as a product. Unlike the homopolymers of lactic acid (PLA) and glycolic acid (PGA) which show poor solubilities, PLGA can be dissolved by a wide range of common solvents, including chlorinated solvents, tetrahydrofuran, acetone or ethyl acetate. PLGA degrades by hydrolysis of its ester linkages in the presence of water. It has been shown that the time required for degradation of PLGA is related to the ratio of its constituent monomer ratio. More specifically, the higher the glycolide content the greater the rate of polymeric degradation. PLGA copolymers with varying ratios of lactide (LA)

and glycolide (GA) monomeric units can exhibit variable degradation rates, and therefore can be 'custom-made' for specific applications requiring specific degradation kinetics.

Microparticles have been proven to be efficient systems for delivery of a wide range of chemotherapeutic drugs to the brain (Ike et al., 1992; Menei et al., 1999). One of the most significant advantages they offer is that they can be injected safely as a suspension, thus permitting site-specific drug delivery to virtually any region in the brain (Emerich et al., 1999). PLGA is considered to be biocompatible with brain tissue (Menei et al., 1996; Emerich et al., 1999; Veziers et al., 2001) and has been employed to deliver a range of anti-neoplastic agents such as 5-fluorouracil, BCNU, carmustine, taxol, and carboplatin by entrapping them into polymeric microspheres for sustained drug release treat brain tumours (Menei et al., 1996; Emerich et al., 2000; Walter et al., 1994; Olivi et al., 1996; Chen et al., 1998). PLGA has been employed to formulate microparticles to deliver drugs such as levodopa (with and without a decarboxylase inhibitor), dopamine, norepinephrine and the neurotrophic factor, GDNF to the brain via striatal implants (Popovic and Brundin, 2006).

The present study is aimed at understanding the incorporation of nicotine into polylactic acid (PLA) and poly(D,L-lactic-co-glycolic) acid (PLGA) microparticles which are then re-incorporated into a cross-linked zinc-alginate-pectinate polyspheric multi-particulate system to be employed as a possible brain implant for the treatment of PD. A Box–Behnken design is employed to prepare 15 PLA-PLGA formulations, which are tested for their drug incorporation efficiency and release potential and subsequently optimised using multiple regression and an

artificial neural network generalized feed-forward model. Based on the rapid burst effect from the microparticles, further incorporation is conducted in a zinc-alginate-pectinate system using ionotropic gelation

6.2 Materials and Methods

A mixture of low molecular weight poly(lactic-co-glycolic) acid (85/15) (PLGA) with an inherent viscosity 0.65dL/g in $CHCl_3$ at 30°C) and low molecular weight polylactic acid (PLA) with an inherent viscosity 0.66dL/g in $CHCl_3$ at 30°C was purchased from Burmingham Polymers Inc. (Bioabsorbabale polymers, MA, USA). Nicotine ((-)-1-methyl-2-(3-pyridyl)-pyrolidine) was purchased from Sigma Pharmaceuticals (Sigma Pharmaceutical Group; M.A., USA). Acetonitrile was purchased from Merck Laboratory Supplies (Pty) Ltd. (Gauteng, South Africa), Liquid paraffin with a distillation range 40–60°C was purchased from Merck Laboratory Supplies (Pty) Ltd. (Gauteng, South Africa). Span 80 was purchased from Rochelle Chemicals (South Africa). Petroleum ether, Dimethylformide (DMF), both of which were 99.5 % pure, were purchased from Rochelle Chemicals (Gauteng, South Africa). Pectin was donated by Herbstreith and Fox KG (Neuenbürg/Württ., Germany), Sodium Alginate was donated by FMC BioPolymer (Drammen, Norway) and Zinc gluconate was purchased from Merck – Schudart (Hohenbrunn, Germany).

6.2.1 Preparation of PLA-PLGA Microparticles

In order to produce the correct formulations to optimise the release profile of nicotine and the entrapment efficiency of the drug, the Box-Behnken design was used. This is an independent

quadratic approach, which does not contain an embedded factorial or fractional factorial, was employed to generate a statistical matrix.

The formulation input factors that were evaluated at 3-levels included:

- Polymer type: PLA (1), PLGA (2) and their combination in a 1:1 ratio (3);
- Stirring time: 3, 9 and 15 hours; and
- Concentration of emulsifying agent Span 80: 0.5% $^{w}/_{v}$, 1.25% $^{w}/_{v}$ and 2% $^{w}/_{v}$.

The 15 combinations of PLA-PLGA microparticles were prepared using an oil-in-oil (O/O) phase separation process in accordance with the Box-Behnken design (Table 6.2).

Table 6.2: Independent variables evaluated using the Box-Behnken Design.

Formulation Number	Polymer Type	Stirring Time (hours)	[Span 80] ($\%^{w}/_{v}$)
1	1	15	1.25
2	2	3	0.50
3	3	9	2.00
4	3	15	1.25
5	2	9	1.25
6	1	3	1.25
7	2	3	2.00
8	2	9	0.50
9	2	15	2.00
10	1	9	0.50
11	3	9	0.50
12	2	15	0.50
13	2	9	2.00
14	3	3	1.25
15	1	9	2.00

440 mg of polymer (PLA, PLGA or combination) was added to 10mL of acetonitrile and left for 12 hours to dissolve without stirring. Upon complete dissolution of the polymers, 300mg of nicotine was added and mixed by means of a magnetic stirrer. Using a 10mL pipette, the polymer-

nicotine dispersion was added in a dropwise manner to 50mL of liquid paraffin containing the appropriate concentration of Span 80. This was conducted under agitation using a Hiedolph stirrer (Labotec®, Gauteng, South Africa) at 500rpm. The stirring speed was decreased to 400rpm after the addition was completed and for the remainder of the process with different stirring times as indicated in the Box-Behnken design (Table 6.2).

Upon completion of the required stirring time, hardening of the microparticles was achieved by the addition of 25mL of petroleum ether. This mixture was then stirred for an additional 10 minutes at 400rpm. An Erlenmeyer flask containing a Bucchner funnel equipped with Whatman® filter paper (0.45μm pore size) was utilized in order to collect the microparticles via vacuum filtration. An additional 25mL of petroleum ether was then added to the residual mixture in the beaker to wash out the remaining microparticles.

The filter paper containing the microparticles was placed under an extractor for 48 hours, to facilitate evaporation of the residual solvent. Subsequently the microparticles, ready for analysis, were stored in glass vials at -5°C.

6.2.2 Determination of Drug Entrapment Efficiency

The drug entrapment efficiency of the microparticles was determined in dimethylformide (DMF) since both nicotine and the polymers were soluble in this solvent. 20mg of nicotine-loaded microparticles was dissolved in 100mL of DMF and thereafter agitated at room temperature with the aid of a homogenizer (VELP® Scientifica Microstirrer, Italy). In order to remove any

contaminants or residual polymer that may have not coated the nicotine, the samples were filtered through a Millipore® filter (0.45 μm pore size). The absorbance values of the samples were read at a wavelength of 260nm and converted to drug concentration by means of a standard curve (obtained using concentrations of nicotine varying from 1 to 3%). Drug entrapment efficiency (DEE) (%) was calculated using Equation 3.2 (Section 3.2.6, Chapter 3).

6.2.3 Determination of *In Vitro* Drug Release Characteristics

Nicotine-loaded particles of each formulation equivalent to 20mg of pure nicotine were placed in 100mL phosphate buffered saline of pH 7.4 (PBS) in sealed 200mL glass jars. These jars were then placed in a shaker bath (Labotec®, Gauteng, South Africa) set at 37°C and agitated at 50 rpm. At 30-minute intervals 1mL samples of the solution were removed, appropriately diluted with PBS and analysed by UV at 260nm. An equal volume of drug-free PBS was added to the glass jars to maintain sink conditions.

6.2.4 Optimisation of the PLA-PLGA Microparticles

Optimisation of the PLA-PLGA microparticles was based on drug entrapment efficiency and drug release. Two different methods were considered to optimise the formulation. The first consisted of the application of Design of Experiments response optimiser function in Minitab (Release 14, Minitab Inc., USA) employing simultaneous optimisation of the responses. The second approach involved the application of Artificial Neural Networks (ANN) (NeuroSolutions V4.32, NeuroDimension Inc., USA) using a Generalized Feed Forward algorithm, also employing a

simultaneous optimisation technique. The employment of two methods enabled a comparison to be obtained between formulations that were prepared.

Multiple regression of the response outputs generated from the Box-Behnken design and pattern recognition and prediction from artificial neural networks were used to optimise the drug entrapment efficiency and release of nicotine from the microparticles.

6.2.5 Double Entrapment of PLA-PLGA Microparticles into Crosslinked Alginate-Pectinate Polyspheres

Due to the fact that entrapment of nicotine into different PLA and PLGA combinations caused the drug to be released within the first 30 minutes, a double entrapment approach was attempted. To accomplish this, pectin, sodium alginate and then a 1:1 combination thereof was used as the second coating. Three $2\%^{w}/_{v}$ polymer solutions composed of pectin, sodium alginate and a 1:1 combination ($2\%^{w}/_{v}$ each) was dissolved in 80mL of de-ionized water. Upon complete dissolution of the polymer solutions, they were made up to 100mL with de-ionized water. Three $2\%^{w}/_{v}$ solutions of zinc gluconate (200mL) were prepared as the crosslinking agents. Approximately 24mg of the optimised nicotine-incorporated microparticles (≈ to 2mg pure nicotine) was added to 20mL of each of the three polymer solutions and stirred for 30 minutes. Each of these 3 polymer dispersions, using a 20mL syringe were then added dropwise into 3 separate beakers containing the crosslinking solution. This dropwise addition allowed for the formation of either PLA-PLGA-zinc-alginate, PLA-PLGA-zinc-pectinate or PLA-PLGA-zinc-alginate-pectinate polyspheres (i.e. polyspheres incorporated with PLA-PLGA microparticles). These resultant polyspheric formulations were agitated for an additional 30 minutes in the crosslinking solution and thereafter

left to cure in a dark area at room temperature for 3 hours. After 3 hours the polyspheres were washed with 3x500mL de-ionized water and allowed to air dry over 4 days, under ambient conditions. Following this, dissolution studies were conducted in a similar manner as described above.

6.2.6 Elucidating Surface Morphology of the Developed Systems

The shape and surface morphology of the microparticles and polyspheres was examined using a JEOL 6400 scanning electron microscope (JEOL, Japan).

6.3 Results and Discussion

6.3.1 Yield of Microparticles

Varying yields of microparticles were found among the different formulations, ranging from 83.30mg to 1164.00mg (Table 4.3). In the case of 83.30mg, the conditions were PLGA as the polymer, 3 hours stirring time and 0.5%$^{w}/_{v}$ Span 80. This low yield may be attributed to a low stirring time as well as the use of minimal concentration of emulsifying agent. Conversely, the highest yield was seen in the formulation that employed PLGA, had a stirring time of 9 hours and used a Span 80 concentration of 1.25%$^{w}/_{v}$. The results thus revealed that the polymer employed is not the only deciding factor for microparticle yield. Rather, the stirring time and emulsifying agent combine in their effects. Prolonged stirring (>9 hours) may have led to poorer yields due to excessive shearing forces on the polymer, consequently leading to fragmentation of the microparticles. Figure 6.2a and 6.2b show the scanning electron micrographs (SEM) of fragmented and optimal microparticles respectively.

(a)

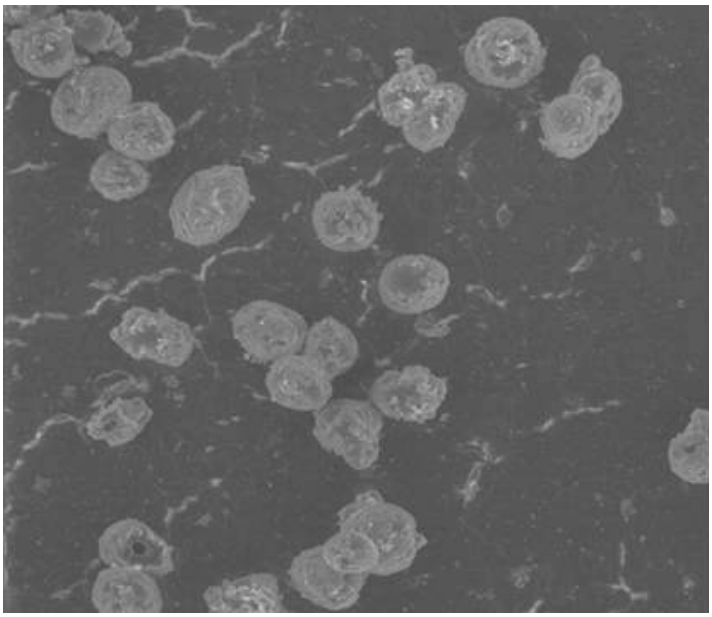

(b)

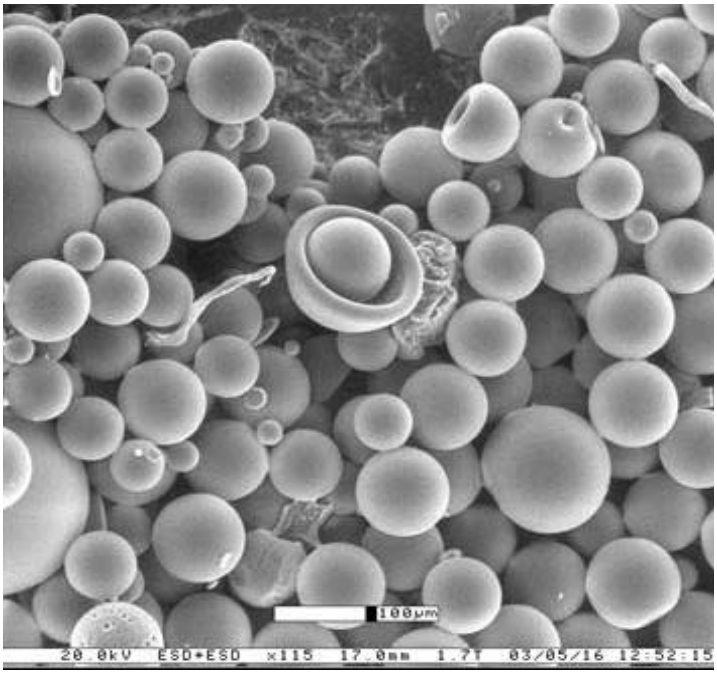

Figure 6.2: Scanning electron micrographs of (a) fragmented microparticles and (b) optimal spherical microparticles.

6.3.2 Evaluation of Drug Entrapment Efficiency

Overall, the results demonstrated that optimal entrapment efficiency was observed from the following formulations (in order of increasing entrapment efficiency) (Table 6.3):

- Formulation 2 (PLGA, 3 hours, [Span 80] 0.5 $\%^{w}/_{v}$);
- Formulation 14 (PLA + PLGA, 3 hours, [Span 80] 1.25 $\%^{w}/_{v}$); and
- Formulation 7 (PLGA, 3 hours, [Span 80] 2 $\%^{w}/_{v}$)

The overall trend observed is that the formulation comprising only PLGA or a combination of the two polymers with a stirring time of 3 hours provided the high entrapment efficiency. The presence of PLA in the formulation yielded a lower entrapment efficiency as it may have decreased the amorphous character of the polymer.

6.3.3 Evaluation of *In Vitro* Release of Nicotine from the Microparticles

The *in vitro* dissolution profiles for all formulations demonstrated near 100% release within the first 30 minutes (Table 6.3). This is due to the fact that the polymers are too porous, probably due to a lack of sufficient consolidation and therefore the ability to restrict the diffusion of nicotine via the pores. A typical scanning electron micrograph reveals the highly porous nature of a microparticle (Figure 6.3), hence leading to rapid drug diffusion.

These profiles were not optimal since our aim was to formulate a controlled and prolonged release implant. These results therefore demonstrated the need to double-incorporate the PLA-PLGA microparticles, to further restrict the release rate of nicotine.

Table 6.3: Values of responses obtained from the formulation of nicotine-loaded PLA-PLGA microparticles.

Formulation Number	Yield of Microparticles (mg)	Drug Entrapment Efficiency ($\%^{W}/_{W}$)	Drug Release (%) after 0.5 hours
1	486.90	44.78	85.12
2	83.30	83.66	94.22
3	1040.40	42.16	66.65
4	981.60	35.88	77.12
5	1164.00	39.62	82.45
6	279.00	16.41	98.44
7	604.20	74.39	94.08
8	858.70	39.9	95.56
9	1441.10	29.53	69.76
10	932.30	28.71	94.23
11	881.80	44.41	80.34
12	431.20	31.42	80.51
13	1139.00	32.57	99.12
14	810.60	82.83	93.26
15	818.90	51.16	98.01

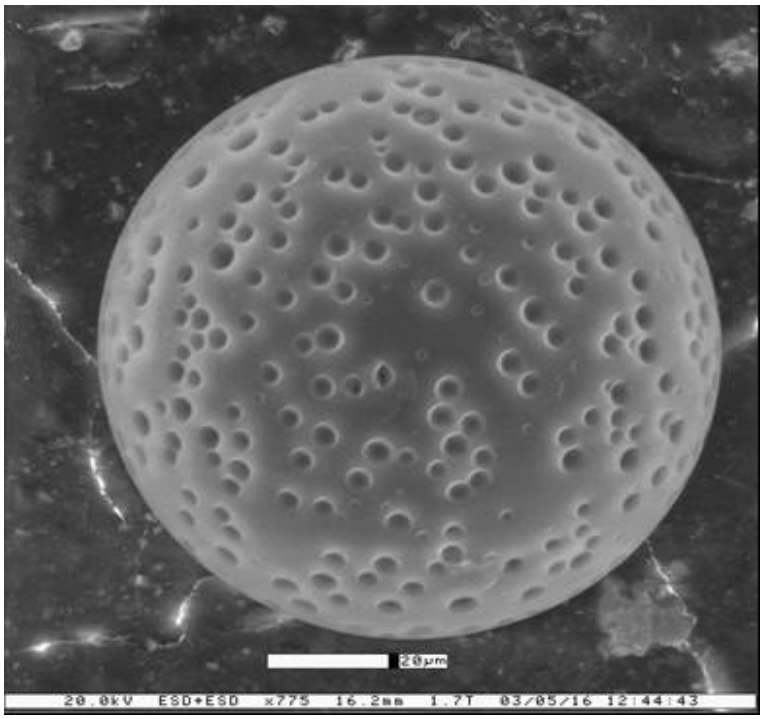

Figure 6.3: Typical scanning electron micrograph of a highly porous PLA-PLGA microparticle.

6.3.4 Statistical Optimisation Studies

The output parameters for the optimisation and the results are provided in Table 6.5. Table 6.4 provides the optimised input parameters generated through stepwise forward and backward regression.

Table 6.4: Optimised parameters used to generate experimental values.

Input Parameters	Box-Behnken	ANN
Polymer Type	3	1.7
Stirring Time (hours)	3	6.7
[Span 80] ($\%^{w}/_{v}$)	0.5	1.4

Table 6.5: Comparison between desired and experimental output parameters with respect to selected data-modelling tools.

Output Parameters	Box-Behnken		Artificial Neural Network	
	Desired	Exp.*	Desired	Exp.*
Drug Entrapment Efficiency	90%	81.29%	90%	89.81%
Drug Release (%) after 1 hour	100.02	106.32	100.00	103.33

*see Table 6.4

The regression and ANN algorithmic analysis predicted two formulations which still provided unfavourable results, since both reflected poorer entrapment efficiencies in comparison to those seen in earlier formulations and possessed release characteristics that were inconsistent and unpredictable (Figure 6.4). Drug was once again almost completely released from the "optimised" microparticles within the first 30 minutes. Since both the Box-Behnken and the ANN formulations showed similar behaviour, we opted to choose only one method for re-entrapment, namely the ANN formulation.

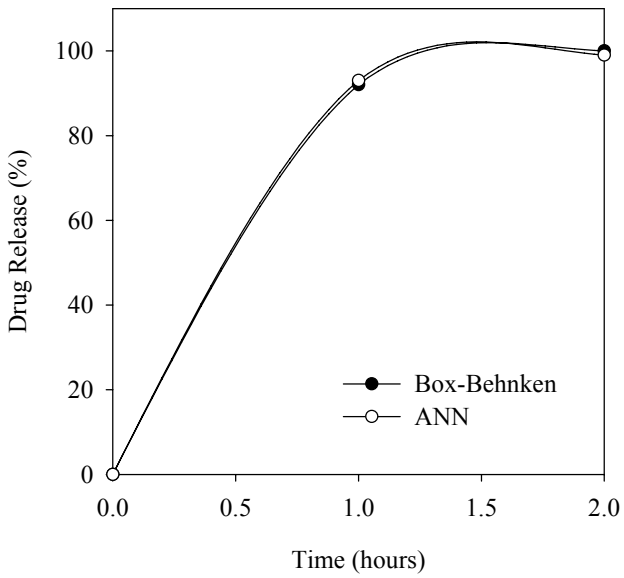

Figure 6.4: % Drug released from optimised PLA-PLGA microparticles as per Box-Behnken design and ANN algorithm (N=3; SD <0.03).

6.3.5 Statistical Inferences between the Experimental and Predicted Values for Responses Measured

Both drug release after 0.5 hours and drug entrapment efficiency (Figure 6.5a-b) reflected a close linear relationship between the experimental and predicted values (R^2=0.89 and R^2=0.80 for drug release and drug entrapment efficiency respectively). Using a t-test, it was also confirmed that no statistical differences ($p>0.05$) existed between the experimental and predicted values for both responses.

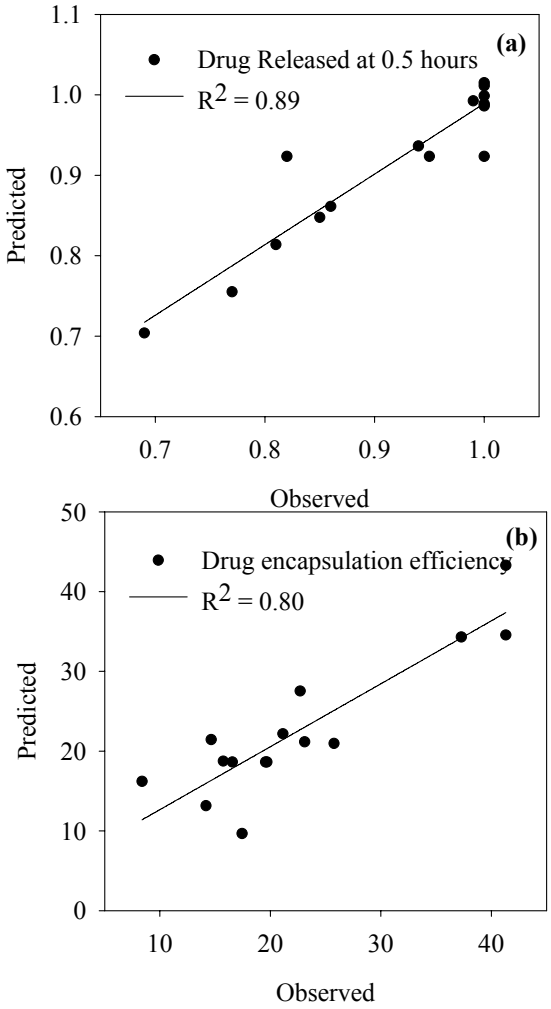

Figure 6.5: Linear relationship between the experimentally-derived and Box-Behnken predicted values for (a) Drug release (fractional) after 0.5 hours, and (b) Drug entrapment efficiency (N=3; SD<0.27).

Equation 6.1 below is the quadratic equation describing the Box-Behnken design:

Response = b_0 + b_1* polymer type + b_2* stirring time + b_3* [Span 80] + b_4 polymer type + b_5 stirring time*stirring time + b_6*[Span 80]*[Span 80] + b_7*polymer type*stirring time + b_8*polymer type*[Span 80] + b_9*stirring time*[Span 80]

Equation 6.1

In all cases of model-fitting, the Normal Plot of the Residuals showed that the data points formed a straight line indicating that the residuals were normally distributed (Figure 6.6a). Furthermore, the plot of the Residuals versus Fits showed a random pattern of the residuals on both sides of zero (Figure 6.6b). Typical plots of these indicators are shown in Figure 6.6a and 6.6b.

The adjusted Andersoñ-Darling statistic, a measure of how far the plot points fall from the fitted line in a probability plot produced a value of <0.2 in all cases. In general, a smaller Andersoñ-Darling statistic indicates that the distribution fits the data better. Essentially, the statistic is a weighted squared distance from the plot points to the fitted line with larger weights in the tails of the distribution. In addition, the p-values (0.302 - 0.417) were obtained for the normal residual plots were higher than the chosen α-level of 0.05, indicating that the data followed a normal distribution.

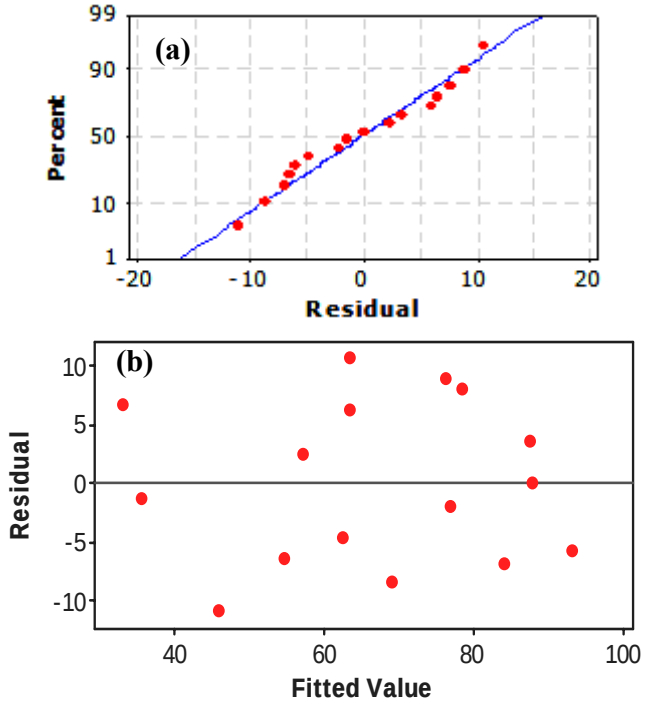

Figure 6.6: Typical profiles for (a) the normal probability plot of the residuals, and (b) the residuals versus the fitted values.

Table 6.6 shows the salient statistical parameters that were used to assess the goodness-of-fit of the models for the respective responses. Note that a p-value higher than 0.05 for the lack-of-fit parameter also indicates better model-fitting. R^2 values above 0.80 were considered as acceptable, based on complexity of the design.

Table 6.6: Salient Parameters employed according to Andersoñ-Darling statistic.

Response	R^2	Lack-of-Fit (p-value)
Drug Release after 0.5 hours	0.89	0.302
Drug Entrapment Efficiency	0.82	0.417

6.3.6 Main Effects on the Responses

The main effect indicates the influence of a single factor on a dependent variable averaged across the levels of the other factors. Figure 6.7a and 6.7b are typical main effects plots.

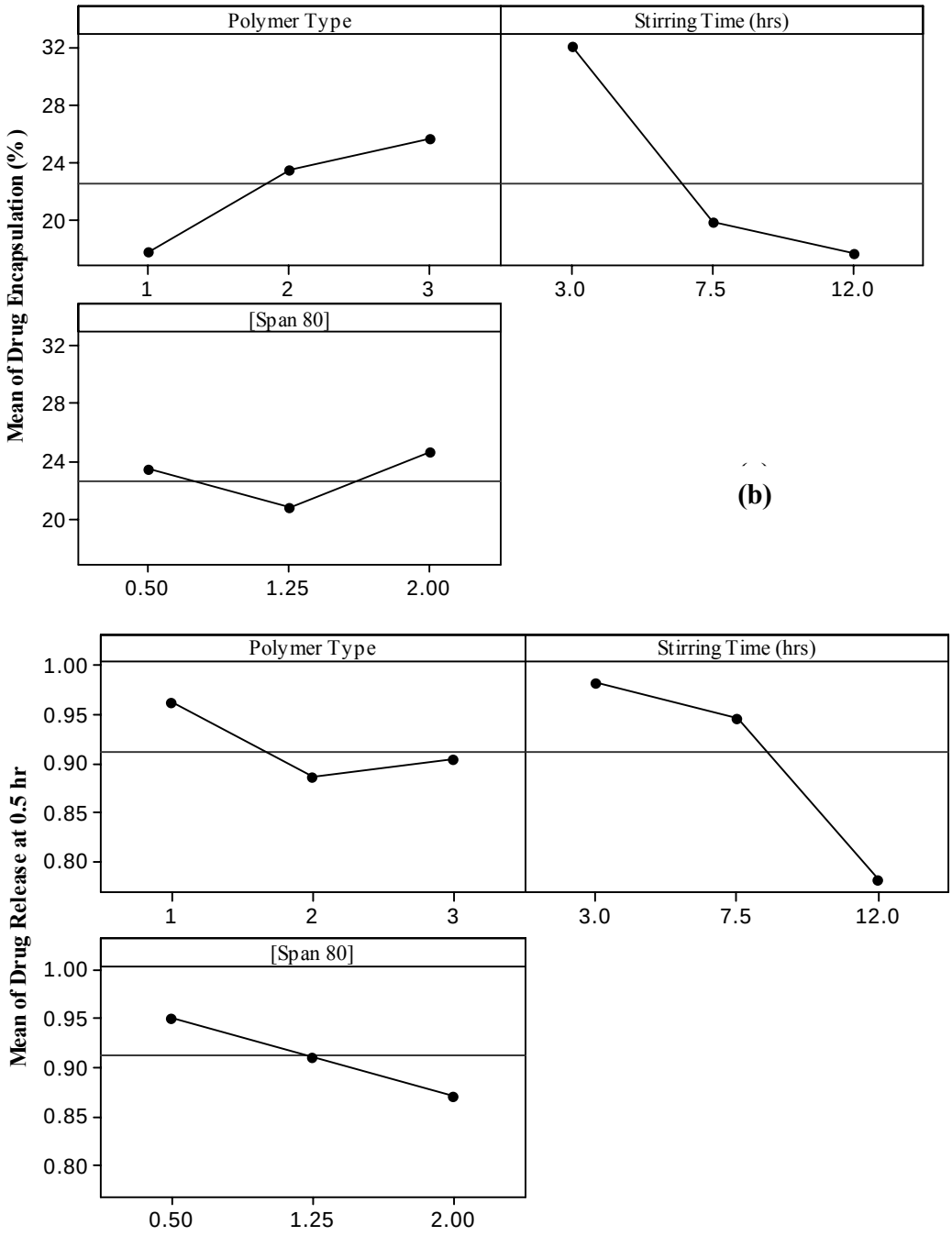

Figure 6.7: (a) Main effects plots (data means) for Drug Entrapment (%), and (b) % Drug release at 0.5 hours.

As observed in Figure 6.7a, the quantity of nicotine incorporated within the microparticles increased with the concentration of PLGA incorporated within its matrix. This may be attributed to the fact that PLGA may impart greater strength around the incorporating matrix and hence allowing for more drug to be entrapped. Stirring time demonstrated an inverse relationship with the entrapment ability and may be attributed to the fragmentation of microparticles as they were exposed to prolonged agitation (see Figure 6.2a). The concentration of emulsifying agent, Span 80, did not appear to show any particular or well-defined trend. However it was observed that entrapment was greatest (25%) at the highest concentration of Span 80 used, i.e. $2\%^{w}/_{v}$. This may be due to reduced interfacial tension between the external solution system and the periphery of the microparticles.

From Figure 6.7b, it was observed that drug release was as expected. Faster release was observed from microparticles that possessed a predominately PLA component in the incorporating material. As stated previously the comparatively more fragile nature imparted into the incorporating matrix by the presence of a greater amount of PLA allowed for more rapid release of nicotine.

The central limit value of each factor (Polymer type – 2 [PLA-PLGA combination], Stirring time – 7.5 hours and Span 80 concentration – $1.25\%^{w}/_{v}$) produced a focal point for significant changes ($p<0.05$) in the drug entrapment and drug release behaviour.

6.3.7 Response Surface Behaviour of Microparticulate System

Surface plots demonstrating the most significant changes for each response are depicted in Figure 6.8a and 6.8b.

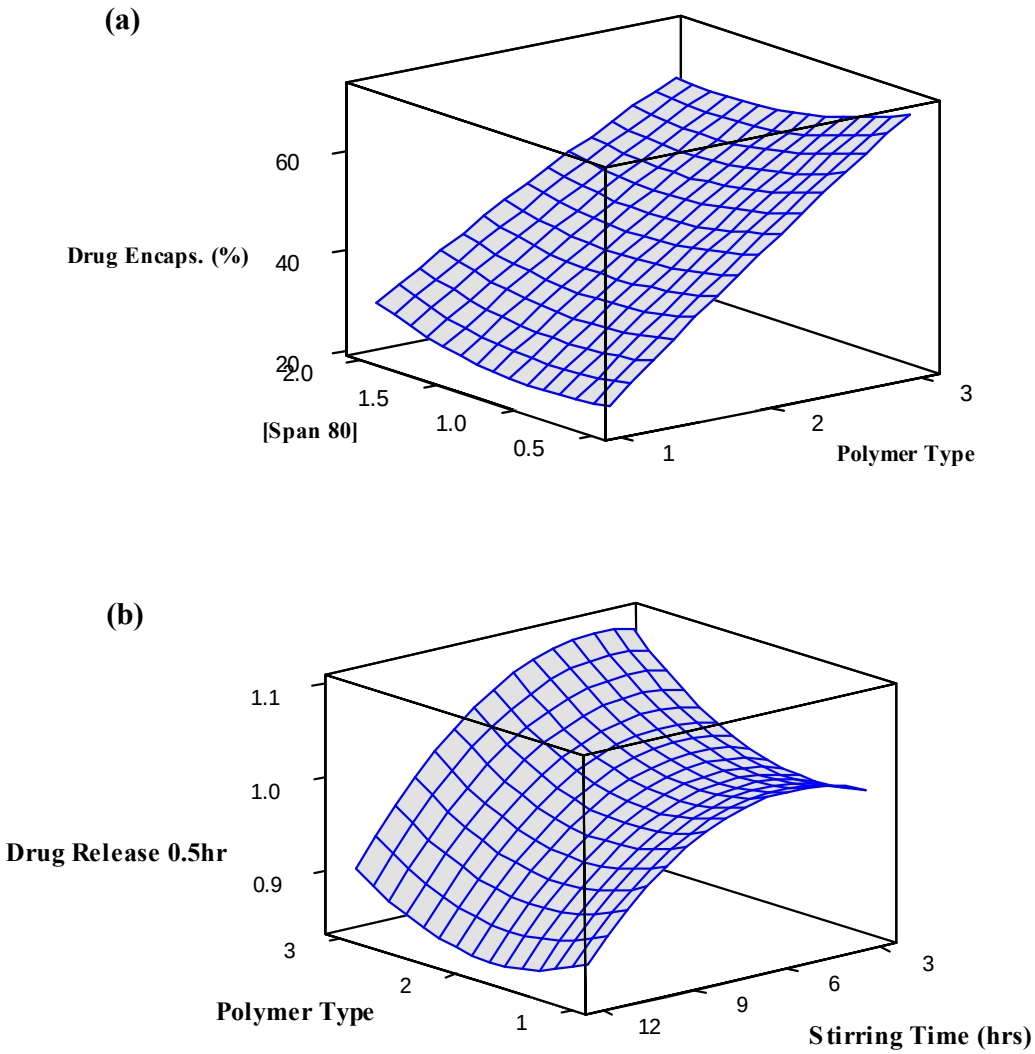

Figure 6.8: Response Surface Plots for (a) Drug encapsulation vs. Polymer type and [Span 80]; and (b) Drug release in 0.5 hours vs. Stirring time (hours) and Polymer type (1 – PLA; 2 – PLA and PLGA and 3 – PLGA).

Figure 6.8a indicated that as the concentration of PLGA was increased, the drug entrapment also increased. The concentration of Span 80 in the presence of a changing polymer composition did not affect the entrapment ability of the microparticles.

Figure 6.8b indicated that a decrease in the stirring time increased drug release. This may be attributed to possible clumping of microparticles, the aggregates of which attracted drug to the surface, due to inadequate stirring.

6.3.8 Double-Entrapment of PLA-PLGA Microparticles within an Alginate-Pectinate Platform

From the above, we have validated the need for re-entrapment of the microparticles to ensure that drug release can be significantly reduced to a rate that can be extended over a period of at least one month and to ensure that PD patients do not need to be implanted on a continuous basis, as this would negate patient compliance. To double-incorporate we needed to select a polymer that could attain this objective and interact favourably with the drug-PLGA matrix. To ensure this, a crosslinking agent was required to allow for the formation of bonds between the two polymers to form stable polyspheric structures.

The two polymers selected as the re-incorporating agents were the polyanionic polymers pectin and sodium alginate. The two polymers, when combined, are thought to interact through a combination of hydrogen bonding, Van der Waals forces and a significant effect is played by the crosslinking agent in the entire process. Both polymers have been extensively studied for their ability to form drug delivery systems that are capable of providing controlled and prolonged drug

delivery (Liu and Krishnan, 1999; Pillay et al., 2002; Walkenström, 2003). In a previous study (Liu and Krishnan, 1999), the use of pectin in particular was shown to produce extremely robust microspheres, which were resistant to degradation in acidic pH and demonstrated modulated release profiles of the incorporated model drugs at an alkaline pH. In combination with alginate it also plays a significant role in influencing the density of the 3-dimensional network of the combined structure. On the other hand, the homogeneity of the microstructure is a direct function of the concentration of the alginate in the mixture (Walkenström, 2003). Studies have shown that a combination of these polymers leads to the development of a synergistic interaction between the two and the subsequent formation of a 3-dimensional structure that has the capacity to incorporate even insoluble materials and not significantly influenced by the surrounding medium/environment (Pillay and Fassihi, 1999). In the present study, it was found that there was a close relationship between the degree of crosslinking and the yield of crosslinked polyspheres (Table 6.7). Zinc gluconate was selected as the crosslinking agent.

6.3.9 Yield of Crosslinked Polyspheres

The degree of crosslinking (η) was approximated using Equation 6.2,

$$\eta \approx \frac{\text{(Experimental polymer yield)} - \text{(Theoretical polymer yield)}}{\text{(Theoretical polymer yield)}} \times 100$$

Equation 6.2

Where η is the comparative degree of crosslinking between the polymer and zinc ions.

Table 6.7: Responses obtained for re-incorporated microparticles.

Crosslinked Polyspheric Matrices	Polysphere Yield (mg)	Drug Entrapment Efficiency (%)	Comparative Degree of Crosslinking (%)
Zinc-alginate	492.00	123.00	23.00
Zinc-pectinate	572.50	143.13	43.13
Zinc-alginate-pectinate	896.60	112.08	12.08

The following characteristics of the double-incorporated polyspheres were observed:

6.3.9.1 Zinc-Alginate Platform

Discrete spherical polyspheres were formed. The theoretical weight of polymer expected was 400mg; however an experimental value of 492.00mg was attained (Table 6.7). This may be attributed to the surface adherence of salt from the crosslinking solution. The close correlation between the theoretical and experimental value suggested that the degree of polymeric crosslinking was close to 100%.

6.3.9.2 Zinc-Pectinate Platform

As a double-incorporated polymer, on visual inspection they did not appear to be uniform, since aggregation and clumping of polyspheres was predominant. The polyspheres also formed significant 'tails' i.e. the polyspheres lost their spherical shape within the solution under the influence of stirring to form elongated/oblong structures. The increased weight (Table 6.7), can be attributed to the absorption of a large number of zinc ions within the pectinate platform. In comparison to zinc-alginate, it appears that the zinc-pectinate underwent a greater degree of crosslinking with zinc ions. The greater the number of ions within the matrix, the greater the bridging between the chains and the said ions. This may decrease polymer solubility, disentanglement and relaxation, thus leading to decreased polymer mobility.

6.3.9.3 Combined Zinc-Alginate-Pectinate Platform

Spherical polyspheres without tails were formed. The zinc-alginate-pectinate combination displayed the lowest degree of crosslinking compared to the other polymer types (Table 6.7). This may be attributed to the fact that a larger concentration of polymer, without a comparatively higher concentration of crosslinking agent was employed. Figure 6.9 is a typical scan of a zinc-alginate polysphere, which is incorporated with PLA-PLGA microparticles.

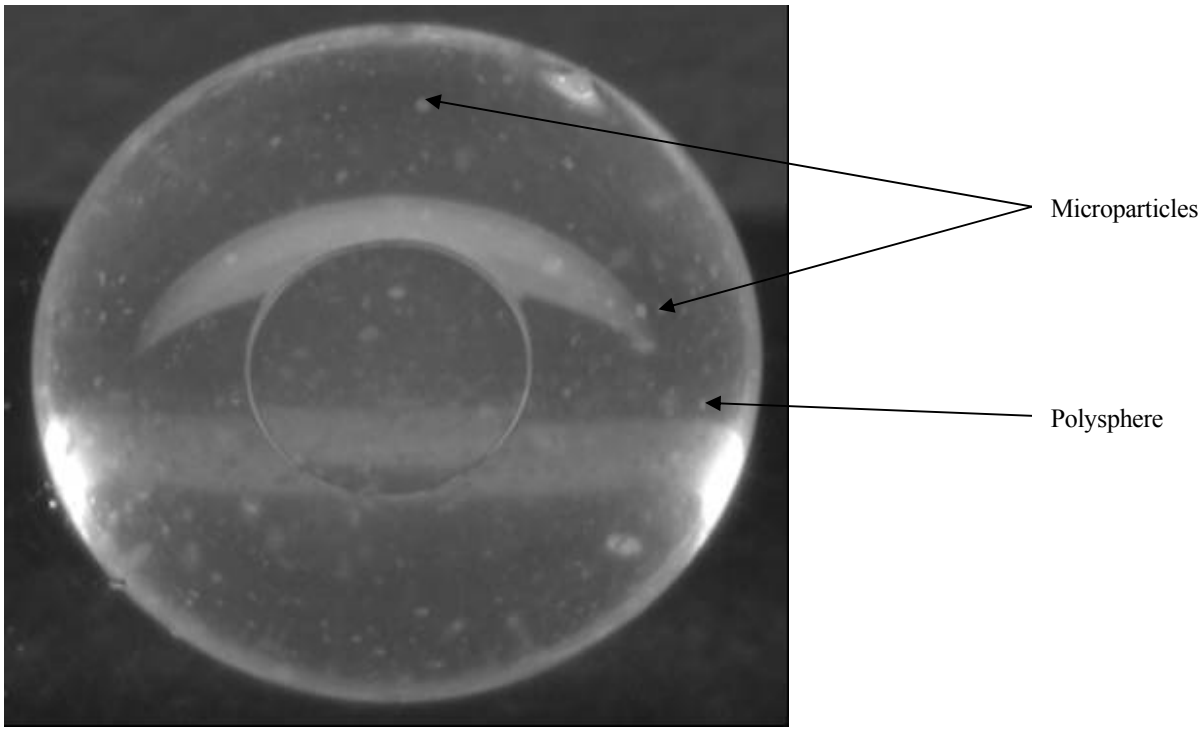

Figure 6.9: High resolution scan of PLA-PLGA microparticles double-incorporated within a zinc-alginate polysphere.

6.3.10 Evaluation of Drug Release from Polyspheres

It has been previously observed that significant sequestration occurs between the zinc ions, polymeric matrix and phosphate ions within the buffer solution (Pillay et al., 1999). This was once again observed, which led to the development of turbid solution due to the precipitation of zinc

phosphate within the dissolution medium. Figure 6.10 depicts the release profiles obtained from the three crosslinked polyionic systems.

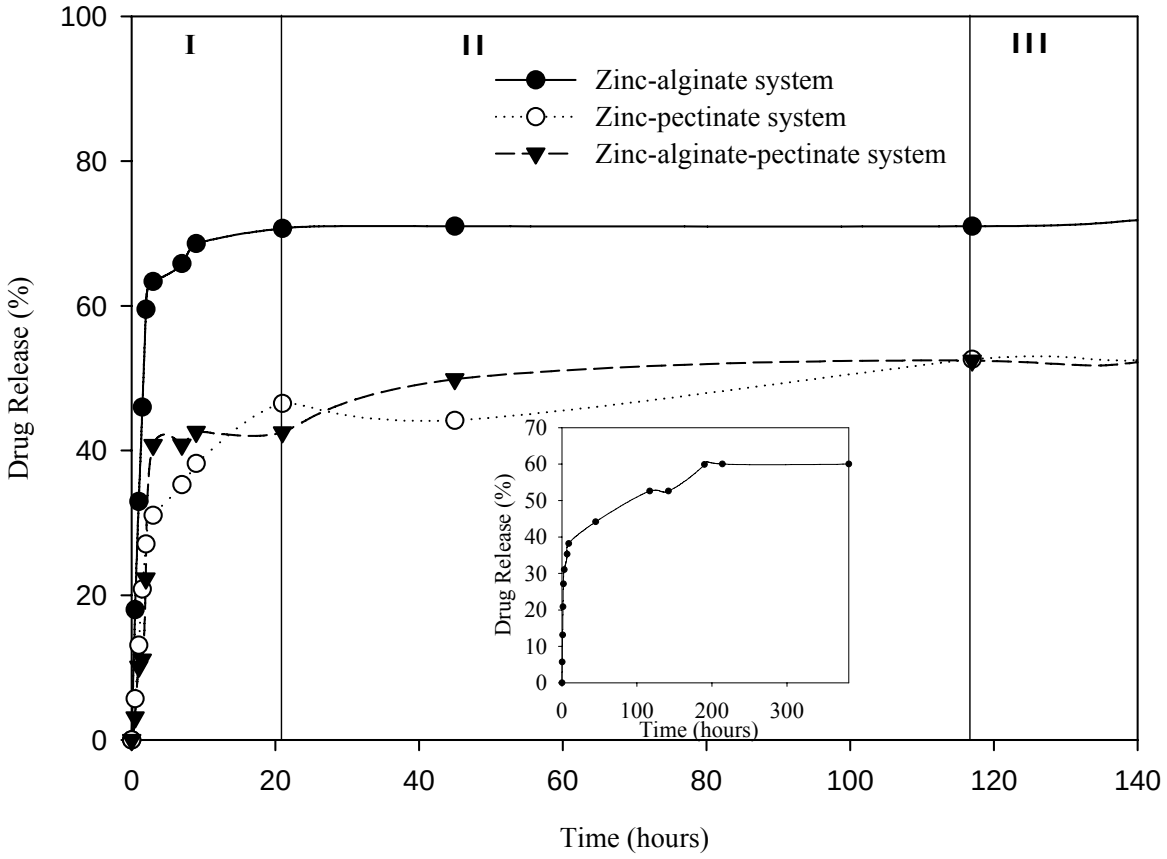

Figure 6.10: Drug release studies of double-encapsulated microparticles from multiparticulate polyspheres. (Insert clearly shows the second phase of drug release).

In all three cases it was noted that a high initial burst effect was obtained, followed by a plateau after a 2 hour period. The second phase of drug release appeared to occur from 6 hours onwards. The addition of pectin into the matrix appeared to significantly reduce drug release in comparison to the zinc-alginate system.

6.4 Concluding Remarks

The need for double entrapment of PLA-PLGA microparticles is warranted in order to allow for the development of a formulation that demonstrates prolonged and controlled release. It was concluded that zinc-pectinate polyspheres were optimal for re-entrapment. The zinc-pectinate platform had a significantly greater degree of crosslinking (43.125%) leading to greater drug entrapment and slower drug release, thus explaining the attenuated burst effect as a result of surface drug followed by slower drug release (Figure 6.10). Zinc-alginate-pectinate polyspheres did not appear to offer any significant advantage over zinc-pectinate polyspheres with respect to drug release and in fact possessed a smaller capacity to re-incorporate the PLA-PLGA microparticles.

Chapter 7

Conclusions and Recommendations

7.1 Conclusions

According to a recent study conducted by Dorsey et al (2007) the number of patients afflicted with PD worldwide in 2005 was approximately 4.1 million. It is projected that as a result of increased average life expectancy the number of individuals affected with this chronic progressive and severely debilitating disease will double by 2030 (Dorsey et al., 2007).

The present study developed a crosslinked multiple-unit multi-polymeric drug delivery device to deliver the model neuroprotectant nicotine with potential for implantation into the substantia nigra pars compacta to provide site-specific drug delivery provided zero-order prolonged release of the drug over a period of 1-2 months for the management of PD. This was achieved through the formulation of a novel reinforced ionotropically crosslinked reinforced alginate gelispheres which were compressed into release-rate modulating polymeric discs. This study has enabled the establishment of the elucidation of factors which influence the ability reinforced polymeric systems to entrap drug (drug entrapment efficiency), modulate drug release and induce changes in the physicomechanical properties and viscoelastic behaviour of the novel polymeric device following exposure to simulated CSF. Extensive tests including textural analyses, enthalpic studies and qualitative analyses through the use of FTIR enabled deductions regarding molecular interactions and configuration to correlate drug release studies. This study indicated that the reinforced system

far exceeds existing crosslinked polysaccharide systems of this nature with respect to its erosional and degradation behaviour. Furthermore, the fact that drug release of a low molecular weight and extremely hydrophilic model drug such as the model neuroprotectant, nicotine could be attenuated in the observed manner indicated the versatile platform that the device represents in terms of drug delivery.

A comprehensive investigation of the influence of the physicomechanical properties of various alginates crosslinked with various combinations of the three crosslinking agents, namely, zinc, calcium and barium revealed their influence on its erosional and textural properties following hydration. Overall textural analysis of the crosslinked gelisphere matrices indicated that the ratio of the constituent monomers of alginate guluronic (G) and mannuronic (M) acid had a profound influence on the nature of the crosslinked gelispheres generated. The divalent cations employed to crosslink alginate during the study demonstrated varying affinity to the monomers, which consequently impacted on the density and erosional behaviour of the matrix. Barium generated densely compact polymeric crosslinked matrices, while zinc-crosslinked gelispheres possessed porous networks. In terms of matrix erosion it was observed that zinc-crosslinked gelispheres demonstrated the most rapid rates of erosion due to the presence of porous matrices which permitted easier diffusion of water molecules into the polymeric network. Calcium-crosslinked gelispheres remained most intact over time following hydration.

Statistical optimisation of hydroxyethylcellulose (HEC) and polyacrylic acid (PAA) reinforced crosslinked alginate gelispheres indicated the following:

- ❖ While all formulations demonstrated first-order drug release kinetics, it was observed that high alginate and high HEC formulations attenuated the burst effect.
- ❖ High drug entrapment efficiencies (DEE) were observed with formulations with a high alginate and high HEC component. Formulations composed of high alginate and high HEC concentration and crosslinked with both crosslinking ions and high PAA concentrations demonstrated high DEE and slow drug release with a minimal burst effect.
- ❖ Textural analysis indicated that the alginate and Ba^{2+} concentrations had the most significant impact on the formation of compact and robust gelispheres.
- ❖ Finally it was observed that post-curing exposure to dilute HCl significantly attenuated matrix swelling and degradation as a result of precipitation of alginic acid within the crosslinked matrix.

Alternative approaches investigated the use of PLGA coatings over compressed polymeric matrices incorporating reinforced gelispheres with high drug-loads and succeeded in sustaining zero-order drug for 21 days. It was concluded that:

- ❖ The presence of hydrophobic PLGA mediates drug release kinetics through matrix erosion, rather than polymeric relaxation.
- ❖ The presence of hydrogels such as HPMC and PEO in the external matrix induced drug release to be mediated through polymer relaxation on the movement of molecules in the matrix.

Formulation of nicotine-loaded PLA-PLGA microparticles incorporated into zinc-crosslinked-pectinate gelispheres through double-entrapment attained prolonged and sustained release. The

factors which influenced drug release from the microparticulate system were optimised to establish that a combination of PLA and PLGA generated reinforced microparticles demonstrated high DEE and slower drug release. Furthermore it was concluded that employing exessive stirring times during formulation resulted in ruptured microparticles.

The primary goal of this study conducted was to develop a reinforced biopolymeric drug delivery system which has the capacity to provide prolonged release of neuroprotective agents through ideal zero-order kinetics in a site-specific manner to the brain. The study aimed to optimise PD patient therapy with respect to compliance and therapeutic efficacy. Extremely promising results were observed from the developed drug delivery systems investigated during this study. Formulation of compressed PLGA discs incorporating nicotine-loaded crosslinked alginate gelispheres reinforced with a combination of polymers (HEC and PAA) and crosslinked agents, namely barium and calcium succeeded in achieving zero-order release kinetics for 50 days.

7.2 Recommendations

The many neuroprotective agents investigated offer exciting opportunities for the development of future treatments. The challenge with many of these agents lies in the development of similar or modified versions that are both, more selective and potent. Furthermore, the development of drug delivery systems that can effectively deliver these molecules through site-specific mechanisms is vital to optimize their use.

The National Institute of Neurological Disorders and Stroke (NINDS) at the National Institute of Health (NIH) in the United States of America has created the Neuroprotection Exploratory Trials in PD (NET-PD), a large scale clinical trial network designed to assess potential neuroprotective agents for use in PD. Of the several compounds that were initially identified by scientists and clinicians in government, academia and industry for evaluation but only a few were promising enough to qualify for further study in neuroprotection clinical trials. According to an update on the investigations conducted by the Committee to Identify Neuroprotective Agents for Parkinson's disease or (CINAPS) to identify suitable potential neuroprotective agents in treating PD in February 2005, four compounds, namely, creatine, coenzyme Q10, minocycline and GM-1 ganglioside were chosen to evaluate in larger, Phase III Clinical Trials.

The developed devices offer a unique platform to deliver a range of the aforementioned neuroprotective agents. Since most of these agents possess higher molecular weights and decreased propensity to become soluble in aqueous media (such as physiological fluid or CSF), it is postulated that drug release would be further attenuated and demonstrate release kinetics which are further prolonged (as opposed to the studied nicotine-loaded systems). Further studies employing neuroactives with larger molecular weights and lower hydrophilicity (than the model drug, nicotine) should be conducted to confirm and establish the versatility and efficacy of the device in providing prolonged zero-order release.

Due to the fact that the device employs simple and mild formulation conditions, the multi-polymeric multi-unit systems developed provide a versatile means of adapting the developed system not only for alternative neuroprotectant agents, but could also be expanded to serve as a

means to deliver other bioactives such as genes, cells and even peptides. Studies employing some of the aforementioned bioactives should be performed to establish their viability following formulation, *in vitro* and *in vivo* analyses.

The geometry of the gelispheres developed during the study is significantly conducive towards drug release. This is due to the fact that spherical particles have the largest surface area available for interaction with physiological fluid. Thus it is proposed that the development of reinforced crosslinked polymeric particles with geometry which is less conducive towards drug release be developed.

It is also proposed that formulating of nano- or microparticulate barium-calcium-HEC-PAA reinforced crosslinked alginate gelispheres such as those developed from the optimised systems be conducted. This can be achieved through the use of processes such as ionotropic pre-gelation. *In vitro* analyses would enable a comparison of drug release kinetics. It is postulated that drug release may occur more rapidly due to the fact that such particles would provide increased surface areas available for surrounding physiological fluids to interact with. However, it is more feasible to incorporate such particles into external compressed polymeric matrices (discs). Furthermore, it would enable the formulation of discs with smaller dimensions, which would be more suitable for implantation.

Due to significant developments in the arena of PD genetics and cell biology, recent studies have indicated an explosive development of improved animal models of PD. In addition the creation of genetic animal models based on genes implicated in PD, investigators have also employed

environmental toxins in novel ways to produce more chronic and gradually progressive models of PD. It is proposed that further *in vivo* studies employing suitable animal models be conducted to establish the viability of the proposed devices. Ideally, the conditions for drug release *in vivo*, in the living brain tissue, need to be simulated. Fundamental aspects to be addressed include an appropriate replication of cerebrospinal fluid (CSF) in terms of pH and osmotic pressure, as well as the degree of agitation and temperature. The overall mass transport mechanisms on a physical and chemical into living brain tissue are not yet fully understood. In addition to this due to the complex morphology of the brain, range of processes can be involved in the transport of the drug following its released from the dosage form to its target site (brain). To date no standardised animal models exist for the evaluation of drug delivery systems which provide site-specific delivery to the brain, CNS or for the delivery of pharmaceutical agents and devices for PD. It is proposed therefore that further research be conducted to establish such a system to standardise and regulate *in vivo* studies conducted for the diseases and develop models which can serve as a more robust reflection of the disease in human subjects, to establish meaningful *in vitro–in vivo* correlations.

References

1. Abbott NJ, Rönnbäck L, Hansson E. Astrocyte–endothelial interactions at the blood–brain barrier. Nature Rev Neurosci. 7:41-53. 2006.

2. Akaike H. A new look at the statistical model identification. IEEE Transactions Automatic Contr. 19(6):716–723. 1974.

3. Al Musa S, Abu Fara D, Badwan AA. Evaluation of parameters involved in the preparation and release of drug loaded crosslinked matrices of alginate. J Control Rel. 57(3): 223-232. 1999.

4. Alexacis T, Boadi D, Quong D, Groboillot A, O'Neill I, Poncelet D, Neufeld R. Microencapsulation of DNA within alginate microspheres and crosslinkled chitosan membranes for in vivo implantation. Appl Biochem Biotech. 50:93-106. 1995.

5. Alvarez-Fuentes J, Fernandez-Arevalo M, Gonzalez-Rodriguez ML, Cirri M, Mura P. Development of enteric-coated timed-release matrix tablets for colon targeting. J Drug Target. 12(9-10):607-12. 2004.

6. Am OB, Amit T, Youdim MBH. Contrasting neuroprotective and neurotoxic actions of respective metabolites of anti-Parkinson drugs rasagiline and selegiline. Neurosci Lett. 355(3):169-172. 2004.

7. Andrews GP, Jones DS. Rheological characterization of bioadhesive binary polymeric systems designed as platforms for drug delivery implants. Biomacromolecules. 7(3):899-906. 2006.

8. Armstrong DW, Wang X, Ercal N. Enantiomeric composition of nicotine in smokeless tobacco, medicinal products, and commercial reagents. Chirality. 10:587–591. 1998.

9. Aslani P, Kennedy RA. Studies on diffusion in alginate beads. I. Effect of crosslinking with calcium or zinc ions on diffusion of acetaminophen. J Control Rel. 42:75–82. 1996.

10. Assal F, Spahr L, Hadengue A, Rubbici-Brandt L, Burkhard PR. Tolcapone and fulminant hepatitis. Lancet. 352 (9132):958. 1998.

11. Badwan A, Abumalooh A, Sallam E, Abukalaf A, Jawan O. A sustained release drug delivery system using calcium alginate beads. Drug Dev Indus Pharm. 11:239–256. 1983.

12. Bae YH, Okano T, Husu R, Kim SW. Thermo-sensitive polymers as on-off switches for drug release. Makromol Chem Rapid Commun. 8:481-485. 1987.

13. Bajpai SK, Sharma S. Investigation of Swelling/Degradation Behaviour of Alginate Beads Cross-linked with Ca2+ and Ba2+ Ions. React Funct Polymer. 59:129–140. 2004.

14. Bajpai SK, Tankhiwale R. Investigation of dynamic release of vitamin B_2 from calcium alginate/chitosan multilayered beads: Part II. React Func Polymers. 2006.

15. Baloğlu E, Özyazıcı M, Hızarcıoğlu SY, Karavana HA. An in vitro investigation for vaginal bioadhesive formulations: bioadhesive properties and swelling states of polymer mixtures. Il Farmaco. 58(5):391-396. 2003.

16. Beal MF. Coenzyme Q10 administration and its potential for treatment of neurodegenerative diseases. Biofactors. 9(2-4):261-6. 1999.

17. Beal MF. Mitochondrial dysfunction and oxidative damage in Alzheimer's and Parkinson's diseases and coenzyme Q10 as a potential treatment. J Bioenerg Biomembr. 36(4):381-6. 2004.

18. Begley DJ. Delivery of therapeutic agents to the central nervous system: the problems and the possibilities. Pharmacol Ther. 104(1):29-45. 2004.

19. Belluardo N, Mudo G, Blum M, Amato G, Fuxe K. Neurotrophic effects of central nicotinic receptor activation. J Neural Transm Suppl. (60):227-45. 2000.

20. Benedetti MD, Bower JH, Maraganore DM, McDonnell SK, Peterson BJ, Ahlskog JE, Schaid DJ, Rocca WA. Smoking, alcohol, and coffee consumption preceding Parkinson's disease: a case-control study. Neurology. 14;55(9):1350-8. 2000.

21. Bharath S, Hsu M, Kaur D, Rajagopalan S, Andersen JK. Glutathione, iron and Parkinson's disease. Biochem Pharmacol. 64(5-6).1037-1048. 2002.

22. Bhardwaj R, Blanchard J. In vitro characterization and in vivo release profile of a poly (D,L-lactide-co-glycolide) based implant delivery system for the α-MSH analog, melanotan-I. Int J Pharm. 170:109–117. 1998.

23. Bodor N, Buchwald P. Brain-targeted drug delivery: experiences to date. Am J Drug Targ. 1:13–26. 2003.

24. Bodor N. A strategy for delivering peptides into the central nervous system by sequential metabolism. Science. 257:1698–1700. 1992.

25. Bordia T, Parameswaran N, Fan H, Langston JW, McIntosh JM, Quik M. Partial recovery of striatal nicotinic receptors in 1-methyl-4-phenyl-1,2,3,6-tetrahydropyridine (MPTP)-lesioned monkeys with chronic oral nicotine. J Pharmacol Exp Ther. 319(1):285-92. 2006.

26. Bordia T, Parameswaran N, Fan H, Langston JW, McIntosh JM, Quik M. Partial recovery of striatal nicotinic receptors in 1-methyl-4-phenyl-1,2,3,6-tetrahydropyridine (MPTP)-lesioned monkeys with chronic oral nicotine. J Pharmacol Exp Ther. 319(1):285-92. 2006.

27. Brem H, Tamargo RJ, Olivi A, Pinn M, Weingart JD, Wharam M, Epstein JI. Biodegradable polymers for controlled delivery of chemotherapy with and without radiation therapy in the monkey brain. J Neurosurg. 80(2):283-90. 1994.

28. Briceño A, Delgado JM, de Delgado GD. The two-dimensional coordination polymer tetraaquamesaconatobarium(II), $[Ba(C_5H_4O_4)(OH_2)_4]_n$ Acta Cryst. 58:m602-m605. 2002.

29. Bridge MH, Williams E, Lyons ME, Tipton KF, Linert W. Electrochemical investigation into the redox activity of Fe(II)/Fe(III) in the presence of nicotine and possible relations to neurodegenerative diseases. BBA. 1690(1):77-84. 2004.

30. Brotchie JM, Lee J, Venderova K. Levodopa-induced dyskinesia in Parkinson's disease. J Neural Transm. 2004

31. Burke RE. Parkinson's disease, cell death and disease of the nervous system. In: Koliatos VE, Rattan RR (editors). Totowa, NJ: Humana Press Inc. Pages 459–75. 1998.

32. Burnette RR. Theory of Mass Transfer. Pages 96-135. Controlled Drug Delivery: Fundamentals and Applications. Robinson JR, Lee VHL (editors). 2nd edition. Marcel Dekker Inc. New York, USA. 1987.

33. Carr R. Evaluating flow properties of solids. Chem Eng. 72:163-8. 1965.

34. Checkoway H, Powers K, Smith-Weller T, Franklin GM, Longstreth WT Jr, Swanson PD. Parkinson's disease risks associated with cigarette smoking, alcohol consumption, and caffeine intake. Am J Epidemiol. 155(8):732-8. 2002.

35. Chen JF, Xu K, Petzer JP, Staal R, Xu YH, Beilstein M, Sonsalla PK, Castagnoli K, Castagnoli N Jr, Schwarzschild MA. Neuroprotection by caffeine and A(2A) adenosine receptor inactivation in a model of Parkinson's disease. J Neurosci. 21(10):RC143. 2001.

36. Chen W, He J, Olson JJ, Lu DR. Direct intracerebral delivery of carboplatin from PLGA microspheres against experimental malignant glioma in rats. Drug Delivery. 5:101–110. 1998.

37. Chien YW. Controlled Drug Delivery: Fundamentals and Applications. Robinson JR, Lee VHL (editors). 2nd edition. Marcel Dekker Inc. New York, USA. Pages 481-16. 1987.

38. Choi, HS, Khang G, Shin HC, Rhee JM, Lee HB. Preparation and Characterization of fentanyl-loaded PLGA microspheres; in vitro release profiles. Int J Pharm. 234:195–203. 2002.

39. Choonara YE, Pillay V, Carmichael T, Danckwerts MP. An in vitro study of the design and development of a novel doughnut-shaped minitablet for intraocular implantation. Int J Pharm. 310(1-2):15-24. 2006

40. Clarke CE, Guttman M. Dopamine agonist monotherapy in Parkinson's disease. Lancet. 360(9347):1767-9. 2002.

41. Clarke PBS, Fu D, Jakubovic A, Fibiger HC. Evidence that mesolimbic dopaminergic activation underlies the locomotor stimulant action of nicotine in rats. J Pharmacol Exp Ther. 246:701-708. 1988.

42. Cohen G, Spina MB. Deprenyl suppresses the oxidant stress associated with increased dopamine turnover. Ann Neurol. 26:689-90. 1989.

43. Cohen S, Lobel E, Trevgoda A, Peled Y. A novel, in situ-forming ophthalmic drug delivery system from alginates undergoing gelation in the eye. J Control Rel. 44(2–3):201–208. 1997

44. Colombo P, Bettini R, Peppas NA. Observation of swelling process and diffusion front position during swelling in hydroxypropyl methyl cellulose (HPMC) matrices containing a soluble drug. J Control Rel. 61(1-2):83-91. 1999.

45. Comella CL, Tanner CM. Therapy of Parkinson's Disease. Koller WC, Paulson G (editors). 2nd edition. Mercel Dekker Inc., New York, USA. Pages 109-22. 1995.

46. Conrad JM, Robinson JR. Sustained drug release from tablets and particles through coating. In: Liberman AS, Lachman SW (editors). Pharmaceutical Dosage Forms: Tablets. Volume 3. Pages 149–220. Marcel and Deccer, New York, USA. 1982.

47. Cools R. Dopaminergic modulation of cognitive function-implications for l-DOPA treatment in Parkinson's disease. Neurosci Biobehav Rev. 2005.

48. CRC Handbook of Chemistry and Physics on CD-ROM, CRC Press. 2004.

49. Critchley M. (editor). James Parkinson. Macmillan and Co Ltd., New York, USA. 1955.

50. Cuña M, Alonso MJ, Torres D. Preparation and in vivo evaluation of mucoadhesive microparticles containing amoxycillin–resin complexes for drug delivery to the gastric mucosa. Eur J Pharm Biopharm. 51(3):199-205. 2001.

51. Dayal P, Pillay V, Babu RJ, Singh M. Box-Behnken Experimental Design in the Development of a Nasal Drug Delivery System of Model Drug Hydroxyurea: Characterization of Viscosity, In Vitro Drug Release, Droplet Size, and Dynamic Surface Tension. AAPS PharmSciTech. 6(4):573-85. 2005.

52. de Rijk MC, Launer LJ, Berger K, Breteler MM, Dartigues JF, Baldereschi M, Fratiglioni L, Lobo A, Martinez-Lage J, Trenkwalder C, Hofman A. Prevalence of Parkinson's disease in Europe: a collaborative study of population-based cohorts. Neurology. 54(11):S21–S23. 2000.

53. Dipiro JT, Talbert RL, Yee GC, Matzke GR, Wells BG, Posey LM. Pharmacotherapy: A Pathophysiologic Approach. 4th edition. Appleton and Lange, Stamford, USA. 1999.

54. Dodd ML, Klos KJ, Bower JH, Geda YE, Josephs KA, Ahlskog JE. Pathological gambling caused by drugs used to treat Parkinson Disease. Arch Neurol. 62:1–5. 2005.

55. Doelker E. Cellulose derivatives. Adv Polym Sci. Berlin. 107:199-265. 1993.

56. Dorsey ER, Constantinescu R, Thompson JP, Biglan KM, Holloway RG, Kieburtz K, Marshall FJ, Ravina BM, Schifitto G, Siderowf A, Tanner CM. Projected number of

people with Parkinson disease in the most populous nations, 2005 through 2030. Neurology. 68:384-386. 2007.

57. Draget KI, Smidsrød O, Skjåk-Bræk. Alginates from algae. Biopolymers. Polysaccharides II: Polysaccharides from eukaryotes. 2002.

58. Draget KI, Stokke BT, Yuguchi Y, Urakawa H, Kajiwara K. Small-angle X-ray scattering and rheological characterization of alginate gels. Alginate acid gels. Biomacromolecules 4:1661-1668. 2003.

59. Du Y, Ma Z, Lin S. Minocycline prevents nigrostriatal dopaminergic neurodegeneration in the MPTP model of Parkinson's disease. Proc Natl Acad Sci USA. 98:14669–14674. 2001.

60. Durig T, Fassihi R. Guar-based monolithic matrix systems: Effect of ionizable and non-ionizable substances and excipients on gel dynamics and release kinetics. J Control Rel. 80:45–56. 2002.

61. Edelman ER, Kost J, Bobeck H, Langer R. Regulation of drug release from polymer matrices by oscillating magnetic fields. J Biomed Mater Res. 19:67-83. 1985.

62. Efentakis M, Koutlis A. Release of furosemide from multiple-unit and single-unit preparations containing different viscosity grades of sodium alginate. Pharm Dev Technol. 6(1):91-8. 2001.

63. Emborg ME. Evaluation of animal models of Parkinson's disease for neuroprotective strategies. J Neurosci Meth. 319(2): 121-43. 2004.

64. Emerich DF, Tracy MA, Ward KL, Figueiredo M, Qian R, Henschel C, Bartus RT. Biocompatibility of poly (DL-lactide-co-glycolide) microspheres implanted into the brain. Cell Transplant. 8(1):47-58. 1999.

65. Fabre E, Monserrat J, Herrero A, Barja G, Leret ML. Effect of MPTP on brain mitochondrial H2O2 and ATP production and on dopamine and DOPAC in the striatum. J Physiol Biochem. 55(4):325-31. 1999.

66. Factor SA, Molho ES. Transient benefit of amantadine in Parkinson's disease: the facts about the myth. Mov Disord. 14:515–517. 1999.

67. Fagerström KO, Pomerleau O, Giordani B, Stelson F. Nicotine may relieve symptoms of Parkinson's disease. Psychopharmacol (Berl). 116(1):117-9. 1994.

68. Fahn S, Cohen G. The oxidant stress hypothasisin idiopathic Parkinon's: Evidence supporting it. Ann Neurol. 32:799-803. 1992.

69. Fahn S. A pilot trial of high-dose alpha-tocopherol and ascorbate in early Parkinson's disease. Ann Neurol. 32:S128-32. 1992.

70. Fahn S. The spectrum of levodopa-induced dyskinesias. Ann Neurol. 47:S2– S11. 2000.

71. Filloux F, Townsend JJ. Pre- and Postsynaptic Neurotoxic Effects of Dopamine Demonstrated by Intrastriatal Injection. Exp Neurol. 119(1):79-88. 1993.

72. Fischel-Ghodsian F, Brown L, Mathiowitz E, Brandenburg D, Langer R. Enzymatically controlled drug delivery. Proc Natl Acad Sci USA. 85:2403-2406. 1988.

73. FMC BioPolymer.NovaMatrix. Releasing Technology Workshop. Alginate, Chitosan and Hyaluronan in Pharmaceutical and Biotechnological Applications: Teaching 'Old' Biopolymers New Tricks. Controlled Release Society Conference 2005.

74. Forno LS. Neuropathology of Parkinson's disease. J Neuropathol Exp Neurol. 55:259–272. 1996.

75. Forzese D. Managing Common Adverse Effects of Levodopa. Consult Pharm. 12:400-12. 1997.

76. Fournier E, Passirani C, Montero-Menei CN, Benoit JP. Biocompatibility of implantable synthetic polymeric drug carriers: focus on brain biocompatibility. Biomaterials. 24(19):3311-31. 2003.

77. Fowler JS, Volkow ND, Wang GJ, Pappas N, Logan J, MacGregor R, Alexoff D, Wolf AP, Warner D, Cilento R, Zezulkova I. Neuropharmacological actions of cigarette smoke: brain monoamine oxidase B (MAO B) inhibition. J Addict Dis. 17(1):23-34. 1998.

78. Frazier JL, Wang PP, Case D, Tyler BM, Pradilla G, Weingart JD, Brem H. Local delivery of minocycline and systemic BCNU have synergistic activity in the treatment of intracranial glioma. J Neuro-Oncol. 64:203–209. 2003.

79. Führer C. Interparticulate attraction mechanisms. In: Alderborn G, Nyström C (editors). Pharmaceutical Powder Compaction Technology. New York, NY, USA. Marcel Dekker. Pages 1–15. 1996.

80. Fujii C, Harada S, Ohkoshi N, Hayashi A, Yoshizawa K. Cross-cultural traits for personality of patients with Parkinson's disease in Japan. Am J Med Genet. 96:1–3. 2000.

81. Furukawa H, Shimojyo R, Ohnishi N, Fukuda H, Kondo A. Affinity selection of target cells from cell surface displayed libraries: a novel procedure using thermo-responsive magnetic nanoparticles. Appl Microbiol Biotechnol. 62(5-6):478-83. 2003.

82. Fuxe K, Janson AM, Jansson A, Andersson K, Eneroth P, Agnati LF. Chronic nicotine treatment increases dopamine levels and reduces dopamine utilization in substantia nigra and in surviving forebrain dopamine nerve terminal systems after a partial di-mesencephalic hemitransection. Naunyn Schmiedebergs Arch Pharmacol. 341(3):171-81. 1990.

83. Gaginella TS, Bass P. Nicotine: release from silicone rubber implants in vivo. Res Commun Chem Pathol Pharmacol. 7(1):213-6. 1974.

84. Gao P, Skoug JW, Nixon PR, Ju TR, Stemm NL, Sung KC. Swelling of hydroxypropyl methylcellulose matrix tablets. Mechanistic study of the influence of formulation variables

on matrix performance and drug release. J Pharm Sci. New York, USA. 85(7):732-740, 1996.

85. Gershanik O, Emre M, Bernhard G, Sauer D. Efficacy and safety of levodopa with entacapone in Parkinson's disease patients suboptimally controlled with levodopa alone, in daily clinical practice: an international, multicentre, open-label study. Prog Neuro-Psychopharm Biol Psych. 27(6):963-971. 2003.

86. Gilchrist T, Martin AM. Wound treatment with Sorbsan – an alginate fiber dressing. Biomaterials. 4:317-20. 1983.

87. Gluck MR, Krueger MJ, Ramsay RR, Sablin OS, Singer TP, Nicklas WJ. Characterisation of the inhibitory mechanism of MPP^+ and 4-phenyl pyridine analogs in inner membrane preparations. J Biol Chem.. 269:3167–3174. 1994.

88. Gold BG, Nutt JG. Neuroimmunophilin ligands in the treatment of Parkinson's disease. Curr Opin Pharmacol.. 2:82–86. 2002.

89. Gombotz WR, Wee SF. Protein release from alginate matrices. Adv Drug Delivery Rev. 31(3):267-285. 1998.

90. Gourlay SG, Forbes A, Marriner T, McNeil JJ. Predictors and timing of adverse experiences during trandsdermal nicotine therapy. Drug Saf. 20(6):545-55. 1999.

91. Grant GT, Morris ER, Rees DA, Smith PJ, Thom D. Biological interaction between polysacarides and divalent cations: The egg-box model. FEBS Lett. 32(1):195. 1973.

92. Grosset KA, Bone I, Grosset DG. Suboptimal medication adherence in Parkinson's disease. Mov Disord. 20(11):1502-7. 2005.

93. Guerin C, Olivi A, Weingart JD, Lawson HC, Brem H. Recent advances in brain tumor therapy: local intracerebral drug delivery by polymers. Invest New Drugs. 22:27–37. 2004.

94. Guidance for Industry: Dissolution Testing of Immediate Release Solid Oral Dosage Forms U.S. Department of Health and Human Services; Food and Drug Administration; Centre for Drug Evaluation and Research (CDER); August 1997.

95. Guo JH, Skinner GW, Harcum WW, Barnum PE. Pharmaceutical applications of naturally occurring water-soluble polymers. Pharm Sci Tech Today. 1(6): 254-261. 1998.

96. Hari PR, Chandy T, Sharma CP. Chitosan/calcium alginate microcapsules for intestinal delivery of nitrofurantoin. J Microencap. 13:319–329.1996.

97. Heller J. Controlled Drug Delivery: Fundamentals and Applications. Robinson JR, Lee VHL (editors). 2nd edition. Marcel Dekker Inc. New York, USA. Pages 179-191. 1987.

98. Hoagland DR, Lieb LL. The Complex Carbohydrates and forms of Sulphur in Marine Algae on the Pacific Coast. J Biol Chem. 23(1):287-97. 1915

99. Hoffman AS, Afrassiabi A, Dong LC. Thermally reversible hydrogels: II. Delivery and selective removal of substances from aqueous solutions. J Control Rel. 4:213-222. 1986.

100. Hoffman AS. Hydrogels for biomedical applications. Adv Drug Deliv Rev. 54(1):3-12. 2002.

101. Hopfenberg HB. D.R. Paul, F.W. Haris (editors), Controlled Release Polymeric Formulations (ACS Symposium Series No. 33). American Chemical Society, Washington, DC. Pages 26–31. 1976.

102. Hsieh DS, Langer R, Folkman J. Magnetic modulation of release of macromolecules from polymers. Proc Natl Acad Sci USA. 78(3):1863-7. 1981.

103. Hui et al. In: Pharmaceutical Dosage Forms: Tablets. Lieberman HA, Lachman L, Schwartz JB (editors). Volume 2. Pages 317-338. 2nd edition. Marcel Dekker, Inc. 1989.

104. Hutton JT, Morris JL. Long-acting Levodopa Preparations. Therapy of Parkinson's Disease. Edited by Koller WC, Paulson G. 2nd edition. Mercel Dekker Inc, New York, USA. Pages 173-87. 1995.

105. Huynh GH, Deen DF, Szoka FC. Barriers to carrier mediated drug and gene delivery to brain tumors. J Control Rel. 110(2):236-259. 2006.

106. Ike O, Shimizu Y, Wada R, Hyon SH, Ikada Y. Controlled cisplatin delivery system using poly(D,L-lactic acid). Biomaterials. 13:230–234. 1992.

107. Ionic Information of Barium. http://www.scescape.net/~woods/elements/barium.html 2004.

108. Ionic Information of Calcium. http://ww.scescape.net/~woods/elements/calcium.html 2004.

109. Ionic Information of Zinc. http://www.scescape.net/~woods/elements/zinc.html 2004.

110. Jamzad S, Fassihi R. Development of a controlled release low dose class II drug-Glipizide. Int J Pharm. 312(1-2):24-32. 2006.

111. Jamzad S, Tutunji L, Fassihi R. Analysis of macromolecular changes and drug release from hydrophilic matrix systems. Int J Pharm.. 292:75–85. 2005.

112. Jankovic J. Complications and limitations of drug therapy for Parkinson's disease. Neurology. 52:S2–S6. 2000.

113. Jankovic J. Levodopa strengths and weaknesses. Neurology. 58:S19–S32. 2000.

114. Ju RTC, Nixon PR, Patel MV. Drug release from hydrophilic matrices 1. New scaling laws for predicting polymer and drug release based on the polymer disentanglement concentration and the diffusion layer. J Pharm Sci. 84:1455–1463. 1995.

115. Kalyani S, Smitha B, Sridhar S, Krishnaiah A. Blend membranes of sodium alginate and hydroxyethylcellulose for pervaporation-based enrichment of t-butyl alcohol. Carbohydrate Polymers. 64(3):425-432. 2006.

116. Katzenschlager R, Sampaio C, Costa J, Lees A. Antichoilinergics for symptomatic management of Parkinson's disease. The Cochrane Database of Systematic Reviews. Issue 3. 2003.

117. Katzung BG. Pharmacological management of Parkinsonism and other movement disorders; Basic and Clinical Pharmacology. 8th edition; Lange Medical Books/McGraw Hill Companies, Inc. 2001.

118. Khan FH, Sen T, Maiti AK, Jana S, Chatterjee U, Chakrabarti S. Inhibition of rat brain mitochondrial electron transport chain activity by dopamine oxidation products during extended in vitro incubation: Implications for Parkinson's disease. BBA Mol Bas Dis. 1741(1-2):65-74. 2005.

119. Kim CK, Lee EJ. The controlled release of blue dextran from alginate beads. Int J Pharm. 79:11–19. 1992.

120. Klos KJ, Bower JH, Josephs KA, Matsumoto JY, Ahlskog JE. Pathological hypersexuality predominantly linked to adjuvant dopamine agonist therapy in Parkinson's disease and multiple system atrophy. Parkinsonism Relat Disord. 11(6):381-6. 2005.

121. Koch S, Schwinger C, Kressler J, Heinzen CH, Rainov NG. Alginate encapsulation of genetically engineered mammalian cells: comparison of production devices, methods and microcapsule characteristics. J Microencaps. 20:303–316. 2003.

122. Koda Kimble MA, Young LY. Applied Therapeutics – The Clinical Use of Drugs. 7th edition. Lippincott Williams and Wilkins. A Wolters Kluwer Company. Philadelphia, USA. 2000.

123. Koller WC, Hubbard JP. Levodopa therapy in Parkinson's disease. Neurology. 40:40–47. 1990.

124. Kong HJ, Mooney DJ. The effects of poly(ethyleneimmine) (PEI) molecular weight on reinforcement of alginate hydrogels. Cell Transplant. 12(7):779-85. 2003.

125. Kontkanen O, Castrén E. Trophic effects of selegiline on cultured dopaminergic neurons. Brain Res. 829(1-2):190-192. 1999.

126. Kost J, Leong K, Langer R. Ultrasound-enhanced polymer degradation and release of incorporated substances. Proc Natl Acad Sci USA. 86(20):7663-6. 1989.

127. Kost J. Ultrasound for controlled delivery of therapeutics. Clin Mater. 13(1-4):155-61. 1993.

128. Krasaekoopt W, Bhandari B, Deeth H. The influence of coating materials on some properties of alginate beads and survivability of microencapsulated probiotic bacteria. Int Dairy J. 14:737-43. 2004.

129. Kriwet B, Kissel T. Interactions between bioadhesive poly(acrylic acid) and calcium ions. Int J Pharm. 127:135–145. 1996.

130. Kuo CK, Ma PX. Ionically crosslinked alginate hydrogels as scaffolds for tissue engineering: Part 1. Structure, gelation rate and mechanical properties. Biomaterials. 22(6):511-521. 2001.

131. Kwon IC, Bae YH, Kim SW. Electrically erodible polymer gel for controlled release of drugs. Nature. 354:291-293. 1991.

132. Langer R. Implantable controlled release systems. Pharmacol Ther. 21(1):35-51. 1983.

133. Lemay S, Blanchet P, Chouinard S, Masson H, Soland V, Bedard MA. Poor tolerability of a transdermal nicotine treatment in Parkinson's disease. Clin Neuropharmacol. 26(5):227-9. 2003.

134. Lemay S, Chouinard S, Blanchet P, Masson H, Soland V, Beuter A, Bedard MA. Lack of efficacy of a nicotine transdermal treatment on motor and cognitive deficits in Parkinson's disease. Prog Neuropsychopharmacol Biol Psychiatry. 28(1):31-9. 2004.

135. Lendlein A, Kratz K, Kelch S. Smart implant materials. Med Device Technol. 16(3):12-4. 2005.

136. Leonard M, De Boisseson MR, Hubert P, Dalençon F, Dellacherie E. Hydrophobically modified alginate hydrogels as protein carriers with specific controlled release properties. J Control Rel. 98(3):395-405. 2004.

137. Leranth C, Roth RH, Elsworth JD, Naftolin F, Horvath TL, Redmond DE Jr. Estrogen is essential for maintaining nigrostriatal dopamine neurons in primates: implications for Parkinson's disease and memory. J Neurosci. 20(23):8604-9. 2000.

138. Lev N, Melamed E. Heredity in Parkinson's disease: new findings. Isr Med Assoc J. 3(6):435-8. 2001.

139. Li VHK, Robinson JR, Lee VHL. Controlled Drug Delivery: Fundamentals and Applications. Robinson JR, Lee VHL (editors). 2nd edition. Marcel Dekker Inc. New York, USA. Pages 3-61. 1987.

140. Linert W, Bridge MH, Huber M, Bjugstad KB, Grossman S, Arendash GW. In vitro and in vivo studies investigating possible antioxidant actions of nicotine: relevance to Parkinson's and Alzheimer's disease. BBA Mol Bas Dis. 1454(2):143-152. 1998.

141. Liu P and Krishnan TR. 1999. Alginate–Pectin–Poly-L-lysine Particulate as a Potential Controlled Release Formulation. J Pharm Pharmacol. 51(2):141-149.

142. Lossinsky AS, Vorbrodt AW, Wisniewski HM. Scanning and transmission electron microscopic studies of microvascular pathology in the osmotically impaired blood-brain barrier. J Neurocytol. 24:795–806. 1995.

143. Ludwig A. The use of mucoadhesive polymers in ocular drug delivery. Adv Drug Deliv Rev. 57(11):1595-1639. 2005.

144. Lueßen HL, de Leeuw BJ, Pérard D, Lehr CM, de Boer AG, Verhoef JC, Junginger HE. Mucoadhesive polymers in peroral peptide drug delivery I. Influence of mucoadhesive excipients on the proteolytic activity of intestinal enzymes. Eur J Pharm Sci. 4:117–128. 1996.

145. Macleod AD, Counsell CE, Ives N, Stowe R. Monoamine oxidase B inhibitors for early Parkinson's disease. Cochrane Collaboration Review. 2005.

146. Maggi L, Bruni R, Conte U. High molecular weight polyethylene oxides (PEOs) as an alternative to HPMC in controlled release dosage forms. Int J Pharm. 195(1-2):229-38. 2000.

147. Maggio R, Riva M, Vaglini F, Fornai F, Molteni R, Armogida M, Racagni G, Corsini GU. Nicotine prevents experimental parkinsonism in rodents and induces striatal increase of neurotrophic factors. J Neurochem. 71(6):2439-46. 1998.

148. Magyar K, Szende B. (−)-Deprenyl, A Selective MAO-B Inhibitor, with Apoptotic and Anti-apoptotic Properties. NeuroToxicol. 25(1-2):233-242. 2004.

149. Mandel S, Weinreb O, Amit T, Youdim MBH. Mechanism of neuroprotective action of the anti-Parkinson drug rasagiline and its derivatives. Brain Res Rev. 48(2): 379-387. 2005.

150. Maruyama W, Takahashi T, Naoi M. (−)-Deprenyl protects human dopaminergic neuroblastoma SH-SY5Y cells from apoptosis induced by peroxynitrite and nitric oxide. J. Neurochem. 70:2510–2515. 1998.

151. Maruyama W, Takahashi T, Youdim M, Naoi M. The anti-Parkinson drug, rasagiline, prevents apoptotic DNA damage induced by peroxynitrite in human dopaminergic neuroblastoma SH-SY5Y cells. J Neural Transm. 109(4):467-81. 2002.

152. Maruyama W, Yamamoto T, Kitani K, Carrillo MC, Youdim M, Naoi M. Mechanism underlying anti-apoptotic activity of a (-)deprenyl-related propargylamine, rasagiline. Mech Ageing Dev. 116:181–191. 2000.

153. Mathiowitz E, Cohen MD. Polyamide microcapsules for controlled release. V. Photochemical release. J Membr Sci. 40:67-86. 1989.

154. Matsubayashi H, Inoue A, Amano T, Seki T, Nakata Y, Sasa M, Sakai N. Involvement of α7- and α4β2-type postsynaptic nicotinic acetylcholine receptors in nicotine-induced excitation of dopaminergic neurons in the substantia nigra: a patch clamp and single-cell PCR study using acutely dissociated nigral neurons. Mol Brain Res. 129(1-2): 1-7. 2004.

155. Matthews RT, Ferrante RJ, Klivenyi P, Yang L, Klein AM, Mueller G, Kaddurah-Daouk R, Beal MF. Creatine and cyclocreatine attenuate MPTP neurotoxicity. Exp Neurol. 157(1):142-9. 1999.

156. McCallum SE, Parameswaran N, Bordia T, McIntosh JM, Grady SR, Quik M. Decrease in alpha3*/alpha6* nicotinic receptors but not nicotine-evoked dopamine release in monkey brain after nigrostriatal damage. Mol Pharmacol. 68(3):737-46. 2005.

157. McDowell RH. Properties of Alginate. 4th edition. London, UK. Alginate Industries Ltd. 1977.

158. Menei P, Boisdron-Celle M, Croue A, Guy G, Benoit JP. Effect of stereotactic implantation of biodegradable 5-fluorouracil-loaded microspheres in healthy and C6 glioma-bearing rats. Neurosurgery. 39:117–124. 1996.

159. Menei P, Venier MC, Gamelin E, Saint-Andre JP, Hayek G, Jadaud E, Fournier D, Mercer P, Guy G, Benoit JP. Local and sustained delivery of 5-fluorouracil from biodegradable microspheres for the radiosensitization of glioblastoma. Cancer. 86:325–330. 1999.

160. Menza MA, Golbe LI, Cody RA, Forman NE. Dopamine-related personality traits in Parkinson's disease. Neurology. 43:505–508. 1993.

161. Menza MA, Golbe LI, Goldstein H, Forman N. Are there personality traits associated with the dopaminergic deficits of parkinson's disease? Biol Psych. 31(5):75-76. 1992.

162. Menza MA, Golbe LI, Goldstein H, Forman N. Parkinson's disease and dopamine-dependent personality traits. Biol Psych. 27(9):55. 1990.

163. Mercuri NB, Bernardi G. The 'magic' of l-dopa: why is it the gold standard Parkinson's disease therapy? Trends Pharmacol Sci. 26(7):341-4. 2005.

164. Miyazaki S, Kubo W, Attwood D. Oral sustained delivery of theophylline using in-situ gelation of sodium alginate. J Control Rel. 67(2):275-80. 2000.

165. Mizuta I, Ohta M, Ohta K, Nishimura M, Mizuta E, Hayashi K, Kuno S. Selegiline and Desmethylselegiline Stimulate NGF, BDNF, and GDNF Synthesis in Cultured Mouse Astrocytes. Biochem Biophys Res Comm. 279(3):751-755. 2000.

166. Moll H. The treatment of postencephalitic Parkinsonism by nicotine. Brain Med J. 1:1079–1081. 1926.

167. Morale MC, Serra PA, L'episcopo F, Tirolo C, Caniglia S, Testa N, Gennuso F, Giaquinta G, Rocchitta G, Desole MS, Miele E, Marchetti B. Estrogen, neuroinflammation and neuroprotection in Parkinson's disease: glia dictates resistance versus vulnerability to neurodegeneration. Neuroscience. 138(3):869-78. 2005.

168. Morens DM, Grandinetti A, Reed D, White LR, Ross GW. Cigarette smoking and protection from Parkinson's disease: false association or etiologic clue? Neurology. 45:1041–1051. 1995.

169. Mortazavi SA, Smart JD. An investigation of some factors influencing the in vitro assessment of mucoadhesion. Int J Pharm. 116:223. 1995.

170. Mukai S, Lipsitz LA. Orthostatic hypotension. Clin Geriatr Med. 18(2):253-68. 2002.

171. Naidu BVK, Sairam M, Raju KVSN, Aminabhavi TM. Thermal, viscoelastic, solution and membrane properties of sodium alginate/hydroxyethylcellulose blends. Carbohydrate Polymers. 61(1):52-60. 2005.

172. Narasimhan B, Peppas NA. Molecular analysis of drug delivery systems controlled by dissolution of the polymer carrier. J Pharm Sci. New York. 86(3):297-304. 1997.

173. Newhouse PA, Kelton M. Nicotinic systems in central nervous systems disease: degenerative disorders and beyond. Pharm Acta Helv. 74(2-3):91-101. 2000.

174. Newhouse PA, Potter A, Singh A. Effects of nicotinic stimulation on cognitive performance. Curr Opin Pharmacol. 4(1):36-46. 2004.

175. Nokhodchi A, Tailor A. In situ cross-linking of sodium alginate with calcium and aluminum ions to sustain the release of theophylline from polymeric matrices. Il Farmaco. 59(12): 999-1004. 2004.

176. Obata T, Aomine M, Inada T, Kinemuchi H. Nicotine suppresses 1-methyl-4-phenylpyridinium ion-induced hydroxyl radical generation in rat striatum. Neurosci Lett. 330(1):122-4. 2002.

177. Obeso JA, Olanow W, Nutt JG. Levodopa motor complications in Parkinson's disease. Trends Neurosci. 23:S2–S7. 2000.

178. Ohya Y, Toyohara M, Sasakawa M, Arimura H, Ouchi T. Thermosensitive biodegradable polydepsipeptide. Macromol Biosci. 5(4):273-6. 2005.

179. Olanow CW, Agid Y, Mizuno Y. Levodopa in the treatment of Parkinson's disease: current controversies. Mov Dis. 19(9): 997-1005. 2004.

180. Olivi A, Ewend EG, Utsuki T, Tyler B, Domb AJ, Brat DJ, Brem H. Interstitial delivery of carboplatin via biodegradable polymers is effective against experimental glioma in the rat. Cancer Chemother Pharmacol. 39:90–96. 1996.

181. Orive G, Ponce S, Hernandez RM, Gascon AR, Igartua M, Pedraz JL. Biocompatibility of microcapsules for cell immobilization elaborated with different type of alginates. Biomaterials. 23:3825–3831. 2002.

182. Painter PC, Coleman MM (editors). Fundamentals of Polymer Science: An Introductory Text. 2nd edition, Technomic Publishing Company, Pennsylvania, USA. 1997.

183. Pardridge WM. Blood–brain barrier delivery. Drug Disc Today. 12(1-2):54-61. 2007.

184. Parkinson J. An Essay on the Shaking Palsy. Sherwood Neely & Jones, London. 1817.

185. Paulson GW, Dadmehr N. Is there a premorbid personality typical for Parkinson's disease? Neurology. 41:73–76. 1991.

186. Peppas NA, Sahlin JJ. A simple equation for the description of solute release III - Coupling of diffusion and relaxation. Int J Pharm. 57:169–172. 1989.

187. Peppas NA. A model of dissolution-controlled solute release from porous drug delivery polymeric systems. J Biomed Mater Res. 17(6):1079-87. 1983.

188. Percival E, McDowell RH. Chemistry and Enzymology of Marine Algal Polysaccharides. Academic Press Inc. Ltd., New York, USA. 1967.

189. Pillay V, Danckwerts MP, Fassihi R, Muhidinov Z. Novel Modulation of Drug Delivery Using Binary Zinc-Alginate-Pectinate Polyspheres for Zero-Order Kinetics Over Several Days: Experimental Design Strategy to Elucidate the Crosslinking Mechanism. Drug Dev Ind Pharmacy. 31:191–207. 2005.

190. Pillay V, Danckwerts MP, Fassihi R. A crosslinked calcium-alginate-pectinate-cellulose acetophthalate gelisphere system for linear drug release. Drug Deliv. 9(2):77-86. 2002.

191. Pillay V, Dangor CM, Govender T, Moopanar KR, Hurbans N. Ionotropic gelation: encapsulation of indomethacin in calcium alginate gel discs. J Microencaps. 15(2):215-26. 1998.

192. Pillay V, Fassihi R. A novel approach for constant rate delivery of highly soluble bioactives from a simple monolithic system. J Control Rel. 67:67–78. 2000.

193. Pillay V, Fassihi R. In vitro release modulation from crosslinked pellets for site-specific drug delivery into the gastrointestinal tract I: Comparison of pH-responsive drug release and associated kinetics. J Control Rel. 59(2):229-242. 1999.

194. Pillay V, Fassihi R. In vitro release modulation from crosslinked pellets for site-specific drug delivery to the gastrointestinal tract II: Physicochemical characterization of calcium-alginate, calcium-pectinate and calcium-alginate-pectinate pellets. J Control Rel. 59(2):243-56. 1999.

195. Pillay V, Fassihi R. In vitro release modulation from crosslinked pellets for site-specific drug delivery into the gastrointestinal tract I: Comparison of pH-responsive drug release and associated kinetics. J Control Rel. 59(2)229-242. 1999.

196. Place VA, Wong P, Barclay BL, Childers JD. International patent number WO 92/01445. 1992.

197. Plackett RL, Burman JP. The design of optimum multi-factorial experiments. Biometrika. 33:305-325. 1946.

198. Polymeropulous MH, Lavedan C, Leory E, Ide SE, Dehejia A, Dutra A, Pike B, Root H, Rubenstein J, Boyer R, Stenroos ES, Chandrasekharappa S, Athanassiadou A, Papapetropoulos T, Johnson WG, Lazzarini AM, Duvoisin RC, Di Iorio G, Golbe LI, Nussbaum RL. Mutation in the α-synuclein gene identified in families with Parkinson's disease. Science. 276:2045-47. 1997.

199. Popovic N, Brundin P. Therapeutic potential of controlled drug delivery systems in neurodegenerative diseases. Int J Phceutics. 314:120-26. 2006.

200. Pradilla BM, Gaini SM, Brem H, Olivi A, DiMeco F. Local delivery of a synthetic endostatin fragment for the treatment of experimental gliomas. Neurosurgery. 57(5):1032-40. 2005.

201. Prasad C, Ikegami H, Shimizu I, Onaivi ES. Chronic nicotine intake decelerates aging of nigrostriatal dopaminergic neurons. Life Sci. 54(16):1169-1184. 1994.

202. Prasad KN, Cole WC, Kumar B. Multiple antioxidants in the prevention and treatment of Parkinson's disease. J Am Coll Nutr. 18(5):413-23. 1999.

203. Przedborski S, Jackson-Lewis V. Mechanisms of MPTP toxicity. Mov Disord. 13(1):35-8. 1998.

204. Przedborski S, Vila M. MPTP: a review of its mechanisms of neurotoxicity. Clin Neurosci Res. 1(6):407-418. 2001.

205. Quik M, Di Monte DA. Nicotine administration reduces striatal MPP+ levels in mice. Brain Res. 917(2):219-224. 2001.

206. Quik M, Jeyarasasingam G. Nicotinic receptors and Parkinson's disease. Eur J Pharmacol. 393(1-3):223-30. 2000.

207. Quik M, Kulak JM. Nicotine and nicotinic receptors; relevance to Parkinson's disease. Neurotoxicol. 23:581–594. 2002.

208. Quik M, McIntosh JM. Striatal alpha6* nicotinic acetylcholine receptors: potential targets for Parkinson's disease therapy. J Pharmacol Exp Ther. 316(2):481-9. 2005.

209. Quik M, Parameswaran N, McCallum SE, Bordia T, Bao S, McCormack A, Kim A, Tyndale RF, Langston JW, Di Monte DA. Chronic oral nicotine treatment protects against striatal degeneration in MPTP-treated primates. J Neurochem. 98(6):1866-75. 2006.

210. Quik M. Smoking, Nicotine and Parkinson's disease. Trends Neurosci. 27(9):561-568. 2004.

211. Rajput AH, Martin W, Saint-Hilaire MH, Dorflinger E, Pedder S. Tolcapone improves motor function in parkinsonian patients with the wearing off phenomenon: a double blind, placebo-controlled, multicenter trial. Neurology. 49:1066–1071. 1997.

212. Rascol O. L-Dopa-induced peak-dose dyskinesias in patients with Parkinson's disease: a clinical pharmacologic approach. Mov Disord. 14:19–32. 1992.

213. Ravina BM, Fagan SC, Hart RG, Hovinga CA, Murphy DD, Dawson TM, Marler JR. Neuroprotective agents for clinical trials in Parkinson's disease: a systematic assessment. Neurology. 60(8):1234-40. 2003.

214. Riley DE, Lang AE. The spectrum of levodopa-related fluctuations in Parkinson's disease. Neurology. 43:1459–1464. 1993.

215. Riley RG, Smart JD, Tsibouklis J, Dettmar PW, Hampson F, Davis JA, Kelly G, Wilber WR. An investigation of mucus/polymer rheological synergism using synthesised and characterised poly(acrylic acid)s. Int J Pharm. 217(1-2):87-100. 2001.

216. Rinne JO, Roytta M, Paljarvi J, Rinne UK. Selegiline (deprenyl) treatment and death of nigral neurons in Parkinson's disease. Neurology. 41:859-61. 1991.

217. Rosen SL. Fundamental Principles of Polymeric Materials. 2nd edition. A Wiley-Interscience Publication, New York, USA. 1993.

218. Ross GW, Petrovitch H. Current evidence for neuroprotective effects of nicotine and caffeine against Parkinson's disease. Drugs Aging. 18(11):797-806. 2001.

219. Roy DS, Rohera BD. Comparative evaluation of rate of hydration and matrix erosion of HEC and HPC and study of drug release from their matrices. Eur J Pharm Sci. 16(3):193-199. 2002.

220. Rusted JM, Newhouse PA, Levin ED. Nicotinic treatment for degenerative neuropsychiatric disorders such as Alzheimer's disease and Parkinson's disease. Behav Brain Res. 113(1-2):121-129. 2000.

221. Sawada H, Shimohama S. Estrogens and Parkinson disease: novel approach for neuroprotection. Endocrine. 21(1):77-9. 2003.

222. Schapira AH. Dopamine agonists and neuroprotection in Parkinson's disease. Eur J Neurol. 9:7-14. 2002.

223. Schapira AH. Neuroprotection and dopamine agonists. Neurology. 58(4):S9-18. 2002.

224. Schapira AH. Neuroprotection in PD-a role for dopamine agonists? Neurology. 61(6):S34-42. 2003.

225. Schneider JS, Roeltgen DP, Mancall EL, et al. Parkinson's disease: improved function with GM1 ganglioside treatment in a randomized placebo-controlled study. Neurology. 50:1630–1636. 1998.

226. Schneider JS, Tinker JP, Van Velson M, Menzaghi F, Lloyd GK. Effects of SIB-1508Y, a novel neuronal nicotinic acetylcholine receptor agonist on motor behavior in parkinsonian monkeys. Mov Disord. 13:637–642. 1998.

227. Schrag A, Ben Shlomo Y, Quinn NP. Cross sectional prevalence survey of idiopathic Parkinson's disease and Parkinsonism in London. BMJ. 321:21–22. 2000.

228. Schrag A, Schott JM. Epidemiological, clinical, and genetic characteristics of early-onset parkinsonism. Lancet Neurol. 5(4):355-63. 2006.

229. Schrag A. Entacapone in the treatment of Parkinson's disease. Lancet Neurol. 4(6): 366-370. 2005.

230. Schwarz G. Estimating the dimension of a model. Ann Statistics. 6(2):461-464. 1978.

231. Serp D, Cantana E, Heinzen C, Von Stockar U, Marison IW. Characterization of an encapsulation device for the production of monodisperse alginate beads for cell immobilization. Biotechnol Bioeng. 70:41–53. 2000.

232. Shepherd JE. Effects of estrogen on congnition mood, and degenerative brain diseases. J Am Pharm Assoc (Wash). 41(2):221-8. 2001.

233. Shivakumar HG, Kumar PTM, Desai KG. Pulsative Drug Delivery System. Pharmaceutics. 2003.

234. Shults CW, Oakes D, Kieburtz K, Beal MF, Haas R, Plumb S, Juncos JL, Nutt J, Shoulson I, Carter J, Kompoliti K, Perlmutter JS, Reich S, Stern M, Watts RL, Kurlan R, Molho E, Harrison M, Lew M; Parkinson Study Group. Effects of coenzyme Q10 in early Parkinson disease: evidence of slowing of the functional decline. Arch Neurol. 59(10):1541-50. 2002.

235. Siegel RA, Falamarzian M, Firestone BA, Moxley BC. pH-controlled release from hydrophobic/polyelectrolyte copolymer hydrogels. J Control Rel. 8:179-182. 1988.

236. Siepmann J. Local controlled drug delivery to the brain. Int J Pharmaceutics. 314(2):99-100. 2006.

237. Silver DE, Ruggieri S. Initiating therapy for Parkinson's disease. Neurology. 50(6):S18-22. 1998.

238. Skoug JW, Mikelsons MV, Vigneron CN, Stemm NL. Qualitative evaluation of the mechanism of release of matrix sustained release of dosage forms by measurement of polymer release. J Control Rel. 27:227–245. 1993.

239. Smidsrød O, Draget KI. Chemistry and physical properties of alginate. Carb Eur. 14:6-13. 1996.

240. Smidsrod O, Skjåk-Bræk G. Alginate as immobilization matrix for cells. Trends Biotechnol. 83:71–78. 1990.

241. Smith TJ. Calcium alginate hydrogel as a matrix for enteric delivery of nucleic acids. Biopharm. 4:54-55. 1994.

242. Soto-Otero R, Méndez-Álvarez E, Hermida-Ameijeiras A, López-Real AM, Labandeira-García JL. Effects of (−)-nicotine and (−)-cotinine on 6-hydroxydopamine-induced oxidative stress and neurotoxicity: relevance for Parkinson’s disease. Biochem Pharmacol. 64(1):125-135. 2002.

243. Srivastava R, Brouillet E, Beal MF, Storey E, Hyman BT. Blockade of 1-methyl-4-phenylpyridinium ion (MPP+) nigral toxicity in the rat by prior decortication or MK-801 treatment: a stereological estimate of neuronal loss. Neurobiol Aging. 14(4):295-301. 1993.

244. Standaert DG, Young AB. Chapter 22: Treatment of Central Nervous System Degenerative Disorders. Goodman and Gillman's The Pharmacological Basis of Therapeutics. Hardman JG, Limbert L (editors). 10th edition. McGraw Hill, USA. 2001.

245. Stanford ECC. On Alginic Acid and Its Compounds. ibid. 5:218-221. 1886.

246. Stanford ECC. A New Method of Treating Seaweed. ibid. 4:519-520. 1885.

247. Stanford ECC. On Algin. Jour Soc Chem Indus. 3:297-301; 301-303. 1884.

248. Stanford ECC. On Algin: A New Substance Obtained from Some of the Commoner Species of Marine Algae Chem News Lond. 47:254-57; 267-269. 1883.

249. Stankov B, Cimino M, Marini P, Lucini V, Fraschini F, Clementi F. Identification and functional significance of nicotinic cholinergic receptors in the rat pineal gland. Neurosci Lett. 156(1-2):131-4. 1993.

250. Stocchi F. Pathological gambling in Parkinson's disease. Lancet Neurol. 4(10):590-592. 2005.

251. Stoof JC, Booij J, Drukarch B. Amantadine as a N-methyl-D-aspartic acid receptor antagonist: new possibilities for therapeutic application? Clin Neurol Neurosurg. 92:S4-S6. 1992.

252. Storm PB, Moriarity JL, Tyler B, Burger PC, Brem H, Weingart J. Polymer delivery of camptothecin against 9L gliosarcoma: release, distribution, and efficacy. J Neuro-Oncol. 56: 209–217. 2002.

253. Sutherland IW. Alginates. Byrom D (editor). Biomaterials: Novel Materials from Biological Sources. Stockton. New York. USA. Pages 309-331. 1991.

254. Tahara K, Yamamoto K, Nishihata T. Overall mechanism behind matrix sustained release (SR) tablets prepared with hydroxypropyl methylcellulose 2910. J Control Rel. 35:59–66. 1995.

255. Tamai I, Tsuji A. Transporter-mediated permeation of drugs across the blood-brain barrier. J Pharm Sci. 89:1371–1388. 2000.

256. Tanner CM, Goldman SM, Aston DA, Ottman R, Ellenberg J, Mayeux R, Langston JW. Smoking and Parkinson's disease in twins. Neurology. 58;581–588. 2002.

257. Tarnopolsky MA. Potential benefits of creatine monohydrate supplementation in the elderly. Curr Opin Clin Nutr Metab Care. 3(6):497-502. 2000.

258. Tatton W, Chalmers-Redman R, Tatton N. Neuroprotection by deprenyl and other propargylamines: glyceraldehydes-3-phosphate dehydrogenase rather than monoamine oxidase-B. J Neural Transm. 110:509–515. 2003.

259. Teismann P, Ferger B. Inhibition of the cyclooxygenase isoenzymes COX-1 and COX-2 provide neuroprotection in the MPTP-mouse model of Parkinson's disease. Synapse. 39(2):167-74. 2001.

260. Tomas-Camardiel M, Rite I, Herrera AJ, de Pablos RM, Cano J, Machado A, Venero JL. Minocycline reduces the lipopolysaccharide-induced inflammatory reaction, peroxynitrite-mediated nitration of proteins, disruption of the blood-brain barrier, and damage in the nigral dopaminergic system. Neurobiol Dis. 16(1):190-201. 2004.

261. Tonnesen HH, Karlsen J. Alginate in drug delivery systems. Drug Dev Ind Pharm. 28:621–630. 2002.

262. Torre ML, Maggi L, Vigo D, Galli A, Bornaghi V, Maffeo G, Conte U. Controlled release of swine semen encapsulated in calcium alginate beads. Biomaterials. 21(14):1493-1498. 2000.

263. Tzourio C, Rocca WA, Breteler MM, Baldereschi M, Dartigues JF, Lopez-Pousa S, Manubens-Bertran JM, Alperovitch A. Smoking and Parkinson's disease. An age-dependent risk effect? The Europarkinson Study Group. Neurology. 49:1267–1272. 1997.

264. Ueng SW, Yuan LJ, Lee N, Lin SS, Chan EC, Weng JH. In vivo study of biodegradable alginate antibiotic beads in rabbits. J Orthop Res. 22:592–599. 2004.

265. Uitti RJ, Tanner CM, Rajput AH, Goetz CG, Klawans HL, Thiessen B. Hypersexuality with antiparkinsonian therapy. Clin Neuropharmacol. 12(5):375-83. 1989.

266. van Veen B, Pajander J, Zuurman K, Lappalainen R, Poso A, Frijlink HW, Ketolainen J. The effect of powder blend and tablet structure on drug release mechanisms of hydrophobic starch acetate matrix tablets. Eur J Pharm Biopharm. 61(3):149-57. 2005.

267. Veziers J, Lesourd M, Jollivet C, Montero-Menei C, Benoit JP, Menei P. Analysis of brain biocompatibility of drug-releasing biodegradable microspheres by scanning and transmission electron microscopy. J Neurosurg. 95(3):489-94. 2001.

268. Vila M, Przedborski S. Genetic clues to the pathogenesis of Parkinson's disease. Nat Med. 10:S58–S62. 2004.

269. Visanji NP, Mitchell SN, O'Neill MJ, Duty S. Chronic pre-treatment with nicotine enhances nicotine-evoked striatal dopamine release and alpha6 and beta3 nicotinic acetylcholine receptor subunit mRNA in the substantia nigra pars compacta of the rat. Neuropharmacol. 50(1):36-46. 2005.

270. Wade A, Weller P. Handbook of Pharmaceutical Excipients. American Pharmaceutical Association, Washington, USA and Pharmaceutical Press, London, UK. 1994.

271. Wadia JS, Chalmers-Radma RME, Ju WJH, Carlile GW, Phillips JL, Fraser AD, Tatton WG. Mitochondrial membrane potential and nuclear changes in apoptosis caused by serum and nerve growth factor withdrawal: time course and modification by (−)-deprenyl. J Neurosci. 18:932–947. 1998.

272. Walkenström P, Kidman S Hermansson AM, Rasmussen PB, Hoegh L. Microstructure and rheological behaviour of alginate/pectin mixed gels. Food Hydrocol. 17(5):593-603(11). 2003.

273. Walter KA, Cahan MA, Gur A, Tyler B, Hilton J, Colvin OM, Burger PC, Domb AJ, Brem H. Interstitial taxol delivered from a biodegradable polymer implant against experimental malignant glioma. Cancer Res. 54:2207–2212. 1994.

274. Wan LSC, Heng PWS, Wong LF. Relationship between swelling and drug release in a hydrophilic matrix. Drug Dev Ind Pharm. 19:1201–1210. 1993.

275. Wang F, Lee T, Wang CH. PEG modulated release of etanidazole from implantable PLGA/PDLA discs. Biomaterials. 23(17):3555-66. 2002.

276. Whistler RL, Smart, CL. Polysaccharide Chemistry. New York: Academic Press, Inc. 1953.

277. White HK, Levin ED. Four-week nicotine skin patch treatment effects on cognitive performance in Alzheimer's disease. Psychopharmacol. 143:158–165. 1999.

278. Williams JA, Dillehay LE, Tabassi K, Sipos E, Fahlman C, Brem H. Implantable biodegradable polymers for IUdR radiosensitization of experimental human malignant glioma. J Neuro-Oncol. 32:181–192. 1997.

279. Williams RO III, Reynolds TD, Cabelka TD, Sykora MA, Mahaguna V. Investigation of excipient type and level on drug release from controlled release tablets containing HPMC. Pharm Dev Technol. 7:181–193. 2002.

280. Wise DL. Biopolymeric Controlled Release Systems: Volume 2. CRC Press, Inc. Florida, USA. 1984.

281. Wong KS, Lu CS, Shan DE, Yang CC, Tsoi TH, Mok V. Efficacy, safety, and tolerability of pramipexole in untreated and levodopa-treated patients with Parkinson's disease. J Neurol Sci. 216(1):81-7. 2003.

282. Xie YX, Bezard E, Zhao BL. Investigating the receptor-independent neuroprotective mechanisms of nicotine in mitochondria. J Biol Chem. 280(37):32405-12. 2005.

283. Xing L, Dawei C, Liping X, Rongqing Z. Oral colon-specific drug delivery for bee venom peptide: development of a coated calcium alginate gel beads-entrapped liposome. J Control Rel. 93:293–300. 2003.

284. Yamada M, Yasuhara H. Clinical Pharmacology of MAO Inhibitors: Safety and Future. NeuroToxicol. 25(1-2):215-221. 2004.

285. Yoo HS, Oh JE, Lee KH, Park TG. Biodegradable nanoparticles containing doxorubicin–PLGA conjugate for sustained release. Pharm Res. 16:1114–1118. 1999.

286. Yoo JY, Kim JM, Khang G, Kim MS, Cho SH, Lee HB, Kim YS. Effect of lactide/glycolide monomers on release behaviors of gentamicin sulfate-loaded PLGA discs. Int J Pharm. 276(1-2):1-9. 2004.

287. Yotsuyanagi T, Ohkubo T, Ohhashi O, Ikeda K. Calcium-induced gelation of alginic acid and pH-sensitive reswelling of dried gels. Chem Pharm Bull. 35:1555–1563. 1987.

288. You JO, Peng CA. Calcium-Alginate Nanoparticles for Nonviral Gene Delivery. Technical Proceedings of the NSTI Nanotechnology Conference and Trade Show. 1:270-273. 2005.

289. Yuan X, Dillehay LE, Williams JR, Williams JA. Synthetic, implantable polymers for IUdR radiosensitization of experimental human malignant glioma. Cancer Biother Radiopharm. 14(3):187-202. 1999.

290. Yuan X, Fahlman C, Tabassi K, Williams JA. Synthetic, implantable, biodegradable polymers for controlled release of radiosensitizers. Cancer Biother Radiopharm. 14(3):177-86. 1999.

291. Yuan X, Tabassi K, Williams JA. Implantable polymers for tirapazamine treatments of experimental intracranial malignant glioma. Radiat Oncol Investig. 7(4):218-30. 1999.

292. Zebli B, Susha AS, Sukhorukov GB, Rogach AL, Parak WJ. Magnetic targeting and cellular uptake of polymer microcapsules simultaneously functionalized with magnetic and luminescent nanocrystals. Langmuir. 21(10):4262-5. 2005.

293. Zhang L, Dawson VL, Dawson TM. Oxidative stress and genetics in the pathogenesis of Parkinson's disease. Neurobiol Dis. 7(4):240-50. 2000.